Stress Granules and RNA-Binding Proteins in Epstein-Barr Virus Infection and Cancer

Alistair Iain Tweedie

Submitted for the degree of

Doctor of Philosophy

University of Sussex

July 2022

Declaration

I hereby declare that this thesis has not been and will not be, submitted in whole or in part to another University for the award of any other degree.

Signature: ……

Abstract

Biomolecular condensates are membrane-less compartments formed within a cell, that have a broad range of functions, depending on the type and localisation. One example of a biomolecular condensate is the stress granule (SG), which forms within the cytoplasm and contains translational machinery, mRNA and RNA binding proteins sequestered to foci following stress-induced translational stalling. Several stresses are known to induce SG formation, commonly via the phosphorylation of eukaryotic initiation factor 2 α (eIF2α) by four main kinases, haem-regulated inhibitor (HRI), double-stranded RNA activated protein kinase R (PKR), PKR-like endoplasmic reticulum kinase (PERK), and general control non-depressible 2 (GCN2). These kinases are commonly activated following viral infection, inhibiting translation, and preventing viral replication; therefore, many viruses have developed mechanisms to evade this process.

Epstein-Barr virus (EBV) is a gamma herpesvirus that infects humans, developing a persistent latent infection within B cells. EBV displays a biphasic growth cycle, exhibiting both latent and lytic cycles and it is well understood that latent EBV infections contribute to the development of several cancers. Whilst many viral processes have been attributed to the formation of these cancers, many others remain to be determined.

While several studies have investigated herpesviruses, eIF2α and SG formation processes, little is known regarding EBV and these mechanisms. We aimed to investigate whether lytic EBV altered SG formation similarly to other lytic viruses. Whilst also focusing on latent EBV, eIF2α and SG formation. Misregulation of SG formation has been associated with several human diseases, including cancer, therefore we aimed to determine whether any link existed between latency and altered SG assembly. We hypothesised that while latent EBV viral product expression is restricted, and may not activate the eIF2α pathway, it may be capable of altering the expression of several key SG-associated components.

Lytic EBV was shown to inhibit SG formation following induction via eIF2α-dependent and independent pathways, providing the first evidence that lytic EBV can circumvent the SG response, albeit through currently unknown mechanisms.

We found that latent EBV infection did induce activation of PKR, PERK or phosphorylation of eIF2α. This was reinforced by our finding that latent EBV infection did not promote SG formation, nor alter chemical-induced SG assembly. However, we provide evidence that latent EBV infection alters the transcription and splicing of a key SG protein, TIA-1. T-cell intracellular antigen-1 (TIA-1), an RNA-binding protein, is central to SG formation and displays both oncogenic and tumour suppressor roles achieved via alternative isoforms. We found that latent EBV infection reduced mRNA levels of TIA-1b, known to act as a tumour suppressor, in B cells, whilst maintaining the levels of TIA-1a, the oncogenic isoform. We suggest that this manipulation of TIA-1 isoform expression may contribute to the development of cancer during persistent latent EBV infection, and may provide a novel target for preventative measures.

This study provides the first basis for the understanding of how the biphasic life cycle of EBV may affect eIF2α, SG formation and associated RNA-binding proteins, to benefit its growth and survival.

Contents

Declaration 2
Abstract 3
List of Figures 8
List of Tables 10
Acknowledgements 11
Abbreviations 12
1 Introduction 16
1.1 Viruses 16
1.1.1 Overview 16
1.1.2 Herpesviruses 18
1.2 The Innate Immune Response 29
1.3 The Integrated Stress Response 33
1.3.1 Overview 33
1.3.2 eIF2 33
1.3.3 eIF2α Phosphorylation 35
1.3.4 ATF4 37
1.3.5 CHOP 38
1.3.6 GADD34 41
1.4 The Unfolded Protein Response 42
1.5 Biomolecular Condensates 44
1.5.1 Overview 44
1.5.2 Phase Separation 44
1.5.3 Functions of Biomolecular Condensates 45
1.5.4 Biomolecular Condensates in Disease 46
1.5.5 Eukaryotic Biomolecular Condensates 48
1.5.6 Stress Granules 51
1.5.7 Nuclear Bodies 63
1.6 RNA Binding Proteins 65
1.6.1 Overview 65
1.6.2 T-cell intracellular antigen-1 (TIA-1) 66
1.6.3 Ras GTPase-activating protein-binding protein 1 (G3BP1) 70
1.6.4 Human antigen R (HuR) 71
1.7 Project Aims 72
2 Materials and Methods 73
2.1 Materials 73
2.1.1 Antibodies 73
2.1.2 siRNA 74
2.1.3 Oligos 75
2.1.4 Plasmids 77
2.1.5 Cells 78
2.2 Cell Culture 79
2.2.1 Culturing 79
2.2.2 Cell Passaging 80
2.2.3 Cell Storage 80
2.2.4 Lytic Induction 81
2.2.5 Cell Synchronisation 81
2.3 Chemical Induction Of Stress 82
2.3.1 Arsenite 82
2.3.2 Hippuristanol 82
2.4 Cell Harvesting 83
2.5 Western Blot (WB) 83
2.5.1 Whole Cell Lysate 83
2.5.2 Protein Quantification 83

2.5.3 SDS-PAGE 84
2.5.4 Semi-Dry Transfer 84
2.5.5 Wet Transfer 84
2.5.6 Ponceau Stain 85
2.5.7 Primary Antibody Incubation 85
2.5.8 Secondary Antibody Incubation 85
2.5.9 Detection 85
2.5.10 Image Analysis 86
2.6 RNA Extraction 86
2.7 cDNA Synthesis 86
2.8 Real-Time Polymerase Chain Reaction (qPCR) 86
2.9 Transfection 87
2.9.1 Electroporation 87
2.9.2 Chemical Transfection 88
2.10 Immunofluorescence (IF) 88
2.10.1 Adherent Cells 88
2.10.2 Suspension Cells 89
2.11 Fluorescence In Situ Hybridization (FISH) 90
2.12 IF and FISH 90
2.13 Automated Cell and Granule Counting 90
2.14 mRNA Stability 91
2.15 Protein Stability 92
2.16 Competent Cells 92
2.17 Transformation 93
2.18 Sequencing 93
2.19 CRISPR/Cas9 Knockout 93
2.19.1 gRNA 93
2.19.2 Cloning 93
2.19.3 Transfection 94
2.19.4 Isolation And Expansion of Single Cell Clones 95
2.20 gDNA Extraction 96
2.21 Polymerase Chain Reaction (PCR) 96
2.22 DNA Gel 97
2.23 Mutagenesis 97
2.24 NGFR Isolation 98
2.25 Nucleolar Purification 99
2.26 RNA PolI Inhibition and Nucleolar Disruption 99
2.27 Statistical Analysis 99
3 Integrated stress response during latent EBV infection 100
3.1 Introduction 100
3.2 Results 108
3.2.1 Characterisation of latency in EBV$^+$ cell lines 108
3.2.2 eIF2α and eIF2αK activation during latent EBV infection 112
3.2.3 ATF4, CHOP and GADD34 116
3.2.4 Induction of eIF2α phosphorylation during latent EBV infection 118
3.3 Discussion 122
4 Stress Granule formation during latent EBV infection 128
4.1 Introduction 128
4.2 Results 132
4.2.1 Characterisation of SGs 132
4.2.2 Optimisation of automated cell and granule counting 135
4.2.3 Latent EBV infection does not induce or alter SG accumulation 137
4.3 Discussion 141
5 RNA-binding proteins and latent EBV infection 146
5.1 Introduction 146

5.2 Results 150
5.2.1 TIA-1 protein levels are lower in latent EBV-infected cells 150
5.2.2 TIA-1 mRNA levels are lower in latent EBV-infected cells 153
5.2.3 Stability of TIA-1 protein and mRNA 156
5.2.4 TIA-1 regulation by HuR 162
5.2.5 TIA-1 knockout 165
5.3 Discussion 174
6 Stress granule formation during lytic EBV infection 181
6.1 Introduction 181
6.2 Results 184
6.2.1 ZTA induces lytic cycle and inhibits SG formation in Zta-AK cells 184
6.2.2 eIF2αK activation in lytic Zta-AK 188
6.2.3 SG formation during lytic EBV infection of adherent cells 191
6.2.4 The role that BGLF5 has on SG formation during lytic EBV infection 194
6.2.5 HEK293 + BGLF5 199
6.3 Discussion 201
7 Final Discussion 207
8 Published Work 216
9 References 217
10 Appendix 265
10.1 Integrated stress response during latent EBV infection 265
10.1.1 Phosphorylated eIF2α fluctuation during latent EBV infection 265
10.1.2 ISR protein expression in response to arsenite exposure in latent EBV-infected cells 272
10.2 RNA-binding proteins and latent EBV infection 273
10.2.1 TIA-1 knockdown 273
10.3 SCIRT lncRNA and nuclear bodies in cancer 275
10.3.1 Introduction 275
10.3.2 Results 278
10.3.3 Discussion 295

List of Figures

Figure 1-1 Viral groups are defined by the nucleic acids that they contain. 17
Figure 1-2 Stages of the EBV lytic cycle. 27
Figure 1-3 IFN induction and signalling following PAMP recognition. 32
Figure 1-4 Integrated stress response (ISR) increases eIF2α phosphorylation, stalls translation and induces SGs. 34
Figure 1-5 Delayed translation initiation promotes ATF4 translation during stress. 40
Figure 1-6 Integrated stress response (ISR) and unfolded protein response (UPR) overlap through the activation of PERK. 43
Figure 1-7 Biomolecular condensates within eukaryotic cells. 49
Figure 1-8 G3BP1 Is responsible for SG accumulation. 56
Figure 1-9 Schematic of TIA-1 function within the cell. 69
Figure 3-1 Inhibition of PKR activation by DNA viruses. 107
Figure 3-2 BL2 and BL31 cells with EBV bacmid are in latency III. 110
Figure 3-3 BL2 and BL31 cells with EBV bacmid are not in lytic phase. 111
Figure 3-4 ISR-associated protein expression levels during latent EBV infection. 114
Figure 3-5 eIF2αK activation, eIF2α phosphorylation and downstream signalling during latent EBV infection. 115
Figure 3-6 Arsenite treatment induces eIF2α phosphorylation during latent EBV infection. 120
Figure 3-7 PERK expression following arsenite stress in EBV$^{+/-}$ BL2. 121
Figure 4-1 SG inhibition by viruses. 131
Figure 4-2 Stress granule characterisation in HeLa Cells. 134
Figure 4-3 Cell Profiler workflow to quantify TIA-1^{+} stress granules in images. 136
Figure 4-4 Latent EBV infection does not affect SG formation. 139
Figure 4-5 Latent EBV in BL31 infection and SG formation. 140
Figure 5-1 TIA-1 and TIAR have similar structures. 149
Figure 5-2 TIA-1 protein levels are lower in latently EBV+ B cells. 151
Figure 5-3 TIAR protein levels do not change in latently EBV+ B cells. 152
Figure 5-4 TIA-1b mRNA levels are lower in latent EBV^{+} cells. 155
Figure 5-5 mRNA degradation is promoted by latent viral infection in BL31, but not in BL2. 158
Figure 5-6 Degradation of TIA-1 mRNA is unchanged during latent infection. 159
Figure 5-7 TIA-1 protein stability is similar between latently infected and uninfected cells. 161
Figure 5-8 HuR mRNA expression is altered by latent viral infection. 164
Figure 5-9 Knockout of TIA-1 in HEK293 cells. 167
Figure 5-10 SGs still form in samples transfected with TIA-1 gRNA. 169
Figure 5-11 Development of TIA-1a and TIA-1b expression vectors. 171
Figure 5-12 TIA-1a/b can be expressed in HEK293 cells. 173
Figure 6-1 Zta-expressing cells inhibit SG formation. 187
Figure 6-2 Lytic EBV does not induce eIF2α phosphorylation, or expression of TIA-1. 190
Figure 6-3 Lytic EBV-infected AGS cells inhibit induced SG formation. 193
Figure 6-4 Lytic induction in EBV-infected HEK293 cells. 197
Figure 6-5 Stress treatment of PMA-treated cells. 198
Figure 6-6 Induced SG accumulation in response to BGLF5 expression. 200
Figure 10-1 Fluctuating eIF2α phosphorylation levels in BL2 and BL31 (EBV$^{+/-}$). 268
Figure 10-2 eIF2α fluctuation during latent EBV infection. 269
Figure 10-3 eIF2α phosphorylation during latent EBV infection following cell synchronisation. 270
Figure 10-4 Expression of ISR-associated proteins following arsenite stress. 272

Figure 10-5 TIA-1 knockdown in EBV – and + BL31. 274
Figure 10-6 lncRNA has multiple functions through different molecular interactions. 277
Figure 10-7 Knockdown of SCIRT decreases nuclear SCIRT foci. 280
Figure 10-8 SCIRT is localised to the nucleolus. 283
Figure 10-9 RNA FISH following PolI inhibition shows the disruption of the nucleolus and dispersal of SCIRT. 284
Figure 10-10 RNA FISH used in combination with IF on purified nucleolus samples show colocalization of SCIRT and Fibrillarin. 285
Figure 10-11 SCIRT localisation over time. 287
Figure 10-12 SCIRT localisation in response to cell density. 288
Figure 10-13 Location of each SCIRT KO strategy. 291
Figure 10-14 SCIRT knockout was performed using CRISPR 292

List of Tables

Table 1-1 Nine herpesviruses are known to infect humans. 20
Table 1-2 Pattern of latent protein expression in latency I, II and III. 24
Table 1-3 Latent EBV products and their associated functions. 25
Table 1-4 Eukaryotic biomolecular condensates located within the nucleus and cytoplasm. 50
Table 1-5 The nine human herpesviruses and their known effect on SG formation. 61
Table 10-1 CRISPR targeting location for each SCIRT KO strategy. 291

Acknowledgements

I would first like to thank my supervisor, Dr Tracy Nissan. Thank you for the years of support, patience, kindness and friendship that you have shown me during this project. You have been a fantastic supervisor to work with and have helped every step of the way.

I am also grateful for being able to have known Dr Stephen Hare. Stephen was one of the kindest, most generous and most genuine people I have ever had the privilege of knowing. He always went out of his way to help where needed and I am thankful to have called him a friend.

Thank you to Prof Simon Morley, who always made the office smile. Your continued patience every time I had a question or needed advice was truly appreciated. You were always happy to chat science-related or not, which brought such a warm atmosphere to our corridor.

I'd like to thank Prof Sarah Newbury, Prof Michelle West, Prof Alison Sinclair, Dr Ben Towler and Dr David Wood for your input and advice along the way, and for sharing so much equipment and materials. Ben and David, I am so grateful for your support and guidance along the way.

To my friends, Daniel, Hayley and Frankie. How things have changed since we first started sharing an office. You are the people that made our corridor so enjoyable to be in. Thank you for putting up with me for so long!

To my family, this would not have been possible without you. Thank you for your unwavering support and for always encouraging me. You have allowed me to be where I am today, and I am truly grateful. Thank you for giving me everything you possibly could.

Lastly, Ashley. Thank you for always being there. Thank you for your unfathomable patience, for your kindness, for your support, for everything.

Abbreviations

Abbreviations	Definition
4E-BP	eIF4E-Binding Protein
ActD	Actinomycin D
ALS	Amyotrophic Lateral Sclerosis
ARE	AU-Rich Elements
ATF4	Activating Transcription Factor 4
ATF6	Activating Transcription Factor 6
ATP	Adenosine Triphosphate
BiP	Binding Immunoglobulin Protein
BL	Burkitt Lymphoma
bZip	Basic Region-Leucine Zipper
CDS	Coding Sequence
cGAS	Cyclic GMP–AMP Synthase
CHOP	C/EBP Homologous Protein
CLRs	C-Type Lectin Receptors
CMV	Cytomegalovirus
CRE	cAMP-Responsive Element
CReP	Constitutive Repressor Of eIF2α Phosphorylation
crRNA	Crispr RNA
DAI	DNA-Dependent Activator Of IRF
DAMPs	Damage-Associated Molecular Patterns
DAPI	4′,6-Diamidino-2-Phenylindole
DEPs	Disassembly Engaged Proteins
DMEM	Dulbecco Modified Eagle Medium
DMSO	Dimethyl Sulfoxide
dsRBD	Double-Stranded RNA-Binding Domain
DTT	Dithiothreitol
Dvl	Dishevelled
EBERs	EBV–Encoded Small RNAs
EBNA	EBV Nuclear Antigen
EBV	Epstein-Barr Virus
eIF2	Eukaryotic Translation Initiation Factor 2
eIF2A	Eukaryotic Translation Initiation Factor 2A
eIF2α	Eukaryotic Translation Initiation Factor 2 α-subunit
eIF4E	Eukaryotic Translation Initiation Factor 4E
ER	Endoplasmic Reticulum
FACS	Fluorescence-Activated Cell Sorting
FBS	Foetal Bovine Serum
FISH	Fluorescence In Situ Hybridization
FTD	Frontotemporal Lobar Degeneration
G3BP1	Ras GTPase-Activating Protein-Binding Protein 1
GADD34	Growth Arrest and DNA Damage-Inducible Protein 34
GAP	Ras-GTPase-Activating Protein
GCN2	General Control Non-Depressible 2
GEF	Guanidine Nucleotide Exchanged Factor

Grb7	Growth Factor Receptor-Bound Protein 7
HCV	Hepatitis C Virus
HHV	Human Herpesviruses
HIV-1	Human Immunodeficiency Virus-1
HRI	Haem-Regulated Inhibitor
HRP	Horseradish Peroxidase
HSV-1	Herpes Simplex Virus-1
HSV-2	Herpes Simplex Virus-2
HuR	Human Antigen R
ICTV	International Committee on Taxonomy of Viruses
IDR	Intrinsically Disordered Regions
IE	Immediate-Early
IF	Immunofluorescence
IFN	Interferon
IFNAR	Interferon-A/B Receptors
IRE1	Inositol-Requiring Enzyme 1
IRES	Internal Ribosome Entry Sites
IRF3	Interferon Regulatory Factor 3
IRF7	Interferon Regulatory Factors 7
ISGF3	The Interferon-Stimulated Gene Factor 3
ISGs	Interferon-Stimulated Genes
ISR	Integrated Stress Response
ISRE	Interferon-Stimulated Response Elements
JAK1	Janus Kinase 1
KD	Knockdown
KH	K-Homology
KI	Knockin
KO	Knockout
KSHV	Kaposi's Sarcoma-Associated Herpesvirus
LB	Luria-Bertani
LCLs	Lymphoblastoid Cell Lines
LLPS	Liquid-Liquid Phase Separation
LMP1	Latent Protein 1
lncRNA	Long-Non-Coding RNA
LSPS	Liquid-Solid Phase Separation
MALAT1	Metastasis-Associated Lung Adenocarcinoma Transcript 1
MAPKs	Mitogen-Activated Protein Kinases
miRNA	Micro RNA
MM231	MDA-MB-231
mTOR	Rapamycin
ncRNA	Non-Coding RNA
NEAT1	Nuclear Paraspeckle Assembly Transcript 1
NGFR	Neuronal Growth Factor Receptor
NIR	Near-Infrared
NLRs	NOD-Like Receptors
NLS	Nuclear Localisation Signal
NPC	Nuclear Pore Complex
O-GlcNAc	O-Linked N-Acetylglucosamine

ORF	Open Reading Frames
PAM	Protospacer Adjacent Motif
PAMPs	Pathogen-Associated Molecular Patterns
PBS	Phosphate Buffered Saline
PcG	Polycomb Group
PCM	Pericentriolar Material
PCR	Polymerase Chain Reaction
PERK	PKR-Like Endoplasmic Reticulum Kinase
PI3K	Phosphoinositide 3-Kinase
PIC	Pre-Initiation Complex
PKC	Protein Kinase C
PKR	Double-Stranded RNA-Activated Protein Kinase R
PMA	Phorbol 12-Myristate 13-Acetate
PML	Promyelocytic Leukaemia
PNC	Perinucleolar Compartment
PP1	Protein Phosphatase 1
PP1c	Protein Phosphatase 1 Catalytic Subunit
PrLD	Prion-Like Domain
PRRs	Pattern Recognition Receptors
PSD	Postsynaptic Densities
PSG	Penicillin-Streptomycin-Glutamine
PTMs	Post-Translational Modifications
qPCR	Real-Time Polymerase Chain Reaction
RAN	Ras-Related Nuclear Protein
RBD	RNA-Binding Domains
RBPs	RNA-Binding Proteins
RG	Arginine-Glycine
RLRs	RIG-Like Receptors
RRM	RNA Recognition Motif
RT	Reverse Transcriptase
RXP	Arg-X-Pro
SCIRT	Stem Cell Inhibitory RNA Transcript
SG	Stress Granule
siNC	Off-Target Negative Control siRNA
snoRNPs	Small Nucleolar Ribonucleoproteins
SOB	Super Optimal Broth
STAT1	Signal Transducer and Activator of Transcription 1
STAT2	Signal Transducer and Activator of Transcription 2
STING	Stimulator Of Interferon Genes
TBEV	Tick-Borne Encephalitis Virus
TBK1	TANK-Binding Kinase 1
TC	Ternary Complex
TDP-43	Tar DNA Binding Protein-43
TIA-1	T-Cell Intracellular Antigen-1
TIAR	TIA-1-Related Protein
TIC	Tumour Initiating Cells
TLRs	Toll-Like Receptors
TORC1	Target Of Rapamycin Complex 1

tracrRNA	Transacting RNA
TYK2	Tyrosine Kinase 2
uORFs	Upstream Open Reading Frames
UPR	Unfolded Protein Response
UTR	Untranslated Region
VHS	Virion Host Shut-off
VZV	Varicella Zoster Virus
WB	Western Blot
YB-1	Y-Box Binding Protein 1

1 Introduction

1.1 Viruses

1.1.1 Overview

Viruses are infectious units that are capable of replicating within living cells. They exhibit a broad range of morphologies and differ in size from 16 nm to over 300 nm in diameter (Modrow et al., 2013). Whilst their morphology is broad, the general structure of a virus is consistent, usually comprised of nucleic acid surrounded by a protein layer, known as the capsid. Some species also possess a lipid membrane. Viruses rely on the metabolic process of the host cell that they infect, hijacking these processes to replicate.

A single infectious virus particle is known as a virion, which can infect the host cell through a variety of mechanisms, including fusion of the plasma membrane, receptor-mediated endocytosis, or pore-mediated penetration, before introducing viral nucleic acid into the cytoplasm. The viral genetic material may then be synthesised to mRNA, depending on the initial nucleic acid, and eventually translated before the viral proteins act to modify the cell's metabolic pathways to replicate more viral particles.

As of now, there are over 10,000 species of virus defined (ICTV, 2021; Lefkowitz et al., 2018). Viruses may contain either DNA or RNA, which may be double or single-stranded and contain sense (+) or antisense (-) strands. Baltimore classification (Baltimore, 1971), uses these features to organise viruses into seven groups, dsDNA viruses, ssDNA viruses, dsRNA viruses, (+)ssRNA viruses, (-)ssRNA viruses, ssRNA-RT viruses, and dsDNA-RT viruses (Figure 1-1). These are labelled groups I-VII respectively. Groups VI and VII represent viruses that make use of reverse transcriptase (RT) before integration into the host cell. Several intermediates may be produced during viral replication, depending on the nuclear material that the virus started with. This project focuses on dsDNA viruses.

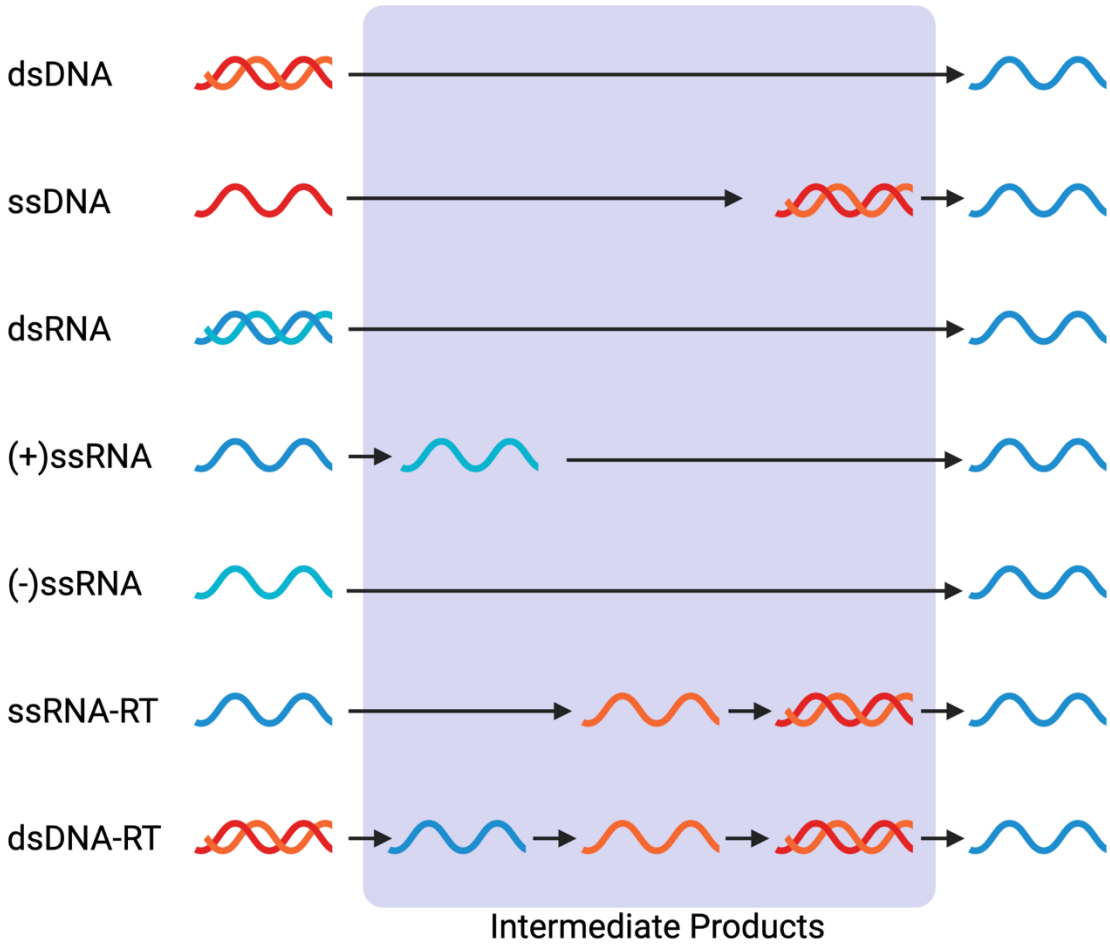

Figure 1-1 Viral groups are defined by the nucleic acids that they contain. Schematic diagram representing the Baltimore grouping of viruses. All nucleic acids are eventually synthesised to mRNA within the host cell, producing several intermediate products during this process. Viruses in the groups ssRNA-RT and dsDNA-RT, make use of reverse transcriptase to produce ssDNA and eventually dsDNA. DNA is represented by red sense and orange anti-sense strands, whilst RNA is represented by dark blue sense and light blue anti-sense strands.

1.1.2 Herpesviruses

Herpesviruses, *Herpesviridae*, are a large family of nuclear-replicating, dsDNA viruses that typically cause a latent infection (Arvin et al., 2007). The lifecycle of herpesviruses generally follows two stages, lytic, where the virus is actively replicating and, latent, where virus replication is dormant. Latency is accomplished through the incorporation of the viral genome, in the form of a closed circular DNA molecule, known as an episome, into the nucleus of the host cell (De Leo et al., 2020). These episomes can assemble into chromatin, similar to host DNA, and replicate using host machinery during cell division. Lytic phase, on the other hand, uses linear viral DNA and transcribes viral machinery to actively replicate within the host cell, creating numerous copies of its DNA (Boehmer & Nimonkar, 2003).

The structure of herpesviruses consists of a large dsDNA genome, icosapentahedral (a polyhedron with 20 faces) capsid, covered in a protein coat and encased in a lipid bilayer envelope (Jeffery-Smith & Riddell, 2021). Their genome is among the largest in nature, ranging from 125 – 245 kbp (Davison, 2002).

Herpesviridae consists of three subfamilies, *Alpha(α)-herpesviridae, Beta(β)-herpesviridae, and Gamma(ɣ)-herpesviridae* characterised by the duration of their replication cycle and host range (ICTV, 2021). α-herpesviruses have been shown to replicate in a broad range of host cells, but preferentially establish latent infection in nerve cells and display a short replication cycle (hours) (Cruz-Muñoz & Fuentes-Panana, 2018; Jeffery-Smith & Riddell, 2021). β-herpesviruses develop a latent infection in secretory glands, reticuloendothelial cells, and kidney cells. They involve a long replication cycle (days) and a much more restricted host cell range. ɣ-herpesviruses develop a persistent latent infection in immune cells, involve the most limited host range of all three groups, and display a slow replication cycle (Drummer et al., 1996).

Entry of herpesviruses into the host cell occurs through a range of mechanisms, depending on the subfamily. The lipid bilayer surrounding the virus contains several group- and species-specific glycoproteins, that mediate binding to specific host cells (Krummenacher et al., 2013). Following the binding of glycoproteins to target cells, fusion machinery is activated and the viral capsid is incorporated into the cell, in most cases, through endocytosis or direct fusion (Akula et al., 2003; Compton et al., 1992; N. Miller & Hutt-Fletcher, 1992). The viral capsid is then transported to the nucleus via the microtubule network, before interacting with the nuclear pore complex and releasing the viral genome into the nucleus (Döhner et al., 2021). After which, the viral genome is transcribed and translated as if it were host DNA. Herpesviruses encode most of the machinery required for replication, including DNA-binding proteins, polymerases, helicase and exonucleases, amongst other proteins (Rampersad & Tennant, 2018).

Whilst over 100 species of herpesviruses exist in nature, only nine are shown to infect human cells and are referred to as human herpesviruses (HHV) (ICTV, 2021) (Table 1-1). This study will focus on HHV-4, also known as Epstein-Barr Virus.

Subfamily	Name	HHV	Latency cell type	Reference
α	Herpes simplex virus-1 (HSV-1)	HHV-1	Sensory neurons	(Nicoll et al., 2012)
	Herpes simplex virus-2 (HSV-2)	HHV-2	Sensory neurons	(Margolis et al., 2007)
	Varicella zoster virus (VZV)	HHV-3	Sensory neurons	(Gershon et al., 2012)
β	Cytomegalovirus (CMV)	HHV-5	Myeloid cells	(Wills et al., 2015)
	Roseolovirus (HHV-6A)	HHV-6A	Myeloid cells	(Yasukawa et al., 1999)
	Roseolovirus (HHV-6B)	HHV-6B	Myeloid cells/Haematopoietic progenitor cells	(Kondo & Yamanishi, 2007; Yasukawa et al., 1999)
	Roseolovirus (HHV-7)	HHV-7	T Cells	(Miyake et al., 2006)
ɣ	Epstein-Barr virus (EBV)	HHV-4	B Cells	(Thorley-Lawson et al., 2013)
	Kaposi's sarcoma-associated herpesvirus (KSHV)	HHV-8	B Cells	(Bechtel et al., 2003)

Table 1-1 Nine herpesviruses are known to infect humans. These HHVs fall into three groups, α-herpesviruses, β- herpesviruses, and ɣ- herpesviruses and differ in their replication cycle, host cell selectivity and latency cell type.

1.1.2.1 Epstein-Barr Virus

Epstein-Barr virus (EBV) is a ɣ-herpesvirus, that preferentially infects B cells. As with most herpesviruses, EBV displays a biphasic growth cycle, exhibiting both latent and lytic cycles.

B cells are lymphocytes derived from hematopoietic stem cells located in bone marrow (in mammals) that produce antibodies during the immune response. Immature B cells differentiate into mature B cells (naïve) within the bone marrow, before migrating to the lymph system. B cells are activated through antigen binding which induces proliferation and differentiation into plasma cells that secrete antibodies. A smaller percentage of B cells are differentiated into memory B cells, a long-lived version that possesses the receptor capable of recognising the initial antigen (Dörner & Radbruch, 2007).

The preferential binding of EBV to B cells occurs through the binding of viral glycoprotein gp350, which carries the EBV binding moiety, to the CD21 receptor found on B cells (Borza & Hutt-Fletcher, 2002; Khyatti et al., 1991; Nemerow et al., 1987). Additional binding occurs between viral glycoprotein gp42 and human leukocyte antigen class II on B cells. EBV develops a persistent latent infection within B cells which has been associated with several human malignancies including Burkitt lymphoma (BL), Hodgkin lymphoma and nasopharyngeal carcinoma (reviewed in Ko, 2015).

EBV has also been shown to infect epithelial cells, albeit in an inefficient and preferentially lytic nature, and it is speculated that oropharyngeal epithelial infection may be a primary source of transmission (Tsang et al., 2014).

1.1.2.1.1 Latency in EBV

Latency is the growth phase in which the virus is not actively replicating, but rather remaining dormant within the cell. The EBV genome exists as a nuclear episome and is replicated once per cell cycle using host DNA polymerase (Kenney & Mertz, 2014).

Latent EBV expresses several proteins, produced during different periods of latency (I, II and III). Several other viral products are produced during this phase, including small non-coding RNAs, known as EBV–encoded small RNAs (EBERs), and several microRNA (miRNA) transcripts (Table 1-2). The latent viral products have a range of functions associated with maintaining infection, controlling signalling pathways, promoting proliferation and ensuring the survival of the host cell (reviewed in Chatterjee et al. 2019; L. S. Young et al., 2000) (Table 1-3). The function of the EBERs, EBER1 and EBER2, remains unclear, however, they are expressed at all stages of latent infection (Arvin et al., 2007). miRNAs are defined as non-coding RNA of around 20 nucleotides in length and are expressed by EBV in several stages of latency. EBV-associated miRNA include BamHI-A rightward fragment-derived miRNAs (BART miRNAs) and BamHI-H rightward fragment 1-derived miRNAs (BHRF1 miRNA) and are thought to be associated with evasion of the host immune response and promotion of proliferation (Iizasa et al., 2020).

EBV infects naïve B cells *in vitro*, causing activation and continuous proliferation of these cells, transforming them into lymphoblastoid cell lines (LCLs), that express the full complement of latent proteins (latency III) (Kozireva et al., 2018; Mrozek-Gorska et al., 2019). In contrast to physiological naïve B cells activation, which can be induced *in vitro* by co-stimulation by IL-4 and CD40L, EBV infection promotes an indefinite proliferation whilst proliferation activation through physiological means is finite (Hollyoake et al., 1995). Several latent EBV products have been implicated in the transformation of B cells through mechanisms including promoting proliferation pathways and evading apoptosis (Saha & Robertson, 2019) (Table 1-3).

In vivo, following EBV infection of B cells, the virus, in latency III, expresses several proteins, namely latent protein 1 (LMP1) and EBV nuclear antigen 2 (EBNA2), that activate the B cell, promoting transformation into proliferating blasts (Amon & Farrell, 2005; Thorley-Lawson & Babcock, 1999). EBNA2 contributes to B cell transformation via

transcriptional activation of a large number of genes that promote proliferation (Portal et al., 2013; Saha & Robertson, 2019; B. Zhao et al., 2011). LMP1 promotes this transformation by mimicking the CD40 receptor signalling pathway, activating B cells and several pathways promoting proliferation (Eliopoulos et al., 1999; Eliopoulos & Young, 1998; B. Zhang et al., 2012). Viral protein expression is then restricted to latency II, through currently unknown mechanisms (Murata et al., 2021), and the B cell transforms into a memory B cell as normal, following exposure to an antigen. Viral gene expression is restricted further to latency I, where only EBNA1 and EBERs are expressed. This restriction of latent products and the transformation of B cells to memory B cells allows for the virus to persist within the body, whilst remaining undetected (Thorley-Lawson & Babcock, 1999).

Latency	Products Expressed										
I	EBERS	miRNA	EBNA1								
II	EBERS	miRNA	EBNA1	LMP1	LMP2A	LMP2B					
III	EBERS	miRNA	EBNA1	LMP1	LMP2A	LMP2B	EBNA-LP	EBNA2	EBNA3A	EBNA3B	EBNA3C

Table 1-2 Pattern of latent protein expression in latency I, II and III. Table showing the viral products produced during each period of latency. Green represents ncRNA and miRNA, red shows nuclear proteins and black represents membrane proteins.

Latent Product	Known associated functions	Reference
EBNA1	Genome replication, viral persistence, transcription regulation, suppress lytic reactivation	(Reisman et al., 1985; Sivachandran et al., 2012; Sugden et al., 1985; Yates et al., 1984, 1985)
EBNA2	B-cell transformation, transcription regulation	(Cohen et al., 1989)
EBNA3A	Transcription regulation, interaction with apoptotic and cell cycle proteins	(Bazot et al., 2014; Harth-Hertle et al., 2013; Maruo et al., 2011; Paschos et al., 2009)
EBNA3B	*In vitro* transformation, cytokine upregulation	(R. E. White et al., 2012)
EBNA3C	Co-activates EBNA2, interacts with apoptotic, cell cycle and tumour suppressor proteins	(Lin et al., 2002; Piovan et al., 2005; Saha, Bamidele, et al., 2011; Saha, Halder, et al., 2011; Saha & Robertson, 2011)
EBNA-LP	B cell transformation, transcription regulation	(Harada & Kieff, 1997; Mannick et al., 1991)
LMP1	Oncogenic, mimics CD40 signalling, B cell transformation	(F. L. Hu et al., 1993; Izumi et al., 1997; Mancao et al., 2005; Mosialos et al., 1995; D. Wang et al., 1985)
LMP2A	Mimics BCR signalling, B cell transformation, interaction with apoptotic and cell cycle proteins, inhibition of epithelial cell differentiation, promotes epithelial cell motility	(Allen et al., 2005; Bieging et al., 2009; Fish et al., 2014; Fukuda & Kawaguchi, 2014; Mancao & Hammerschmidt, 2007; Morrison & Raab-Traub, 2005; Swanson-Mungerson et al., 2010)
LMP2B	Interfere with LMP2A function, increases lytic activation	(Rechsteiner et al., 2008; Rovedo & Longnecker, 2007)
EBERs	Induce growth, modulate the innate immune response, regulate translation	(Fok et al., 2006; Houmani et al., 2009; Iwakiri et al., 2009; Komano et al., 1999; Samanta et al., 2006)
BHRF1 miRNA	Interaction with apoptotic proteins, modulates the immune response, *in vitro* transformation, promotes cell cycle progression	(Regina Feederle et al., 2011; Seto et al., 2010; Xia et al., 2008)
BART miRNA	Interaction with apoptotic proteins, promote apoptosis	(Choi et al., 2013; Haneklaus et al., 2012)

Table 1-3 Latent EBV products and their associated functions. Table showing latent EBV products and known associated functions. Table adapted from Chatterjee et al. (2019).

1.1.2.1.2 Lytic Replication in EBV

EBV also undergoes lytic replication, in which it is actively replicating, producing infectious virions, and allowing transmission between hosts. Lytic replication of EBV occurs mostly in oral epithelial cells, however, may also occur within B cells. As with all ɣ-herpesviruses, latent infection is preferred over lytic replication, so this stage is relatively short-lived (Drummer et al., 1996). Primary infection is thought to occur mostly within oral epithelial cells, where the virus enters the cells whilst in lytic phase before making its way to B cells where it develops a persistent latent infection (Kenney, 2007).

EBV is capable of reactivating to lytic from the latent phase, however, the mechanism is poorly understood (Laichalk & Thorley-Lawson, 2005). The expression of two immediate-early (IE) lytic genes is responsible for the induction of further lytic products (Kenney & Mertz, 2014). Viral transcription factors BZLF1 (Zta/ZEBRA) and BRLF1 (Rta) are induced upon activation of the lytic cycle and in turn induce the expression of early (E) lytic genes encoding for viral replication proteins, before late (L) viral genes are expressed that promote the production of infectious virions (Kenney & Mertz, 2014) (Figure 1-2). Lytic infection produces a much larger complement of products than latency, with around 80 lytic proteins produced (Morales-Sánchez & Fuentes-Panana, 2018). Furthermore, whilst latent infection involves host transcriptional machinery, lytic infection uses viral DNA polymerase, produced at the early stage of lytic infection (Furnari et al., 1992).

During lytic reactivation, the circular latent EBV episome must be linearised. It is thought that this occurs through a rolling circle replication process following the binding of Zta to a lytic-specific origin of replication (Sinclair et al., 2006). This produces multiple linear copiers of the genome, which are then cut by unknown enzymes producing single units of the genome, which are packaged into virions (Figure 1-2).

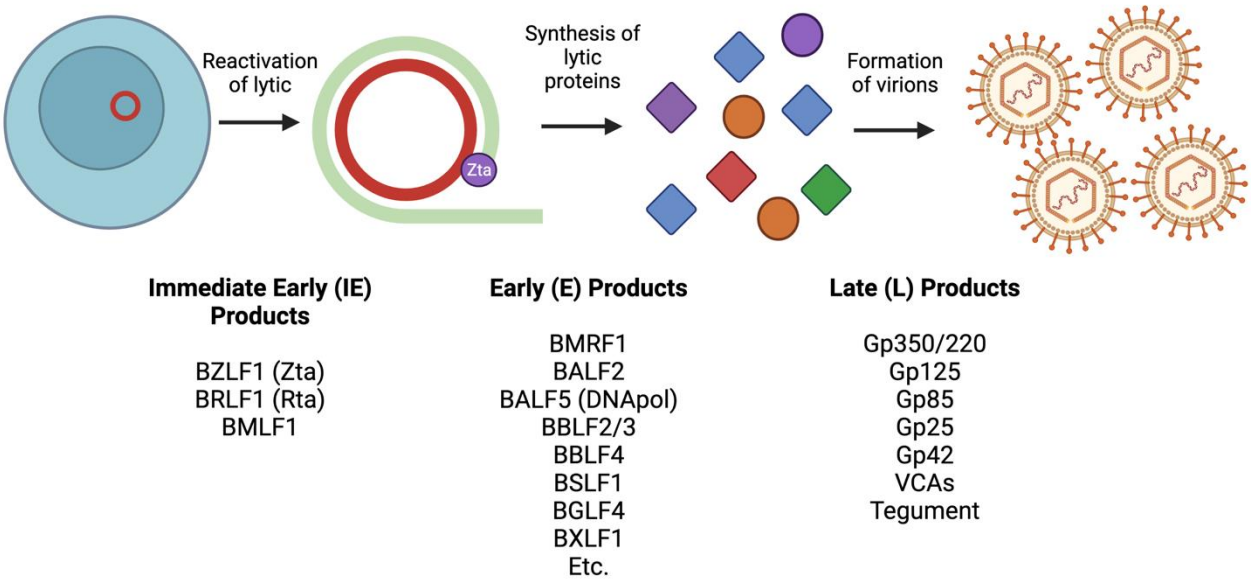

Figure 1-2 Stages of the EBV lytic cycle. Simplified diagram showing the steps following reactivation of EBV lytic cycle in B cells. Immediate early (IE) products are induced following reactivation, which acts as transcription and replication factors to induce further lytic products. Zta binds to the circular latent genome and linearises it through rolling circle replication. The linear genome is packaged into virions by late viral products

1.1.2.1.3 The Association of EBV and Human Disease

Both lytic and latent growth phases of EBV have been associated with several human diseases. However, unlike other herpesviruses, the majority of human diseases associated with EBV stem from latent infection (Chiu & Sugden, 2016).

Lytic EBV infection, whilst usually asymptomatic following primary infection, may cause infectious mononucleosis (IM), which is also known as glandular fever, in adults (Sarwari et al., 2016). IM causes fever, swelling of lymph nodes, and pharyngitis. The majority of cases involve a positive prognosis and usually do not require treatment, however, complications can arise increasing the severity of the disease (Glynn et al., 2007). These complications include rupture of the spleen, hepatitis and airway obstruction (Fugl & Andersen, 2019). The majority of symptoms of IM are thought to be caused by a vigorous T cell response, targeting and eliminating infected cells (Papesch & Watkins, 2001).

Over 90% of the world's adult population carries latent EBV, so it is not surprising that this has been associated with many human diseases (Thompson & Kurzrock, 2004). Before EBV was discovered by Antony Epstein, Yvonne Barr and Bert Achong, Denis Burkitt speculated that a common childhood cancer seen in regions of Africa may have been caused by a virus (Burkitt, 2005). At the time, no such association of a virus causing cancer had been made previously. However, when samples of this cancer, Burkitt lymphoma, were analysed, it was found that they contained virus particles, later defined as EBV (Epstein et al., 1964). This was only the first of cancers linked to EBV, with many others now associated with EBV infection, specifically latent, including Hodgkin lymphoma (Weiss et al., 1989), nasopharyngeal carcinoma (Wolf et al., 1973) and gastric carcinoma (Osato & Imai, 1996). Whilst the mechanism of EBV in tumorigenesis remains speculative, several processes have been linked to the development of disease, including chromosomal translocations, evading apoptosis and promoting proliferation (reviewed in Thompson & Kurzrock, 2004).

1.2 The Innate Immune Response

To understand the effect that EBV may have on the host, it is important to discuss the immune response. There are two forms of immune response in the human body. The first is adaptive immunity, in which the body, acting through cells such as B cells and T cells, develops an acquired immunity to a specific pathogen (Akira et al., 2006). Upon recognising that pathogen a second time, adaptive immunity produces a specific response targeting the invading pathogen. This response commonly involves the release of antibodies to neutralize a target antigen.

The other side of the immune response is the innate immune response. The innate immune response is the body's first line of defence against unspecific invading pathogens and infections (Muralidharan & Mandrekar, 2013). This not only includes cellular defences, but also, physical barriers such as the skin, or the lining of the gut. Following a breach of this physical barrier by an invading pathogen, for example, bacteria or a virus, the immune system attempts to stop this. Pattern recognition receptors (PRRs) are used to detect specific components of the invading pathogen, such as viral RNA or DNA, and elicit a response through interferons (IFNs) (Koyama et al., 2008). Interferons are signalling proteins that modulate the immune response.

These specific pathogenic components recognised by PRRs are known as pathogen-associated molecular patterns (PAMPs) (Onomoto et al., 2014). PRRs may also detect damage-associated molecular patterns (DAMPs), found accompanying damaged or dead host cells. PAMPs are specific structures shared by pathogenic organisms, such as lipids, proteins, and nucleic acids (D. Li & Wu, 2021). Several classes of PPRs have been described, including the membrane-bound Toll-like receptors (TLRs), NOD-like receptors (NLRs), cytoplasmic RIG-like receptors (RLRs) and C-type lectin receptors (CLRs) (Walsh et al., 2013). Additional cytoplasmic PRRs are also present in several cells, including DNA-sensing receptor cyclic GMP–AMP synthase (cGAS) and the RNA-

activated protein kinase, PKR (Taro Kawai & Akira, 2009; Kumar, 2021). The most well-understood PPRs are TLRs, which recognise hydrophobic molecules and nucleic acids and, RLRs, which recognise viral RNA (Akira et al., 2006; Taro Kawai & Akira, 2009). NLRs recognise numerous cytosolic PAMPs from primarily bacterial pathogens, such as peptidoglycan or flagellin, as well as PAMPS produced by host cells and environmental sources (Franchi et al., 2009; Y. K. Kim et al., 2016). CLRs are also cytosolic and recognise primarily fungal carbohydrate structures, however, they may also detect PAMPs from other sources, such as bacteria, viruses and host cells (Hoving et al., 2014).

In regards to EBV, several PPRs have been shown to recognise viral components, including TLR2, TLR3, TLR9 and the RLR retinoic acid-inducible gene I (RIG-I) (Ablasser et al., 2009; Fiola et al., 2010; Gaudreault et al., 2007; Iwakiri et al., 2009; Walsh et al., 2013). These PRRs are thought to recognise lipoproteins/lipopeptides (TLR2), dsRNA (TLR3/RIG-I) and non-methylated CpG-containing nucleic acids (TLR9) (Alexopoulou et al., 2001; Hemmi et al., 2000; Yoneyama et al., 2004; Zähringer et al., 2008). Specifically, PAMPs recognised by these PRRs include virion components, such as glycoprotein, dUTPase and EBER RNA.

Following recognition of PAMPs by PRRs, several diverse pathways are induced promoting the induction of proinflammatory cytokines, chemokines, and IFNs (Muralidharan & Mandrekar, 2013) (Figure 1-3). The general result of each signalling pathway leads to the induction of proinflammatory cytokines, including TNFα, IL-6, and IL-1β, through the activation of transcription factors nuclear factor-kappa B (NF-κB) and AP-1 (Hayden et al., 2006; Zenz et al., 2008). IFN is also induced via transcription factors interferon regulatory factors 3 (IRF3) and 7 (IRF7), which are phosphorylated and translocated to the nucleus resulting in the induction of IFNs. IκB kinase-ε (IKKε) and TANK-binding kinase 1 (TBK1), activated by the binding of a number of PRRs, are responsible for the phosphorylation of IRF3 and IRF7 (McNab et al., 2015). Several

cytoplasmic PRRs, such as cGAS and RIG-I, use an additional adaptor protein, stimulator of IFN genes (STING) to activate TBK1 and IKKε.

Type I IFNs are the main family of cytokines associated with viral infection (Stetson & Medzhitov, 2006). IFNs activate the expression of hundreds of IFN-stimulated genes (ISGs), through the binding of a heterodimeric transmembrane receptor composed of interferon-α/β receptors (IFNAR) 1 and 2. This binding then activates tyrosine kinases Janus kinase 1 (JAK1) and tyrosine kinase 2 (TYK2), which in turn phosphorylate and activate signal transducer and activator of transcription 1 (STAT1) and 2 (STAT2) (D. E. Levy & Darnell, 2002). STAT1 and STAT2 then dimerise and translocate to the nucleus, where they form a complex with IRF9, known as the ISG factor 3 (ISGF3) complex (McNab et al., 2015). This complex binds to IFN-stimulated response elements (ISRE) within the genome, inducing the expression of the ISGs. Additionally, JAK2 and TYK2 activation may also lead to activation of mitogen-activated protein kinases (MAPKs) and the phosphoinositide 3-kinase (PI3K) pathway, whilst other STAT dimers induce alternative pathways and gene induction (McNab et al., 2015) (Figure 1-3).

The expression of these ISGs results in several processes, including activating an antiviral state which limits viral replication, modulating other innate immunity functions, and activation of the adaptive immune response (Ivashkiv & Donlin, 2014). One important role of this pathway is to suppress translation initiation, which may be achieved through the induction of protein kinase RNA-activated (PKR). PKR, along with several other kinases, is responsible for phosphorylating eukaryotic translation initiation factor 2α (eIF2α), which inhibits the guanine nucleotide exchange factor eIF2B, stalling translation (Ivashkiv & Donlin, 2014). This process and PKR are part of the integrated stress response (ISR) (discussed further in the next section) and are commonly activated following viral infection, suggesting that the innate immune response is tightly linked to the ISR.

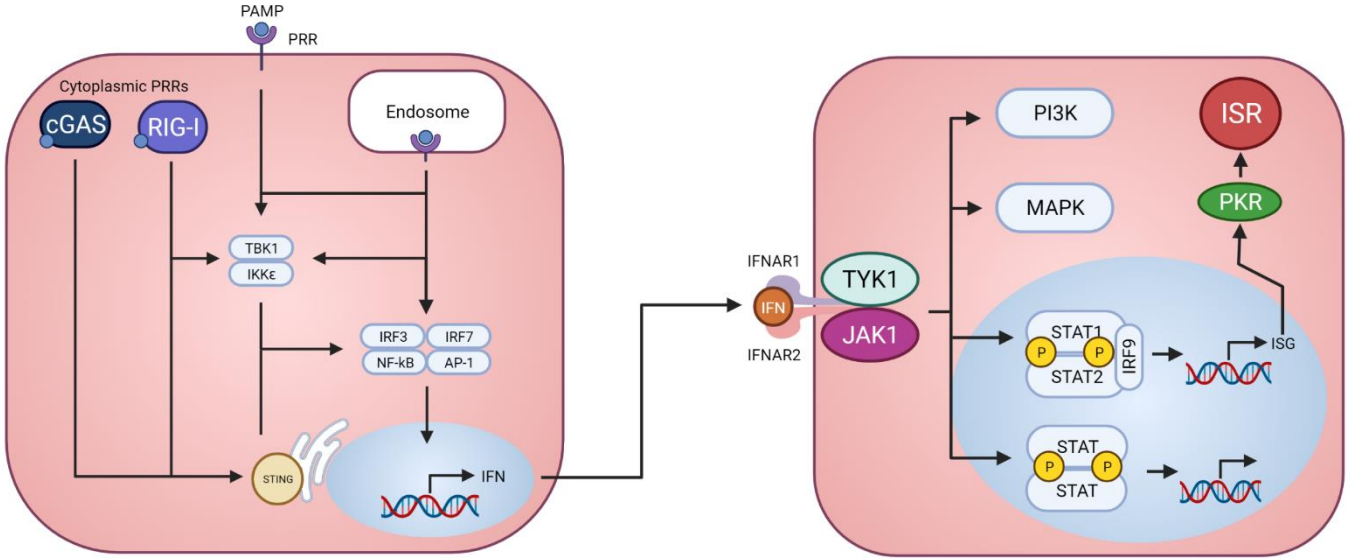

Figure 1-3 IFN induction and signalling following PAMP recognition. Simplified diagram showing several canonical pathways of PAMP recognition by PRRs. Membrane-bound PRRs depicted represent TLRs in this example, and two cytoplasmic PRRs are shown including cGAS and RIG-1. Association of different PRRs by PAMPs induce multiple mechanisms for activation of nuclear factor-kappa B (NF-κB), AP-1, and IFN induction via transcription factors interferon regulatory factors 3 (IRF3) and 7 (IRF7). IFN binds to receptors IFNAR1 and IFNAR2, which in turn activates TYK1 and JAK1. This activation has several effects, including STAT1 and STAT2 phosphorylation and translocation to the nucleus, followed by association with IRF9. This complex induces the expression of ISG through binding to ISREs. PKR is induced as an ISG, increasing cytoplasmic levels of this stress associated kinase and member of the ISR. TYK1 and/or JAK1 activation also results in several other processes, including PI3K activation, MAPK signalling and additional STAT homo and heterodimers that induce a range of genes. Adapted from McNab et al.(2015).

1.3 The Integrated Stress Response

1.3.1 Overview

Central to the effect that viral infection has on mammalian cells, is the integrated stress response (ISR). The ISR is a host response to a variety of cellular stresses and induces specific gene expression and inhibits protein synthesis. It is a core process in the assembly of stress granules (SGs), cytoplasmic foci formed from stalled translational machinery, RNA-binding proteins (RBPs) and mRNA, that function as a site of mRNA triage and storage during stress (discussed further in the next section). The ISR revolves around the regulation of translation initiation factor 2 (eIF2) via phosphorylation on the α subunit (eIF2α), the kinases that perform this process and several downstream effects (Figure 1-4). The activation of the ISR following viral infection is an important process in the body's immune response, limiting viral replication through translational inhibition and functioning as an antiviral pathway (McCormick & Khaperskyy, 2017).

1.3.2 eIF2

eIF2 is a translation initiation factor, that, when bound to GTP, recruits the initial Met-$tRNA_i^{Met}$ to the ribosomal pre-initiation complex beginning cap-dependent translation in eukaryotes (Adomavicius et al., 2019). After the initial start codon recognition, eIF2-GDP is generated through hydrolysis, activated by the GTPase-activating protein eIF5. To facilitate further translation initiation, eIF2-GTP must be re-generated by interaction with its guanine nucleotide exchange factor, eIF2B. Phosphorylation of eIF2α at serine 51 increases its affinity to eIF2B, which both prevents the GDP:GTP exchange and sequesters eIF2α in a high-affinity complex with eIF2B (Hershey, 1989). An elevation of phosphorylated eIF2α by 20–30% has been suggested to be sufficient for sequestration of eIF2B to limit translation initiation, depending on cell type and organism (Brostrom & Brostrom, 1997). These combined effects inhibit translation initiation and promote SG formation.

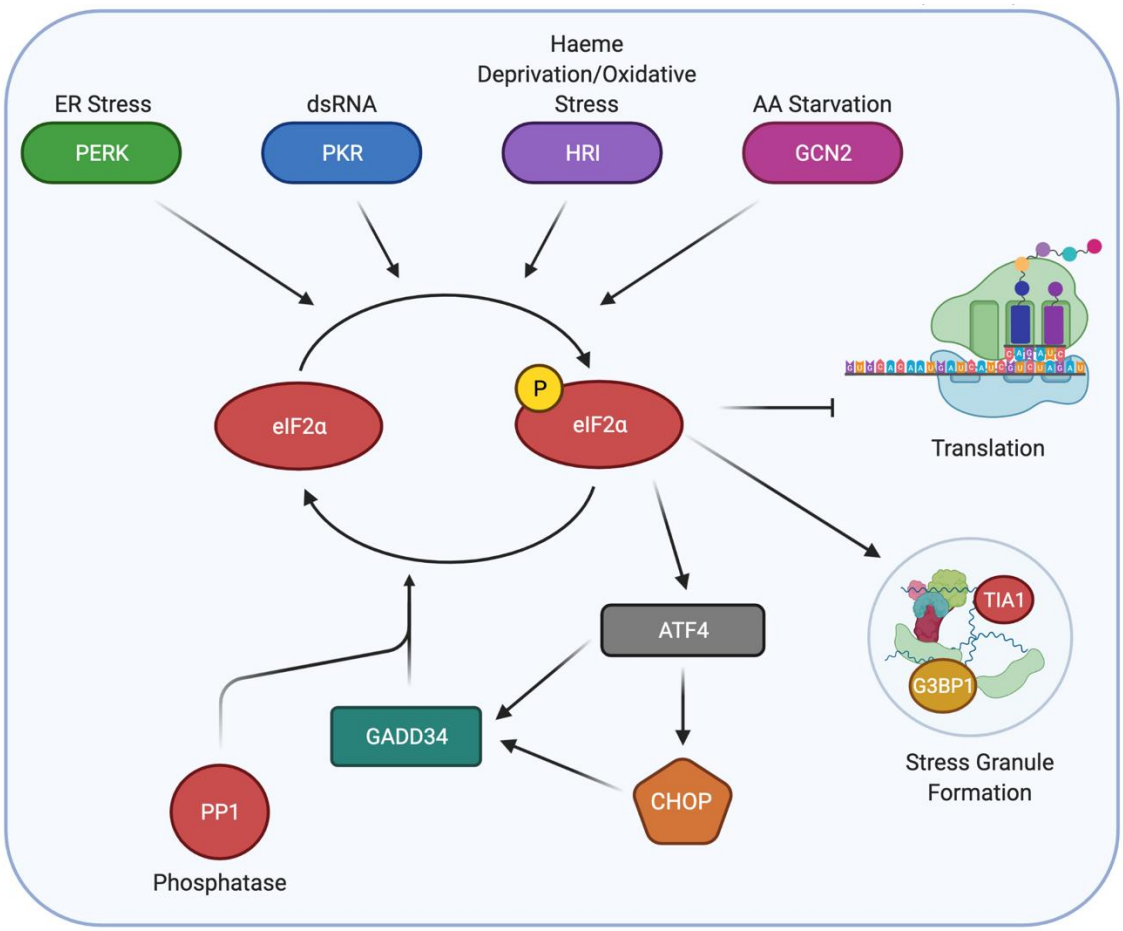

Figure 1-4 Integrated stress response (ISR) increases eIF2α phosphorylation, stalls translation and induces SGs. ISR detects ER Stress, dsRNA, haeme deprivation and oxidation stress, and amino acid starvation and promotes the dimerization and activation of the eIF2αKs PERK, PKR, HRI, and GCN2, respectively. Once activated, these kinases phosphorylate eIF2α, which stalls translation and promotes the formation of stress granules. Phosphorylated eIF2α also promotes the selective translation of uORF containing mRNA, including ATF4, CHOP, and GADD34. GADD34 associates with the eIF2α phosphatase PP1 to dephosphorylate eIF2α during stress recovery.

1.3.3 eIF2α Phosphorylation

Phosphorylation of eIF2α occurs in response to diverse stresses. The ISR is regulated by four eIF2α kinases (eIF2αKs) in humans: haem-regulated inhibitor (HRI), double-stranded RNA-activated protein kinase R (PKR), PKR-like endoplasmic reticulum kinase (PERK), and general control non-depressible 2 (GCN2) (Burgess & Mohr, 2018) (Figure 1-4). HRI is activated through haem deprivation, GCN2 is activated by nutrient and amino acid deprivation, PKR is commonly activated by dsRNA, and PERK is linked to endoplasmic reticulum (ER) stress. This study focuses primarily on PKR and PERK, and their activation during EBV infection.

PKR is frequently activated during viral infection as it contains a regulatory module consisting of an N-terminal double-stranded RNA binding domain (dsRBD) that recognises dsRNA (Lemaire et al., 2008). It has previously been shown that dsRNA is produced by positive-strand RNA, dsRNA, and DNA viruses (Weber et al., 2006), and more recently, also in several negatively-stranded RNA viruses (Son et al., 2015). The production of dsRNA appears to be a trait shared by most viruses, which is an important substrate in host immune response. However, it remains unclear how DNA viruses (including herpesvirus) can produce dsRNA. It is suggested that dsRNA is formed through overlapping and complementary transcripts created as intermediates during replication (Sciortino et al., 2013), or as viral products similar to Epstein–Barr virus-encoded small RNAs (EBERS) that can bind to PKR (McKenna et al., 2007). Upon dsRNA binding to the dsRBD, PKR is activated through dimerization and trans-autophosphorylation, allowing it then to phosphorylate eIF2α, stalling translation and promoting stress granule assembly. It is therefore important for viral replication, that the virus can alter or block this mechanism, so as not to prevent protein synthesis and replication upon dsRNA detection by PKR.

PERK may also be activated in response to viral infection, through endoplasmic reticulum (ER) stress associated with viruses that express membrane glycoproteins, such as the herpesviruses (J. P. White & Lloyd, 2012). Under non-stressed conditions PERK is located on the ER membrane as a homodimer, bound by chaperone binding immunoglobulin protein (BiP/GRP78) (Z. Liu et al., 2015). However, during ER stress, PERK is dissociated from BiP, which triggers the stacking of PERK homodimers allowing trans-autophosphorylation, and activation of PERK. Activated PERK can phosphorylate eIF2α and stall translation, promoting the accumulation of SGs. Therefore, it is important for viruses that express proteins associated with the ER, to mediate the stress that is associated with it.

Herpesviruses activate PERK during lytic replication, when viral glycoproteins are produced at increased levels in the ER, leading to misfolding, activating PERK and the unfolded protein response (UPR) (Leung et al., 2012). The UPR is a stress response tightly associated with the ISR, tasked with overcoming the accumulation of misfolded proteins (discussed in the next section).

EBV is capable of activating PERK via LMP1, which drives the proliferation of infected cells (Dong et al., 2008). This suggests that PERK may be activated by both latent viral products, LMP1, and lytic, viral glycoproteins, during EBV infection. However, it remains unclear whether latent EBV infection produces suitable levels of LMP1 protein to induce PERK activation.

In regards to PKR activations, it has previously been suggested that the EBER proteins inhibit the activation of PKR in *vitro* (McKenna et al., 2007), but whether this also applies *in vivo* is uncertain. One study found that the EBERs were incapable of preventing PKR phosphorylation *in vivo*, in Akata BL cells (Ruf et al., 2005). Additionally, an *in vivo* mouse model, with the deletion of both EBERs did not alter viral infection and persistence

(Gregorovic et al., 2015). This leaves an interesting question, why the EBERs can inhibit PKR *in vitro*, but not *in vivo*?

Whilst it remains to be determined whether latent EBV affects PKR and whether an inhibitory mechanism exists in this phase. We speculate that lytic EBV, however, would likely activate PKR during viral replication through the expression of dsRNA replication intermediates and glycoproteins, unless the virus employs a mechanism to prevent this.

1.3.4 ATF4

Whilst phosphorylation of eIF2α stalls global translation, it alternatively promotes the translation of specific genes (Lu et al., 2004). These specific genes contain short upstream open reading frames (uORFs) within the 5' untranslated region (UTR) that allow translation via re-initiation mechanisms or internal ribosome entry sites (Chan et al., 2013; Rzymski et al., 2010). Activating transcription factor 4 (ATF4) is one such gene that is translated more during stress.

ATF4 contains two uORFs which promote the differential expression of the protein during different stress conditions (Lu et al., 2004; Vattem & Wek, 2004) (Figure 1-5). It is thought that these multiple uORFs contribute to an inhibitory effect on ATF4 during unstressed conditions, as the scanning ribosome is reinitiated at the next coding region after passing uORF1 (Vattem & Wek, 2004). This coding region is uORF2, which exhibits an inhibitory effect on ATF4 as it overlaps the coding region and causes the ribosome to dissociate without translating the gene (S. K. Young & Wek, 2016). During stress, ribosomes require longer before they are competent to reinitiate translation, due to a decreased level of eIF2-GTP. This causes the ribosome to pass uORF2 before reinitiating at the ATF4 coding region (Lu et al., 2004; Vattem & Wek, 2004). Therefore, in unstressed conditions, ATF4 translation is suppressed, but during cellular stress and eIF2α phosphorylation, it is induced.

ATF4 is a basic region-leucine zipper (bZip) transcription factor which binds to a cAMP-responsive element (CRE) (Ameri & Harris, 2008). During stress, the increased levels of ATF4 promote the expression of several stress response genes (Pakos-Zebrucka et al., 2016). ATF4 binds to several dimerization partners that allow for transcriptional control on these genes, which includes C/EBP Homologous Protein (CHOP), which has also been associated as a binding partner of ATF4 (Ameri & Harris, 2008; Harding et al., 2000). ATF4 induces the expression of eIF2α diphosphatase, growth arrest and DNA damage-inducible protein 34 (GADD34) and UPR-associated protein, BiP (Kojima et al., 2003; Y. Ma et al., 2002).

1.3.5 CHOP

C/EBP Homologous Protein (CHOP) is important for the regulation of cell survival and stress-induced apoptosis and is induced following ATF4 expression (Palam et al., 2011). CHOP expression has been extensively linked to ER stress, as several members of the UPR have been shown to also induce CHOP expression (Marciniak et al., 2004). However, it has been shown that CHOP is induced by phosphorylation of eIF2α by all eIF2αKs (Lozon et al., 2011; Suragani et al., 2012; Van de Velde et al., 2016). Following induced mRNA expression of CHOP by ATF4 and UPR-associated proteins, CHOP is preferentially translated similarly to ATF4. CHOP contains one uORF upstream of the coding sequence (CDS), which during unstressed conditions acts as an inhibitor to the expression of the protein (Palam et al., 2011). During stress, however, the uORF is bypassed and the CDS of CHOP is expressed. It was suggested that this occurs through inefficient translational initiation, by low levels of eIF2-GTP and poor start codon consensus in the uORF, leading to leaky scanning by the ribosome, and preferential initiation at a more optimal start codon consensus, the CHOP CDS (Palam et al., 2011).

CHOP acts as a transcription factor that is responsible for the expression and silencing of many pro-apoptotic genes and promotes the expression of the ISR-associated gene

GADD34 (Marciniak et al., 2004; Ron & Habener, 1992). It was also shown to act with ATF4 during ER stress to promote protein synthesis, oxidative stress and cell death (Han et al., 2013).

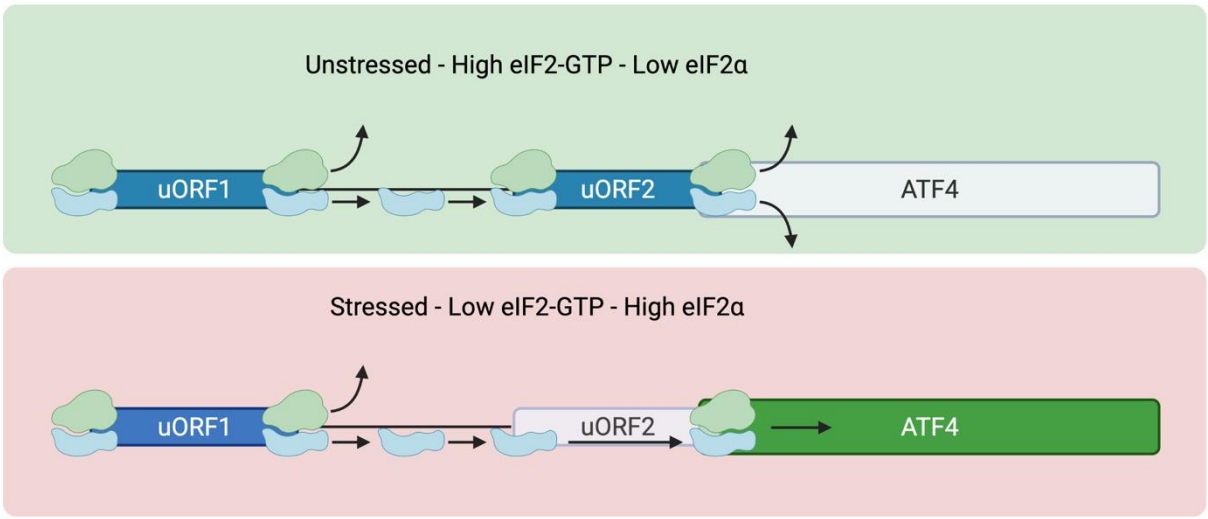

Figure 1-5 Delayed translation initiation promotes ATF4 translation during stress. Simplified diagram showing the two uORFs upstream of the ATF4 gene. During unstressed conditions, levels of eIF2α are low and therefore, eIF2-GTP is abundant and does not limit the initiation of ribosomal complexes. Scanning ribosomes initiate on uORF1, before terminating and reinitiating at uORF2. uORF2 overlaps the CDS of ATF4 which results in termination and dissociation following translation of uORF, preventing ATF4 protein expression. During cellular stress, eIF2 phosphorylation reduces levels of eIF2-GTP, which causes delayed translation reinitiation. This delay causes the scanning ribosome to pass uORF2 before reinitiation occurs at the ATF4 initiation codon, promoting the expression of the protein. Adapted from S. K. Young & Wek (2016).

1.3.6 GADD34

Growth arrest and DNA damage-inducible protein 34 (GADD34), induced by both ATF4 and CHOP, is an important member of the ISR and is responsible for promoting the dephosphorylation of eIF2α. Dephosphorylation is mediated by the protein phosphatase 1 (PP1) complex, consisting of PP1 catalytic subunit (PP1c) and GADD34, or constitutive repressor of eIF2α phosphorylation (CReP) (Choy et al., 2015). CReP is constitutively active in unstressed cells, promoting dephosphorylation of eIF2α and maintaining translation (Jousse et al., 2003). GADD34 on the other hand is induced during periods of cellular stress, via eIF2α phosphorylation, to reduce eIF2α phosphorylation and restore translation, once the stress has been overcome (Y. Ma & Hendershot, 2003).

GADD34, as with ATF4 and CHOP, is preferentially translated during periods of stress. GADD34 contains two uORFs, however, uORF1 contains a poor initiation codon consensus, leading to its bypass in both stress and unstressed conditions (Y. Y. Lee et al., 2009). In unstressed conditions translation is initiated on uORF2 and due to the localisation of a Pro-Pro-Gly sequence next to the termination codon, inefficient ribosome termination occurs, promoting ribosome release before GADD34 translation can occur (S. K. Young et al., 2015). During stress, and eIF2α-phosphorylation, uORF2 is bypassed in a similar manner to CHOP, through poor initiation codon consensus, leading to preferential initiation at GADD34 CDS (Y. Y. Lee et al., 2009; S. K. Young et al., 2015).

1.4 The Unfolded Protein Response

ER stress can manifest in several ways but is generally caused by unfolded proteins and insufficient protein-folding capacity in the ER, which induces the unfolded protein response (UPR). The UPR is a cellular stress response designed to overcome the stress caused by these unfolded proteins. It is a three-pronged system (Figure 1-6), composed of activating transcription factor 6 (ATF6), inositol-requiring enzyme 1 (IRE1), and PERK (P. Walter & Ron, 2011).

When the UPR is activated, the active forms of ATF6 and IRE1 assist the cell in combating ER stress. The chaperone, BiP, is the key regulator in this process. BiP is a member of the heat shock protein 70 family and recognises misfolded proteins in its substrate-binding domain (Kopp et al., 2019). In the absence of unfolded protein, BiP is bound to several proteins including PERK, ATF6 and IRE1, maintaining these in their inactive forms (Lewy et al., 2017; Ye et al., 2000). Following the accumulation of unfolded protein, BiP dissociates from these proteins and preferentially binds to the unfolded protein (Bertolotti et al., 2000).

In this situation, ATF6 is cleaved by S1P and S2P proteases which promotes the transcription of genes to enhance protein folding capacity, while IRE1 is a kinase that engages in non-conventional splicing of the mRNA encoding for the XBP1 transcription factor (Lewy et al., 2017; Ye et al., 2000). When spliced, XBP1 mRNA is translated into its active form, which drives the transcription of genes facilitating ER expansion. Finally, PERK, as described above, phosphorylates eIF2α. Increased eIF2α phosphorylation inhibits translation initiation, thus reducing the load on the ER. Therefore, the UPR and ISR are tightly associated through the inclusion of PERK in both processes.

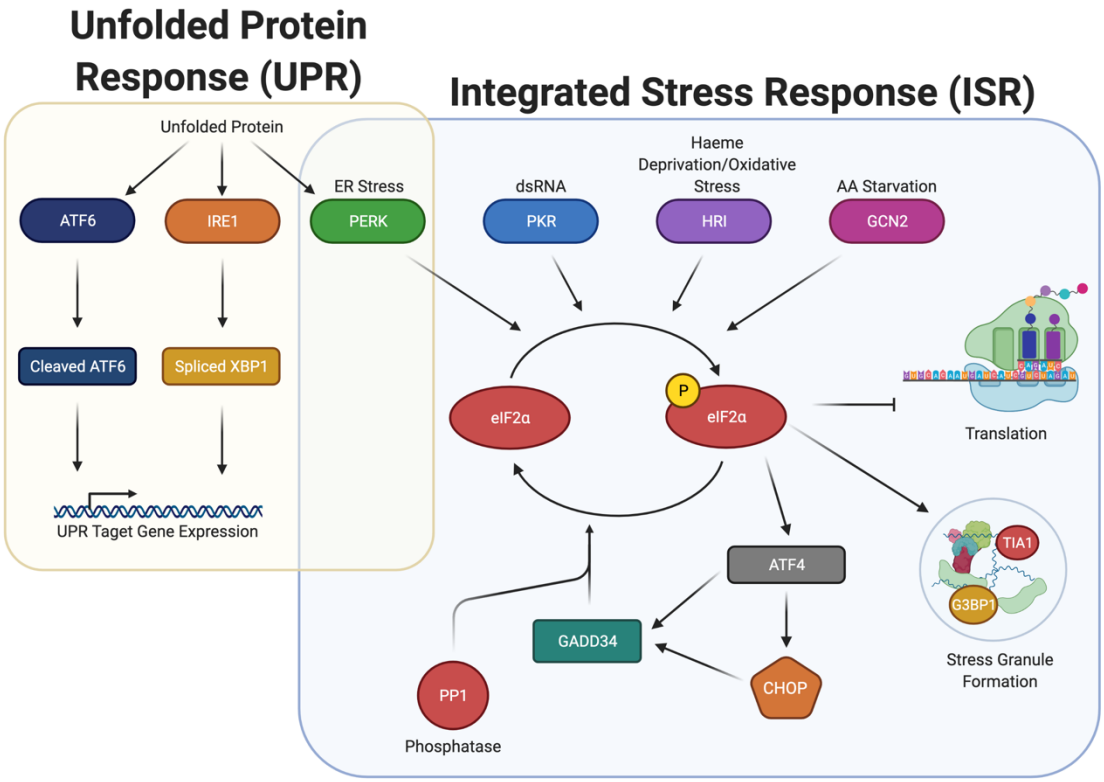

Figure 1-6 Integrated stress response (ISR) and unfolded protein response (UPR) overlap through the activation of PERK. ISR detects ER Stress, dsRNA, haeme deprivation and oxidation stress, and amino acid starvation and promotes the dimerization and activation of the eIF2αKs PERK, PKR, HRI, and GCN2, respectively. Once activated, these kinases phosphorylate eIF2α, which stalls translation and promotes the formation of stress granules. Phosphorylated eIF2α also promotes the selective translation of uORF containing mRNA, including ATF4, CHOP, and GADD34. GADD34 associates with the eIF2α phosphatase PP1 to dephosphorylate eIF2α during stress recovery. The ISR is closely associated with the UPR, connected through PERK. Upon detection of unfolded proteins, ATF6, IRE1, and PERK are all activated, promoting cleavage of ATF6, splicing of XBP1, and the induction of eIF2α phosphorylation. Cleaved ATF6 and spliced XBP1 promote the expression of UPR target genes to elicit a response to unfolded protein.

1.5 Biomolecular Condensates

1.5.1 Overview

The control of biochemical reactions within eukaryotic cells is a tightly regulated process. Organelles act as the site for many of these biochemical processes, and have a broad range of functions, depending on the type and localisation. To elicit and control many complex reactions, the spatial localisation of key components is vital within the cell. Whilst many organelles involve the compartmentalisation of components within a membrane, usually formed by lipid bilayers, several organelles are not bound by a membrane. These are known as biomolecular condensates.

Biomolecular condensates are membrane-less compartments within eukaryotic cells, that have a range of functions, commonly linked to the composition of protein and nucleic acids associated with them (Banani et al., 2017). Biomolecular condensate is a broad term used to encapsulate all foci that contain membrane-less accumulations of nucleic acids and proteins, without conferring more than is known about function, composition or mechanism as previous definitions may have (e.g. hydrogel, compartment) (Glauninger et al., 2022).

Biomolecular condensates are involved in numerous cellular processes in both the nucleus and cytoplasm and include objects such as the nucleolus, Cajal bodies, stress granules, P-bodies, and RNA transport granules (Figure 1-7). The absence of a membrane allows for the rapid recruitment and exchange of components (Brangwynne et al., 2009). They can be formed through several mechanisms, however, the most well-understood, is phase separation (Y. Shin & Brangwynne, 2017).

1.5.2 Phase Separation

Phase separation is the physiochemical process in which two separate phases are produced from a mixture of molecules within the same initial phase (S. Jiang et al., 2020).

This involves the formation of a biomolecular condensate, commonly containing protein and nucleic acids, separated from the surrounding cellular material. The most well-known example of phase separation, and specifically liquid-liquid phase separation (LLPS), is the separation of oil and water. First described as an early interpretation of phase separation in 1912 (Hardy, 1912). Around this time several scientists were beginning to unravel the mystery behind phase separation, through the discovery of the nucleolus and the separation of insoluble particles within a solution (Hardy, 1905; Montgomery, 1898). However, dramatically, it was not until around 100 years later that these concepts were adopted to explain the formation of membrane-less organelles (Dumetz et al., 2008; H. Walter, 1999; H. Walter & Brooks, 1995), and labelled biomolecular condensates (Banani et al., 2017). Whilst the majority of biomolecular condensates are thought to be the result of LLPS (Hyman et al., 2014), other phase separations, such as liquid-solid phase separation (LSPS) occur, however, have regularly been associated with neurogenerative disease (Baradaran-Heravi et al., 2020; Ding et al., 2020; Patel et al., 2015; Ray et al., 2020).

1.5.3 Functions of Biomolecular Condensates

Biomolecular condensates in healthy cells are thought to fall into several functional groups (Banani et al., 2017; Lyon et al., 2021; Y. Shin & Brangwynne, 2017). Although the current agreement differs, generally these groups include organisational hubs, reaction sites and sites of sequestration. First, biomolecular condensates acting as organisational hubs are used to organise internal space. Bodies within the nucleus, such as the nucleolus, paraspeckles and other nuclear bodies are examples of organisational hubs providing organisation of chromatin, proteins, and nucleic acids (Fox et al., 2005; Gibson et al., 2019; Lafontaine et al., 2021).

Another function of biomolecular condensates is acting as the site of biochemical reactions, in which the concentration and specificity of certain molecules may control the

reaction. One such example of this is the activation of cyclic GMP–AMP synthase (cGAS) by DNA binding resulting in the formation of biomolecular condensates containing the activated cGAS (Du & Chen, 2018). The dynamic nature of a biomolecular condensate allows for product and substrate exchange across the phase barrier, providing specificity to the reaction. One study using an engineered biomolecular condensate system, showed the specificity between two substrates when both were present, with only one recruited to the enzyme within the condensate (Peeples & Rosen, 2020).

Finally, and most relevant to this study, is the role of biomolecular condensates in sequestration. This involves the removal of molecules, such as proteins and nucleic acids, away from cellular processes to regulate their function. This sequestration commonly results in the inhibition of the reaction. The most well-known example of this type of biomolecular condensate is stress granules (SGs), which are the focus of this project and will be discussed further later in this chapter. Briefly, as a result of cellular stress, several molecules are recruited to biomolecular condensates known as SGs until the stress is overcome. Upon recruitment of these molecules, many of their processes are known to be inhibited. One example of this is target of rapamycin complex 1 (TORC1), linked to the glucose response and cell growth, in which TORC1 signalling is repressed until release from the SG (Wippich et al., 2013).

Whilst these functional groups provide a basis for understating the role of biomolecular condensates within the cell, they are by no means exhaustive or exclusive. As biomolecular condensate research continues to be a widely studied field, a greater understanding of how they function will be achieved, potentially linking more roles to their existence.

1.5.4 Biomolecular Condensates in Disease

In eukaryotic cells, there have been many biomolecular condensates discovered within the nucleus and cytoplasm (Figure 1-7, Table 1-4). Whilst many of these condensates

are ubiquitous in all cells, several, such as germ granules in germ cells, are exclusive to a specific type of cell. Furthermore, other granules, including SGs, are condition-dependent and only form in the correct environment. Whilst biomolecular condensates function in healthy cells, the accumulation of some condensates has also been associated with several human diseases (reviewed in Spannl, Tereshchenko, Mastromarco, Ihn, & Lee, 2019).

Numerous neurodegenerative diseases have been linked to the formation of biomolecular condensates, usually containing key proteins associated with these diseases (Ding et al., 2020; Patel et al., 2015; Ray et al., 2020). Amyotrophic lateral sclerosis (ALS) is a neurodegenerative disease that progresses to the loss of motor neurons that control muscles within the body and has been associated with the RNA-binding protein FUS (Patel et al., 2015). It was shown that FUS was able to form LLPS biomolecular condensates that solidified over time promoting the acceleration of ALS. Another study associated α-Synuclein (α-Syn), a neuronal protein, and its formation of biomolecular condensates as a precursor to its aggregation, a direct factor in Parkinson's disease (Ray et al., 2020).

Cancer has also been associated with the formation and dysregulation of biomolecular condensates. p53, one of the most well-studied tumour suppressor genes, is regularly mutated in certain cancers (Donehower et al., 2019). The protein was shown to form biomolecular condensates to regulate its function, speculated to act as a functional switch, being released when required and sequestered when not (Kamagata et al., 2020). However, it was been shown that certain mutations can cause the protein to preferentially localise in condensates along with amyloid-like proteins (C. B. Levy et al., 2011), considered to add to the loss of function effect exhibited by the mutant p53 (Y. Zhang et al., 2020). SGs have also been implicated in cancer progression. Y-box binding protein 1 (YB-1), a DNA and RNA binding protein, is involved with several functions relating to pre-mRNA processing, mRNA stability, mRNA packaging, translation and

DNA repair (Budkina et al., 2021; Lyabin et al., 2014). YB-1 is associated with SGs through the binding of SG protein G3BP1 (Somasekharan et al., 2015). This study found that YB-1 inactivation reduced G3BP1 expression and SG formation, leading to reduced tumour invasion and metastasis in mouse models.

The association of biomolecular condensates and human disease is an ever-growing subject. Increased understanding of these condensates will likely lead to further associations, with not only neurodegeneration and cancer but potentially other diseases not yet known to be related.

1.5.5 Eukaryotic Biomolecular Condensates

A great number of biomolecular condensates have been discovered to form in eukaryotic cells (Banani et al., 2017). Table 1-4 focuses on cytoplasmic and nuclear localised eukaryotic biomolecular condensates, however, other condensates are known to form in alternative locations such as the plasma membrane, but beyond the scope of this project. This project primarily focuses on the formation of SGs, along with the investigation of currently unknown nuclear bodies.

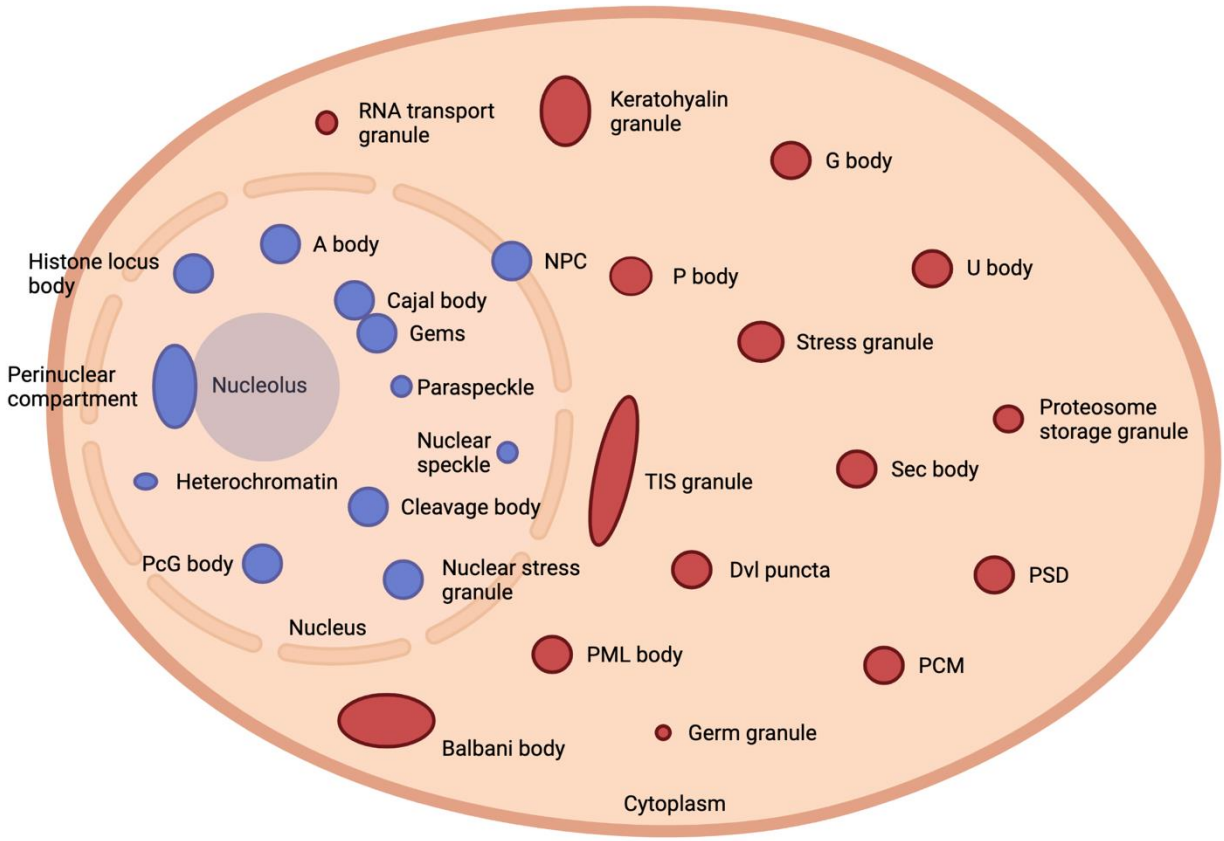

Figure 1-7 Biomolecular condensates within eukaryotic cells. Examples of cytoplasmic and nuclear biomolecular condensates found within eukaryotic cells. Condensates may be ubiquitous, cell type dependent, or condition dependent. Adapted from Banani et al. (2017); Spannl et al. (2019). Localisation and references of each biomolecular condensate are shown in Table 1-4.

Location	Name	Reference
Cytoplasm	Balbiani body	(Boke et al., 2016)
	Germ granule/P granule	(Voronina et al., 2011)
	Keratohyalin granules	(Quiroz et al., 2020)
	Glycolytic (G) body	(Jin et al., 2017)
	Pericentriolar material (PCM)	(Zwicker et al., 2014)
	Processing body	(Sheth & Parker, 2003)
	Promyelocytic leukaemia (PML) body	(Bernardi & Pandolfi, 2007; Lallemand-Breitenbach & de Thé, 2010)
	Proteasome storage granule	(Laporte et al., 2008)
	RNA transport granule	(Kanai et al., 2004)
	Sec body	(Zacharogianni et al., 2014)
	Dishevelled (Dvl) puncta	(Capelluto et al., 2002; Smalley et al., 2005)
	Stress granule	(Collier & Schlesinger, 1986; Kedersha et al., 1999)
	Postsynaptic densities (PSD)	(Banker et al., 1974)
	TIS granule	(W. Ma & Mayr, 2018)
	Uridine-rich snRNP (U) body	(J. L. Liu & Gall, 2007)
Nucleus	Amyloid (A) body	(Audas et al., 2016)
	Cajal body	(Gall et al., 1999)
	Cleavage body	(L. Li et al., 2006)
	DNA damage foci	(Fijen & Rothenberg, 2021)
	Gems (Gemini of Cajal body)	(Q. Liu & Dreyfuss, 1996)
	Heterochromatin	(Strom et al., 2017)
	Histone locus body	(Nizami et al., 2010)
	Nuclear pore complex (NPC)	(Strambio-De-Castillia et al., 2010)
	Nuclear speckles	(Spector & Lamond, 2011)
	Nuclear stress granule	(Sandqvist & Sistonen, 2004)
	Nucleolus	(Lafontaine et al., 2021)
	Paraspeckle	(Bond & Fox, 2009)
	Perinucleolar compartment (PNC)	(S. Huang et al., 1998)
	Polycomb group (PcG) body	(Pirrotta & Li, 2012)

Table 1-4 Eukaryotic biomolecular condensates located within the nucleus and cytoplasm. Table adapted from Banani et al. (2017); Spannl et al. (2019).

1.5.6 Stress Granules

1.5.6.1 Overview

Stress granules (SGs) are cytoplasmic biomolecular condensates that form through LLPS, in response to multiple cellular stresses. These stresses have been shown to include viral infection, heat shock, oxidative stress, and starvation (Hofmann et al., 2021). SGs generally assemble in response to these stresses through stress-induced inhibition of translation initiation. Translation initiation, involves the assembly of the ribosomal subunits on mRNA, through recruitment and interactions with several initiation factors before scanning the mRNA for the start codon.

In mammals, stress-induced inhibition of translation initiation is commonly accomplished by activation of kinases that phosphorylate eIF2α. eIF2 is associated with the eIF2-GTP-Met-tRNAi ternary complex (TC), which recruits the initial methionine to the ribosome during initiation (Merrick & Pavitt, 2018). Phosphorylation of eIF2 generally occurs via the activation of one of the eIF2αK by specific stress, that in turn, phosphorylates the α subunit of eIF2 at serine 51. Following phosphorylation of eIF2α, GDP:GTP exchange is prevented on the eIF2 complex. Without GDP:GTP exchange, initiator tRNA fails to be recruited to the ribosome, stalling translation. This results in stalled 48S translation initiation complexes on mRNAs and a reduction in translating ribosomes due to further elongation without initiation. These mRNAs, cleared of ribosomes, bind to RNA binding proteins, which facilitate the process of SG assembly. Over time, assembled SGs can gain altered properties as well as recruit many additional mRNAs and proteins. Although a number of the components are conserved in all SGs, the composition may vary depending on the stress that induces them (Buchan & Parker, 2009).

Another mechanism for SG assembly relates to the formation of eIF4F, a complex comprised of several initiation factors, and responsible for binding to the 5’ cap on the mRNA. In response to metabolic stress, eIF4E, a component of the eIF4F complex, is

prevented from binding to the other members of this complex through its interaction with eIF4E-binding protein (4E-BP), normally prevented through phosphorylation of 4E-BP by rapamycin (mTOR) (Panas et al., 2016; Sonenberg & Hinnebusch, 2009). The failure of eIF4E to be recruited to the eIF4F complex prevents recruitment to the 5' cap and stalls translation. The eIF4F complex may also be disrupted through additional processes, such as inhibition or disruption of eIF4A and eIF4G (Fujimura et al., 2012; W. J. Kim et al., 2007), resulting in stalled translation and SG formation.

The function of SG formation has long been speculated, however, it is considered to be a site for mRNA storage and triage whilst the cellular stress is overcome (P. J. Anderson & Kedersha, 2008; Kedersha & Anderson, 2002). This promotes several benefits to the cell including, promoting cell survival, controlling protein production, and reducing energy usage (Arimoto et al., 2008; Panas et al., 2016; Walters & Parker, 2015).

1.5.6.2 SG Composition

SG composition may differ through the stress that induces them, as does their size (Mahboubi, Kodiha, et al., 2013). Generally, SGs have been described as being 0.1 µm – 2.0 µm in diameter (P. J. Anderson & Kedersha, 2009), however, other studies have observed larger SGs depending on the induction and length of stress (Mahboubi, Kodiha, et al., 2013). As SGs are formed upon translation initiation inhibition, they contain many of the components and machinery from this process. This includes the 48S preinitiation complex, a piece of initiation machinery comprising of the 40S ribosomal subunit, eIF4F complex, eIF2, and associated mRNA (P. J. Anderson & Kedersha, 2009). Additionally, a broad range of proteins are recruited in the process of SG formation including RNA-binding proteins, such as G3BP1, TIA-1 and HuR, along with many other proteins that function as RNA helicases, transcription factors, nuclear transport factors, nucleases, kinases, and signalling molecules (P. J. Anderson & Kedersha, 2009; Mahboubi, Seganathy, et al., 2013; Tourrière et al., 2003).

1.5.6.3 SG Assembly

Following stress-induced translational stalling, free mRNA is released from polysomes and accumulates within the cytoplasm (Kedersha et al., 2005). This is an important step in SG formation, as inhibition of polysome disassembly prevents SG accumulation (Mazroui et al., 2006). At this point in the process, several mechanisms for SG assembly have been proposed including phase separation of proteins containing intrinsically disordered regions (IDRs) (Kroschwald et al., 2015), the accumulation of a solid core of proteins and RNA, that recruit additional RNA and RBPs (Jain et al., 2016), and the interaction between G3BP1 and the 40S ribosomal subunit (Kedersha et al., 2016). Although the exact mechanism remains unclear, all these proposed processes involved the interaction of proteins containing IDRs.

G3BP1 appears to play a key role in SG formation and has been shown to exist in an inactive closed conformation dimer in the absence of stress (Figure 1-8). G3BP1 contains a positively charged Arginine-Glycine (RG)-rich region, that interacts with its acidic disordered region, holding the protein in a closed conformation (Guillén-Boixet et al., 2020). However, upon binding of free RNA, the RG-rich region is released, and the conformation is altered, which results in the binding of G3BP1 to additional RNA, creating clusters. These G3BP1-RNA condensates were then shown to recruit additional RBPs in what is considered the maturation of the SG (Guillén-Boixet et al., 2020). This mechanism aligns with that proposed by Kedersha et al. (2016) in that interaction of G3BP1 with the 40S ribosomal subunit (along with other RBPs) is central to SG assembly. Silencing of G3BP1 in several cell lines has been shown to disrupt SG formation (Aulas et al., 2015; J. P. White et al., 2007), whilst deletion of G3BP1 disrupted condition-specific SG formation, including eIF2α phosphorylation and eIF4F SG pathways (Kedersha et al., 2016). This suggests that G3BP1 is key in SG formation, however, alternative stresses may promote SGs through a separate mechanism.

Additional RBPs, such as TIA-1, have been closely tied to SG accumulation and shown to be required for their formation. RBPs will be discussed further later in this chapter.

1.5.6.4 Posttranslational Modifications (PTMs)

Post-translational modifications (PTMs) have been linked to the assembly, regulation and disassembly of SGs (Hofweber & Dormann, 2019; Ohn & Anderson, 2010). As previously discussed, one of the key processes in the formation of SGs is the phosphorylation of eIF2α, however, several other PTMs have been described.

The PTM associating O-linked N-acetylglucosamine (O-GlcNAc) to serine and threonine residues on translational machinery was shown to be vital to aggregating untranslated messenger ribonucleoprotein to SGs (Arimoto et al., 2008). Arginine demethylation of G3BP1 and another SG-associated protein, UBAP2L, was shown to promote SG formation (C. Huang et al., 2020; W. C. Tsai et al., 2016).

There have been several other PTMs on SG-associated proteins leading to the assembly defined, including SUMOylation, poly(ADP-ribosyl)ation, arginine methylation and additional phosphorylation, as well as modifications on the RNA (Gill et al., 2021; Hofmann et al., 2021). It appears that PTM on SG proteins and RNA is central to their ability to form foci.

1.5.6.5 SG Disassembly

The process of SG disassembly is a reasonably taken-for-granted topic and is significantly less studied than that of assembly. It is known that SGs are generally reversible in most cells, and disperse over 1 – 2 hours (P. J. Anderson & Kedersha, 2002b). It was suggested that SG disassembly occurred in two phases, whereupon translational restart, mRNA is removed from the SG (Wheeler et al., 2016). This then causes structural instability within the SG as RBP are no longer held together, and in turn, they are dispersed, and the SG is cleared. The process of disassembly being step-wise was also found through the labelling of several core SG proteins (Marmor-Kollet et

al., 2020). This study found several key SG proteins, which they termed disassembly engaged proteins (DEPs), were recruited to SGs during recovery from stress and were involved in the SUMOylation of several SG proteins, linking this PTM to disassembly.

Interestingly, PTMs have also been linked to the disassembly of SGs by several other studies (Duan et al., 2019; C. Huang et al., 2020; N. P. Tsai et al., 2008). Whilst arginine demethylation of UBAP2L was shown to promote SG formation (W. C. Tsai et al., 2016). Silencing and overexpression of the protein disrupted SG disassembly, suggesting that PTM on this protein may play a key role in this SG dynamics (C. Huang et al., 2020). N. P. Tsai et al. (2008) found that growth factor receptor-bound protein 7 (Grb7), a key SG protein that interacts directly with HuR, was hyperphosphorylated following termination of stress, leading to its dissociation from binding partners and eventual separation from the SG. It has also been shown that inhibition of poly(ADP-ribosyl)ation led to a delay in SG disassembly (Duan et al., 2019).

Although the mechanism of SG disassembly has not yet been deciphered, it is clear that PTMs play a central role in the dispersal of SG-associated proteins. Disrupted clearance of SGs has also been shown to be a key process in the development of protein aggregates and the onset of neurodegenerative diseases (Duggan et al., 2020; Wolozin & Ivanov, 2019). Reinforcing the importance of understanding this process and how it may be affected in human disease

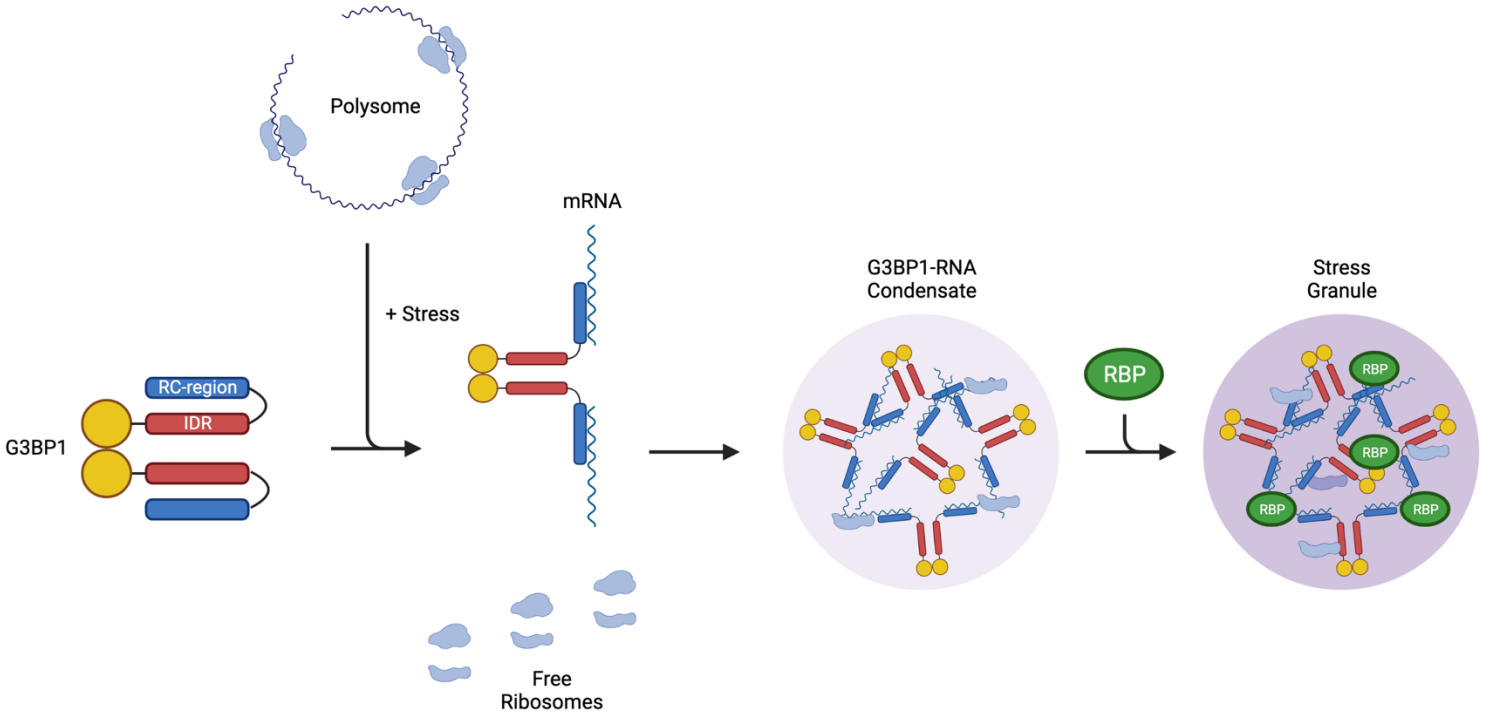

Figure 1-8 G3BP1 Is responsible for SG accumulation. Schematic diagram showing the role that G3BP1 plays in the formation of SGs. G3BP1 exists in a closed conformation in the absence of stress, through interactions between the negatively charged intrinsic disorder region (IDR) and the positively charged RC-rich region (RC-region). Upon stress, the polysome is dissembled and free mRNA accumulates in the cytoplasm. This free mRNA competes with the IDR for binding to the RC-rich region, promoting an open confirmation and increasing G3BP1 affinity to bind to further RNA. This results in clustering of open G3BP1-RNA complexes and small ribosomal subunits forming a biomolecular condensate. The recruitment of additional RBPs and other SG-associated translational machinery form a mature SG.

1.5.6.6 SGs and Innate Immunity

There are well-established connections between SGs, the innate immune response, and viral infection (Cláudio et al., 2013; McCormick & Khaperskyy, 2017; Onomoto et al., 2014). In the last few years, research has shown a convergence between innate immunity pathways and SGs. Two examples are the cytosolic DNA sensor cyclic GMP-AMP synthase (cGAS) and inflammasomes, which activate inflammatory responses including pyroptosis, a lytic form of cell death caused because of intracellular infection.

Cyclic GMP-AMP synthase is an important cytoplasmic DNA sensor for the detection of microbial or self-DNA. The core SG protein G3BP1 has been shown to associate with cGAS and be critical for its production of type I IFN (Z. S. Liu et al., 2019). However, this study suggested that cGAS was not related to SG formation since cGAS was not found in SGs. In addition, knockdown of TIA1, which eliminated SGs, did not affect cGAS signalling. Furthermore, cytoplasmic cGAS foci induced with interferon stimulatory DNA did not colocalize with G3BP1.

However, the extent of SGs' role in cGAS activation remains unclear. A subsequent study supported the finding that G3BP1 regulated cGAS (S. Hu et al., 2019). In contrast to the previous work, the researchers found that the cGAS foci contained G3BP1, PKR, and phosphorylated eIF2α. Defining these foci as SGs is supported by PKR activation and elevated eIF2α phosphorylation, dependent on cGAS; however, it remains to be confirmed whether these G3BP1 foci are bona fide SGs.

The inflammasomes are a multiprotein component of the innate immune response that are assembled in response by PRRs following the recognition of a PAMP (Broz & Dixit, 2016). They promote the activation of inflammatory caspases, which cleave specific cytokines to induce inflammation-associated cell death, known as pyroptosis. The NACHT, LRR, and PYD domains-containing protein 3 (NLRP3) inflammasome is a specific inflammasome containing the PRR, NOD-like receptor NLRP3, and recognises

several PAMPs produced during viral infection (C. Zhao & Zhao, 2020). It is directly affected by the formation of SGs. The DEAD-box helicase DDX3X can interact with and regulate the NLRP3 inflammasome (Samir et al., 2019). Overexpression of DDX3X has been previously shown to cause SG formation and is impaired when downregulated, although it is likely not involved in SG disassembly (Cui et al., 2020; Shih et al., 2012). The interaction of DDX3X with the inflammasome combines with its role in SG biology as documented in Samir et al. (2019), which demonstrated that SG assembly can prevent the activation of inflammasomes, while pre-assembled inflammasomes are unaffected by SG formation. In contrast to cGAS however, G3BP1 depletion did not affect the function of inflammasomes. This suggests that different immune pathways may be differently affected by SGs and SG proteins.

An interesting connection between innate immunity and SGs is the ability of eIF2αK to regulate the signalosomes, which have been shown to have the ability to form amyloid fibrils (Girardin et al., 2020; Sohn & Hur, 2016). These include the NLRP3 and AIM2 inflammasome, and MAVS, TRIF, and RIPK1/RIPK3 amyloid-like fibrils. There is also a connection between innate immunity and amyloid-driven neurodegeneration (Ryu et al., 2018). SGs have numerous links to both neurodegeneration and alternative structures promoted by prion-like proteins (Wolozin & Ivanov, 2019). These connections suggest that infection may result in a variety of effects dependent on SGs and phase separation of signalling proteins.

1.5.6.7 Stress Granules and Viruses

In infection biology, viruses were found to assemble SGs in response to viral infections soon after the discovery of SGs. Sensors for cellular stresses, such as the presence of ER stress, dsRNA, or amino acid starvation activate one of four eIF2αKs. Viruses were recognized early as potential activators as they often contain dsRNA or cause ER stress, commonly from viral protein production (P. J. Anderson & Kedersha, 2002b).

Translation inhibition that results in SG assembly is an important response of the cell to restrict viral protein production and replication. A clue to the importance of SGs is the multiple ways in which viruses affect them (J. P. White & Lloyd, 2012). Manipulation of SGs by viruses can include eIF2α-independent SG assembly, inhibition of SG assembly (either by other stresses or by viruses), or even subversion of SG proteins for new functions and novel non-SG-like aggregates, which are used for viral purposes, including viral replication.

More recent evidence suggests that SGs function in innate immunity in combatting viruses, independently of the role of translation inhibition (Eiermann et al., 2020; Lloyd, 2012; McCormick & Khaperskyy, 2017; Onomoto et al., 2014). These functions are primarily linked to the sequestration of proteins and RNA within SGs, including translation initiation factors, RNA binding proteins involved in viral replication and signalling molecules. Beyond affecting translation, sequestration inhibits viral replication and cellular apoptosis. Further evidence of the importance of SGs in combatting viral infections is that many viruses show increased viral production without SGs. Conversely, in other cases in which SG assembly cannot be subverted by viruses, there is a reduction in viral infection due to SGs.

Several viruses manipulate TIA-1 and SG formation to aid their replication, through a variety of mechanisms, these include, the positive-stranded RNA virus, poliovirus, which promotes the formation of TIA-1 positive granules that lack other SG components (J. P. White & Lloyd, 2011), whilst also cleaving G3BP1 (J. P. White et al., 2007). HSV-1, a DNA virus, promotes TIA-1 accumulation in the cytoplasm but prevents SG formation (Esclatine et al., 2004a). West Nile and dengue virus (both positive-stranded RNA viruses) products interfere and interact with TIA-1/TIAR to prevent SGs from forming (Emara & Brinton, 2007). Additionally, during tick-borne encephalitis virus (TBEV) infection, also a positive-stranded RNA virus, viral RNA interacted with TIA-1 and TIAR and sequestered these proteins away from SGs (Albornoz et al., 2014). It was also noted

that cells with depleted TIA-1 led to a significant increase in extracellular viral infectivity (Albornoz et al., 2014).

The process of viruses suppressing, modulating, or hijacking the formation of stress granules appears to also be a characteristic of the herpesviruses. Current research suggests that the majority of herpesviruses that have been studied suppress the formation of SGs via the eIF2α pathway (Burgess & Mohr, 2018; Finnen et al., 2014; Sharma et al., 2017; Ziehr et al., 2016) (Table 1-5). Understanding how EBV infection may do the same is a principal aim of this study.

Herpesvirus	SG Response	Effect/Potential Effect of SG Response
HSV-1	Inhibited	VHS prevents SG formation through PKR inhibition (Dauber et al., 2011)
HSV-2	Inhibited	VHS prevents SG formation through PKR inhibition (Dauber et al., 2016; Finnen et al., 2014)
VZV	Unknown	ORF63 is involved in the suppression of eIF2α phosphorylation (Ambagala & Cohen, 2007)
EBV	Unknown	No Data
CMV	Inhibited	pTRS1 and pIRS1 prevent SG formation by interfering with PKR (Ziehr et al., 2016)
HHV-6A	Unknown	HHV-6A induced the accumulation of phosphorylated PKR and phosphorylated eIF2α (Sharon & Frenkel, 2017)
HHV-6B	Unknown	No Data
HHV-7	Unknown	No Data
KSHV	Inhibited	ORF57 binds to PACT and prevents it from activating PKR (Sharma et al., 2017)

Table 1-5 The nine human herpesviruses and their known effect on SG formation.

1.5.6.8 SGs and Disease

As touched upon previously, the formation of stress granules has been associated with multiple human diseases, mostly, neurodegeneration and cancer (Spannl et al., 2019). SGs link with neurodegenerative disorders has been regularly shown through the association of SG proteins and these diseases. Tar DNA binding protein-43 (TDP-43), a RBP shown to be important for correct SG dynamics (Khalfallah et al., 2018), was found to be hyperphosphorylated in sporadic ALS and frontotemporal lobar degeneration (FTD) (Neumann et al., 2006). Further studies identified a mutation on TDP-43 associated with ALS (Sreedharan et al., 2008). Several other SGs proteins have been linked to ALS and FTD, including TIA-1, FUS and hnRNPA1 (Mackenzie et al., 2017; Molliex et al., 2015; Patel et al., 2015).

SGs were abundant in brain samples taken from patients with Alzheimer's disease and colocalised with the regularly neurodegeneration-associated protein tau (Vanderweyde et al., 2012). The self-aggregating properties of RBPs are likely to be an important factor in the formation of neurodegenerative disease, and any mutation occurring within them may lead to abnormal aggregations. It has been suggested that chronic and persistent formation of stress granules is cytotoxic leading to the formation of cytoplasmic inclusions *in vitro*, suggesting a potential mechanism for the pathology of ALS and FTD (P. Zhang et al., 2019).

SG formation and associated proteins have been linked to several cancers. As mentioned previously, YB-1, a translation factor and binding partner of G3BP1, is overexpressed and localised in the nucleus in numerous human cancers (reviewed in Maurya et al., 2017). It is unclear how YB-1 regulates the proliferation of cancer, however, Maurya et al. (2017) speculate on the potential to use YB-1 as a biomarker in the detection and prognosis of the disease. Another association between SG assembly and cancer is the connection between mutated DEAD-box RNA helicase, DDX3X and hyper-assembly of SGs (Valentin-Vega et al., 2016). Previous studies had linked

mutated DDX3X to several cancers (Bol et al., 2015; Brandimarte et al., 2014; L. Jiang et al., 2015; Ojha et al., 2015). Valentin-Vega et al. (2016) found that mutated DDX3X within medulloblastoma cells, promoted hyper-assembly of SGs, adding to further translational inhibition and potentially contributing to tumorigenesis.

Numerous links between SGs and human disease have been found. As a tightly regulated process, there is the potential for it to go wrong, and rather than be beneficial to the cell, have disastrous effects instead. This emphasises the importance of SG formation functioning correctly, and begs the question, what effect would a virus modifying this process have on human disease?

1.5.7 Nuclear Bodies

Whilst SGs remain at the centre of this study, some focus must be given to nuclear bodies. Nuclear bodies are a broad group of biomolecular condensates that include any membrane-less accumulation within the nucleus. More well-known examples of nuclear bodies include the nucleolus and Cajal bodies, but also include other condensates such as paraspeckles and nuclear stress bodies (Figure 1-7). They are known to have several functions, including acting as reaction sites, regulating gene expression, and storing and modifying RNA and proteins (Mao et al., 2011).

The nucleolus is a prime example of a nuclear body. This relatively large biomolecular condensate exists in nearly every eukaryotic cell and is the site of rRNA transcription, rRNA processing and ribosomal assembly (Dubois & Boisvert, 2016). The mammalian nucleolus consists of three different phases within the condensate, a fibrillar centre, a dense fibrillar component and a granular component (Mao et al., 2011).

Another example of nuclear bodies are paraspeckles. Paraspeckles are small (0.5 – 1.0 μm) dynamic structures, containing only a small number of proteins thought to be associated with transcription and RNA processing (Fox et al., 2002). Whilst they have

been shown to not localise to sites of transcription, it has been reported that an inactive form of RNA polymerase II is found within them (Xie et al., 2006). As with several other nuclear bodies, the structure of paraspeckles is thought to be centred around a long-non-coding RNA (lncRNA) scaffold. lncRNA will be discussed in a later chapter, however, they are RNA molecules of more than 200 nucleotides that are generally not translated. Several lncRNAs have been associated with the formation of nuclear granules, and are shown to be key in the construction and stabilisation of nuclear condensates (Chujo & Hirose, 2017).

1.6 RNA Binding Proteins

1.6.1 Overview

Central to the assembly of SGs, are the RNA binding proteins (RBPs), such as T-cell intracellular antigen-1 (TIA-1), TIA-1-related (TIAR) and Ras GTPase-activating protein-binding protein 1 (G3BP1), which oligomerize on non-translating mRNA present in the granules. These, and other RBPs, have multiple low-affinity interactions with ss and dsRNA, as well as proteins, and can elicit several functions through these interactions (Dreyfuss et al., 2002; Guillén-Boixet et al., 2020; Hofmann et al., 2021; Sanders et al., 2020; Yang et al., 2020). The proteins involved often contain IDRs and/or low complexity prion-like repeat sequences. Weak dynamic interactions act together to undergo the process of LLPS, which allows for proteins and RNA to concentrate within foci to create a distinct fluid environment. SG formation sequesters many additional RBPs along with mRNA, translational machinery, and key SG proteins, depending on the stress acting upon the cell.

RBPs are usually made up of one, or multiple structural motifs, known as RNA-binding domains (RBD). These domains include RNA Recognition Motif (RRM), the double-stranded RNA-binding domain (dsRBD), the K-Homology (KH) domain, a motif that binds single-stranded RNA and DNA, and the zinc finger domains (Lunde et al., 2007). The modularity of RBPs through these multiple domains, along with the addition of auxiliary domains, alternative splicing, and post-translational modifications, provides a broad RNA-specificity and function (Glisovic et al., 2008). RBPs have been shown to have several roles in RNA modification and processing, translational regulation, mRNA localization and nuclear export.

Post-transcriptional regulation of gene expression is a useful tool employed in the human genome, commonly controlled by RBPs (Glisovic et al., 2008). It provides various mechanisms of control for gene expression, vital for differential expression of genes

within different cells. One such control is alternative splicing, which provides different mRNAs encoding for different proteins, using the same initial pre-mRNA (Smith & Valcárcel, 2000). As pre-mRNA contains numerous exons, as well as introns, alternative splicing allows for the inclusion or exclusion of these exons promoting alternative mRNA products. Interactions between pre-mRNA and RBPs, through their RBDs, are the main influencers of alternative splicing (Witten & Ule, 2011).

1.6.2 T-cell intracellular antigen-1 (TIA-1)

TIA-1 is an RBP shown to be involved with translational silencing, alternative splicing, and stress granule formation (Dember et al., 1996; Piecyk et al., 2000) (Figure 1-9). TIA-1 is comprised of three RRMs along with a glutamine-rich C-terminal auxiliary domain (Tian et al., 1991).

TIA-1 can promote alternative splicing through recruitment of the U1 small nuclear ribonucleoprotein (U1 snRNP) to pre-mRNA via direct binding to the U1-specific polypeptides U1-C (Förch et al., 2002). Furthermore, TIA-1 has been shown to bind to splicing activators adjacent to the 5' splice sites to enhance splicing (Del Gatto-Konczak et al., 2000). TIA-1 localisation differs depending on function, and it has been demonstrated that TIA-1 can continuously shuttle between the nucleus and cytoplasm (T. Zhang et al., 2005). This is important to TIA-1 function, as it is involved in multiple roles occurring in both, the nucleus, and cytoplasm.

TIA-1 plays a part in other RNA expression mechanisms, including mRNA silencing and translational repression (Rayman & Kandel, 2017). TIA-1 acts as a translational repressor through binding to mRNA via specific sequence motifs, commonly AU-rich elements (ARE), containing transcripts encoding for pro-inflammatory proteins, and reducing levels of protein expression (Yamasaki et al., 2007). TIA-1 binds to AREs within the 3'UTR, which are present in several mRNAs, including Cyclooxygenase-2, TNF-α, β2-Adrenergic Receptor (Dixon et al., 2003; Kandasamy et al., 2005; Piecyk et al., 2000).

In the cytoplasm, a key function of TIA-1 is to sequester untranslated mRNA to SGs during stress-induced eIF2α phosphorylation (Kedersha et al., 1999). As TIA-1 can shuttle in and out of the nucleus, it can relocate to cytoplasmic foci, and recruit untranslated mRNA through broad binding specificity exerted by its multiple RRMs (Dember et al., 1996; Kedersha et al., 2000). TIA-1 has a glutamine-rich C-terminal auxiliary domain that also represents a prion-like domain (PrLD), necessary for protein aggregation and stress granule formation (Gilks et al., 2004; Kedersha et al., 1999; McInerney et al., 2005; Rayman & Kandel, 2017). PrLDs are sequences of low complexity, enriched polar, uncharged amino acids and have been associated with neurodegenerative disease (Couthouis et al., 2011). However, TIA-1 aggregation is highly regulated as part of the stress granule mechanism, and overexpression of TIA-1 has been linked with the induction of SGs (Kedersha et al., 1999). More recently, another study suggested that found that overexpression of TIA-1 reduced cell proliferation (Sánchez-Jiménez et al., 2015). TIA-1 has been shown to colocalise with tau, a protein regularly associated with neurodegeneration, and reducing levels of TIA-1 in mice protects against neurodegeneration and inhibits tau misfolding (Apicco et al., 2018; Vanderweyde et al., 2016).

Numerous isoforms of TIA-1 exist, however, alternative splicing causing an inclusion or exclusion of exon 5 leads to the expression of TIA-1a and TIA-1b, respectively, the two most common isoforms (P. J. Anderson & Kedersha, 2002a; Izquierdo & Valcárcel, 2007b). Whilst these isoforms do not differ dramatically in size, the exon 5 inclusion is just 33 bps, their functions are affected by this difference. TIA-1b exhibits an enhanced splicing ability over TIA-1a, and TIA-1a promotes proliferation of cells, whilst TIA-1b inhibits proliferation and promotes apoptosis (Hamada et al., 2016; Izquierdo & Valcárcel, 2007b; Sánchez-Jiménez et al., 2015).

Emerging evidence is beginning to associate TIA-1 with the regulation of tumours. Sánchez-Jiménez et al. (2015) reported that knockdown of TIA-1 in transformed cells

promoted cellular proliferation and tumour growth, and low TIA-1 expression levels in lung cancer patients correlated with a poor prognosis. This study further reinforced their findings by inducing TIA-1 expression in mice, which inhibited the growth of xenotumours. This apparent tumour suppressor function has since been suggested to be isoform-specific, specifically TIA-1b, while in contrast, TIA-1a was shown to have oncogenic activity (Hamada et al., 2016). This study found that cells expressing only TIA-1a grew significantly more colonies than the wild type, whilst the TIA-1b cells, had far fewer colonies that the wild type. They concluded that TIA-1a promoted proliferation, whilst TIA-1b inhibited this process and induced cell death, which has been reinforced by another study (Carrascoso et al., 2018). Although conflicting with the original study on TIA-1 and tumour growth, these studies suggest an oncogenic and tumour suppressor role for TIA-1a and TIA-1b, respectively. Further research is required to further the understanding of the role that TIA-1 in tumour growth. However, if this mechanism is as proposed, it provides an interesting balance between the two isoforms. If manipulated by a virus, such as EBV, that aims to promote proliferation and inhibit SG formation, there may also be additional consequences such as tumour growth.

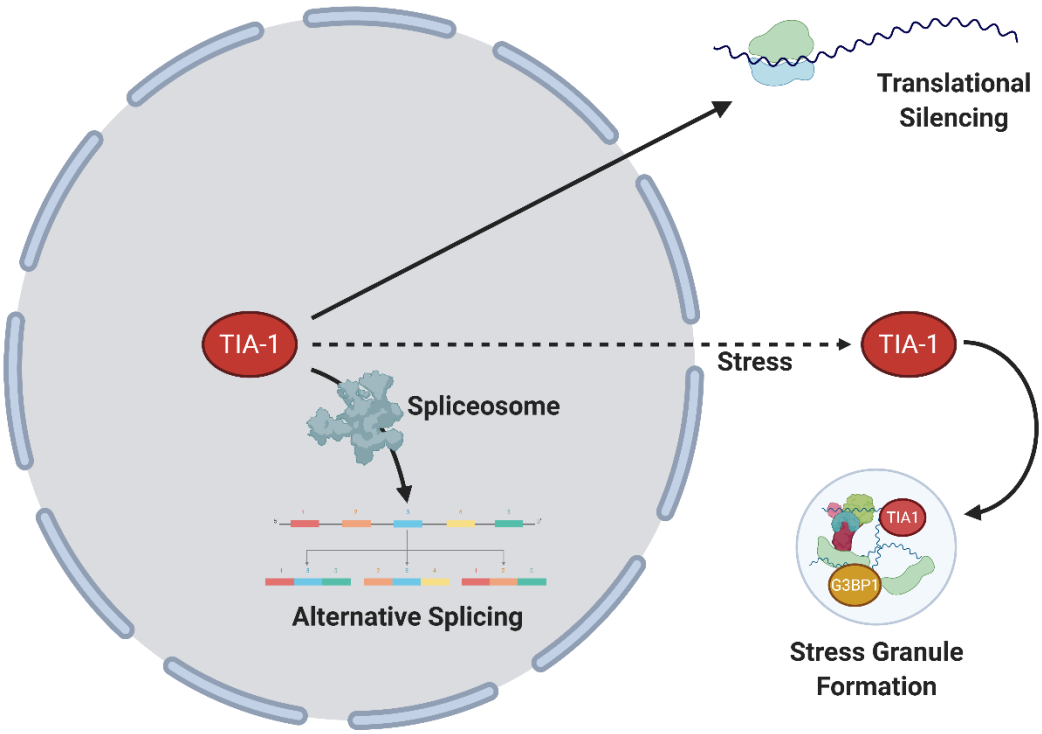

Figure 1-9 Schematic of TIA-1 function within the cell. TIA-1 is nuclear RBP, however, may shuttle between the nucleus and cytoplasm depending on function. During cellular stress, TIA-1 is exported to the cytoplasm where it promotes the formation of SGs. TIA-1 may also translationally silence mRNA in the cytoplasm, through binding directly to the mRNA and inhibiting translational machinery from binding. Finally, TIA-1 works to promote alternative splicing within the nucleus though binding and interactions with the spliceosome.

1.6.3 Ras GTPase-activating protein-binding protein 1 (G3BP1)

Another SG-associated protein is Ras GTPase-activating protein-binding protein 1 (G3BP1), a cytosolic protein that was originally thought to bind to the SH3 domain of Ras-GTPase-activating protein (GAP), involved in Ras signalling (Parker et al., 1996). However, more recent evidence suggests that G3BP1 is not associated with Ras-GAP, and therefore not a genuine binding partner (Annibaldi et al., 2011). What is known is that G3BP1 is a critical factor in stress granule formation, and overexpression of G3BP1 induces SG formation, whilst knockdown inhibits it (Tourrière et al., 2003).

Whilst not the focus of this study, G3BP1 is a key SG protein, and it is tightly linked to this process. G3BP1 has also been shown to be an important antiviral factor, through binding and promoting RIG-I recognition of RNA viruses, activating the innate immune response (Onomoto et al., 2012). Furthermore, G3BP1 is critical for DNA binding and activation of cGAS, through binding directly to cGAS and promoting the oligomerisation of cGAS, priming and activating this process (Z. S. Liu et al., 2019). It has also been shown that G3BP1 is vital for recruiting PKR to SGs following viral infection, initiating eIF2α phosphorylation, along with the role in initiating SG formation discussed previously (Reineke & Lloyd, 2015).

G3BP1 has several other functions relating to controlling mRNA and gene expression (reviewed in Kang et al., 2021). G3BP1 was shown to stabilise mRNA expression and promote protein expression. One example of this is its association with cdk7 mRNA and subsequent stabilisation before increased protein translation leads to cellular growth (Lypowy et al., 2005). G3BP1 has also been implicated in the degradation of mRNA through its role as an endoribonuclease. It was shown that G3BP1 can cleave the 3′ UTR of c-myc, a proto-oncogene that promotes several genes associated with cellular proliferation (Tourrière et al., 2001). G3BP1 has many additional functions outside the process of SG formation and is key to regulating and affecting numerous mechanisms.

1.6.4 Human antigen R (HuR)

Human antigen R (HuR/ELAVL1) is the final RBP that will be discussed in this chapter. Throughout this study, it became clear that this protein was important, not only in SG formation but associated with EBV and the effect that the virus has on TIA-1 regulation.

HuR, as with many other RBPs, binds to ARE in the 3' UTR of target mRNAs to assert its function. Whilst being primarily located within the nucleus, HuR can shuttle between the nucleus and cytoplasm (Fan & Steitz, 1998). This shuttling ability allows the protein to localise to the cytoplasm during cellular stress and accumulate in SGs (Bley et al., 2015). HuR has been associated with post-transcriptional regulation of numerous target mRNA, thought to be related to DNA damage and the stress response (reviewed in Hinman & Lou, 2008). Furthermore, as with TIA-1, HuR is implicated in alternative splicing (Izquierdo, 2008). Interestingly, it was shown that HuR and TIA-1 bound to the same target mRNA and had opposite regulation of alternative splicing (W. Zhao et al., 2014). This process is investigated further in later chapters.

1.7 Project Aims

The mechanism of biomolecular condensate formation is a highly regulated process. SG formation and viral infection involve not only the central ISR pathway but also the innate immune response and the UPR. SG formation includes numerous components, such as RBPs which themselves are stringently regulated.

We hypothesise that latent EBV will evade eIF2αK activation and thus eIF2α phosphorylation, via its restricted viral product expression. The absence of dsRNA and low levels of LMP1 will likely fail to induce activation of PKR or PERK, respectively. This suggests that SG will not form due to latent EBV infection, and therefore no mechanism may exist to prevent this process. We aim to confirm the activation and phosphorylation levels of PKR, PERK and eIF2α, whilst investigating SG formation through chemical induction.

Next, we aimed to investigate the effect of latent EBV on RBPs. Previous studies have revealed that viruses can manipulate RBPs to not only modify the SG process but to aid the viral lifecycle. We hypothesised that latent EBV alters RNP transcription and splicing to promote proliferation and evade apoptosis whilst contributing to the development of latent EBV-associated cancer.

Finally, in line with previous research into lytic human herpesviruses, we aimed to determine whether the actively replicating EBV may activate the ISR, and possess mechanisms to evade SG formation. We hypothesise that lytic EBV will prevent SG formation induced by the virus and through chemical induction, via similar mechanisms as seen with HSV-1, HSV-2 and KSHV.

2 Materials and Methods

2.1 Materials

2.1.1 Antibodies

2.1.1.1 Primary Antibodies

Name (Clone)	Supplier	Product Code	Lot Number	Specificity
ATF4	Abcam	ab184909	GR3212613-4	Rabbit mAb
c-myc	Abcam	ab32072		Rabbit mAb
EBV EBNA2	MW Lab	NA	NA	Rabbit pAb
EBV ZEBRA/Zta (BZ1)	Santa Cruz	sc-53904	A1518	Mouse mAb
eIF2α	Cell Signalling Technology	2103S	04/2011 Lot: 3	Mouse mAb
Fibrillarin	Abcam	ab5821	GR3369971	Rabbit pAb
G3BP1	Abcam	ab56574	GR236188-1	Mouse mAb
PERK	Abcam	ab77654	GR168400-17	Rabbit pAb
Phospho-eIF2α	Abcam	ab32157	GR3254220-2	Rabbit mAb
Phospho-eIF4E	Abcam	ab76256	GR210598-6	Rabbit mAb
Phospho-PERK	Abcam	ab192591	GR185975-86	Rabbit pAb
Phospho-PKR	Invitrogen	PA5-37704	SK2480418	Rabbit pAb
Phospho-PKR	Merck Millipore	07-532	2918608	Rabbit pAb
PKR	Abcam	ab226846	GR3305104-1	Rabbit pAb
TIA-1	Abcam	ab40693	GR3240852-1	Rabbit pAb
TIA-1	Santa Cruz	sc-1751	G2704	Goat pAb
TIAR	BD Biosciences (Fisher)	610352 15895409	8164601	Mouse mAb
α-Tubulin	Thermo Fisher Scientific	32-2500	UD286180	Mouse mAb
β-Actin	Abcam	ab8226	GR231973-1 GR3249122-1	Mouse mAb

2.1.1.2 Secondary Antibodies

Name (Clone)	Supplier	Product Code	Lot Number	Specificity
Alexa Fluor 555 IgG	Life Technologies	A21428	2272588 1511349	Rabbit
Alexa Fluor 633 IgG	Life Technologies	A21053	2304277 1579047	Mouse
Alexa Fluor 555 IgG	Life Technologies	A21422	1480471	Mouse
Anti-Mouse IgG HRP	GE Healthcare	NXA931V	9838250	Mouse
Anti-Rabbit IgG HRP	Cell Signalling	7074S	01/2018	Rabbit
IRDye 800CW Goat Anti-Rabbit	Li-Cor	926-32211	D00304-15	Rabbit
IRDye 680RD Goat Anti-Mouse	Li-Cor	926-68070	D00804-13	Mouse

2.1.2 siRNA

ID	Manufacturer	Target	Sequences (If known)
L-013042-02-0005	Horizon Discovery	ON-TARGETplus Human TIA1 siRNA	SMARTpool
D-001810-01-05	Horizon Discovery	ON-TARGETplus Non-targeting siRNA #1	SMARTpool
SCIRT 1B	Ambion	RP5-1120P11.1 (siSCIRT#1)	GUUUGUAGAUGUAAUCAAA
SCIRT c1B	Ambion	RP5-1120P11.1 (siSCIRT#2)	CACUGUUGUUGGUUGAAUU

2.1.3 Oligos

ID	Target	Sequence (5'-3')	Reference
MW84	GAPDH Forward	TCAAGATCATCAGCAATGCC	(Schlick et al., 2011)
MW85	GAPDH Reverse	CATGAGTCCTTCCACGATACC	(Schlick et al., 2011)
OL01	TIA-1 Forward	TCCCGCTCCAAAGAGTACATATGAG	(W. Zhao et al., 2014)
OL02	TIA-1 Reverse	AAACAATTGCATGTGCTGCACTTTC	(W. Zhao et al., 2014)
OL03	TIA-1 (Exon 5 overlap) Forward	GCCCAAGACTCTATACGTCGGTAACC	(Izquierdo & Valcárcel, 2007b)
OL04	TIA-1 (Exon 5 overlap) Reverse	GGTGCAAAAGCAGCTTTTATATCTTC	(Izquierdo & Valcárcel, 2007b)
OL05	TIA-1 Intron Forward	GCTGAGGCAGGAGAATCACT	This thesis
OL06	TIA-1 Intron Reverse	TGAGATGGTGTCTGGCTCTG	This thesis
OL07	CHOP Forward	ACCAAGGGAGAACCAGGAAACG	(Chiang et al., 2017)
OL08	CHOP Reverse	TCACCATTCGGTCAATCAGAGC	(Chiang et al., 2017)
OL09	GADD34 Forward	CCTCCTAGGCTGCCCCT	(T. H. Kim et al., 2014)
OL10	GADD34 Reverse	ATGGACAGTGACCTTCTCGG	(T. H. Kim et al., 2014)
OL11	ATF4 Forward	GTCCCTCCAACAACAGCAAG	(T. H. Kim et al., 2014)
OL12	ATF4 Reverse	CTATACCCAACAGGGCATCC	(T. H. Kim et al., 2014)
OL13	18S Forward	CATTGGAGGGCAAGTCTGG	(Saunus et al., 2007)
OL14	18S Reverse	TCCCAAGATCCAACTACGAGC	(Saunus et al., 2007)
OL19	TIAR Forward	CAACTGGAAAATCCAAAGGCTATGG	(W. Zhao et al., 2014)
OL20	TIAR Reverse	GACGCAATTCCTCCACAGTACACAG	(W. Zhao et al., 2014)
OL23	HuR (Long 3'UTR) Forward	GTGGTGCTGGGTGGGTTCCG	(Homa et al., 2013)
OL24	HuR (Long 3'UTR) Reverse	GCTCCCAACAGCAGCACGGT	(Homa et al., 2013)
OL25	HuR (Total) Forward	GTTTGGGCCGTTTGGTGCCG	(Homa et al., 2013)

OL26	HuR (Total) Reverse	GCGGTAGCCGTTCAGGCTGG	(Homa et al., 2013)
OL27	TIA-1a Forward	GGACGGAAGATAATGGGTAAGGAAG	(Hamada et al., 2016)
OL28	TIA-1a Reverse	CTGACAACGGTACTACTGCTTGTATC	(Hamada et al., 2016)
OL29	TIA-1b Forward	GGACGGAAGATAATGGGTAAGGAAG	(Hamada et al., 2016)
OL30	TIA-1b Reverse	CAAAGACATGGAAATGATTGCTTGTATC	(Hamada et al., 2016)
OL35	Zta (BZLF1) Forward	AATGCCGGGCCAAGTTTAAGCAAC	(W. Zhang et al., 2016)
OL36	Zta (BZLF1) Reverse	TTGGGCACATCTGCTTCAACAGGA	(W. Zhang et al., 2016)
OL39	TIA-1 Gene Forward	ATTGGGGTTTCATTGTTCCCG	This thesis
OL40	TIA-1 Gene Reverse	TGGCAGACATCCAGCATCTT	This thesis
OL43	TIA-1 Exon 2 Long gDNA Forward	GCCAACCAGTTGACACCACA	This thesis
OL46	TIA-1 EX5 Insert Reverse	GCAGTCAAAAGAAAGATACAAGCAGTAGTACCGTTGTCAGCACACAGCGTTCACAAGATAATCATTTCCATGTCTTTGTTGG	This thesis
OL50	TIA-1 EX5 NEB Insert Forward	ACACAGCGTTCACAAGATCATTTCCATGTCTTTGTTG	This thesis
OL51	TIA-1 EX5 NEB Insert Reverse	GCTGACAACGGTACTACTGCTTGTATCTTTCTTTTGAC	This thesis

2.1.4 Plasmids

Number	Plasmid Name	Bacterial Resistance	Reference
P01	PX458	Ampicillin	(Ran et al., 2013)
P02	PX459	Ampicillin	(Ran et al., 2013)
P03	PX458_2A_GFP_sgRNA_TIA1	Ampicillin	(Meyer et al., 2018)
P04	pFRT_TO_eGFP_TIA1b	Ampicillin	(Meyer et al., 2018)
PO5	pFRT_TO_eGFP_TIA1a	Ampicillin	This thesis
B332	pCDNA3.1(+)-BGLF5 ORF	G418	(R Feederle et al., 2009)
P1919	F-plasmid in recombinant EBV	Chloramphenicol	(R Feederle et al., 2009)
P509	BZLF1 expression plasmid	Ampicillin	(R Feederle et al., 2009)
PP1 UP1	PX459_sgRNA_SCIRT_Promotor_Upstream_1	Ampicillin	This thesis
PP1 UP2	PX459_sgRNA_SCIRT_Promotor_Upstream_2	Ampicillin	This thesis
PP1 DS1	PX459_sgRNA_SCIRT_Promotor_Downstream_1	Ampicillin	This thesis
PP1 DS2	PX459_sgRNA_SCIRT_Promotor_Downstream_2	Ampicillin	This thesis
EX1 UP1	PX459_sgRNA_SCIRT_Exons_Upstream_1	Ampicillin	This thesis
EX1 UP2	PX459_sgRNA_SCIRT_Exons_Upstream_2	Ampicillin	This thesis
EX1 DS1	PX459_sgRNA_SCIRT_Exons_Downstream_1	Ampicillin	This thesis
EX1 DS2	PX459_sgRNA_SCIRT_Exons_Downstream_2	Ampicillin	This thesis
LO1 UP1	PX459_sgRNA_SCIRT_Whole_Locus_Upstream_1	Ampicillin	This thesis
LO1 UP2	PX459_sgRNA_SCIRT_Whole_Locu_Upstream_2	Ampicillin	This thesis
LO1 DS1	PX459_sgRNA_SCIRT_Whole_Locu_Downstream_1	Ampicillin	This thesis
LO1 DS2	PX459_sgRNA_SCIRT_Whole_Locu_Downstream_2	Ampicillin	This thesis

2.1.5 Cells

Full Name	Cell Type	Tissue/Disease	Source/Reference
HeLa	Adherent	Uterus/Adenocarcinoma	ATCC, Manassas, VA, USA
MDA-MB-231	Adherent	Breast/Adenocarcinoma	ATCC, Manassas, VA, USA
MCF7	Adherent	Breast/Adenocarcinoma	ATCC, Manassas, VA, USA
HEK293	Adherent	Kidney/Normal	ATCC, Manassas, VA, USA
MRC-5	Adherent	Lung/Normal	European Collection of Cell Cultures (ECACC)
BL2	Suspension	Burkitt Lymphoma/EBV$^-$	(Schlick et al., 2011)
BL31	Suspension	Burkitt Lymphoma/EBV$^-$	(Schlick et al., 2011)
BL2wtBAC2	Suspension	Burkitt Lymphoma/EBV$^+$	(Schlick et al., 2011)
BL31wtBAC2.2	Suspension	Burkitt Lymphoma/EBV$^+$	(Schlick et al., 2011)
MutuI	Suspension	Burkitt Lymphoma/EBV$^+$	(Gregory et al., 1990)
MutuIII	Suspension	Burkitt Lymphoma/EBV$^+$	(Gregory et al., 1990)
Rev-AK	Suspension	Burkitt Lymphoma/EBV$^+$	(Ramasubramanyan et al., 2015)
Zta-AK	Suspension	Burkitt Lymphoma/EBV$^+$	(Ramasubramanyan et al., 2015)
AGS	Adherent	Stomach/Gastric Adenocarcinoma	ATCC, Manassas, VA, USA
AGSA1	Adherent	Stomach/Gastric Adenocarcinoma	Dr Manal Moalwi (Unpublished)
AGSA2	Adherent	Stomach/Gastric Adenocarcinoma	Dr Manal Moalwi (Unpublished)
AGSEBVAK1	Adherent	Stomach/Gastric Adenocarcinoma	Dr Manal Moalwi (Unpublished)
AGSEBVAK2	Adherent	Stomach/Gastric Adenocarcinoma	Dr Manal Moalwi (Unpublished)
HEK293 B95.8 EBV	Adherent	Kidney/Normal EBV$^+$	(R Feederle et al., 2009)
HEK293 B95.8 EBV ΔBGLF5	Adherent	Kidney/Normal EBV$^+$	(R Feederle et al., 2009)

2.2 Cell Culture

2.2.1 Culturing

HeLa, MDA-MB-231, MCF7, HEK293, and MRC-5 cells (kindly donated by Prof Simon Morley) cultured in Dulbecco modified eagle medium (DMEM) (PAN Biotech; P04-04510) supplemented with 10% foetal bovine serum (FBS) (PAN Biotech; P40-47500), 1X Penicillin-Streptomycin-Glutamine (PSG) (Gibco; 10378016) and passaged 1:5/10 three times a week, or when 70-80% confluent.

BL2 and BL31 cell lines used as EBV negative, along with corresponding cell lines transfected with EBV Bacmid 2 expressing complete EBV genome, used as EBV positive (BL31wtBAC2, BL31wtBAC2) (kindly donated by Prof Michelle West (Schlick et al., 2011)). BL2 and BL31 cultured in RPMI 1640 without Glutamine (Gibco; 31870074) containing 20% FBS, 1X PSG, 0.5 mM Thioglycerol (Sigma; M6145), 10 mM Na Pyruvate (Sigma; P5280). BL2wtBAC2.2 and BL31wtBAC2 were cultured in the media with the same composition as BL2 and BL31 with the addition of 100 µg/ml Hygromycin (Gibco; 10453982) as a selection marker. All BL cell lines were passaged 1:3 three times a week, or when 70-80% confluent.

MutuI and MutuIII cell lines are BL cell lines containing mutated EBV viruses that remain in latency I and latency III respectively (kindly donated by Prof Michelle West (Gregory et al., 1990)). Cells were cultured in RPMI 1640 without Glutamine containing 20% FBS, 1X PSG, 0.5 mM Thioglycerol, 10 mM Na Pyruvate. Cells were passaged 1:3 three times a week, or when 70-80% confluent.

Rev-AK/Zta-AK cell lines (kindly donated by Prof. Alison Sinclair (Ramasubramanyan et al., 2015)) cultured in RPMI 1640 without Glutamine containing 10% FBS, 1X PSG, 0.5 mM Thioglycerol, 10 mM Na Pyruvate. Passaged 1:3 three times a week, or when 70-80% confluent.

AGS cells were kindly donated by Manal Moalwi and Prof. Alison Sinclair, along with AGS cells mock-infected (AGSA1/AGSA2) and AGS infected with EBV (AGSEBVAK1/AGSEBVAK2) (unpublished). All AGS cells were cultured in DMEM/F-12, HEPES (Gibco; 11330057) supplemented with 10% FBS, 1X PSG and passaged 1:5 three times a week, or when 70-80% confluent. Media for transfected cells was supplemented with 400 µg/ml G418 (Gibco; 10131027) as a selection marker.

HEK293 expressing wild-type B95.8 EBV (p2089) and HEK293 expressing BGLF5 knockout EBV were kindly donated by Prof. Henri-Jaques Delecluse (DKFZ, Heidelberg) (R Feederle et al., 2009). Cells were cultured in RPMI 1640 without Glutamine containing 10% FBS, 1X PSG, supplemented with 100 µg/ml Hygromycin as a selection marker. Passaged 1:5 three times a week, or when 70-80% confluent.

All cells were grown at 37ºC in a humidified atmosphere with 5% CO_2.

2.2.2 Cell Passaging

At 70-80% confluency, cells were passaged. The correct volume of suspension cells was transferred to a fresh flask and topped up to the appropriate volume with fresh media. Adherent cells were washed with Phosphate Buffered Saline (PBS) (Sigma; D8537) before detachment using TrypLE (Gibco; 10718463). Cells were then transferred to a fresh flask, along with new media.

2.2.3 Cell Storage

Cells were pelleted and resuspended in FBS containing 10% dimethyl sulfoxide (DMSO) (Sigma; D8418) and transferred to cryogenic tubes (Fisher; 11385644). Cells were gently frozen at -1°C/minute in a Mr Frosty™ Freezing Container (Fisher; 5100-0001) overnight at -20°C. Cells were transferred to liquid nitrogen for long-term storage.

2.2.4 Lytic Induction

2.2.4.1 Zta-AK/Rev-AK

Lytic cycle was induced in Zta-Ak using doxycycline hydrochloride (Sigma; D3072). Cells were grown to 70-90% confluency before splitting 1:2 24 hours before treatment. 1 µg/ml doxycycline was added to cells and incubated at 37^{o}C 5% CO_2 for 24 hours. Following induction, BD Accuri™ C6 Plus Flow Cytometer (BD Biosciences) was used to measure the percentage of cells expressing GFP.

2.2.4.2 AGS

AGS cells infected with EBV were induced into lytic cycle using phorbol 12-myristate 13-acetate (PMA/TPA). Cells were seeded at 1-2x10^5 cells/ml and seeded onto appropriately sized plates and allowed to attach overnight. Cells were treated with 50 ng/ml PMA and incubated for 24 hours.

2.2.4.3 B95.8 EBV/BGLF5 KO

HEK293 expressing wild-type B95.8 EBV (p2089) and HEK293 expressing BGLF5 knockout EBV were induced into lytic cycle using PMA (50 ng/ml, 24 hours) or transfected with the BZLF1 expression vector.

2.2.5 Cell Synchronisation

Suspension cells were grown to 70-90 % confluency in a large flask and passaged 1:1 to a total volume of 300 ml. The cells were incubated overnight at 37 ^{o}C 5% CO_2 before 9 µM RO-3306 (Merck; SML0569) was added and incubated for a further 20 hours. Cells were spun down and pelted gently before being washed three times in PBS and resuspended into 4 x 100 ml media.

1 hour following release from the cell cycle arrest, the first extraction was performed. 5 ml was removed from each flask and pelleted down. Three pellets were immediately

flash-frozen in liquid nitrogen and the fourth was resuspended in 3 ml of ice-cold 70% EtOH in PBS and stored at 4 ^{o}C for FACS analysis.

Extractions were performed at numerous time points across 48 hours.

FACS samples suspended were washed twice in PBS before resuspending in 500 µl PBS (containing 0.1 mg/ml RNase A and 0.03 mg/ml propidium iodide solution) and incubating at RT for 30 min. Samples were analysed on BD Accuri using appropriate filter sets.

2.3 Chemical Induction Of Stress

2.3.1 Arsenite

Adherent cells were cultured to 70-80% confluency in a 5 cm petri dish or 6-well plate before the media was removed, and 2 ml of fresh media was added. Cells treated with 2 µl of 0.5 M sodium arsenite (Sigma; S7400) (final conc. 0.5 mM) and incubated at 37^{o}C 5% CO_2 for 45 minutes. Suspension cells were grown to 70-80% confluency, and 5 ml of cells were transferred to falcon tubes before adding 5 µl of 0.5 M sodium arsenite (final conc. 0.5 mM) and incubated at 37^{o}C 5% CO_2 for 45 minutes.

2.3.2 Hippuristanol

Adherent cells were cultured to 70-80% confluency in a 5 cm petri dish or 6-well plate, media removed, and 2 ml of fresh media added. Cells were treated with 2 µl of 1 mM hippuristanol (kindly donated by Prof Simon Morley) (final conc. 1 µM) and incubated at 37^{o}C 5% CO_2 for 45 minutes. Suspension cells were grown to 70-80% confluency, and 5 ml of cells were transferred to falcon tubes before adding 5 µl of 1 mM Hippuristanol (final conc. 1 µM) and incubated at 37^{o}C 5% CO_2 for 45 minutes.

2.4 Cell Harvesting

Adherent cells had media removed and were scraped in 200 µl cold PBS before transferring to Eppendorf tubes or were detached in a suitable volume of TrypLE (Fisher; 12604013) before the enzyme was deactivated in media containing serum, and gently centrifuged (<400 g) to pellet cells.

Suspension cells were transferred directly to Eppendorf tubes along with media. Samples were centrifuged at 400 g, 5^{o}C for 10 minutes.

Both adherent and suspension cell pellets were transferred to Eppendorf tubes in PBS and re-pelleted at 13,000 g for 30-60 seconds before being flash-frozen in liquid nitrogen and stored at – 80^{o}C.

2.5 Western Blot (WB)

2.5.1 Whole Cell Lysate

A cell pellet was thawed on ice and 100 µl of 1x Gel Sample Buffer/10^6 cells (Laemmli buffer; 50 mM Tris pH6.8, 4% SDS, 10% β-Mercaptoethanol, 0.01% Bromophenol blue, 10% Glycerol, 1 mM EDTA) added, and gently mixed. Samples were kept on ice and sonicated at 25%, 5x 10 seconds with 10 seconds intervals on Vibra-Cell™ sonicator (Sonics). Following sonication, samples were centrifuged at full speed for 10 seconds and heated on a heat block at 95°C for 10 minutes. Samples were vortex briefly before centrifuging again at full speed for 10 seconds and stored at -20°C.

2.5.2 Protein Quantification

Protein concentration was determined by either Bradford assay (Bio-Rad; 5000006) or Qubit assay (Fisher; 10543343) according to manufacturers' instructions.

2.5.3 SDS-PAGE

Tris-glycine SDS-polyacrylamide resolving gel was prepared using 5-15% acrylamide, followed by 5% acylamide used for the stacking gel.

Samples (Cell lysate: 10 µg – 30 µg; Whole cell lysate: 5 - 30 µl) were added to 15 µl of gel sample buffer and resolved on an SDS-PAGE gel in 1 x SDS running buffer (25 mM Tris, 192 mM glycine, 0.1% SDS, pH 8.3).

SDS-PAGE was run at 150 V for 50 – 90 minutes depending on the size of the protein and the percentage of the gel, in a Bio-Rad Mini-PROTEAN Tetra Electrophoresis System.

2.5.4 Semi-Dry Transfer

Filter paper and 0.2 µm pore size nitrocellulose membrane were soaked in semi-dry buffer (25 mM Tris, 192 mM glycine, pH 8.3, 0.375% SDS, 20% EtOH) for 5 minutes before transfer to equilibrate the membrane. The membrane was placed on top of filter paper, followed by the gel and covered with further filter paper before loading into a Trans-Blot Turbo Transfer System (Bio-Rad; 1704150). The gel was transferred to the membrane at 25 V for 30 minutes.

2.5.5 Wet Transfer

Filter paper and 0.2 µm pore size nitrocellulose membrane were soaked in wet-blot buffer (25 mM Tris, 192 mM glycine, pH 8.3, 20% Methanol) for 5 minutes before transfer to equilibrate the membrane. The membrane was placed on top of filter paper, followed by the gel and covered with further filter paper before being loaded into a Bio-Rad Mini Trans-Blot cell. This cell was run on the Bio-Rad Mini-PROTEAN Tetra Electrophoresis System with wet-blot buffer for 16 hours at 20 V and 4^{o}C.

2.5.6 Ponceau Stain

Following the transfer, the membrane was stained using Ponceau stain (Sigma; P7170) for 1 minute at RT whilst rocking. The membrane was then washed three times in distilled water and the protein visualised, and the cut if required.

2.5.7 Primary Antibody Incubation

Membrane was blocked for >30 minutes in blocking buffer (TBS-tween [20 mM Tris, 150 mM NaCl, 0.1% Tween 20], 3% BSA), rocking at RT.

Primary antibodies were added to 5 ml blocking buffer at the manufacturer's recommended dilution and incubated with the membrane in heat-sealed bags overnight at 4^{o}C whilst rocking.

Antibodies in blocking buffer were used up to five times and stored at -20^{o}C.

2.5.8 Secondary Antibody Incubation

Membranes were removed from primary incubation and washed three times for 5 minutes in TBS-tween. Membranes were incubated with secondary antibodies at the manufacturer's recommended dilution in 5 ml of blocking buffer, for 1 hour at RT whilst rocking.

Following incubation, membranes were washed three times for 5 minutes in TBS-tween.

2.5.9 Detection

2.5.9.1 Chemiluminescence

Pierce ECL Western Blotting Substrate (Fisher; 32106) was used according to the manufacturer’s protocol to detect secondary antibodies associated with horseradish peroxidase (HRP). Li-Cor Odyssey Fc was used to detect chemiluminescence.

2.5.9.2 NearIR

Following secondary incubation and washing, membranes were imaged on the Li-Cor Odyssey Fc, detecting wavelengths of 700 and 800.

2.5.10 Image Analysis

Li-Cor Image Studio™ Lite was used for all analysis of western blot images.

2.6 RNA Extraction

Cell pellet ($5x10^6$ cells) was defrosted on ice and then lysed using 1 ml Tri reagent (Sigma; T9424) and vortexed until the pellet was dissolved (1-4 minutes). 200 µl Chloroform was added, and samples were vortexed for 4 minutes to mix. Samples were then centrifuged at 13,000 rpm for 15 minutes at 4°C. Three separate phases formed, with the upper aqueous layer containing RNA. This layer was transferred to a fresh Eppendorf tube containing an equal volume of 70% ethanol and added directly to an RNeasy kit (QIAGEN; 74104) column, following the manufacturer's protocol.

2.7 cDNA Synthesis

Using Applied Biosystems™ High-Capacity RNA-to-cDNA™ Kit (Applied BioSystems; 10704217), cDNA was synthesised from 0.5 – 1 µg RNA extracted from cell pellet, as per manufacturers protocol.

2.8 Real-Time Polymerase Chain Reaction (qPCR)

Primer stocks were diluted into working stock using 7.5 µl of 100 mM Primer in 492.5 µl water (1.5 mM final conc.). A 96-well plate was set up containing 7.5 µl Go-Taq SYBR (Promega; A6001), 1.5 µl Forward primer, 1.5 µl Reverse Primer and 1.5 µl Nuclease-free water. Standard curve samples were created using an initial 1:10 dilution of cDNA followed by five further serial dilutions at 1:4. Samples were diluted 1:10 – 1:20

depending on RNA concentration before cDNA synthesis. 3 µl of cDNA sample or standard curve sample was added to each well.

qPCR was run on an Applied Biosystems StepOnePlus™ RT PCR System and analysed using the Applied Biosystems One-Step programme.

2.9 Transfection

2.9.1 Electroporation

Thermo Scientific NEON transfection console set up as per manufacturer's instructions. Suspension cells were counted to determine volume for $5x10^6$ cells. 10 ml of antibiotic-free media was aliquoted into small tissue culture flasks before a working stock of DNA/siRNA was created at the appropriate concentration. Volume for $5x10^6$ cells was transferred to a centrifuge tube and repeated for each condition and repeat before centrifuging at 400 g for 5 - 10 minutes to pellet the cells. Pellet was washed in 5 ml of PBS and pelleted again. The supernatant was removed and the pellet was resuspended in 110µl buffer T ($5x10^6$ cells/110µl Buffer T). The appropriate concentration of DNA/siRNA was added to each sample and gently mixed. The sample was electroporated according to cell type using a 100 µl Neon tip:

Cell Type	Pulse Voltage (v)	Pulse width (ms)	Pulse Quantity
BL	1300	30	1
HEK293	1100	20	2
MCF7	1100	30	2
MM231	1100	30	2

Transfected samples were transferred to a flask containing 10 ml of antibiotic media and incubated for 24 - 48 hours.

2.9.2 Chemical Transfection

Transfection reagents were determined by the cell type and transfection task, they included Lipofectamine RNAiMAX (Fisher; 13778), Lipofectamine 2000 (Fisher; 11668), Lipofectamine 3000 (Fisher; L3000) and HiPerfect (QIAGEN; 30170).

2.9.2.1 Transfection

Cells were seeded in a 6-well plate one day before transfection, at an appropriate density to provide 80 - 90% confluency the next day.

Immediately before transfection, media in each well was replaced with fresh media and transfection was performed according to the manufacturer's protocol. Cells were incubated for 24-72 hours.

2.9.2.2 Reverse Transfection

Manufacturers' protocols were followed relating to transfection reagents. Cells were detached and seeded into a 6-well plate at a seeding density of 0.1-1x10^6 cells/well. Transfection reagents along with DNA/RNA were then added directly to the detached cells and gently mixed. Cells were incubated for 24-72 hours.

2.10 Immunofluorescence (IF)

2.10.1 Adherent Cells

Cells were seeded at a cell density of 1x10^5 cells/ml and grown in 6-well plates containing coverslips (sterilized in 100% ethanol) overnight. Cells were fixed in 4% formaldehyde in PBS for 10 minutes before being gently washed in PBS and then permeabilized in 0.5% Triton X-100 for 10 minutes.

Coverslips were blocked for 30 minutes in TBS-tween containing 1% BSA before being incubated with primary antibodies diluted to the manufacturer’s recommendations in TBS-tween (1% BSA) for 1 hour. Coverslips were washed in TBS-tween and incubated

with secondary antibodies conjugated to Alexa Flour dyes, also diluted to the manufacturer's recommended dilution in the TBS-tween (1% BSA), for 1 hour. Coverslips were washed in TBS-tween before being mounted onto microscope slides using Duolink Mounting Medium with DAPI (Duolink; 82040-0005) and sealed using clear nail varnish. Slides were stored at 4 ^{o}C in the dark.

Cells were imaged with Zeiss LSM880 fluorescence confocal microscope.

2.10.2 Suspension Cells

Cells were grown to 70 - 80% confluency, before 15 ml of cells, in media, were transferred to a falcon tube and centrifuged at 400 g for 5 minutes. The supernatant was aspirated off and cells were resuspended in 2 ml 4% formaldehyde in PBS for 10 minutes. Cells were centrifuged, the formaldehyde removed, and cells washed in PBS before further centrifugation. PBS was removed and 2 ml of 0.5% Triton X-100 was added for 10 minutes. Centrifugation, aspiration, and PBS wash steps were repeated. Cells were resuspended in PBS to a cell density of $1x10^6$ before 50 µl of cell/PBS mixture was dropped onto an ethanol-sterilized coverslip and spread evenly with the tip of the pipette. Coverslips were air-dried in a tissue culture hood.

Coverslips were blocked for 30 minutes in TBS-tween containing 1% BSA before being incubated with primary antibodies diluted to the manufacturer’s recommendations in TBS-tween (1% BSA) for 1 hour. Coverslips were washed in TBS-tween and incubated with secondary antibodies conjugated to Alexa Flour dyes, also diluted to the manufacturer's recommended dilution in the TBS-tween (1% BSA), for 1 hour. Coverslips were washed in TBS-tween before being mounted onto microscope slides using Duolink Mounting Medium with DAPI (Duolink; 82040-0005) and sealed using clear nail varnish. Slides were stored at 4 ^{o}C in the dark

Cells were imaged with Zeiss LSM880 fluorescence confocal microscope.

2.11 Fluorescence In Situ Hybridization (FISH)

MCF-7 and MDA-MB-231 cells were seeded onto 13 mm glass coverslips at a density of 1-2x10^5 cells and adhered overnight. Thirty-three tiled oligonucleotides were designed across the length of two lncRNAs, SCIRT and MALAT1 with Stellaris RNA FISH probe designer (LGC Biosearch Technologies). Probes for cytoplasmic control GAPDH were commercially available from Stellaris (SMF-2026-1). Cells were fixed in 4% formaldehyde in PBS for 10 min at room temperature and then permeabilized in 0.5% Triton-X in PBS for 10 minutes at room temperature. The coverslips were then washed with pre-hybridization buffer (2x SSC, 10% Formamide) for 1 minute and incubated in a humidified chamber with 125 nM probes with Quasar 670 dye targeting SCIRT and probes with Quasar 570 dye targeting GAPDH RNA/MALAT1 in hybridization buffer (2x SSC, 10% Formamide, 10% Dextran Sulfate, 0.2 mg/ml BSA, 1 mg/ml Yeast tRNA, 2 mM VRC) in the dark at 37^{o}C for 4 hours. The coverslips were then incubated in the pre-hybridization buffer for 15 minutes at 37^{o}C twice, then washed in 2x SSC three times, before being mounted on a microscope slide with Duolink Mounting Medium with DAPI (Duolink; 82040-0005) and sealed with clear nail varnish.

Cells were imaged with Zeiss LSM880 fluorescence confocal microscope.

2.12 IF and FISH

Protocols for IF and FISH were combined. Following IF, an additional fixation step was used to ensure the protein was fixed before processing slides for FISH.

2.13 Automated Cell and Granule Counting

IF images were loaded into Cell Profiler (www.cellprofiler.org) and a custom pipeline was used to count cells and granules. Using single Z-stack images for each channel, the pipeline first smooths the channel associated with the DNA (DAPI) to remove any artefacts or intensity differences shown in each nucleus. The program performs this

smoothing using a Gaussian filter, that convolves the image with a normal distribution that's full length at half maximum is the size of the expected artefacts (Carpenter et al., 2006). The pipeline then identifies nuclei within this image that meet the size and threshold parameters, determined from the average size of typical nuclei within this cell type, and the intensity of the background and object signals. A similar process is performed with the images that show the G3BP1 signal. The input image is smoothed to ensure the signal covers the whole cytoplasm, and cells are identified where the smoothed G3BP1 signal propagates from the nucleus. The cytoplasm is determined by subtracting the nucleus image from the cells and expanding by 2 pixels to ensure that any objects on the edge of the cytoplasm are included in future calculations. To determine TIA-1^{+} SGs, the raw TIA-1 image is smoothed reasonably harshly to remove all speckles. This smoothened image is then subtracted from the raw image to correct for differences in background signal intensity. Cell profiler then enhances the speckles found in this image, by calculating objects of the appropriate SG size, and the difference in signal intensity relative to background pixels neighbouring the object. TIA-1 granules are identified by the pipeline when found to meet size parameters, calculated by measuring numerous SGs from early experiments, followed by pixel intensity thresholds that calculate the difference in signal between objects and neighbouring background and identify only those that fall within the parameters that have been determined to only include SGs. SGs are identified by relating the expanded cytoplasm with TIA-1 granules and quantified.

2.14 mRNA Stability

Cells were grown to 80 – 90 % confluency before passaging 3:1 the day before treatment. On the day of treatment, 5 µg/ml ActinomycinD (Sigma; A9415) was added to each sample, and gently mixed. 10 ml of cells were extracted and pelleted before the supernatant was removed, and the cells flash-frozen in liquid nitrogen. The treated cells

were transferred back to the incubator, and extractions were performed at regular intervals for 24 hours.

Following the final extraction, RNA was extracted from each cell pellet, and cDNA was synthesised before running on a qPCR as previously described.

2.15 Protein Stability

Cells were grown to 80 – 90 % confluency before passaging 3:1. The following day, 33 µg/ml Cycloheximide (Sigma; 01810) was added to each sample, and gently mixed. 10 ml of cells were extracted and pelleted before the supernatant was removed, and the cells flash-frozen in liquid nitrogen. The treated cells were transferred back to the incubator, and extractions were performed at regular intervals for 24 hours.

The protein was extracted from each cell pellet and run on a WB as previously described.

2.16 Competent Cells

DH5α cells (gifted by Dr Stephen Hare), were streaked onto Luria-Bertani (LB) agar plates and grown overnight at 37 ^{o}C. A single colony of DH5α was picked and transferred to 25 ml of Super Optimal Broth (SOB) media in a 250 ml flask and incubated for 6 – 8 hours at 37°C with vigorous shaking. Following incubation three 250 ml flasks, each containing 20 ml of SOB media, were inoculated using 1 ml, 400 µl and 200 µl of the starter culture respectively. Each flask was incubated at 18 ^{o}C for 14 hours with moderate shaking. The OD_{600} was read for each culture regularly until one reached 0.55, after which, the other cultures were discarded, and the correct density culture was placed into an ice bath for 10 minutes. The cells were harvested by centrifugation at 2,000 g for 10 minutes at 4 ^{o}C, and the supernatant was removed. The cells were resuspended in 6 ml ice-cold Inoue transformation buffer (55 mM MnCl2, 15 mM CaCl2, 250 mM KCl, 10 mM PIPES pH 6.7) and incubated on ice for 10 minutes. The cells were pelleted at 2,000 g for 10 minutes at 4 ^{o}C and the supernatant was removed and resuspended in 2 ml of ice-

cold Inoue transformation buffer. 140 µl of DMSO (7%) was added to the solution, gently mixed, and placed on ice for 10 minutes. The chemically competent DH5α cells were frozen in 50 µl aliquots in liquid nitrogen and stored at – 80°C.

2.17 Transformation

50 µl aliquots of chemically competent cells were thawed on ice, and 1 – 5 µl of DNA was added directly to cells and gently mixed. Cells were then spread onto LB agar plates containing the appropriate selection and grown overnight at 37 ^{o}C.

2.18 Sequencing

All sequencing was performed using Eurofins (eurofinsgenomics.eu) Sanger sequencing and analysed using Benchling (benchling.com).

2.19 CRISPR/Cas9 Knockout

2.19.1 gRNA

gRNA was designed using Genome browser (USCC), based on their on-target and off-target scores provided by Genome browser.

2.19.2 Cloning

gRNA oligo pairs were ordered from Merck. Each primer pair included the gRNA sequence, along with the reverse complement partner with the following overhang added to the appropriate oligo:

Forward: 5’ CACCG---------- 3’
Reverse: 5’ AAAC----------C 3’

1 µl of each oligo (100 µM) was phosphorylated and annealed in a 10 µl reaction mixture containing 1 µl 10x T4 DNA Ligase Buffer (NEB; B0202S), 0.5 µl T4 polynucleotide

kinase (NEB, M0201S) and 6.5 µl H_2O. The reaction was incubated at 37ºC for 30 mins, followed by 95ºC for 5 mins before decreasing 5ºC/min to 25ºC.

The annealed oligo pairs were cloned into two plasmids, pSpCas9(BB)-2A-Puro (PX459) V2.0 plasmid (Addgene; 62988) and pSpCas9(BB)-2A-GFP (PX458) (Addgene; 48138), through a single step digestion-ligation method. This involved a 10 µl reaction containing 100 ng PX458/PX459 plasmid, 2 µl annealed oligo pair (diluted 1:250), 1x Tango buffer (Thermo Fisher, BY5), 1 mM dithiothreitol (DTT), 1 mM adenosine triphosphate (ATP), 0.5 µl T7 DNA ligase (NEB, M0318S) and 1 µl FastDigest BbsI (Thermo Fisher, FD1014). The reaction mixture was incubated at 37ºC for 5 mins and 23ºC for 5 min, repeating for 6 cycles.

Each construct was transformed into chemically competent DH5α cells using a simplified transformation. 1 – 5 µl of the construct was added directly to 50 µl of thawed competent DH5α cells and mixed gently. The cells were spread onto LB agar plates with the appropriate selection (100 µg/ml Ampicillin) and incubated at 37ºC overnight. Following incubation, several single colonies were picked and grown in 5 µl LB broth containing 100 µg/ml Ampicillin overnight at 37ºC. Extraction of the plasmids from DH5α was performed using a QIAprep Spin Miniprep Kit (QIAGEN; 27104) as per the manufacturer's protocol. Confirmation that the construct contained the correct insertion sequence was obtained through sequencing each plasmid with the U6 primer (5'-GCCTATTTCCCATGATTCCTTC-3') (Eurofins). Each construct was stored at -20ºC.

2.19.3 Transfection

Transfection into MCF7 cells was performed using Lipofectamine 3000 with optimal conditions determined previously by the Castellano Lab. 2.5 µg construct DNA was transfected into MCF7 cells using 5 µl Lipofectamine 3000 as per the manufacturer's protocol. Briefly, cells were seeded into a 6-well plate to be 70 – 90 % confluent at the

point of transfection, the transfection reagents were incubated together for 20 minutes before adding to the cells and incubating at 37ºC 5% CO_2 for 48 hours.

Transfection into HEK293 cells was performed using the NEON Transfection System as previously described. 0.5 - 3 µg plasmid DNA was electroporated into the cells and grown for 48 hours.

2.19.4 Isolation And Expansion of Single Cell Clones

Cells that were transfected with a plasmid that contained a puromycin resistance gene were selected using this marker. Optimal selection conditions were determined using a toxicity kill curve, in which MCF7 cells were seeded into a 96-well plate and varying concentrations of puromycin (0 – 2 µg/ml) were added to the cells. Selection was determined as the lowest concentration that killed most (>90 %) of the cells over 72 hours, 0.5 µg/ml. 24 hours following transfection, cells were then treated with 0.5 µg/ml puromycin for 48 hours, after which the cells were detached and seeded into two 96-well plates at a density of 0.3 cells/well to obtain single colonies. Cells were grown for 2-4 weeks until colonies were visible.

Cells that were transfected with a plasmid contained a GFP marker that allowed for selection to be performed by Fluorescence-activated cell sorting (FACS). Following transfection, cells were grown for 48 hours before detaching and preparing for cell sorting. Cells were resuspended at 10^6 - 10^7 cells/ml in PBS containing 1% serum, and 5 mM EDTA and passed through a 30 µm cell strainer (Corning; 352235) to prevent clumping and obtain single cells. Cells were sorted on a BD FACS melody (BD Biosciences) by side scatter and forward scatter to remove dead cells and doublets, followed by GFP providing only transfected cells. Single GFP-positive cells were seeded individually into the wells of a 96-well plate containing 100 µl appropriate media and grown for 2-4 weeks until observable colonies.

Once individual colonies reached confluence within the 96-well plate, the cells were transferred to a 25 cm^2 flask and grown to confluence. Half the cells were pelleted for DNA extraction, whilst the other half were transferred to liquid nitrogen for storage.

2.20 gDNA Extraction

Cell pellets were thawed on ice, before adding 100 µl/5x10^5 cells of extraction buffer (10mM Tris pH 8.2, 1mM EDTA, 25mM NaCl, 1 mg/ml Proteinase K) and homogenised through vortexing. Homogenised cells were incubated at 37^{o}C for 30 minutes, before 5 minutes at 95^{o}C. Cells were centrifuged at 13,000 g for 10 minutes and the pellet was discarded.

2.21 Polymerase Chain Reaction (PCR)

PCR was performed using Phusion™ High-Fidelity DNA Polymerase (Thermo Scientific; F530S). 50–250 ng of template DNA per 50 µl reaction was used, along with 5X Phusion HF, 200 µM dNTPs, 0.5 µM forward primer, 0.5 µM reverse primer, 3 % DMSO, and 1-unit Phusion DNA polymerase.

The annealing temperature was determined using www.thermofisher.com/tmcalculator, and optimal durations and cycles were dependent on the template DNA. The reaction mixture was run on a thermocycler:

Cycle Step	Temperature	Time	Cycles
Initial Denaturation	98 ^{o}C	30 s	1
Denaturation	98 ^{o}C	5 – 10 s	25 - 35
Annealing	X ^{o}C	10 – 30 s	
Extension	72 ^{o}C	15 – 30 s/kb	
Final extension	72 ^{o}C	5 – 10 mins	1
	4 ^{o}C	Hold	

PCR amplification was followed by QIAquick PCR Purification (QIAGEN; 28104) of the PCR products following the manufacturer's protocol.

2.22 DNA Gel

0.8 – 2 % agarose was dissolved into 1x TAE buffer (40 mM Tris, 20 mM acetic acid, and 1 mM EDTA) and heated in the microwave until completely dissolved. 3 µl/100 µl SYBR™ Safe DNA Gel Stain (Thermo Fisher; S33102) was added once the buffer had cooled to ~50ºC, before pouring into the DNA gel cassette, and adding a comb. Once completely set, the gel was placed in a DNA running tank containing 1x TAE buffer that covered the gel. 5 µl of DNA was mixed with 1 µl 6X DNA Gel Loading Dye (Thermo Fisher; R0611) and loaded onto the gel, along with a 1kb DNA ladder (Invitrogen; 10787018). The gel was run at 150 V for 1 – 4 hours depending on the size of the DNA, and the percentage of the gel. Following completion of the separation, the gel was imaged on the Li-Cor Odyssey Fc at a wavelength of 600 nm for 2 minutes. The image was processed in Image Studio Lite.

2.23 Mutagenesis

pFRT_TO_eGFP_TIA1 was a gift from Thomas Tuschl (Addgene; 106094) and renamed pFRT_TO_eGFP_TIA1b.

TIA-1a isoform was created using primers containing the desired mutation were designed using NEBasechanger.neb.com and ordered from Merck:

Name	Sequence	Annealing Temp
TIA-1 EX5 NEB Insert Forward	ccaacaaagacatggaaatgattatcttgtgaacgctgtgtgctgacaac ggtactactgcttgtatctttcttttgactgc	56ºC
TIA-1 EX5 NEB Insert Reverse	gcagtcaaaagaaagatacaagcagtagtaccgttgtcagcacacagc gttcacaagataatcatttccatgtctttgttgg	56ºC

Mutagenesis was performed using Q5® Site-Directed Mutagenesis Kit (NEB; E0554). A reaction mixture was set up using 1X Q5 Hot Start High-Fidelity Master Mix, 0.5 µM

Forward Primer, 0.5 µM Reverse Primer, 25 ng template DNA. The reaction was cycled through the following conditions:

Cycle Step	Temperature	Time	Cycles
Initial Denaturation	98 °C	30 s	1
Denaturation	98 °C	10 s	25
Annealing	56 °C	30 s	
Extension	68 °C	30 s/kb	
Final extension	68 °C	2 mins	1
	4 °C	Hold	

1 µl of the PCR product was added to 1X KLD reaction buffer and 1X KLD reaction mix and incubated at RT for 5 mins. 5 µl of the KLD treated mixture was transformed into 50 µl competent DH5α as previously described and grown overnight at 37 °C on an LB agar plate with the appropriate selection. Several colonies were picked and grown overnight at 37 °C in LB broth, also containing selection. Plasmids were extracted using a QIAprep Spin Miniprep Kit (QIAGEN; 27104) as per the manufacturer's protocol.

The mutated construct and original template construct were sent for sequencing (Eurofins) to confirm the presence of the insertion. Plasmids were stored at -20 °C.

2.24 NGFR Isolation

Rev-AK and Zta-AK cells expressing the expression vector were isolated using MACSelect NGFR MicroBeads (Miltenyi; 130-091-330). First, cells were induced by doxycycline, as previous described, before pelleting and resuspending in 320 µl of MAC separation buffer (PBS, 0.5% BSA) per $4x10^7$ cells. 80 µl of MACSelect NGFR MicroBeads were added to this volume and incubated on ice for 15 minutes. MS MACS Column was placed into the magnetic field of the separator and rinses with 500 µl MAC separation buffer. The cell suspension was placed on the column and the unlabelled cells were collected as uninduced (negative beads). The column was washed four times with 500 µl MAC separation buffer before the column was removed from the separator,

and induced cells flushed through with 1 ml of MAC separation buffer (positive beads). Samples were stored at -20 ^{o}C.

2.25 Nucleolar Purification

Cells were harvested as previously described, before being washed three times in ice-cold PBS. Cell resuspended in 5 ml/5x10^6 cells of buffer A (10 mM Hepes, pH 7.9, 10 mM KCl, 1.5 mM $MgCl_2$, 0.5 mM DTT) and incubated on ice for 5 minutes. Cells were homogenised in a 7 ml Dounce homogeniser 10 – 30 times until 90% of cells burst. Cellular material was pelleted at 218 g for 5 minutes at 4^{o}C, and the supernatant was stored at -80^{o}C as the cytoplasmic fraction. Pellet resuspended in 3 ml of S1 solution (0.25 M Sucrose, 10 mM $MgCl_2$) and layered over 3 ml of S2 solution (0.35 M Sucrose, 0.5 mM $MgCl_2$). The mixture was centrifuged at 1430 g for 5 minutes at 4^{o}C, before resuspending the pellet in 3 ml of S2. Sample sonicated at 40% for six 10-second bursts, with a 10-second interval. Sample layered over 3 ml of S3 solution (0.88 M Sucrose, 0.5 mM $MgCl_2$) and centrifuged at 3000 g for 10 minutes at 4^{o}C. The supernatant was retained as a nucleoplasmic fraction and stored at -80^{o}C. The pellet containing nucleoli was resuspended in 0.5 ml S2 and centrifuged at 1430 g for 5 minutes at 4^{o}C. The pellet containing purified nucleoli was resuspended in 0.5 ml S2 and stored at -80^{o}C.

2.26 RNA Poll Inhibition and Nucleolar Disruption

Cells were grown onto slides as previously described. BMH-21 (Sigma; SML1183) (1 µM final concentration) was added to the cells and incubated for 3 hours at 37^{o}C 5% CO_2. Following incubation, cells were washed with PBS, before fixing and permeabilising as previously described.

2.27 Statistical Analysis

All statistical analysis was performed using GraphPad Prism 9. Multiple comparisons were made using a two-way analysis of variance (ANOVA).

3 Integrated stress response during latent EBV infection

3.1 Introduction

The integrated stress response (ISR) is a key host antiviral mechanism, in which the phosphorylation of eIF2 is central. eIF2 is a critical element in the regulation of translation and is tightly controlled.

In translation, following recognition of the start codon by the 43S pre-initiation complex (40S ribosomal subunit bound by eIF1, eIF1A, eIF3 and eIF5, along with an eIF2-GTP-Met-tRNAi ternary complex), a conformational change occurs reducing the affinity of eIF2-GDP to Met-tRNAi causing the release of eIF2-GDP, phosphate, and eIF5 (Algire et al., 2005). To continue further rounds of translation initiation, eIF2-GDP must be reactivated by its guanidine nucleotide exchanged factor (GEF), eIF2B, that associates with eIF2 and aids the exchange of GDP with GTP. Under stress conditions, the α subunit of eIF2 is phosphorylated causing eIF2 to have a greater affinity to eIF2B, preventing its dissociation, whilst acting as an inhibitor of GEF function (Hinnebusch & Lorsch, 2012). This acts as a vital regulatory mechanism, as this inhibition prevents eIF2 from associating with the initiation complex, stalling translation.

eIF2 is comprised of three subunits, α, β and γ, sized at 36 kDa, 38 kDa and 52 kDa respectively (Ernst et al., 1987), each of which is highly conserved across species, emphasising the importance of eIF2 in translational regulation (Erickson et al., 1997).

The α subunit is well known for being the regulatory component of eIF2, in which phosphorylation on serine 51 promotes eIF2-eIF2B inhibitory binding, along with an S1 binding domain that is speculated to be a site of RNA binding (Gribskov, 1992). Originally discovered in yeast, it was found that phosphorylation of eIF2α at serine 51 formed a complex with eIF2B, in which two eIF2 molecules bind on either side of eIF2B. This binding was enhanced through direct interactions of the phosphate groups of eIF2α and

eIF2B, whilst creating conformational changes promoting tighter interactions between eIF2α α-helix and eIF2B (Gordiyenko et al., 2019).

eIF2β contains several phosphorylation sites, relating to phosphorylation by casein-kinase-2, protein kinase C and cAMP-dependent protein kinase (Welsh et al., 1994). Along with the binding site for eIF5 (Sizova et al., 1998), and guanidine nucleotide-binding domains with unknown functions (Naranda et al., 1995). eIF2β also contains the binding site for eIF2B (Kimball et al., 1998).

Finally, eIF2γ contains guanine nucleotide-binding domains, which, when mutated dramatically reduce GDP binding, suggesting that eIF2γ is the location for GDP binding within eIF2 (Naranda et al., 1995).

Interestingly, it is currently unknown where the binding of Met-tRNAi takes place, however, cross-linking of Met-tRNAi to eIF2β labels four peptides within the protein (Gaspar et al., 1994). This group also found that eIF2γ may be involved in Met-tRNAi binding through the same technique. Furthermore, another group found a Met-tRNAi binding site through analysis of the crystal structure (Roll-Mecak et al., 2004).

In this chapter, we focus on the phosphorylation of eIF2α and how EBV may affect or manipulate this pathway. Four main kinases are responsible for phosphorylating eIF2α in mammals, PKR, PERK, GCN2 and HRI, and it is here, along with directly influencing eIF2α, where several viruses manipulate SG assembly (Y. Liu et al., 2020). eIF2α phosphorylation is likely to impede viral invasion, through the global shut-down of protein synthesis, and with that, viral replication, however, sustained eIF2α phosphorylation, would eventually lead to apoptosis of the cell. Therefore, any invading virus must moderate this response to survive.

Hepatitis C virus (HCV) has been shown to interfere with the activation of PERK and has developed the means to inhibit this response, dampening both the UPR and ISR through

multiple mechanisms (Asselah et al., 2010; Egan et al., 2013; Pavio et al., 2003; Tardif et al., 2004). Other viruses have been shown to manipulate the ER stress pathway, including the bovine viral diarrhoea virus (Jordan et al., 2002) and the Japanese encephalitis virus (Su et al., 2002). PERK activation appears to be common during viral infection, and could be caused by a variety of reasons, such as viral protein production, ER remodelling and direct activation of kinases, however, many viruses have mechanisms to evade the stress responses associated with this activation (Lewy et al., 2020).

It has been shown that members of the ɣ-herpesvirus family, including EBV and KSHV, manipulate the UPR to promote lytic gene expression (Bhende et al., 2007; Matar et al., 2014; Wilson et al., 2007; Yu et al., 2007). In EBV, specifically, XBP1 was shown to activate transcription of two EBV immediate-early gene promotors and XBP1 RNAi inhibited lytic EBV gene expression (Bhende et al., 2007).

PKR is activated by dsRNA, commonly produced during viral infection (Son et al., 2015; Weber et al., 2006). PKR expression is induced through the interferon system, a large family of cytokines that are released in response to several viral infections (reviewed in Jaramillo et al., 1995). The PKR promoter contains an IFN-stimulated response element (ISRE) that is induced in response to type I IFN (Kuhen & Samuel, 1997).

HSV-1 has been shown to readily produce dsRNA during infection (Jacquemont & Roizman, 1975; Kozak & Roizman, 1975), however, HSV-1 produces the viral protein, U_S11, that interacts with, and is phosphorylated by, PKR blocking its activation of eIF2α (Cassady et al., 1998; Lussignol et al., 2013). U_S11 was shown to bind specifically to dsRNA, thought to play an important role in inhibiting PKR activity (Khoo et al., 2002). Multiple other mechanisms that block, modify or hijack PKR activation have been exhibited by several other DNA viruses (reviewed in Cesaro & Michiels, 2021) (Figure 3-1).

It has also been demonstrated that certain viruses may affect eIF2α phosphorylation through alternative methods other than the commonly associated kinases. One such example is infected cell protein 34.5 (ICP34.5), that when expressed, forms a complex with PP1c and dephosphorylates eIF2α in HSV-1 and HSV-2 infection (Cassady et al., 1998; Y. Li et al., 2011). This process emulates the mechanism of GADD34; however, the virus introduces a viral protein to manipulate this process preventing translational stalling and SG assembly.

The eIF2α phosphorylation pathway is a key process that viruses must overcome to successfully infect a host cell. In conclusion, several eIF2αKs will likely be activated during viral infection, and without manipulation, translation will stall, and stress granules will form. However, as discussed, many viruses evade this anti-viral process, and as seen in HSV-1 and HSV-2 the human herpesviruses are no different.

This chapter focuses on latent EBV infection and eIF2α pathways and aims to determine whether the latent virus can activate this process, and in doing so, does a viral mechanism exist that allows EBV to evade any translational stalling and SG formation that consequently occurs? Several studies have investigated lytic infection regarding eIF2α phosphorylation, eIF2αK and human herpesviruses, however, in terms of EBV, it is especially important to understand how the persistent latent infection remains undetected by these antiviral pathways. It is thought that around 90% of the global adult population carries asymptomatic EBV, which occurs through establishing latency in memory B-lymphocyte (Babcock et al., 1998; Khan et al., 1996). Furthermore, EBV-associated malignancies were responsible for 1.8% of all cancer deaths in 2010 (Khan & Hashim, 2014), with nearly all EBV-linked cancers attributed to latency (Hamilton-Dutoit et al., 1993; Herbst et al., 1991; Niedobitek et al., 1995; Rowe et al., 1987; Sbih-Lammali et al., 1996).

EBV and the effects of eIF2α phosphorylation, along with its kinases, have scarcely been investigated. It has been speculated that the EBERs, viral small non-coding RNA produced during latent infection, may bind and regulate PKR, and has been shown *in vitro*, however, this remains controversial as it is yet to be shown *in vivo* (Clarke et al., 1991; Sharp et al., 1993). EBERs contain a significant secondary structure, including stable stem loops (Glickman et al., 1988), which in theory, would provide a perfect opportunity for the virus to associate with PKR. It was shown, however, that neither EBV infection, nor EBERs alone prevented PKR phosphorylation *in vivo*, and eIF2α phosphorylation was not prevented in EBV infected cells, compared to uninfected cells, following interferon treatment (Ruf et al., 2005). Localisation data revealed that the EBERs were localised within the nucleus of infected cells (Howe & Steitz, 1986), however, it has since been shown that they are present in the cytoplasm during interphase, suggesting a translation role (Schwemmle et al., 1992).

The lack of evidence of interactions between PKR and EBERs *in vivo*, suggests that the EBERs are not responsible for viral evasion of the eIF2α phosphorylation pathway. Furthermore, in an *in vivo* mouse model, deletion of both EBERs did not affect viral infection and persistence compared to wild-type (Gregorovic et al., 2015), suggesting that protein synthesis was not inhibited.

ER stress is a common occurrence during viral infection, as many viruses express viral glycoproteins within the ER, with the potential to induce the UPR (reviewed in Banerjee & Mukhopadhyay, 2016). Therefore, it is an interesting subject in the determination of how EBV may induce or evade the stress response. Thapsigargin-induced ER stress was shown to promote lytic replication within LCLs, emphasising that ER stress is an important trigger for viral replication (Taylor et al., 2011). However, importantly this study indicates that eIF2α, although phosphorylated as a response to Thapsigargin, is not linked to this induction of lytic replication.

LMP1, is a latent EBV viral protein, essential for B-cell transformation, through mimicking CD40 signalling that activates growth and survival pathways (Kaye et al., 1993; L. W. Wang et al., 2017). It has also been associated with eIF2α phosphorylation via the activation of PERK (Lam et al., 2004). It was shown, that high levels of LMP1 in EBV^-, and EBV^+ BL cells resulted in eIF2α phosphorylation (Lam et al., 2004). Furthermore, it was shown that in BL cells, intermediate levels of LMP1 drove proliferation, whereas high levels inhibited protein synthesis via activation of PERK resulting in activation of both ISR and UPR (Dong et al., 2008). Interestingly, a recent study found that LMP1 inhibited PERK activation, through direct binding and inhibition, downregulating UPR-associated genes in nasopharyngeal carcinoma patients, and promoting tumour progression (He et al., 2021). The later study speculated that the discrepancy with previous reports may be due to differing latency between the two types of cancer. BL commonly contains EBV expressing latency I and III, whereas nasopharyngeal carcinoma usually carries EBV in latency II. It was suggested that as EBNA2 is expressed during latency III, but not during latency II, EBNA2 could promote c-myc transactivation leading to greater activation of UPR (Kaiser et al., 1999). Another suggestion was B-cell prolificacy in expressing IgG at high levels inducing the UPR (Gass et al., 2002). A great deal more research is required to understand LMP1 and its effect on eIF2α and the stress pathways.

EBNA3C, a latent viral nuclear protein, has been shown to interact with GADD34 (Garrido et al., 2009). It was shown to prevent GADD34 recruitment of PP1a, inhibiting eIF2α dephosphorylation. While eIF2α phosphorylation was increased, the associated downstream UPR events were not activated. It is suggested that EBNA3C protects against the UPR, whilst appearing to neglect the increase in eIF2α. Could this be down to EBV having additional mechanisms that protect against eIF2α-induced translational stalling and stress granule formation, or is the virus able to manipulate this situation also?

Although latent EBV infection promotes a much more restricted level of viral gene expression than lytic, there is still a huge potential for viral products to interact, modify and hijack the eIF2α pathway. As referenced in this chapter, several latent proteins have been shown to interact with stages of the ISR, however, it remains inconclusive as to whether these latent products are capable of activating this process when expressed during infection.

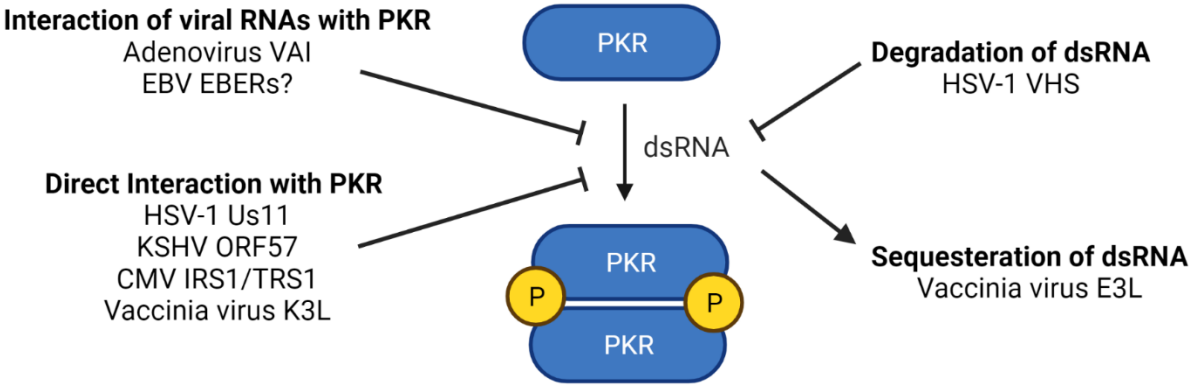

Figure 3-1 Inhibition of PKR activation by DNA viruses. Several mechanisms exist in DNA viruses to prevent PKR activation. Adenovirus small RNA VAI interacts with PKR, blocking its ability to bind dsRNA and activate. The same process has been proposed for EBV EBERs. Other viral components bind directly to PKR preventing its activation. dsRNA is also targeted by DNA viruses. HSV-1 viral protein VHS promotes degradation of dsRNA, while vaccinia virus product E3L sequesters dsRNA away from PKR preventing activation. (Adapted from Cesaro & Michiels, 2021)

3.2 Results

3.2.1 Characterisation of latency in EBV$^+$ cell lines

The BL2/BL2wtBAC2 and BL31/BL31wtBAC2.2 systems (kindly gifted by Prof. Michelle West (Schlick et al., 2011)) provided an appropriate means to compare differences between latent EBV infected cells and uninfected. BL2 and BL31 are EBV$^-$ Burkitt lymphoma cell lines, derived from two separate patient samples, while their EBV$^+$ counterparts (BL2wtBAC2 and BL31wtBAC2.2, respectively) were created through infection with wild-type recombinant EBV bacterial artificial chromosome (BAC/bacmid) (Calender et al., 1987).

It had previously been shown that the BL2 and BL31 cells infected with the EBV bacmid, expressed the full complement of latent proteins, suggesting that these cells were in latency III (Anderton et al., 2008). To investigate whether BL31wtBAC2.2 (BL31wtBAC) and BL2wtBAC2 (BL2wtBAC) remained in latency III, western blotting (WB) was used, probing for EBNA2 (Figure 3-2). EBNA2 is exclusively expressed during latency III, whilst absent during latency I and II. MutuI and MutuIII systems (kindly gifted by Prof. Michelle West (Gregory et al., 1990)) are EBV$^+$ cells that contain a mutated virus unable to leave latency I or latency III, respectively, and in this experiment are used as a negative and positive control for the detection of EBNA2. Lanes showing BL2, BL31 and MutuI protein expression show a complete absence of EBNA2, reinforcing the lack of EBV in BL2 and BL31, whilst showing EBNA2 is not expressed during latency I. In contrast, lanes containing BL2wtBAC, BL2wtBAC and MutuIII, revealed the detection of EBNA2 confirming the presence of latency III EBV in each of these samples.

Furthermore, confirmation that both EBV$^+$ BL2 and BL31 cell lines contained non-lytic EBV, was shown through WB probing for viral lytic protein ZTA (Figure 3-3). Zta protein was absent in all BL2 and BL31 samples, regardless of infection, whilst present in positive control cell line Zta-AK. Zta-AK is a lytic inducible cell line, that is described in

greater detail in a later chapter. However, it contains an inducible expression plasmid containing Zta, that was induced before this experiment.

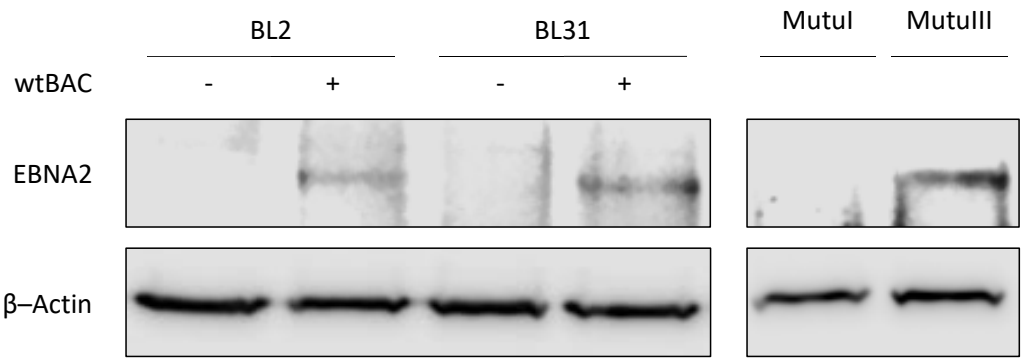

Figure 3-2 BL2 and BL31 cells with EBV bacmid are in latency III. Protein was extracted from BL2, BL31 along with their EBV+ counterparts expressing the wild-type recombinant bacmid, as well as latency I, MutuI, and latency III, MutuIII cell lines. Protein was resolved on 10% SDS-PAGE and western blotted probed with antibodies against latency III protein, EBNA2, and loading control, β-actin.

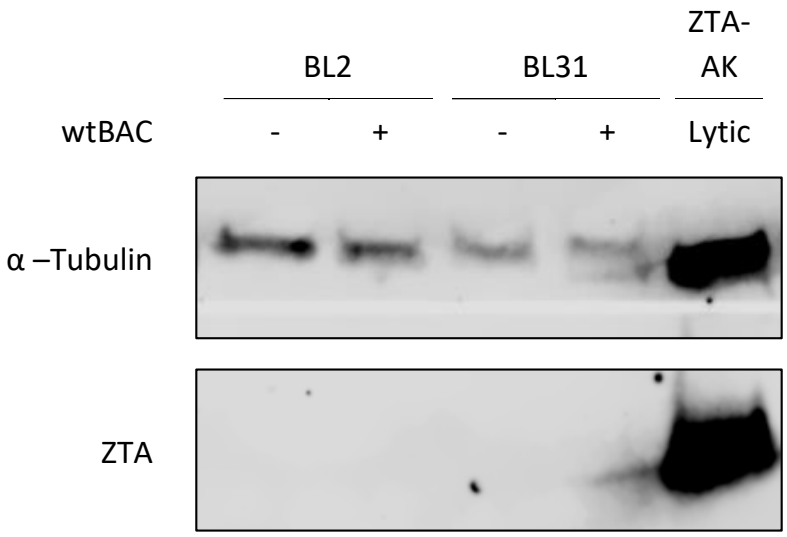

Figure 3-3 BL2 and BL31 cells with EBV bacmid are not in lytic phase. Protein was extracted from BL2, BL31 along with their EBV+ counterparts expressing the wild-type recombinant bacmid, as well as lytic sample, ZTA-AK. I, MutuI, and latency III, MutuIII cell lines. Protein was resolved on 10% SDS-PAGE and western blotted probed with antibodies against latency III protein, EBNA2, and loading control, β-actin.

3.2.2 eIF2α and eIF2αK activation during latent EBV infection

The eIF2αKs, PKR and PERK, are commonly associated with the phosphorylation of eIF2α during viral infection, linked to dsRNA detection and ER stress, respectively. A significant link between HRI activation and viral infection in mammals, has yet to be found, while GCN2 activation, suppression and modification have been shown in only a handful of mammalian viral infections, although this data is increasing (reviewed in Y. Liu et al., 2020). Therefore, it was decided that this study would focus on the most likely kinases to be activated during EBV infection, PKR and PERK.

Using BL2, BL31 and EBV^+ counterparts, PERK and PKR activation was assessed through the detection of their phosphorylated forms. WB probing for total and phosphorylated levels of PERK, PKR and eIF2α (Figure 3-4) revealed no significant difference in activation between EBV^- and EBV^+ samples in both BL2 and BL31 cell lines (Figure 3-5).

Whilst both EBV-infected cell lines show an increase of at least 1.5-fold of phosphorylated PERK compared to uninfected cell lines, with BL31 expressing a nearly 2-fold increase, this is not significant. This suggests that PERK is not activated by latent EBV infection, either through ER stress or latent product expression, such as LMP1.

PKR activation also is not induced by EBV infection. Interestingly, total PKR levels are significantly increased in both EBV^+ cell lines, however, phosphorylated PKR remained low (Figure 3-4). The ratio of phosphorylated PKR to total shows a potential trend of decreasing in both infected cell lines, when compared to uninfected counterparts, however, not significant. Therefore, whilst latent EBV infection appears to activate the innate immune response and stimulate the expression of PKR, no latent product activates this eIF2αK.

Finally, eIF2α phosphorylation was also shown to be unaffected by exposure to the latent virus. No significant difference is seen between both EBV+ and EBV+ cell lines (Figure 3-5). ATF4 protein expression, commonly induced in response to eIF2α phosphorylation, also shows no significant difference between infected and uninfected cell lines (Figure 3-5C), consistent with our finding that eIF2α phosphorylation is not induced following latent EBV infection.

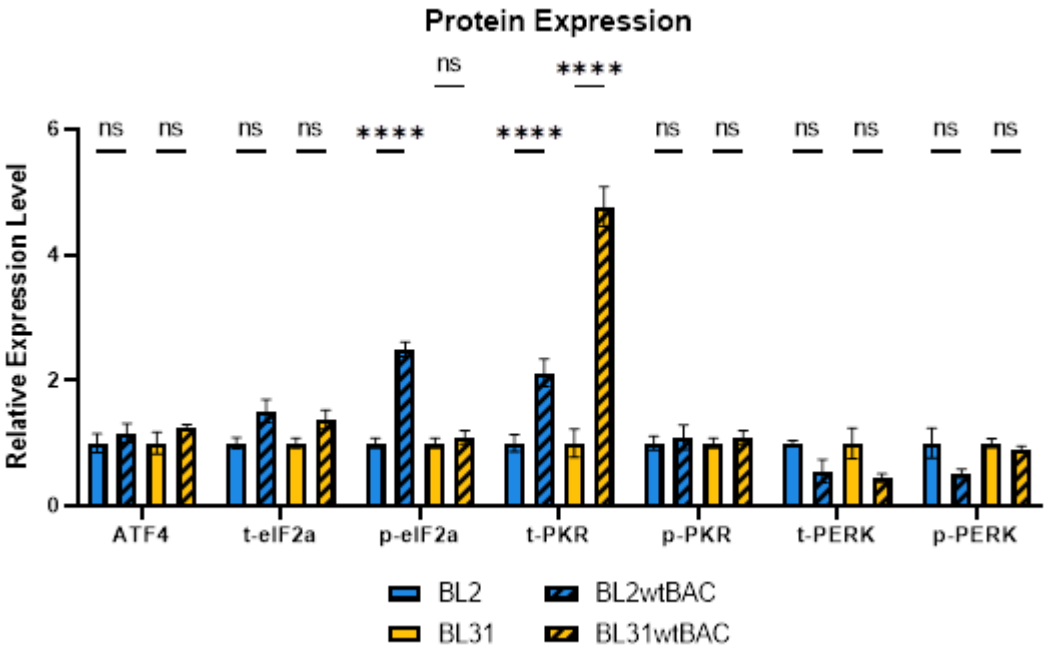

Figure 3-4 ISR-associated protein expression levels during latent EBV infection. Protein levels detected from Figure 3-5A, normalised against α-tubulin, and set relative to the uninfected sample. Error bars represent s.e.m. n=3 (Two-way ANOVA, ns = P > 0.05, * = P ≤ 0.05, ** = P ≤ 0.01, *** = P ≤ 0.001, **** = P ≤ 0.0001).

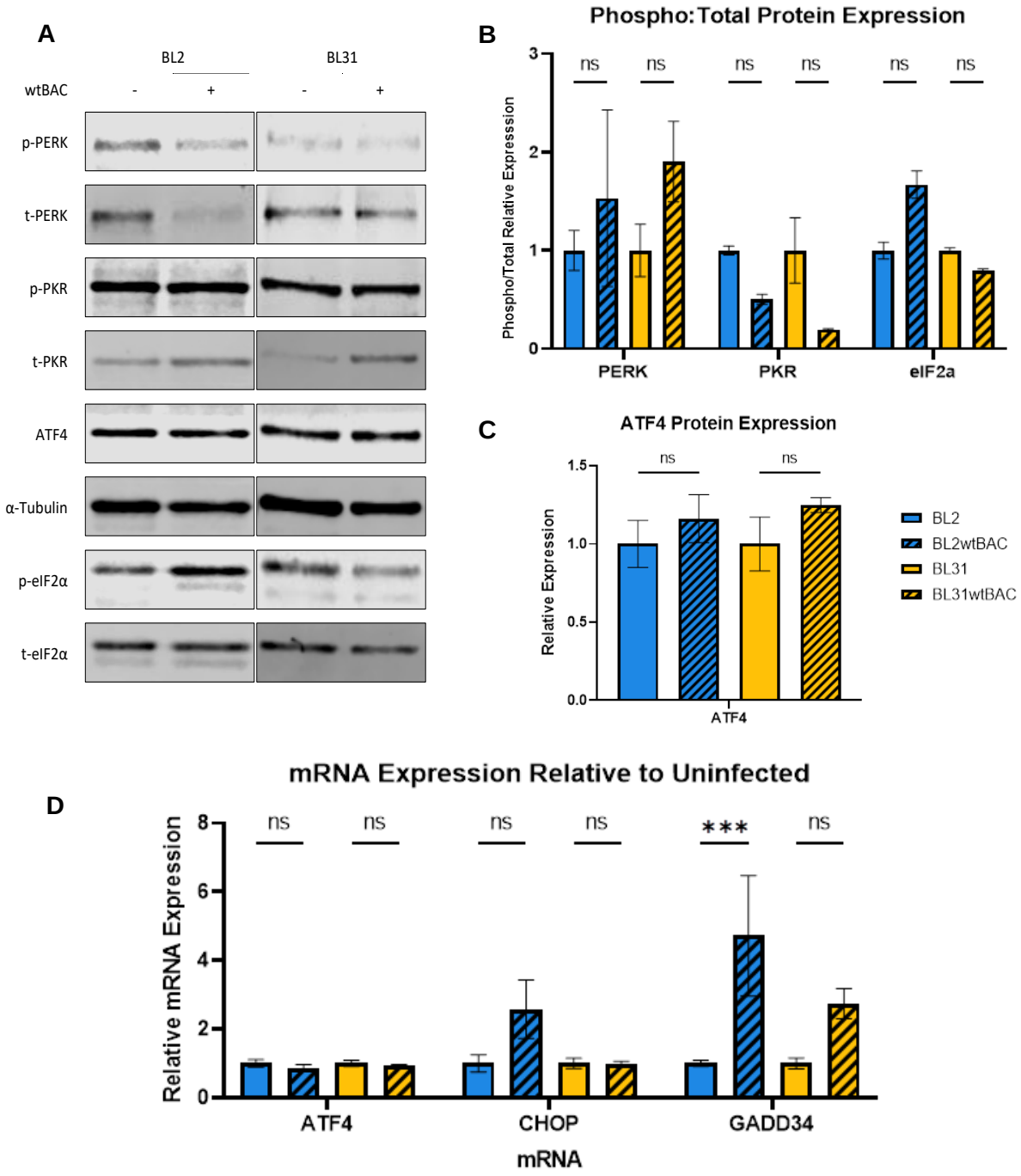

Figure 3-5 eIF2αK activation, eIF2α phosphorylation and downstream signalling during latent EBV infection. **(A)** Western blot analysis of BL2, BL31 and latent EBV positive counterparts, BL2wtBAC2 and BL31wtBAC2.2, respectively. Protein was extracted from each sample and resolved on 10% SDS-PAGE and immunoblotted with antibodies probing by phosphorylated and total levels of PERK, PKR and eIF2α, along with ATF4 and loading control α-tubulin. **(B)** Quantification of WB (A) showing ratio of phosphorylated protein levels against total and relative to uninfected sample to give fold change. **(C)** Quantification of ATF4 protein expression (A) relative to uninfected protein levels. **(D)** qPCR data showing relative mRNA expression between three eIF2α downstream transcripts, ATF4, CHOP and GADD34, normalised against GAPDH. mRNA expression levels for each gene are relative to the uninfected sample. Error bars represent s.e.m. n=3 (Two-way ANOVA, ns = $P > 0.05$, * = $P \leq 0.05$, ** = $P \leq 0.01$, *** = $P \leq 0.001$, **** = $P \leq 0.0001$).

3.2.3 ATF4, CHOP and GADD34

Several mRNAs that are induced downstream of eIF2α phosphorylation were investigated in latent EBV-infected cells. Following eIF2α phosphorylation, global protein synthesis is generally inhibited, however, translation of several mRNAs containing uORFs in their 5' UTR, is increased through multiple mechanisms (Wek, 2018).

Many of these preferentially translated proteins have central roles in the stress response, such as GADD34, ATF4, and CHOP, which can be used as readouts for activation of the ISR, and eIF2α phosphorylation. Their roles in stress are diverse. ATF4 is a transcription factor promoting the expression of genes involved in the ISR including GADD34 and CHOP (Figure 1-4). GADD34 is a scaffolding protein that promotes dephosphorylation of eIF2α by targeting the PP1 phosphatase to phosphorylated eIF2α, whereas CHOP is a pro-apoptotic transcription factor regulated by ATF6, another ER stress-induced transcription factor.

qPCR amplifying regions within ATF4, CHOP and GADD34 mRNA revealed that ATF4 mRNA levels did not differ between latent EBV infected cells and their uninfected counterparts, confirming, as expected, that the latent virus does not affect the expression of the ATF4 gene (Figure 3-5D).

GADD34 mRNA expression revealed an increase in both EBV-infected cell lines compared to uninfected cells. GADD34 showed a ~2.5-fold increase in EBV^+ BL31 relative to uninfected cells, albeit not significant, whilst EBV^+ BL2 showed a significant ~4.5-fold increase in GADD34 mRNA compared to uninfected cells. Whilst the data representing BL31 does not show a significant difference between EBV^+ and EBV^- samples, it does suggest a trend that is reinforced by BL2.

CHOP mRNA expression was 2-fold greater in BL2 EBV^+ cells compared to EBV^- BL2, however not significantly, whilst EBV^+ BL31 cells, show a similar level of CHOP mRNA

expression as EBV^- BL31. Whilst no significant difference is observed in mRNA levels of CHOP, the data presented for BL2 show a potential trend that aligns with the significant increase of GADD34 mRNA expression in EBV^+ samples. Speculatively, the increased levels of CHOP mRNA expression in EBV^+ BL2 may be driving GADD34 expression further, as along with ATF4, CHOP is also thought to induce GADD34 expression (Brush et al., 2003; Kojima et al., 2003; Novoa et al., 2001, 2003).

3.2.4 Induction of eIF2α phosphorylation during latent EBV infection

Finally, this study aimed to investigate the eIF2α pathways in latently infected cells following induced stress by arsenite and to determine whether the latent infection altered this response. Arsenite has regularly been used to induce cellular stress and stress granule formation and is an effective inducer of eIF2α phosphorylation through activating several eIF2αKs (Zhou et al., 2008). To test whether latent EBV infection manipulated the eIF2α pathway, cells were either treated with 0.5 mM sodium arsenite (As, NaAs, arsenite), or an equal volume of nuclease-free water (untreated control).

It was shown that increased eIF2α phosphorylation was observed in all arsenite-treated cells, compared to untreated cells (Figure 3-6A). Quantification and normalisation against total levels of eIF2α within each cell exhibited an increase of between 5- and 10-fold compared to untreated samples (data not shown).

Interestingly, phosphorylation of eIF2α in response to arsenite stress did differ between cell lines, in which a significant difference is observed between EBV^- and EBV^+ BL31 arsenite treated samples. Our data suggests that EBV-infected cells displayed increased levels of eIF2α phosphorylation. However, both EBV^- and EBV^+ BL2 arsenite treated cells exhibited a similar level of eIF2α phosphorylation, with a decrease in phosphorylation in EBV^+ cells. Taken together, it is likely that these trends are due to cell line variability, rather than an effect of the virus, as both, an increase and decrease of eIF2α phosphorylation are seen in EBV^+ BL31 and BL2 respectively when compared to EBV^- cells. Therefore, we can suggest that latent EBV does not affect arenite-induced eIF2α phosphorylation.

PKR phosphorylation, on the other hand, shows, when normalised against total PKR levels, no response to arsenite-induced stress. This suggests that PKR is unaffected by this chemical (Figure 3-6C). A slight increase in PKR phosphorylation is observed following arsenite treatment in BL2, although this is not emulated in BL31, and along with

a broad standard error of the mean, suggests that this response is not caused by arsenite exposure. All other cell lines, infected and uninfected, show a similar phosphorylation level of PKR in untreated and arsenite-treated cells. PERK was also shown to exhibit a similar level of phosphorylation in response to arsenite stress in both EBV-infected and uninfected BL2 cells (Figure 3-7), suggesting that this eIF2αK is also unaffected by arsenite treatment.

Interestingly, although eIF2α is phosphorylated in response to arsenite stress, this does not correlate to ATF4 protein expression (Figure 3-6B). Arsenite stress appears to dampen ATF4 protein expression in all cell lines, contradictory to the current understanding of the eIF2α pathway, and the literature. However, this decrease is not significant and only ranges between 0.4- and 0.2-fold lower than the untreated control. It is likely that the decrease/lack of response to increased eIF2α phosphorylation, is down to a staggered activation of ATF4. As protein was extracted immediately following stress treatment, ATF4 protein is unlikely able to be induced at a rate that would be noticed in this experiment.

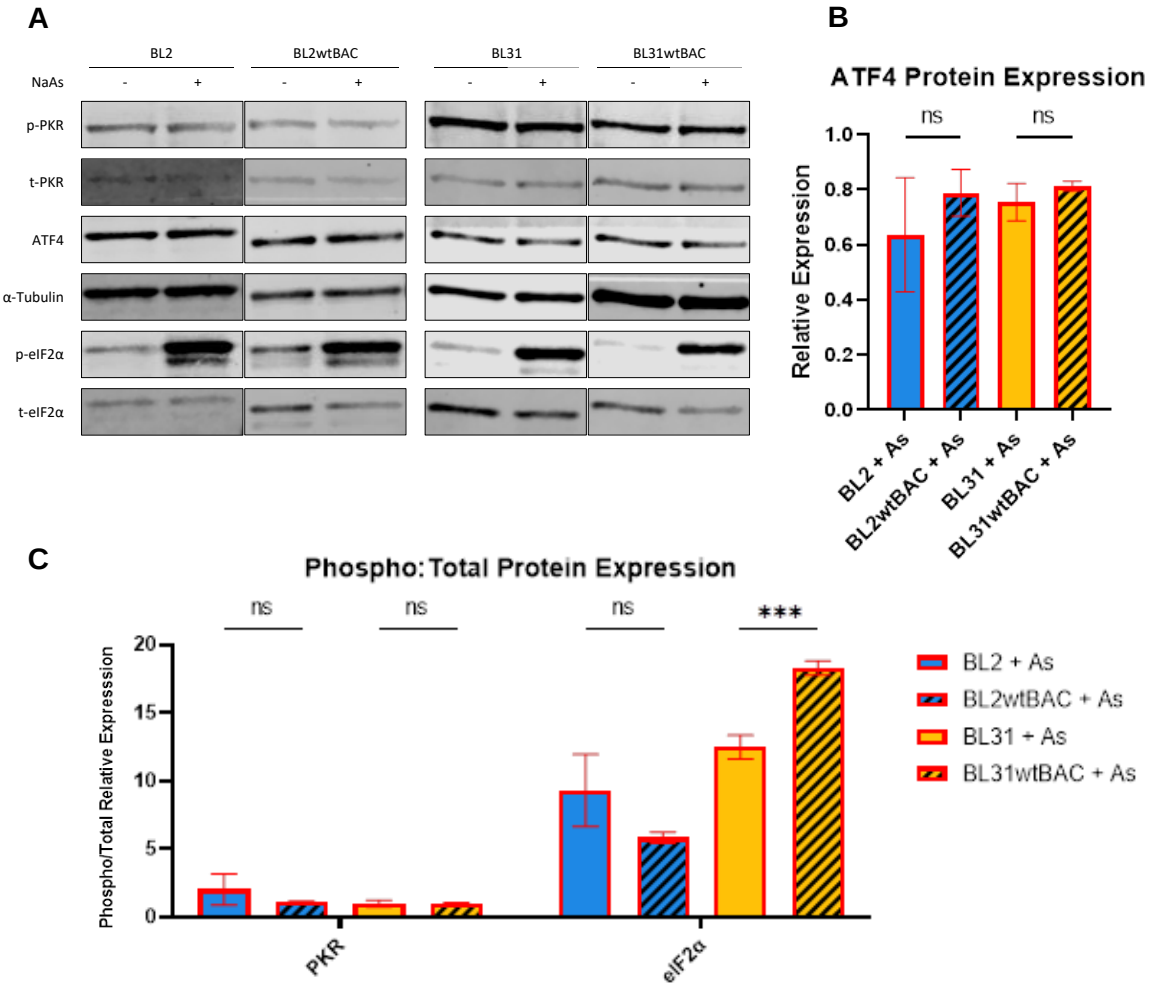

Figure 3-6 Arsenite treatment induces eIF2α phosphorylation during latent EBV infection. (A) WB analysis of EBV negative (BL2, BL31) and EBV positive samples (BL2wtBAC2, BL31wtBAC2.2) following 45-minute 0.5 mM sodium arsenite (As) exposure or untreated control. Protein was extracted from each sample and resolved on 10% SDS-PAGE, before immunoblotting with antibodies for phosphorylated and total eIF2α PKR and α-tubulin as loading control. **(B)** Quantification of ATF4 protein levels shown on WB (A), normalised to α-tubulin, and set relative to untreated control **(C)** Quantification of WB (A) showing ratio of phosphorylated protein levels normalised against total and relative to untreated control for each cell lines. Error bars represent s.e.m. n=3 (Two-way ANOVA, ns = P > 0.05, * = P ≤ 0.05, ** = P ≤ 0.01, *** = P ≤ 0.001, **** = P ≤ 0.0001).

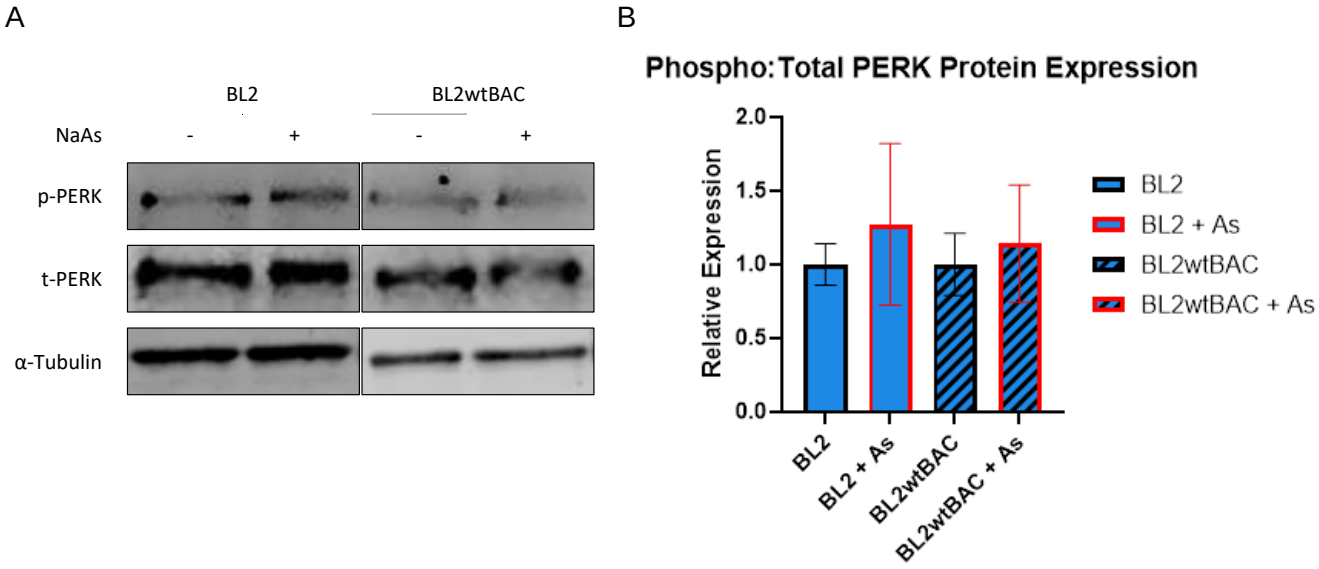

Figure 3-7 PERK expression following arsenite stress in EBV$^{+/-}$ BL2. (A) WB analysis of EBV negative and EBV positive BL2 cells following 45-minute 0.5 mM sodium arsenite (NaAs) exposure or untreated control. Protein was extracted from each sample and resolved on 10 % SDS-PAGE, before immunoblotting with antibodies for phosphorylated and total PERK and α-tubulin as loading control. **(B)** Ratio of phosphorylated protein levels against total and relative to uninfected sample to give fold change. Error bars represent s.e.m. n=3 (Two-way ANOVA, ns = P > 0.05, * = P ≤ 0.05, ** = P ≤ 0.01, *** = P ≤ 0.001, **** = P ≤ 0.0001).

3.3 Discussion

The EBV bacmid infection system (Calender et al., 1987) provides a convenient *in vitro* method to understand how EBV infection affects the cell. The two cell lines used in this study (BL2 and BL31) provided cell variability as although both are Burkitt lymphoma cell lines, they are derived from two distinct patient samples. The EBV^+ samples of BL2 and BL31, that carry the EBV bacmid, have been described elsewhere (Anderton et al., 2008; Kelly et al., 2005). This study aimed to adopt this model to understand whether latent EBV infection affected the ISR within the host cell. Therefore, it was initially important to confirm that both EBV^+ cell lines, were in latency and that this latency was expressing the full complement of viral latent products (latency III). EBNA2 is exclusively expressed during latency III and it was shown to be present in both EBV^+ BL cell lines (Figure 3-2). EBNA2 was also detected in MutuIII, an EBV^+ cell line expressing latency III products, but absent from MutuI, the latency I counterpart. It was also found that EBV^+ cell lines did not express detectable levels of the early lytic gene, Zta (Figure 3-3), confirming that these cells had not entered lytic cycle. The presence of several other latent proteins had previously been confirmed in both EBV^+ BL31 and BL2 cells (Anderton et al., 2008). Taken together, it can be concluded that the EBV^+ cells used (BL2wtBAC and BL31wtBAC), contain EBV in latency III and express the full complement of latent products. This allows for any host response to these viral latent products to be investigated.

Latency provides the virus with a means to remain within host cells, whilst only expressing a limited number of viral gene products, whether these products activate the host immune response remained to be determined. We found that two eIF2αKs, PKR and PERK, were unaffected in response to latent EBV infection. Whilst a trend of increased PERK activation was observed in EBV^+ cells, this was not significant suggesting that the virus does not induce ER stress and activate PERK. PKR activation was also not observed in EBV-infected cells (Figure 3-5).

PKR is commonly activated in virus-infected cells, as this kinase can bind to dsRNA, a frequent product of most viruses (Dauber & Wolff, 2009; Weber et al., 2006). Furthermore, PKR expression is known to be induced following stimulation of the innate immune response by viruses (Kuhen & Samuel, 1999). We show that expression of PKR protein levels increased in latently infected cell lines (Figure 3-4), compared to uninfected, suggesting that the latent virus does activate the innate immune response, and therefore ISGs such as PKR. However, the increase in PKR protein does not correlate to a similar increase in phosphorylated PKR. Phosphorylated PKR remains similar in all cell lines, EBV^- and EBV^+ (Figure 3-4). When normalised against this increased PKR expression, the EBV^+ cell lines exhibit a trend of decreased PKR phosphorylation, albeit not significant (Figure 3-5). This trend provides an intriguing insight as to how the latent virus may evade detection through PKR. We speculate that latent EBV evades PKR activation through the lack of expressing a latent product capable of activating this kinase.

It has previously been determined that PKR can bind to dsRNA of lengths between 30 and 80 bps (Manche et al., 1992; Minks et al., 1979), however, more recent studies have found PKR capable of binding 19 – 21 bp siRNA/dsRNA also (Puthenveetil et al., 2006; Sledz et al., 2003). Several dsRNA products produced during latent protein production may be capable of binding to the PKR dsRNA binding domain. However, it remains unclear as to whether they interact with PKR, or even are expressed to suitable levels to elicit a response. Our data suggest that they do not activate PKR, but an inhibitory mechanism cannot be ruled out.

Other latent HHVs have been found to interfere with the ISR through PKR. KSHV expresses latent protein, vIRF-2, that inhibits PKR through direct interaction (Burýšek & Pitha, 2001). Another KSHV latent protein, LANA, was shown to inhibit responses downstream of PKR activation (Esteban et al., 2003). The presence of a mechanism to evade PKR activation would suggest that dsRNA is produced during latent KSHV

infection. Therefore, it would not be implausible to speculate that this may also occur during latent EBV infection. The results shown in this chapter suggest that latent EBV evades PKR activation, either directly or through its restrictive product expression. The EBERs have been associated with PKR inhibition, specifically, EBER1 (Clarke et al., 1991; Sharp et al., 1993), and a binding model of EBER1 to the dsRNA binding domain of PKR has been established (Vuyisich et al., 2002). These observations remain controversial, not only as this interaction has yet to be shown *in vivo*, but the EBERs are thought to be localised within the nucleus (away from PKR) and have been linked to several other binding partners (Glickman et al., 1988; Howe & Steitz, 1986; Toczyski et al., 1994). However, it was suggested that the EBERs can be detected in the cytoplasm during interphase, suggesting that they may be involved in translation, and therefore may have the ability to affect the ISR (Schwemmle et al., 1992).

PERK activation was absent in latent EBV-infected cells. This suggests that latent EBV's restricted expression of viral gene products is not capable of inducing ER stress within the cell. It has been previously been shown that EBV latent protein, LMP1, induces PERK activation (Lam et al., 2004). LMP1 is responsible for B cell transformation, through mimicking CD40 signalling that activates growth and survival pathways (Kaye et al., 1993; L. W. Wang et al., 2017). Whilst LMP1 is vital for several latent EBV processes, activation of PERK may induce eIF2α phosphorylation, stalled translation and SG formation, stopping these processes. Lam et al. (2004) found that the top 5% of the highest LMP1 expressing cells, increased eIF2α phosphorylation 3-fold. Therefore, there is a potential for the virus to promote this response via activation of PERK. Our data, however, suggests that PERK is not activated by the expression of LMP1 or other latent products within these latently infected cell lines. It can be speculated that LMP1 is not expressed to suitable levels to affect the activation of PERK during latent infection.

eIF2α phosphorylation levels in EBV infected cells compared to uninfected cells, revealed no significant difference in both cell lines (Figure 3-5). eIF2α phosphorylation

was shown to increase in one cell line, whilst a decrease in the other, albeit not significantly, suggesting the absence of a trend, and lack of eIF2α phosphorylation following latent EBV infection. This collaborates the lack of either PKR or PERK activation from the latent virus.

The mRNA levels of ATF4 and CHOP, which may be induced by eIF2α phosphorylation suggest that there is no difference between uninfected and latent EBV-infected samples, BL2 and BL31 (Figure 3-5D). ATF4 protein levels also showed little difference in either cell line compared to their uninfected counterparts (Figure 3-5B). Taken together this data reinforces our observations regarding PKR, PRK and eIF2α phosphorylation levels, and latent infection does not activate the ISR.

Interestingly, we observe an increase in GADD34 in latent EBV^+ cells (Figure 3-5D). This novel finding suggests that the latent virus induces the expression of GADD34 without an increase in eIF2α phosphorylation or ATF4/CHOP mRNA expression. The increase in GADD34 in latent EBV^+ cells would provide an opportunity to counteract any phosphorylation of eIF2α, that may occur during latent infection. Although intriguingly, this is not observed. How the virus induces GADD34 expression without the increase of eIF2α phosphorylation remains unclear, however, could show the first evidence that EBV is capable of counteracting the ISR and limiting eIF2α phosphorylation.

Finally in this chapter, it was shown that phosphorylation of eIF2α was inducible in latently infected cells, to a similar level as uninfected cells, when exposed to arsenite stress (Figure 3-6). The oxidative stress induced through exposure to arsenite is severe, however, if a mechanism exists within EBV^+ cells to counteract the phosphorylation of eIF2α, such as increased GADD34 expression, it may dampen the activation seen in arsenite-treated cells. Increased phosphorylation of eIF2α was observed in all infected and uninfected cell lines following exposure to arsenite. However, little difference was observed in eIF2α phosphorylation levels in arsenite-treated samples, normalised to

untreated levels, between infected and uninfected samples. BL31 infected cells showed a significantly increased level of eIF2α phosphorylation compared to uninfected cells, while BL2 showed the opposite. As this response did not correlate to both virus-infected samples, it is therefore realistic to suggest that this difference is due to cell variability rather than the effect of the virus. This finding would suggest that the increased levels of GADD34 present in EBV^+ cells are not capable of reducing the phosphorylation of eIF2α induced by arsenite. However, whether this is the case with less severe stress inducers would provide an interesting basis as to how and whether latent EBV may overcome less severe stresses, that could be associated with its lifecycle. Furthermore, investigating the mRNA levels of GADD34 in EBV^+ following arsenite exposure may provide further evidence of differential expression following EBV infection.

PKR and PERK phosphorylation remained unaffected, revealing that arsenite stress did not induce either of these kinases in these cells, and would likely be working through GCN2, or HRI, known to be activated following oxidative stress. ATF4 protein expression also remained unaffected following exposure to arsenite, regardless of the high level of eIF2α phosphorylation in all cells. As ATF4 expression is downstream of eIF2α phosphorylation, the response will be staggered, and likely would take longer than provided in this experiment. One study found that following exposure to 100 μM sodium arsenite, ATF4 protein was only detectable from 2 hours following exposure (Nathaniel Roybal et al., 2005). Therefore, although an increase in ATF4 protein expression was not observed in any cells following arsenite exposure, it can be suggested that this expression would increase following further incubation time.

In conclusion, latent EBV infection does not induce eIF2α phosphorylation, PERK or PKR activation. Downstream gene expression of GADD34 is increased in latently infected cells, suggesting a potential mechanism to counteract any phosphorylation of eIF2α that could occur through the activation eIF2αKs in response to viral products. However, our findings suggest that this does not occur during latent infection. Further studies

investigating GADD34 protein expression, and potential inducers, may shed light on how this gene is upregulated during latent EBV infection, and how this may benefit the virus.

4 Stress Granule formation during latent EBV infection

4.1 Introduction

The role of viruses in stress granule formation has been extensively investigated over the last 20 years (P. J. Anderson & Kedersha, 2002b; Eiermann et al., 2020; J. P. White & Lloyd, 2012). Whilst these studies have investigated viruses from all groups, the majority focus on RNA viruses, neglecting DNA viruses, such as herpesviruses. This has left a void in our understanding of how the biphasic life cycle of herpesviruses may affect SG formation. In this chapter, SG formation during latent EBV infection is characterised.

eIF2αK activation, eIF2α phosphorylation and associated downstream effects are commonplace in virus-infected cells (Eiermann et al., 2020). This increased activation of the eIF2α pathway promotes the formation of SGs unless the virus has evolved a mechanism to prevent this. SG formation can be both beneficial and detrimental to viral replication. On one hand, the sequestration and localisation of all necessary translational machinery provide the virus with a unique opportunity to hijack and utilise this process, on the other, the stalling of translation that accompanies SG formation, negatively affects viral protein expression. Therefore, many viruses have developed mechanisms to either prevent/overcome SG formation or influence the process to benefit viral replication (reviewed in White & Lloyd, 2012). Viruses preventing SG formation have been shown to inhibit eIF2α and eIF2αK activation directly, or act further downstream, such as inhibiting or modifying the process during assembly of SGs (Figure 4-1). Several RNA viruses, such as Junin virus, Influenza A virus, and Japanese encephalitis virus have been shown to prevent SG formation through eIF2α phosphorylation inhibition (Khaperskyy et al., 2012; Linero et al., 2011; Tu et al., 2012). The DNA herpesvirus, HSV-1, was also shown to inhibit eIF2α phosphorylation, preventing SG formation (Dauber et al., 2011). The mechanisms involved in these processes commonly involve the inhibition of eIF2αKs or blocking phosphorylation of eIF2α by viral proteins. RNA

viruses, West Nile viruses and Dengue virus interfere with TIA-1 recruitment to the SG, blocking their formation (Emara & Brinton, 2007). Several other viruses (mostly RNA viruses), including foot and mouth virus and poliovirus, produce viral proteases that can cleave G3BP1, preventing SG assembly (Visser et al., 2018; J. P. White et al., 2007). This is only a handful of examples representing the current understanding of viral infection and SG formation; however, it demonstrates how RNA viruses represent most of the past research in this field.

Furthermore, most studies have focused on actively replicating viruses, rather than viruses that exhibit latency seen in herpesviruses, therefore it is difficult to speculate whether these viruses, expressing a much more restricted level of viral products, are capable of inducing SG formation. It had previously been suggested that an increase of eIF2α phosphorylation by 20–30% would be sufficient to sequester eIF2B into an inactive complex (Brostrom & Brostrom, 1997), stalling translation and promoting SG formation. Therefore, it is possible, through the increase and fluctuation of eIF2α phosphorylation observed in the previous chapter, that SGs may form in these cells.

It has been shown that several members of the human herpesvirus family express products that inhibit SG accumulation, namely VHS1 in HSV-1/HSV-2, and ORF57 in KSHV (discussed further in chapter 5). However, these viral products are only expressed during the lytic cycle, which begs the question, does latent infection involve a similar process, or even, does it need to? The restricted viral product expression of latent EBV infection means that only a small number of components may be detected by the SG response.

dsRNA, detected by PKR is unlikely to be produced as a product of latent replication, as suggested to occur during lytic replication of several other viruses (Sciortino et al., 2013; Weber et al., 2006). As the latent EBV genome exists as a circular closed plasmid, it behaves similarly to host chromosomal DNA and is replicated once during the cell cycle

by host machinery (Tsurumi et al., 2005). However, the expression of the EBERs, or other miRNA produced during latency, may be detected by PKR by their secondary structure. Data presented in the previous chapter, however, suggests that PKR is not activated during latent EBV infection. Furthermore, the virus does not produce glycoproteins during latency, and we showed that latent product expression does not promote the activation of PERK. Therefore it is likely that SG formation will not be induced during latent EBV infection.

Sharma & Zheng (2022) showed that only KSHV cells in lytic cycle were able to prevent arsenite-induced SG formation, while cells with latent KSHV infection showed an abundance of TIA-1^{+} SGs. To assess whether this may also be the case during latent EBV infection, SG formation was induced through chemical exposure.

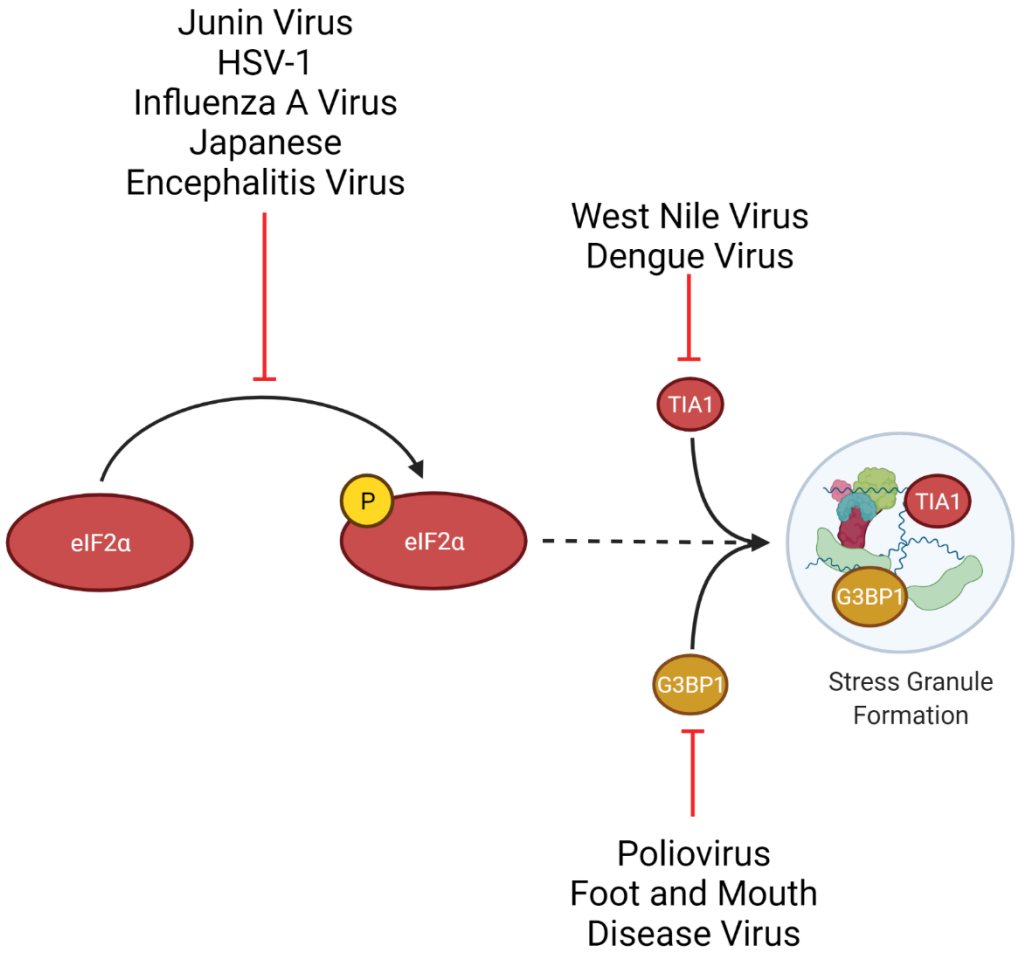

Figure 4-1 SG inhibition by viruses. Several viruses employ mechanisms to evade the SG response. Junin virus, herpes simplex virus (HSV-1), influenza A virus and Japanese encephalitis virus inhibit the phosphorylation of eIF2α through a variety of mechanisms, either directly inhibiting eIF2α activation or a kinase responsible for phosphorylating eIF2α. Viruses may also inhibit SG formation downstream of eIF2α phosphorylation, by interfering with SG elements such as G3BP1 or TIA-1. Poliovirus and foot and mouth disease virus possess a protease to cleave G3BP1 preventing it from assembling SGs. West Nile virus and Dengue virus sequester TIA-1 away from SG components, inhibiting their formation.

4.2 Results

4.2.1 Characterisation of SGs

It was important to first optimize a method to visualise SGs under certain conditions. As previously described, G3BP1 and TIA-1 are commonly associated with SGs and are regularly used to detect them (P. J. Anderson & Kedersha, 2002b; Fay et al., 2017; Kedersha et al., 1999). Antibodies probing for these SG markers provide a simple means to identify SGs, through signal intensity, size, and localisation with one another.

In this study, HeLa cells were initially used to optimize stress and antibody conditions, as they have been extensively used in SG biology (Budkina et al., 2021; Kedersha et al., 1999, 2005; Reineke et al., 2012, 2015). They exhibit a suitable sized cytoplasm, in which SGs form, that allows for numerous SGs to be imaged in each cell. Unlike B cells, which consist of a much smaller cytoplasm surrounding the nucleus, which was used to characterise SG formation and EBV infection later in this section.

Sodium arsenite is an effective stress inducer in most cell types and has been used to induce SGs in numerous studies investigating similar mechanisms (Burgess & Mohr, 2018; Fay et al., 2017; Finnen et al., 2014; Kedersha et al., 1999; Yang et al., 2020).

Figure 4-2A shows HeLa cells following stress induced by arsenite, the cell exhibits TIA-1^+ and G3BP1^+ foci forming in the cytoplasm, indicative of stress granule characteristics. In the untreated cells, G3BP1 is spread throughout the cytoplasm, whilst TIA-1 is present in both the nucleus and cytoplasm as expected. Confirming that SGs formed in HeLa cells following exposure to arsenite and could be detected by TIA-1 and G3BP1 antibodies.

Following this initial characterisation of SGs, optimisation of the time that the cells were exposed to arsenite was performed. Treatment of cells with 0.5 mM sodium arsenite was regularly used in previous studies, however, varying time exposure between 30–60

minutes was used (Burgess & Mohr, 2018; Fay et al., 2017; Finnen et al., 2014; Kedersha et al., 1999; Yang et al., 2020). Figure 4-2B shows the results of varying the exposure time of HeLa cells to 0.5 mM sodium arsenite. Using the same markers and antibodies in Figure 4-2A, no stress granules are present in untreated cells, and interestingly, also following 30 minutes of treatment. Stress granules can be seen in both 45- and 60-minute exposures to arsenite, however, the cells appear more normal and healthier at the lower exposure time, suggesting that the 60-minute exposure may affect the cell detrimentally through prolonged inhibition of translation. The 45-minute exposure also shows a larger quantity of stress granules within HeLa cells, compared to the longer exposure. Taken together, 45 minutes was shown to be the most appropriate time exposure for these cells.

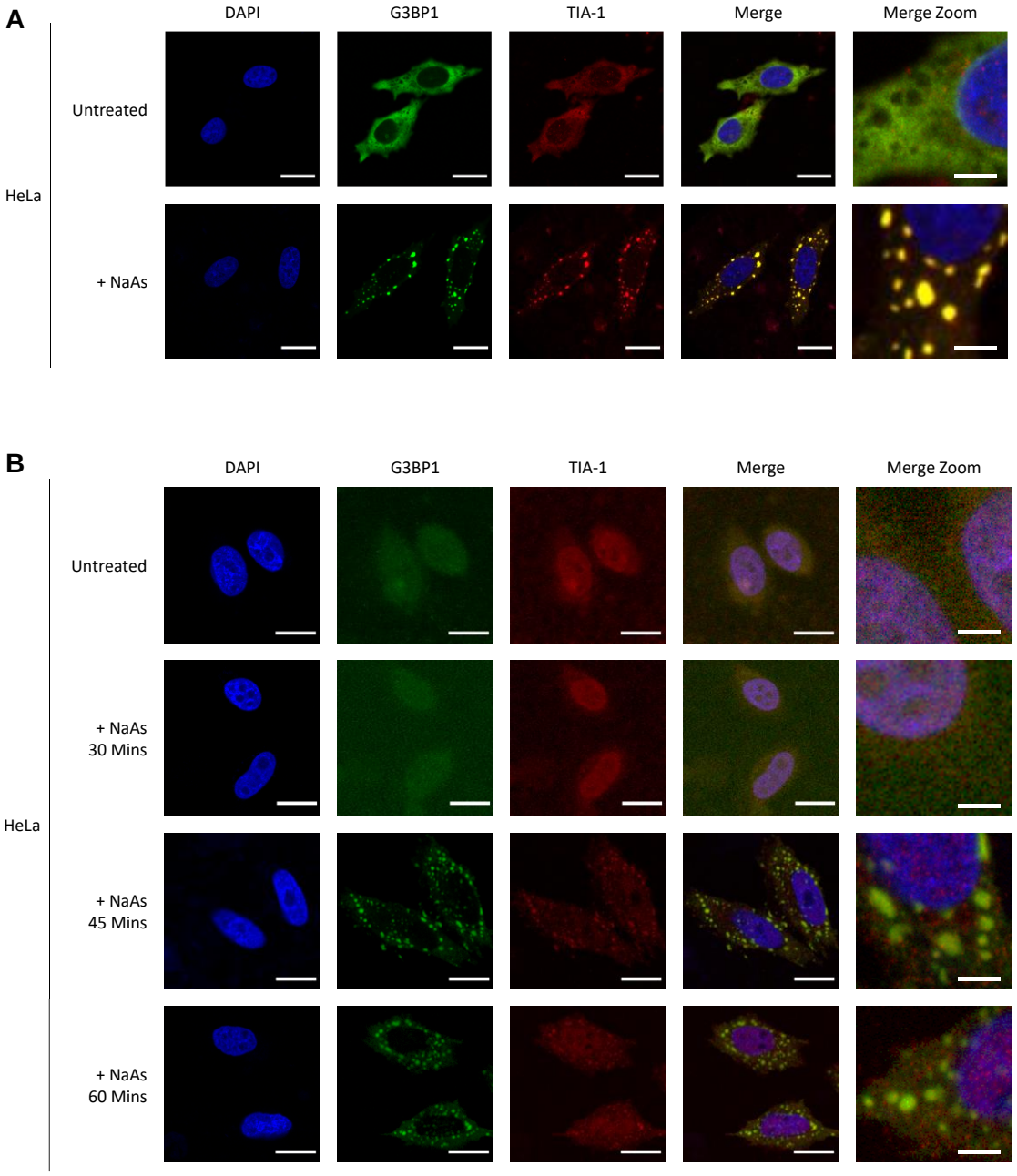

Figure 4-2 Stress granule characterisation in HeLa Cells. (A) HeLa cells were grown onto coverslips before treating with 0.5 mM sodium arsenite (NaAs), or water (untreated) for 45 minutes. Cells were fixed, permeabilized and stained for G3BP1 (green) and TIA-1 (red) using corresponding antibodies and imaged using confocal microscopy. The nuclei were stained using mounting media containing DAPI. **(B)** Arsenite treatment exposure optimisation. Cells were treated with sodium arsenite for 30, 45 and 60 minutes, along with an untreated control, before fixing, permeabilising and staining as described in (A). **(A & B)** Scale bar = 20 µm, Zoom scale bar = 5 µm

4.2.2 Optimisation of automated cell and granule counting

The number of stress granules that were exhibited in initial experiments revealed a need for automated quantification of the granules and the cells. This would also remove any bias and provide comparable parameters for SG detection in each condition.

Cell Profiler (www.cellprofiler.org) is a program designed to analyse cell images through a pipeline that can be automated (Carpenter et al., 2006). This program provided a useful process in which SGs could be detected and counted within numerous cells.

A standard recommendation is that >100 SG should be counted across 3-5 images to obtain a correct representation of SG formation within that condition (Fay et al., 2017). Therefore, it was determined that for all images in which SGs were quantified, >100 SGs would be counted across 3 biological replicates of each condition. A pipeline was created in Cell Profiler 4.2.1 (for windows) to quantify TIA-1$^+$ SGs, the number of cells and the intensity of the signal throughout the cell. Several other values were obtained from Cell Profiler for future analysis within this pipeline, however, not directly referenced in this study.

Figure 4-3 shows the workflow on which the pipeline is based. Firstly, the IF images taken on the confocal microscope are uploaded to Cell Profiler, as separate channels using a single Z-slice, manually determined to be the most central image of the cell. The pipeline involves the identification of the nucleus and cells, combining this information to determine the cytoplasm, before expanding the cytoplasm by 2 pixels to ensure any objects on the border of the cytoplasm are included in the quantification. SGs are identified using the TIA-1 signal, which is corrected by smoothing, subtracting, and enhancing to provide an optimum image for quantification. TIA-1$^+$ SGs that meet the size, localisation and signal intensity criteria are then counted and quantified. The data for each cell showing among other things, the quantity of SGs per cell, was exported and analysed.

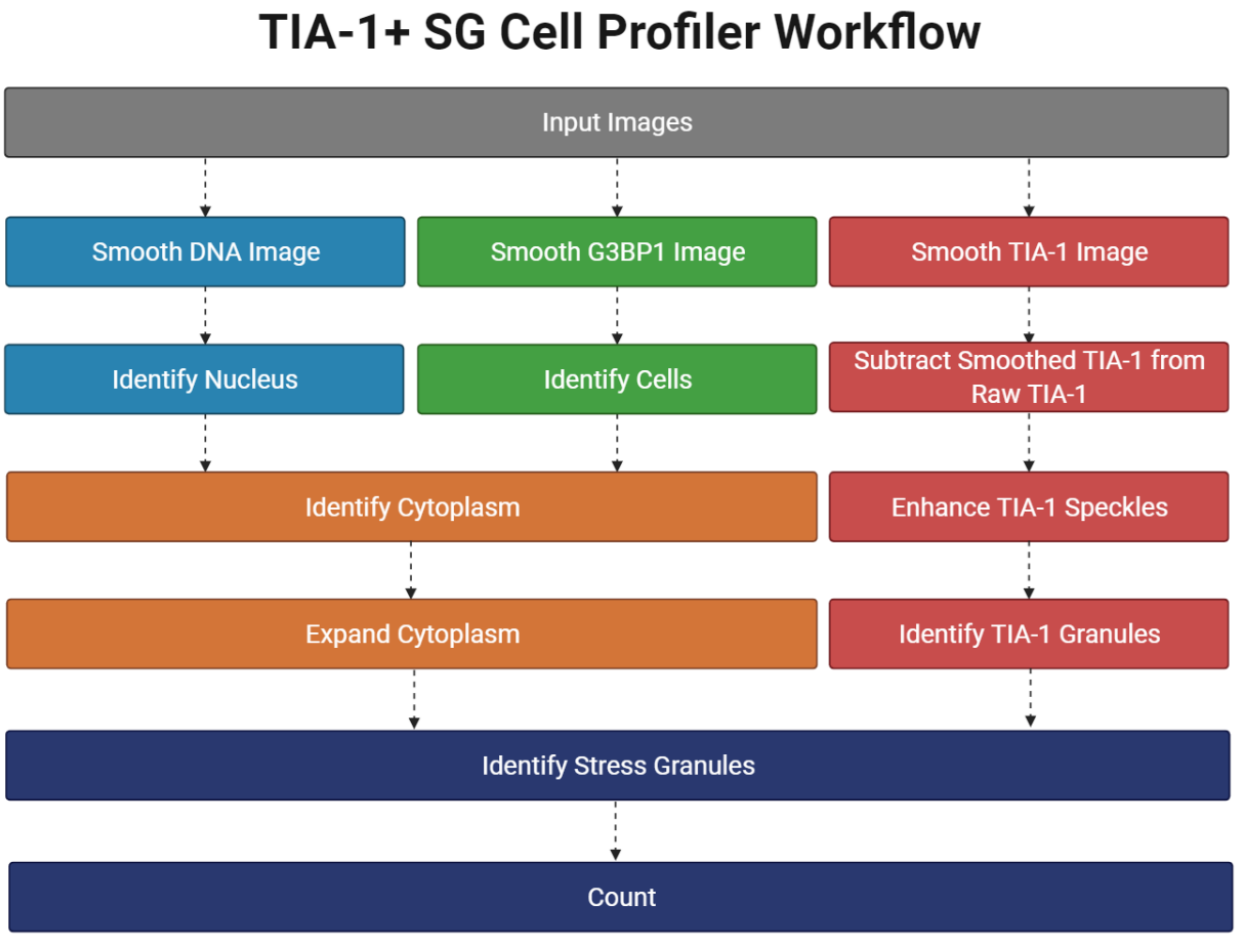

Figure 4-3 Cell Profiler workflow to quantify TIA-1$^+$ stress granules in images. IF images from a single Z-slice showing DNA, G3BP1 and TIA-1 were uploaded into Cell Profiler as separate channels. DNA was processed first, with smoothing to ensure each nucleus was not segregated by differences in signal intensity, followed by identification of each nucleus. Images showing G3BP1 were treated in the same manner, smoothing to spread the G3BP1 signal throughout the cytoplasm, before identifying the cells. The cytoplasm was identified through subtracting the nucleus from the cells and expanded to cover objects that may lay on the edge of the cytoplasm. The TIA-1 signal was smoothed and subtracted from the raw image to remove background. Any speckles were enhanced by the program and TIA-1+ granules were identified. Stress granules were determined through associating the extended cytoplasm image with TIA-1 foci, and these granules were counted and quantified, along with each cell.

4.2.3 Latent EBV infection does not induce or alter SG accumulation

This study aimed to determine whether latent EBV infection affected stress granule formation in host cells. This was performed using immunofluorescence and chemically induced cellular stress. Initially, this study aimed to deduce whether the latent EBV infection alone induced stress granule formation. Figure 4-4 shows that there is no difference in the number of SGs per cell between uninfected and latent EBV-infected BL2 cells. This can be seen in the IF images (Figure 4-4A), through the absence of colocalised G3BP1 and TIA-1 foci, and when TIA-1$^+$ SGs are quantified by Cell Profiler in Figure 4-2B. Cell Profiler quantified TIA$^+$ SGs following the pipeline shown previously (Figure 4-3). A basal level of ~0.5 SGs/cell is shown in both infected and uninfected cell lines, showing no significant difference between the two.

This experiment made use of two different mechanisms for the induction of SGs, arsenite, known to induce stress through several eIF2αKs and in turn phosphorylate eIF2α, and, hippuristanol, a potent inhibitor of eIF4A (Cencic & Pelletier, 2016). It was shown in the previous chapter, that arsenite increases eIF2α phosphorylation in both uninfected and latent EBV-infected cells (Figure 3-6). As discussed, the activation of the eIF2α pathway is a key mechanism for the formation of SGs and is commonly manipulated by viruses. Therefore, the use of alternative stress, hippuristanol, provides a useful tool to determine whether the virus affects the eIF2α pathway. Hippuristanol induces SGs formation through an eIF2α-independent pathway, in which it inhibits eIF4A from binding to RNA, maintaining a closed conformation and stalling translation (Cencic & Pelletier, 2016). The process of stalling translation then promotes the formation of SGs. Following incubation of either 0.5 mM sodium arsenite or 1 µM hippuristanol for 45 minutes, both cell lines exhibited distinct stress granules shown by the presence of colocalised G3BP1 and TIA-1 foci (Figure 4-4A). Upon quantification of these stress granules (Figure 4-4B), the number of SGs per cell significantly increased in both chemical exposed conditions, compared to untreated, in both cell lines. Furthermore, no

significant difference is observed between each method of SG induction, in each cell line, suggesting that both arsenite and hippuristanol have the same affect regardless of whether the cell is infected with the latent virus or not. A similar result was also seen in BL31 and its infected counterpart (Figure 4-5).

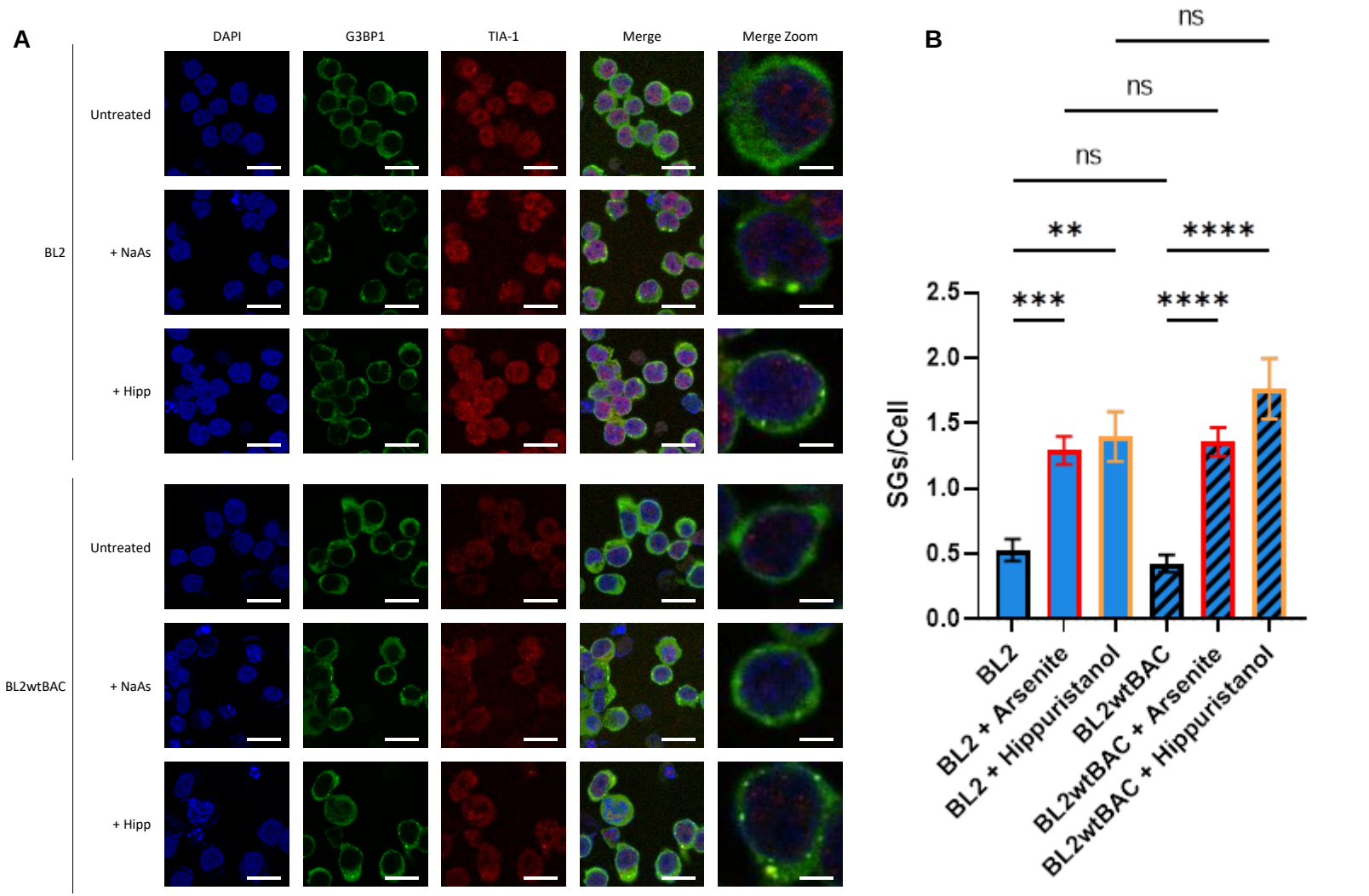

Figure 4-4 Latent EBV infection does not affect SG formation. (A) SG markers TIA-1 and G3BP1 were used to show the presence of SGs following stress. BL2 and BL2wtBAC cells were incubated with NaAs (0.5mM), hippuristanol (1 µM) or water (untreated) for 45 minutes before fixation and permeabilization. Cells were stained for G3BP1 (green) and TIA-1 (red) using corresponding antibodies and imaged using confocal microscopy. The nuclei were stained using mounting media containing DAPI. Scale bar = 20 µm, Zoom scale bar = 5 µm. **(B)** Quantification of IF (A) was performed using cell profiler to count TIA-1^{+} stress granules per cell. Total number of cells per condition >100. Error bars represent s.e.m. n=3 (Two-way ANOVA, ns = P > 0.05, * = P ≤ 0.05, ** = P ≤ 0.01, *** = P ≤ 0.001, **** = P ≤ 0.0001).

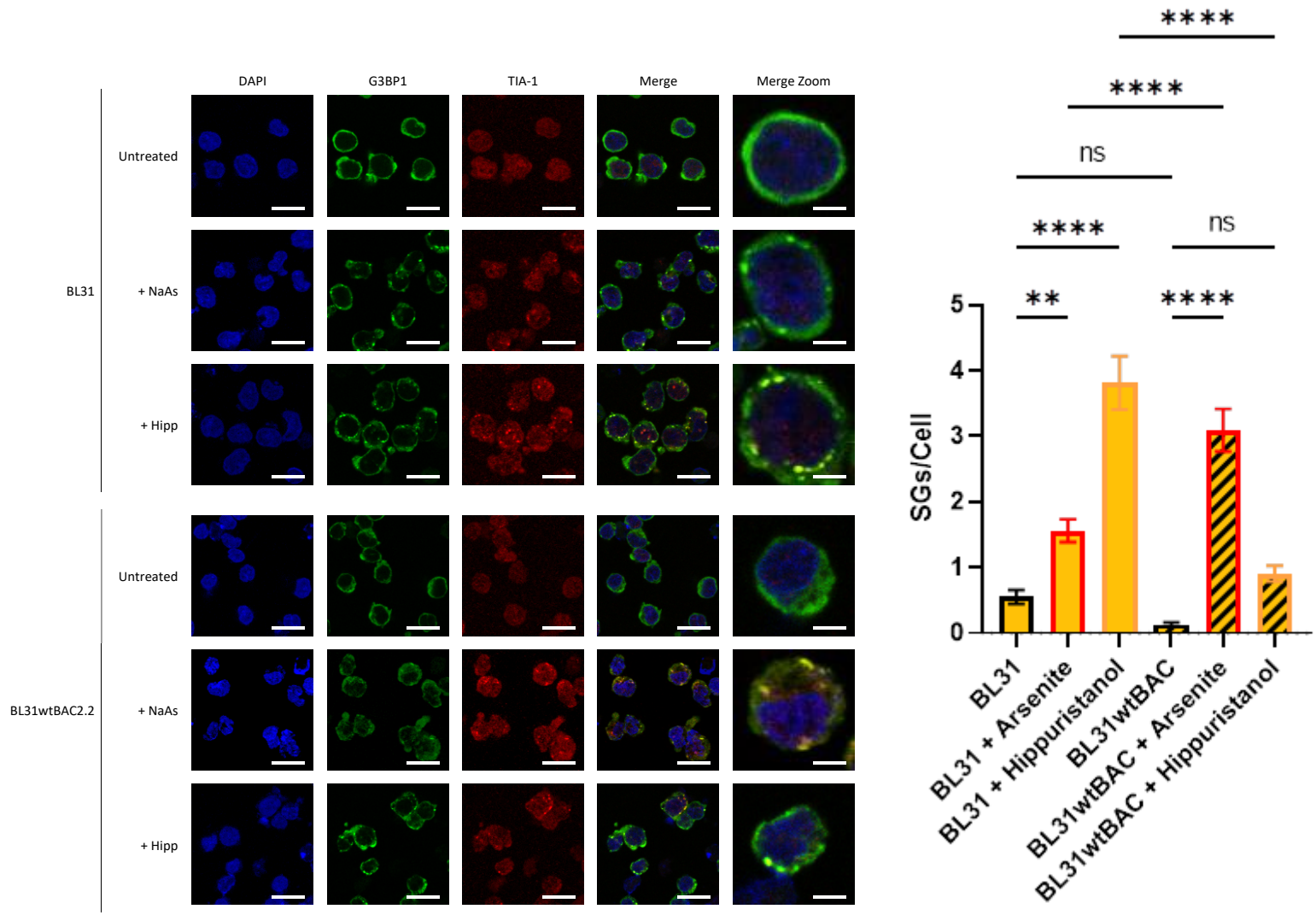

Figure 4-5 Latent EBV in BL31 infection and SG formation. (A) SG markers TIA-1 and G3BP1 were used to show the presence of SGs following stress. BL31 and BL31wtBAC cells were incubated with NaAs (0.5mM), hippuristanol (1 µM) or water (untreated) for 45 minutes before fixation and permeabilization. Cells were stained for G3BP1 (green) and TIA-1 (red) using corresponding antibodies and imaged using confocal microscopy. The nuclei were stained using mounting media containing DAPI. Scale bar = 20 µm, Zoom scale bar = 5 µm. **(B)** Quantification of IF (A) was performed using cell profiler to count TIA-1^{+} stress granules per cell. Total number of cells per condition >100. Error bars represent s.e.m. n=3 (Two-way ANOVA, ns = $P > 0.05$, * = $P \leq 0.05$, ** = $P \leq 0.01$, *** = $P \leq 0.001$, **** = $P \leq 0.0001$).

4.3 Discussion

The results presented in this chapter show that SG formation within cells can be analysed and characterised through several processes and investigates the effect that latent EBV infection has on this mechanism. The first objectives of this chapter were to optimise the process for chemically inducing stress granules and confirm that they could be imaged in B cells, using known SG markers. The initial characterisation of SGs in HeLa cells (Figure 4-2A) confirmed that SGs could be induced through the exposure of the cells to sodium arsenite and that these SGs could be imaged using SG markers, G3BP1 and TIA-1. Although HeLa cells have long been known to carry numerous mutations, contain chromosomal irregularities and exhibit genetic abnormalities, even more so than most cancer-derived cell lines (Macville et al., 1999; Mittelman & Wilson, 2013), they provided an efficient cell line to initially characterise SGs in. HeLa cells proliferate notoriously fast and exhibit a relatively large cytoplasm when compared to BL cell lines, that were used for EBV experiments. This allowed for the cells to be grown quickly and provided a large area in which SGs could form and be characterised. The effect that sodium arsenite had on the cells was dramatic (Figure 4-2). It had been shown in the previous chapter that arsenite was capable of inducing eIF2α phosphorylation to between 5– and 20-fold more than untreated samples (Figure 3-6). Using the same exposure concentration and time (0.5 mM, 45 minutes) was also sufficient to induce SG formation. SG markers G3BP1 and TIA-1 provided a strong colocalized signal in arsenite-treated cells, whilst remaining relatively spread out throughout the cytoplasm (G3BP1) and the cell (TIA-1) in untreated samples.

The results shown in Figure 4-2B shows that the optimum exposure time to arsenite was 45 minutes. Kedersha et al. (1999) had shown that 30 minutes was sufficient to induce SG formation in DU145 (human prostate cancer cell line) and COS-7 (monkey kidney cell line), however, in HeLa this time did not show observable SGs. This is likely due to cell variability, as these results are consistent with observations made in other studies

using HeLa (Buchan et al., 2008; Tolay & Buchberger, 2021). At 45 minutes, however, a strong SG accumulation can be observed. SG accumulation also occurs following 60 minutes of exposure to arsenite; however, these cells begin to exhibit abnormal morphology, become rounder, have deformed nuclei, and begin to detach from the flask. This suggests that these cells are beginning to undergo apoptosis and would not be appropriate to study for the stress response. It was therefore decided to use 45 minutes as the exposure time to sodium arsenite for future experiments with other cell lines.

The requirement for automated SGs quantification was clear immediately following initial characterisation. Figure 4-2A shows numerous (>10) SGs per cell following arsenite-induced stress. Furthermore, there is a high risk of selection bias when manually counting SGs. As arenite induces a dramatic increase in SGs compared to untreated, it is difficult to anonymise the images from each condition, therefore an automated process in which SGs are counted by a program when they meet certain parameters was preferred. Cell Profiler, a program designed to measure and analyse phenotypes within cell images (Carpenter et al., 2006), allows for a pipeline to be created to measure SGs within the images of this study. As shown in the results of this chapter, the pipeline developed involves several steps that aim to first identify cells, nuclei, and cytoplasm, before identifying and quantifying TIA-1^{+} SGs within the cell. G3BP1^{+} SGs, along with SGs containing both signals, were also quantified, however, the signal obtained from TIA-1 was superior to G3BP1 in intensity and specificity, therefore it was decided to use TIA-1 to quantify SGs.

Following the characterisation of SGs, and the development of a method to quantify SGs within cells, this study moved to investigate the remaining aims of this chapter. To understand whether latent EBV infection promoted SG assembly and whether chemical induction of SGs was affected by the latent virus.

Firstly, it was shown that there was no difference in SG formation between uninfected and latent EBV-infected BL cells (Figure 4-4). This is an interesting discovery, as it may suggest one of two things. One, the latent infection does not express viral products during latency that activate the stress response and induce SG formation. Or two, the latent virus has mechanisms to evade this response following its activation.

Previous studies however have shown that PERK activation may be induced by latent EBV product, LMP1 (Lam et al., 2004). However, it was shown in the previous chapter that neither PKR nor PERK is activated during latent EBV infection (Figure 3-5). It is therefore likely that latent EBV products are not capable of inducing ER stress or activating PKR.

eIF2α phosphorylation was shown to not be affected by latent viral infection, however, mRNA expression of GADD34, the protein linked to dephosphorylation of eIF2α, was increased (Figure 3-5). Combining this knowledge with the results presented in this chapter, it can be suggested that the virus does employ a mechanism to evade SG formation. PKR activation is prevented, and processes to oppose eIF2α phosphorylation are promoted, albeit through an unknown mechanism. This suggested that the restricted expression of viral products during latency may have the ability to activate the stress response, but the virus prevents this from stalling translation and forming SGs.

SG formation in viruses has become an extensively studied field over the last 20 years and several mechanisms deployed by viruses to evade, manipulate and hijack this process have been discovered (P. J. Anderson & Kedersha, 2002b; Eiermann et al., 2020). However, latent infection has been neglected, especially as latent EBV infection was associated with 137,900–208,700 cancer deaths in 2020 (Wong et al., 2022). Most studies focus on actively replicating viruses, that produce numerous viral products in the host cell that have the potential to activate the stress response. The restricted viral product expression of latency provides an interesting basis for research into the stress

response of infected cells, especially viral evasion mechanisms associated with this limited expression. It is well understood that latent EBV infection is the primary cause of several cancers (El-Sharkawy et al., 2018). Therefore, latent viral products are affecting the cell in such a way to promote proliferation and development of cancer, however, do not induce the SG response.

Secondly, it was shown that there is no difference in SG assembly between uninfected and latent EBV-infected BL cells following artificial stress induction by arsenite or hippuristanol. Arsenite, as previously mentioned, is known to induce SGs through oxidative stress that activates several eIF2αKs which in turn phosphorylate eIF2α and promote the formation of stress granules. Figure 4-4 reveals that in both uninfected and latent EBV-infected BL2 cells, arsenite induces a strong SG response, showing between 1 – 2 SGs per cell. A similar level of SG formation in both uninfected and infected cells would suggest that the virus is unable to prevent activation of eIF2α via arsenite stress, regardless of the increased GADD34 expression shown in the previous chapter (Figure 3-5).

It has been shown in several studies that other herpesviruses can prevent SG formation following arsenite stress. HSV-2 interferes with arsenite-induced SG formation downstream of eIF2α signalling (Finnen et al., 2014, 2016), while KSHV is thought to prevent arsenite-induced SG formation by interfering with PKR activation (Sharma et al., 2017). However, the latter report focuses on PKR activation in response to arsenite exposure, which was shown in Figure 3-6 to not be activated in uninfected or latent EBV-infected BL cells in this study. Furthermore, these examples suggest that lytic products are responsible for the evasion of arsenite-induced SG formation. The lack of related viral products or homologs expressed during latent EBV infection along with the results obtained shows that the mechanisms employed by these lytic viruses, do not occur in latent EBV infection.

Finally, hippuristanol-induced SGs were examined in latent EBV-infected cells. Hippuristanol is a useful tool in understanding SG evasion mechanisms as it allows for SGs to be induced via an eIF2α independent pathway. This provides insight as to whether any potential SG inhibition occurs downstream of eIF2α. Although in this chapter as it has been shown that arsenite can induce stress granule formation, it is unlikely that hippuristanol would have a different effect. The results shown in Figure 4-4 reveal that, as expected, hippuristanol-induced SG formation shows no difference between uninfected and latent EBV-infected cells. Hippuristanol produces a slightly stronger SG response in both uninfected and infected cells compared to arsenite, consistent with observations made through the course of our investigations (data not shown).

In conclusion, the data presented in this chapter reveals that latent EBV infection does not induce SG formation. This correlates with observations made in the previous chapter showing that eIF2α phosphorylation is not increased during latent EBV infection. Furthermore, the latent infection does not alter chemical-induced SG formation regardless of increased mRNA expression of GADD34. Whilst eIF2α, and eIF2αKs were unaffected by latent infection, we next aimed to investigate whether EBV affected SG-associated RNA-binding proteins directly, which we discuss in the next chapter.

5 RNA-binding proteins and latent EBV infection

5.1 Introduction

RNA binding proteins (RBPs) are proteins that bind to single or double-stranded RNA and have the ability to impact the role of gene expression (Dreyfuss et al., 2002). Although their structure differs, they are generally composed of several structural RNA-binding domains (RBD). These domains include RNA Recognition Motif (RRM), the most abundant RBD, the double-stranded RNA-binding domain (dsRBD), the K-Homology (KH) domain, a motif that binds single-stranded RNA and DNA, and the zinc finger domains (Lunde et al., 2007). These multiple domains, along with additional auxiliary domains, provide RBPs with a broad function and RNA-specificity (Glisovic et al., 2008).

T-cell-restricted intracellular antigen-1 (TIA-1) is an RBP, associated with translational silencing, alternative splicing, and stress granule formation (Del Gatto-Konczak et al., 2000; Kedersha et al., 1999; Le Guiner et al., 2001; Piecyk et al., 2000). TIA-1 comprises three RRMs along with a glutamine-rich C-terminal auxiliary domain (Tian et al., 1991), of which a similar structure can also be found in the closely related RBP, TIA-1-related protein (TIAR) (Figure 5-1). TIAR shares 79-91% homology in its RBDs with TIA-1, and 51% homology in the carboxyl terminus (Dember et al., 1996). There are numerous isoforms of TIA-1 that exist in nature, including TIA-1a and TIA-1b, formed through alternative splicing of exon 5 and represent the two major isoforms of this protein (P. J. Anderson & Kedersha, 2002a). Each isoform exhibits a similar level of distribution, however, differ in their splicing activity and specificity, with TIA-1b showing an enhanced splicing ability (Izquierdo & Valcárcel, 2007b). TIA-1a, the longer isoform, contains the 11 amino acid exon 5 inclusion within RRM2, while TIA-1b lacks this exon. Although the exact function of this exon is not known, TIA-1b ability for enhanced splicing, suggests that the exclusion of this exon is beneficial to this process. This is similar to the mechanism of AUF1 splicing, where the inclusion of an exon versus exclusion,

decreases the RNA binding affinity and specificity (Wagner et al., 1998). TIAR contains a similar exon inclusion/exclusion of 17 amino acids within its RRM1, producing TIARa and TIARb respectively (P. J. Anderson & Kedersha, 2002a). TIAR depletion was shown to promote the skipping of exon 5 in TIA-1 pre-mRNA splicing, leading to an increase in the TIA-1b/a ratio, thus increasing TIA-1 splicing activity (Izquierdo & Valcárcel, 2007b). This data suggests that a compensatory mechanism between TIAR and TIA-1 may exist.

TIA-1 can shuttle between the nucleus and cytoplasm, which is important for the multiple functions that TIA-1 performs in both locations. While TIA-1 does not contain a nuclear localisation signal (NLS), a region within its RRM2 domain is responsible for nuclear localisation (T. Zhang et al., 2005). This occurs through a Ras-related nuclear protein (RAN)-GTP-dependent pathway, the main pathway associated with the NLS. The same study also identified a region within the TIA-1 RRM3 domain responsible for nuclear export, which along with nuclear localisation by RRM2, was shown to be affected by their RNA-binding capacity.

TIA-1 binding to pre-mRNA and components of the spliceosome regulates alternative splicing in the nucleus. The spliceosome is a large RNA-protein complex responsible for removing introns from pre-mRNA (Lamond, 1993). TIA-1 has been shown to associate with the spliceosome component U1 snRNP, recruiting it to specific regions on pre-mRNA (Förch et al., 2002). In this mechanism, TIA-1 has been shown to affect alternative splicing, via direct binding of splicing activators near the 5’ splice site (Del Gatto-Konczak et al., 2000). TIA-1 is also associated with mRNA silencing and translational repression (Rayman & Kandel, 2017). These functions occur through the binding of TIA-1 to AU-rich elements (AREs) with the 3’UTR of several mRNAs, holding the mRNA in a translationally repressed state, and reducing protein expression (Yamasaki et al., 2007). TIA-1 has also long been associated with the formation of SGs, binding and recruiting untranslated mRNA to these foci during periods of cellular stress (Kedersha et al., 1999).

The PrLD located with the TIA-1 C-terminal domains provides the ability to self-aggregate and promotes the formation of granules (Kedersha et al., 1999).

Depletion of TIA-1 is known to inhibit SG formation, and several viruses have been shown to target TIA-1 to interfere with this process (Albornoz et al., 2014; Emara & Brinton, 2007; Esclatine et al., 2004b; Gilks et al., 2004; Kedersha et al., 1999, 2000; J. P. White & Lloyd, 2011). The mechanism adopted by these viruses includes the formation of abnormal TIA-1 foci, sequestration of TIA-1 and direct interference and inhibition with TIA-1. Our study investigates whether latent EBV may also target TIA-1.

Finally, the role of TIA-1 in tumour formation and suppression is an interesting topic. Several studies have implicated TIA-1 in both the formation and suppression of tumour growth (Carrascoso et al., 2018; Hamada et al., 2016; Sánchez-Jiménez et al., 2015). It was first reported that low levels of TIA-1 in lung cancer patients were correlated with a poor prognosis (Sánchez-Jiménez et al., 2015). The same study found that silencing TIA-1 promoted cell proliferation, while expression of TIA-1 in the xenotumours of mice inhibited their growth. Hamada et al. (2016) found that TIA-1a promoted the proliferation of cells, whilst TIA-1b inhibited cell growth and promoted apoptosis. This suggests that TIA-1 isoforms have contrasting roles in tumour development and suppression, in which TIA-1a is oncogenic, whilst TIA-1b is a tumour suppressor.

Latent EBV is commonly associated with the development of several cancers, therefore we aimed to investigate whether latent EBV manipulated TIA-1 expression, and in doing so modified the balance between oncogenic and tumour suppressor function. We hypothesised that a mechanism may exist in latent EBV infection that altered isoform expression of TIA-1 aiding viral growth but contributing to the development of EBV-associated tumours.

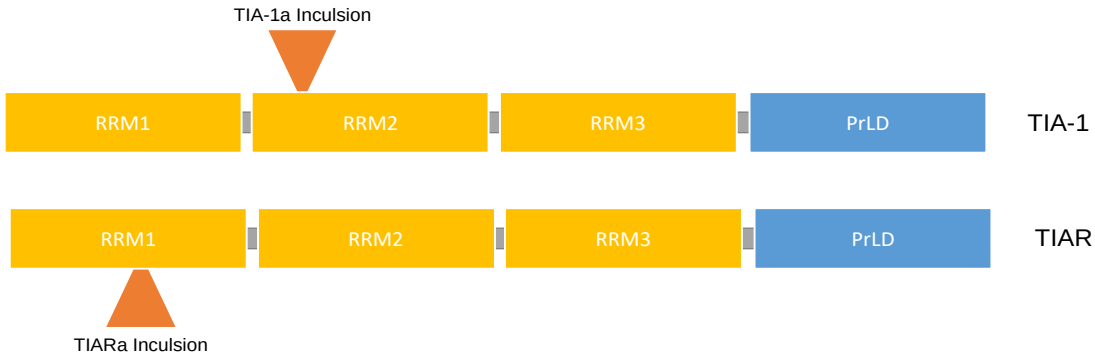

Figure 5-1 TIA-1 and TIAR have similar structures. They each contain three RRMs and a PrLD. TIA-1a/TIARa contain a short exon within their transcripts that is not present within TIA-1b/TIARb, this is controlled by alternative splicing. Figure adapted from (Anderson & Kedersha, 2002a).

5.2 Results

5.2.1 TIA-1 protein levels are lower in latent EBV-infected cells

Using the same latent EBV system as described in earlier chapters (BL2, BL2wtBAC, BL31, BL31wtBAC), the difference in TIA-1 protein expression was assessed between EBV^- and EBV^+ infected cells.

Figure 5-2 reveals that TIA-1 protein levels differ between infected and uninfected BL cells, most dramatically in the smaller isoform, TIA-1b. Figure 5-2A shows the larger TIA-1a isoform (top band) remains at a similar intensity between EBV^- and EBV^+ cells in both cell lines. Whilst the smaller isoform, TIA-1b (bottom band) appears to decrease in both EBV^+ cell lines when compared to the uninfected cells. Following quantification of each band separately and combined, there is a significant decrease in levels of TIA-1b following EBV infection, whilst TIA-1a remains similar regardless of the presence or absence of EBV (Figure 5-2B). When both bands are quantified together, a total decrease of TIA-1 is seen in the EBV-infected sample of both cell lines.

G3BP1 was also included in these experiments as it is known to be an important SG protein and modified by viruses such as poliovirus (J. P. White et al., 2007). However, as shown in Figure 5-2A, G3BP1 protein levels remain constant regardless of whether the cells contain latent EBV or not.

TIAR protein levels were also assessed, to exclude any unspecific binding of the TIA-1 antibody to TIAR, and asses previously reported association with TIA-1 expression and splicing (Izquierdo & Valcárcel, 2007b). Multiple bands are also present for TIAR protein levels; however, the intensity of each isoform does not change between latent EBV infected cells and uninfected cells in both BL2 and BL31 (Figure 5-3).

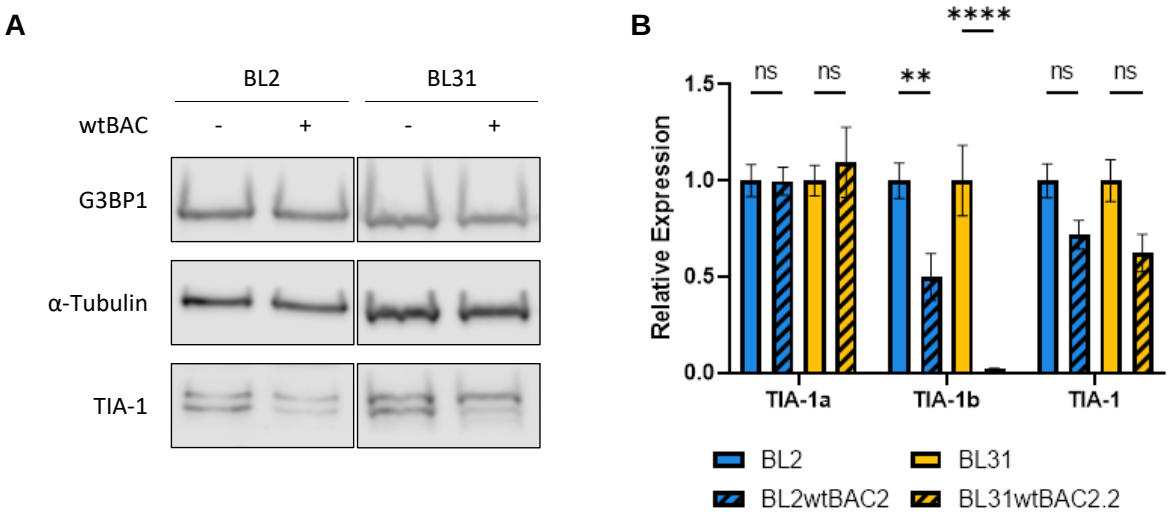

Figure 5-2 TIA-1 protein levels are lower in latently EBV+ B cells. (A) Protein was extracted from BL2, BL31 and EBV+ cell lines, BL2wtBAC and BL31wtBAC. Protein was resolved on 10% SDS-PAGE before immunoblotting against antibodies probing for TIA-1 and, loading control, α-tubulin. **(B)** Quantification of WB (A) showing levels of TIA-1a (top band), TIA-1b (bottom band) and TIA-1 (both bands) protein, normalised against α-tubulin and relative to EBV$^-$ sample. Error bars represent s.e.m. n=3 (Two-way ANOVA, ns = P > 0.05, * = P ≤ 0.05, ** = P ≤ 0.01, *** = P ≤ 0.001, **** = P ≤ 0.0001).

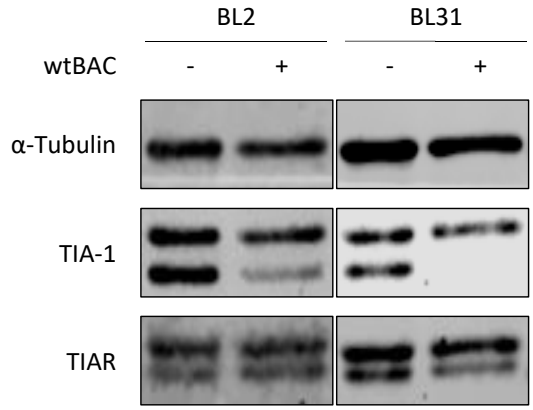

Figure 5-3 TIAR protein levels do not change in latently EBV+ B cells. Protein was extracted from BL2, BL31 and EBV+ cell lines, BL2wtBAC and BL31wtBAC. Protein was resolved on 10% SDS-PAGE before immunoblotting against antibodies probing for TIA-1, TIAR and, loading control, α-tubulin.

5.2.2 TIA-1 mRNA levels are lower in latent EBV-infected cells

Following the significant decrease in TIA-1 protein levels shown in EBV^+ compared to EBV^- cell lines, the mRNA was investigated to determine whether the virus was affecting the protein through transcriptional control or mRNA degradation.

First, qPCR primers were designed to span across exon 5, the exon excluded in TIA-1b, but included in TIA-1a. These primers allowed for the quantitative PCR to be performed and the final product to be separated on an agarose gel, providing a ratio for each isoform (Figure 5-4A). In each EBV^+ cell line, there is an increased ratio of TIA-1a amplified than TIA-1b, when compared to both EBV^- cell lines. This suggests that TIA-1b mRNA levels are lower in EBV^+ cells than in EBV^- cells. Figure 5-4B shows the mRNA expression levels of TIA-1, this time, however, using non-isoform specific primers, to avoid any discrepancies due to the size differences, with the ratios determined from Figure 5-4A separating the total levels into TIA-1a and TIA-1b. Total TIA-1 mRNA levels are lower in EBV-infected cells compared to uninfected, similar to that of the protein. Using the ratios of expression of each isoform, it can be determined that TIA-1b is decreased in the EBV-infected cells, whilst TIA-1a remains similar. This was repeated using the exon spanning primers and provided similar results (data not shown).

Finally, isoform-specific primers for TIA-1a and TIA-1b were used to reinforce the results shown in this chapter. Isoform-specific primers spanning through exon junctions did not initially allow for optimum qPCR conditions, and therefore were not immediately adopted. However, one study designed and used these primers successfully to show altered levels of TIA-1 isoforms in a similar experiment (Izquierdo & Valcárcel, 2007b). Therefore, following their design, these primers were used to confirm the results. Figure 5-4C confirms the results shown in A and B, revealing that TIA-1b is lower in both EBV-infected cell lines when compared to their EBV^- counterparts. This decrease is shown to be roughly half of the uninfected levels, although only statistically significant in BL31.

Interestingly, there is also a slight decrease in TIA-1a levels, which was also shown in Figure 5-4B, however, this remains similar to both uninfected cell lines.

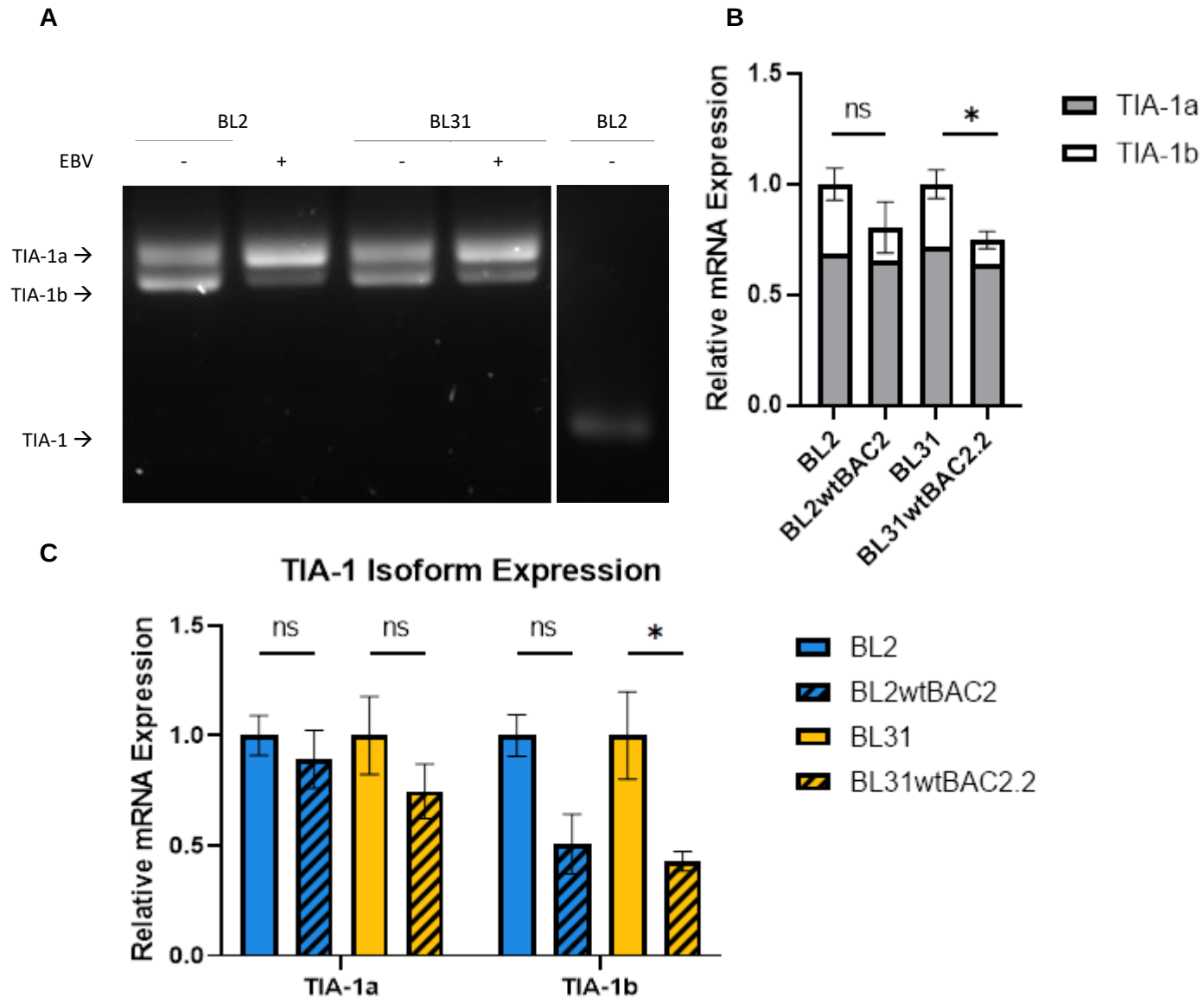

Figure 5-4 TIA-1b mRNA levels are lower in latent EBV⁺ cells. (A) RNA was extracted from EBV- BL2, BL31, and EBV+ BL2 and BL31 and synthesised to cDNA. qPCR was performed using primers spanning exon 5 and final products were separated on 2% agarose gel electrophoresis. Right panel represents isoform primer control, using primers that do not span isoforms and EBV- BL2 cDNA. **(B)** Quantification of qPCR performed on BL2 and BL31 EBV+/- using non-isoform specific primers, and the quantification of (A) representing the isoform ratio. **(C)** qPCR analysis of samples from (B) using isoform specific primers. **(B & C)** mRNA levels were normalised against GAPDH and relative to uninfected sample. Error bars represent s.e.m. n=3 (Two-way ANOVA, ns = P > 0.05, * = P ≤ 0.05, ** = P ≤ 0.01, *** = P ≤ 0.001, **** = P ≤ 0.0001).

5.2.3 Stability of TIA-1 protein and mRNA

Interestingly, the lower levels of TIA-1 mRNA in latent EBV infected cells suggest that the virus may be affecting the transcription of the gene, or promoting mRNA degradation. To assess this, first, the differences between TIA-1 pre-mRNA and mRNA were investigated. Primers spanning either from an intron into an exon for pre-mRNA, or across two exons for mRNA, were designed to detect differences in pre-mRNA and mRNA levels. If mRNA decay is occurring due to the virus, pre-mRNA levels will be similar in both EBV^- and EBV^+ cell lines, whilst as shown previously, TIA-1 mRNA levels will decrease in EBV^+ cell lines.

TIA-1 mRNA levels were once again shown to be lower in latent EBV infected cells than non-infected cells, whilst interestingly pre-mRNA exhibited two different profiles in each cell line (Figure 5-5). BL2 shows a transcriptional control profile, in which TIA-1 pre-mRNA is lower in EBV^+ cells, compared to EBV^-, similar to the mRNA, suggesting that the gene is being transcriptionally controlled. However, in BL31 the profile suggests that the mRNA is being decayed, as TIA-1 pre-mRNA levels are similar in EBV^+ and EBV^- cells, suggesting that transcription of the gene is occurring at the same rate in each cell line, however, the virus is promoting mRNA decay.

To further assess this, the mRNA decay profiles of each cell line and their latent EBV counterpart were examined. Actinomycin D (ActD) is a potent transcription inhibitor that prevents the unwinding of DNA, inhibiting RNA polymerase, and is commonly used to assess mRNA decay (Avendaño & Menéndez, 2008; Ratnadiwakara & Änkö, 2018). Each cell line was exposed to ActD before TIA-1 mRNA levels were monitored over 24 hours. Figure 5-6 shows the level of TIA-1 mRNA remaining throughout this experiment, along with isoform-specific mRNA levels of TIA-1a and TIA-1b. Figure 5-6A shows that mRNA degradation of both BL2 and BL31 is similar across 24 hours, BL2wtBAC and BL31wtBAC exhibit a slower degradation of TIA-1 mRNA. This difference is amplified

with TIA-1b mRNA, in which both EBV-infected cell lines, exhibit a slower degradation of TIA-1b mRNA than the uninfected cell lines (Figure 5-6C). Interestingly, TIA-1a mRNA degradation in BL2wtBAC is similar to both uninfected cell lines, whilst BL31wtBAC is slower. However, due to the complexity of this experiment, only one biological replicate was obtained for each sample, therefore any differences may only be considered initial data and not be over-examined without further investigation.

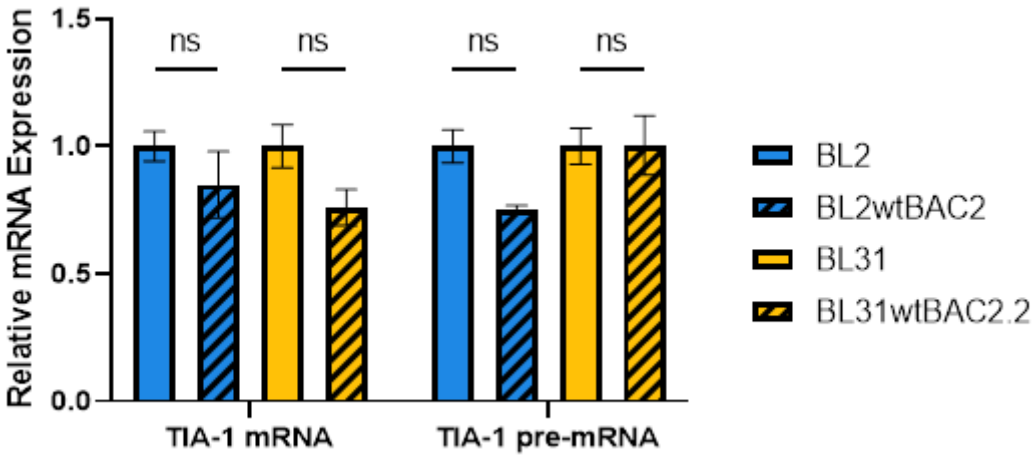

Figure 5-5 mRNA degradation is promoted by latent viral infection in BL31, but not in BL2. qPCR analysis showing TIA-1 mRNA and pre-mRNA levels in BL2 and BL31 along with EBV positive counterparts. Normalised against GAPDH and expression relative to uninfected samples. Error bars represent s.e.m. n=3 (Two-way ANOVA, ns = P > 0.05).

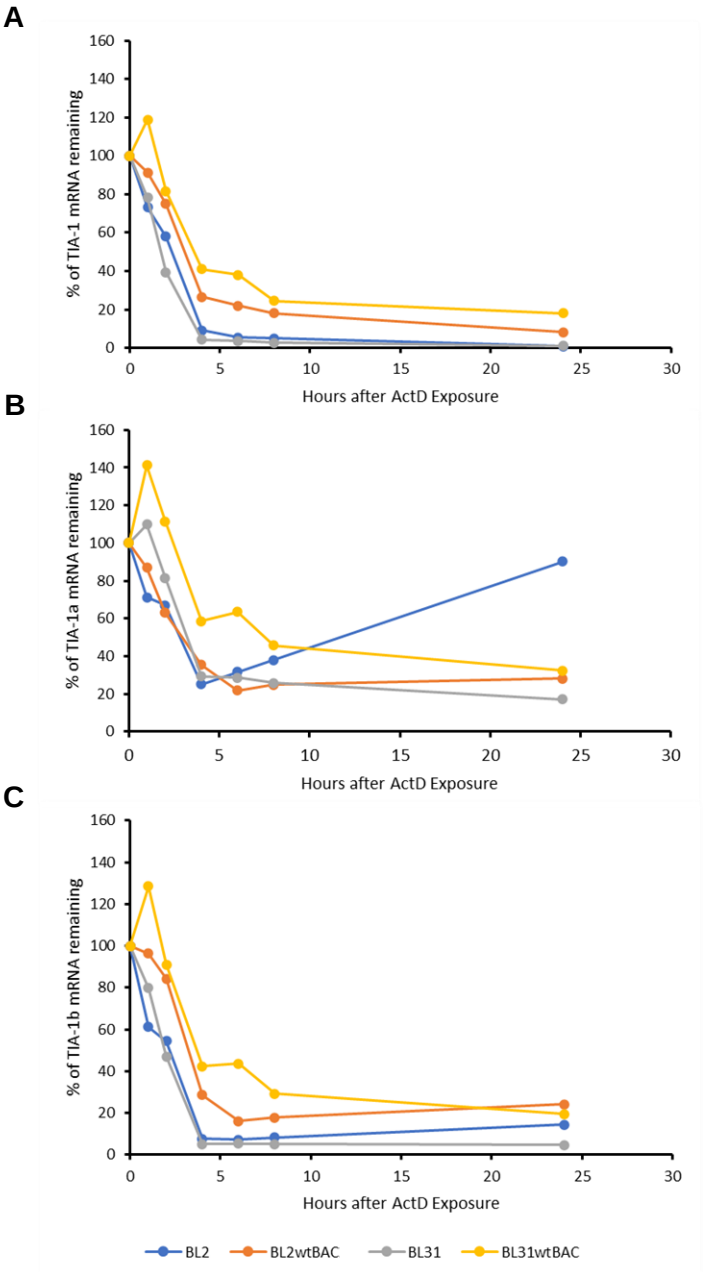

Figure 5-6 Degradation of TIA-1 mRNA is unchanged during latent infection. qPCR analysis following ActD (5 µg/ml) treatment of BL2, BL31 and EBV + counterparts, BL2wtBAC and BL31wtBAC. RNA extractions were performed over a series of time points for 24 hours, before cDNA synthesis and qPCR was performed using primers for TIA-1 (A), TIA-1a (B) and TIA-1b (C), normalised against 18S rRNA. mRNA levels were standardized against time 0 as 100% expression. n=1.

Finally, TIA-1 protein stability was assessed to determine whether latent EBV infection promoted increased degradation of TIA-1. Cycloheximide is a commonly used drug that inhibits protein synthesis, through the interference of translocation and blocking elongation, allowing for protein stability after inhibition to be assessed (Obrig et al., 1971; Schneider-Poetsch et al., 2010). TIA-1 protein levels were determined periodically over time, following treatment with cycloheximide. It was shown that TIA-1 proteins had a similar level of stability between uninfected and infected cell lines, suggesting that the decrease in TIA-1 protein levels in infected cells was not down increased protein instability promoted by the virus (Figure 5-7). C-myc was used as a positive control to show that protein synthesis had been inhibited, as this protein has a short half-life of 20 – 30 minutes (Salghetti et al., 1999), which can be seen in each cell line in this experiment.

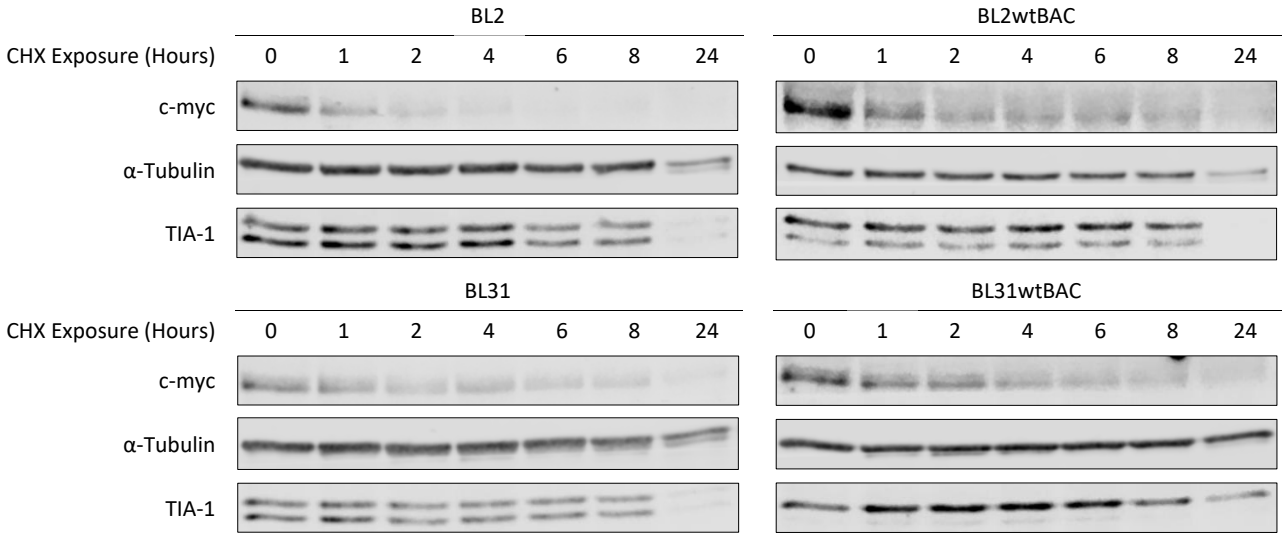

Figure 5-7 TIA-1 protein stability is similar between latently infected and uninfected cells. Western blot analysis of BL2, BL2wtBAC2, BL31 and BL31wtBAC2.2 over 24 hours following cycloheximide treatment (33 µg/ml). Protein was extracted over 24 hours and resolved on 10% SDS-PAGE. WB was performed using antibodies probing from TIA-1, along with α-Tubulin as loading control, and c-myc as protein synthesis inhibition positive control**.**

5.2.4 TIA-1 regulation by HuR

We next aimed to investigate how TIA-1 isoforms may be regulated during latent EBV infection. It is well understood that TIA-1 can regulate alternative splicing (Del Gatto-Konczak et al., 2000; Förch et al., 2000, 2002) and had previously been shown to be regulated by TIAR (Izquierdo & Valcárcel, 2007b). While our previous data had shown that TIAR does not change in response to latent EBV infection, we speculated that another RBP may have the ability to regulate TIA-1. TIA-1 has also been shown to self-regulate isoform expression, in which overexpression of one isoform altered levels of several other TIA-1 isoforms (Le Guiner et al., 2001).

Another RBP linked to cellular stress is Hu antigen R (HuR), that associates with the 3' UTR of mRNA, promoting stability (Tran et al., 2003), and is a known component of SGs (Jain et al., 2016). Interestingly, HuR was alternatively spliced in response to EBV infection (Homa et al., 2013). It was also revealed to work in tandem with TIA-1 and TIAR in the alternative splicing of SIRT1, a protein linked to metabolism and stress response (W. Zhao et al., 2014). It was shown that HuR promoted exon exclusion within SIRT1 mRNA, whilst TIA-1 and TIAR inhibited exon exclusion. In addition, it was shown that HuR and TIA-1 regulation was tightly associated, with lower HuR decreasing TIA-1 levels, whilst lower TIA-1, increased HuR levels (Tomoko Kawai et al., 2006).

A previous study had shown that HuR isoforms were altered upon latent EBV infection, in which the shorter isoform was preferentially expressed over the longer isoform in proliferating lymphoblastoid cell lines (Homa et al., 2013).

Figure 5-8 shows the mRNA expression levels of HuR in the form of all isoforms, and only the long isoform, along with TIA-1 levels. BL31 and EBV^+ BL31wtBAC express similar levels of both HuR total and HuR long, suggesting that there is no difference in isoform expression following EBV infection. This, however, is not replicated in BL2, where total HuR levels are slightly decreased in EBV^+ BL2wtBAC, but HuR long isoform

levels are significantly decreased, suggesting that the difference is made up by the short isoform. The difference between each cell line does not allow for any conclusions to be made, while data for BL2 would suggest that the virus may be promoting the preferential splicing of the shorter HuR isoform over the longer, BL31 suggests that there is little difference between isoform sizes in infected and uninfected cells.

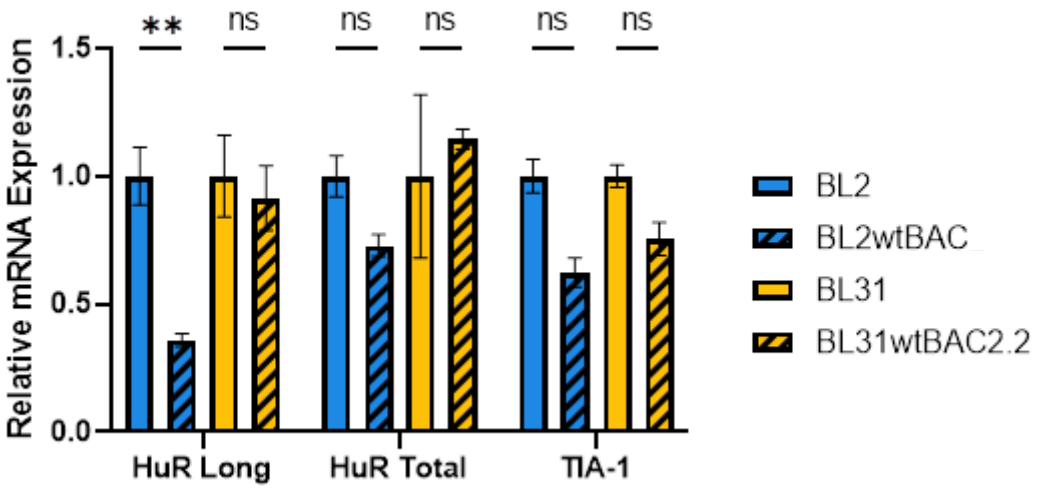

Figure 5-8 HuR mRNA expression is altered by latent viral infection. mRNA levels of total HuR and HuR long isoform were determined through qPCR, normalised against GAPDH, in cDNA samples synthesised from RNA extracted in BL2 and BL31 EBV-/+. TIA-1 mRNA was used as a comparison. mRNA levels were found relative to uninfected samples. Error bars represent s.e.m. n=3 (Two-way ANOVA, ns = $P > 0.05$, * = $P \leq 0.05$, ** = $P \leq 0.01$, *** = $P \leq 0.001$, **** = $P \leq 0.0001$).

5.2.5 TIA-1 knockout

The next process of this study was to create a TIA-1 knockout in an adherent cell line, investigate the effect that this has, as well as provide a TIA-1$^-$ cell line that each isoform may be transfected into. A successful technique had previously been demonstrated by Prof. Thomas Tuchel, using a CRISPR-Cas9 plasmid, containing gRNA targeting TIA-1 (Meyer et al., 2018). This plasmid also contained eGFP allowing for cells that had successfully taken up the plasmid to be sorted via FACS. The process and plasmid (PX458_2A_GFP_sgRNA_TIA1) were adopted for our study.

Following transfection of the plasmid into HEK293 cells, along with a negative control using just the backbone plasmid (PX458), the cells were sorted to ensure only cells containing the plasmid remained. Four colonies were selected from the TIA-1 KO samples (KO1-4), and one negative control (KO0) and the gDNA was extracted and the regions covering the gRNA were amplified. The sequencing obtained following this amplification is shown in Figure 5-9A. The sequencing primer ran right to left, revealing that once it passes the PAM site on each KO sample, several errors occur in the sequence, whilst the negative control resembles the expected genomic sequence (top line). This would suggest that a cut was induced, and errors were created in all KO samples. The PCR products were run on a DNA gel to visualize any differences in size caused by CRISPR, however, as shown in Figure 5-9B, there are no clear differences between the KO samples and the NC.

Next, the protein expression was investigated to determine whether the errors induced by the CRISPR had promoted the degradation of the mRNA. Interestingly, when TIA-1 was probed for using the monoclonal antibody (ab140595) that has been used throughout this experiment, no TIA-1 was seen in any of the KO samples, and remained in the negative control, KO0 (Figure 5-9C). However, to ensure that the protein was knocked out, rather than the antibody is unable to bind to the altered sequence, a

polyclonal antibody was used (sc-1751). Following incubation with this antibody, clear bands can be seen in all KO samples, suggesting that TIA-1 remained in these samples.

The mRNA data, obtained by qPCR of these samples, also suggested that TIA-1 mRNA remained present following KO (Figure 5-9D). The mRNA levels of TIA-1, TIA-1a and TIA-1b, in KO1-3, were relatively similar to those obtained for KO0 suggesting expression of the TIA-1 gene is the same. KO4 however, shows a consistent decrease in TIA-1 expression, between isoforms and total compared to the negative control. This would suggest that the mRNA has decreased, but a certain level of expression remains. This decrease of 0.5-fold may suggest that this is a heterozygous knockout, in which the gene is knocked out in one allele but remained in the other.

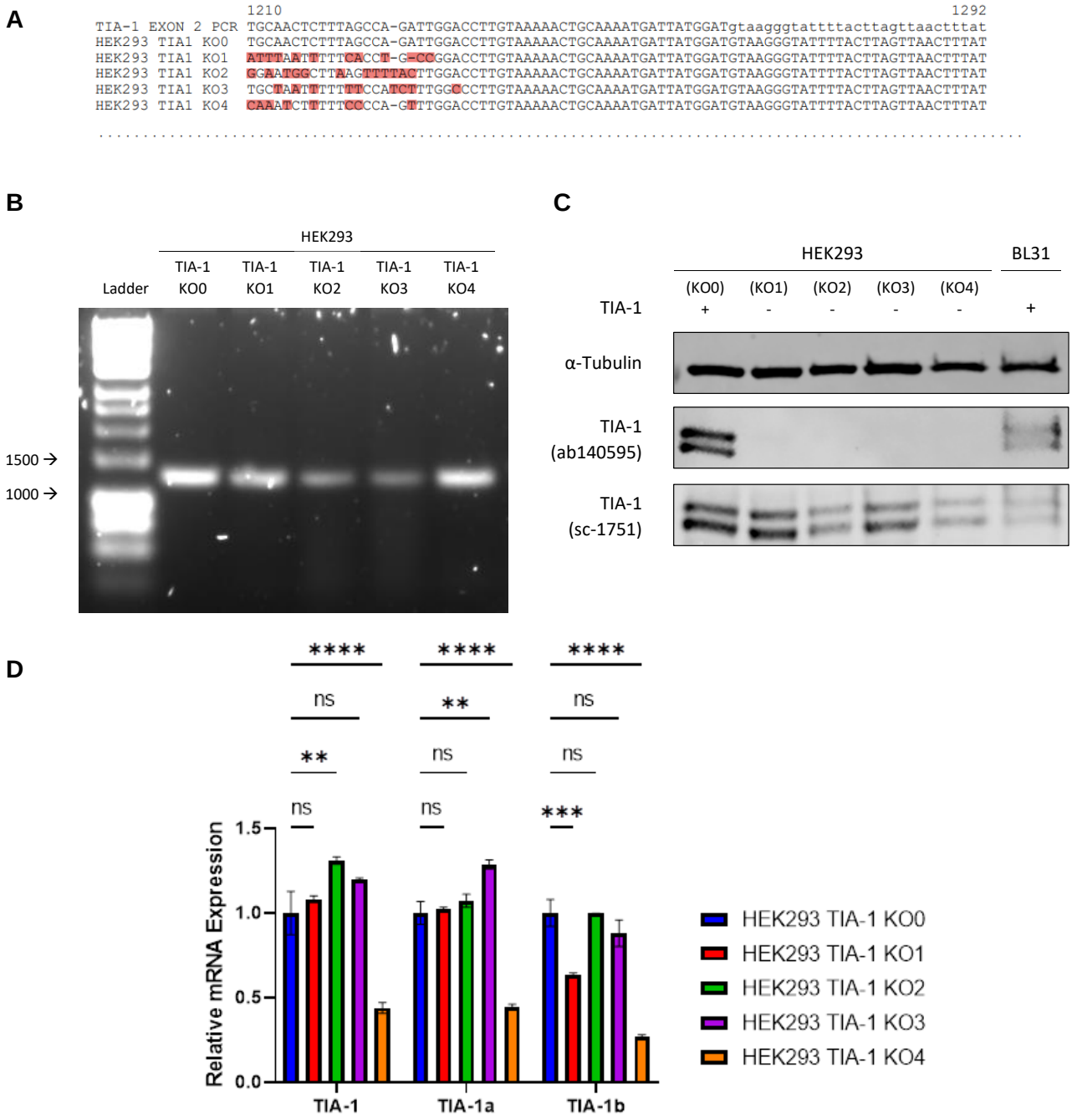

Figure 5-9 Knockout of TIA-1 in HEK293 cells. (A) gDNA was extracted from HEK293 cells that had either been transfected with CRISPR vector lacking gRNA (KO0) or containing gRNA targeting TIA-1 (KO1-4). PCR amplified across gRNA cut site at exon 2 and products were sequenced. First line represents the template, and mismatches are shown in red. **(B)** PCR products obtained from (A) were separated on 0.8% agarose gel with the expected product size of 1288 bps. **(C)** Protein was extracted from each transfected sample and resolved on 10% SDS-PAGE along with positive TIA-1 control, BL31. Samples were immunoblotted with antibodies against TIA-1, monoclonal (ab140595) and polyclonal (sc-1751) along with loading control, α-tubulin. **(D)** cDNA was synthesised from RNA extracted from each sample and amplified using qPCR. mRNA levels of TIA-1a, TIA-1b and TIA-1 were normalised against GAPDH and set relative to NC sample (KO0). Error bars represent s.e.m. n=1 (Two-way ANOVA, ns = $P > 0.05$, * = $P \leq 0.05$, ** = $P \leq 0.01$, *** = $P \leq 0.001$, **** = $P \leq 0.0001$).

Although the results thus far had suggested that the KO was not successful, the cells were taken forward for further analysis. It has been previously suggested that cells lacking TIA-1, exhibited impaired SG formation (Gilks et al., 2004). Therefore, using G3BP1 as a marker, it can be seen if the KO cells maintained SG function. Figure 5-10 reveals that, as expected, the NC cell line exhibits normal SG function in response to arsenite and hippuristanol-induced stress. The KO cell line (KO1) also shows SG formation in response to arsenite and hippuristanol, shown by the presence of G3BP1 foci. The TIA-1 signal in the KO cell line is noticeably weaker than the NC, likely due to inefficient binding of the antibody, however, faint SG foci can still be seen.

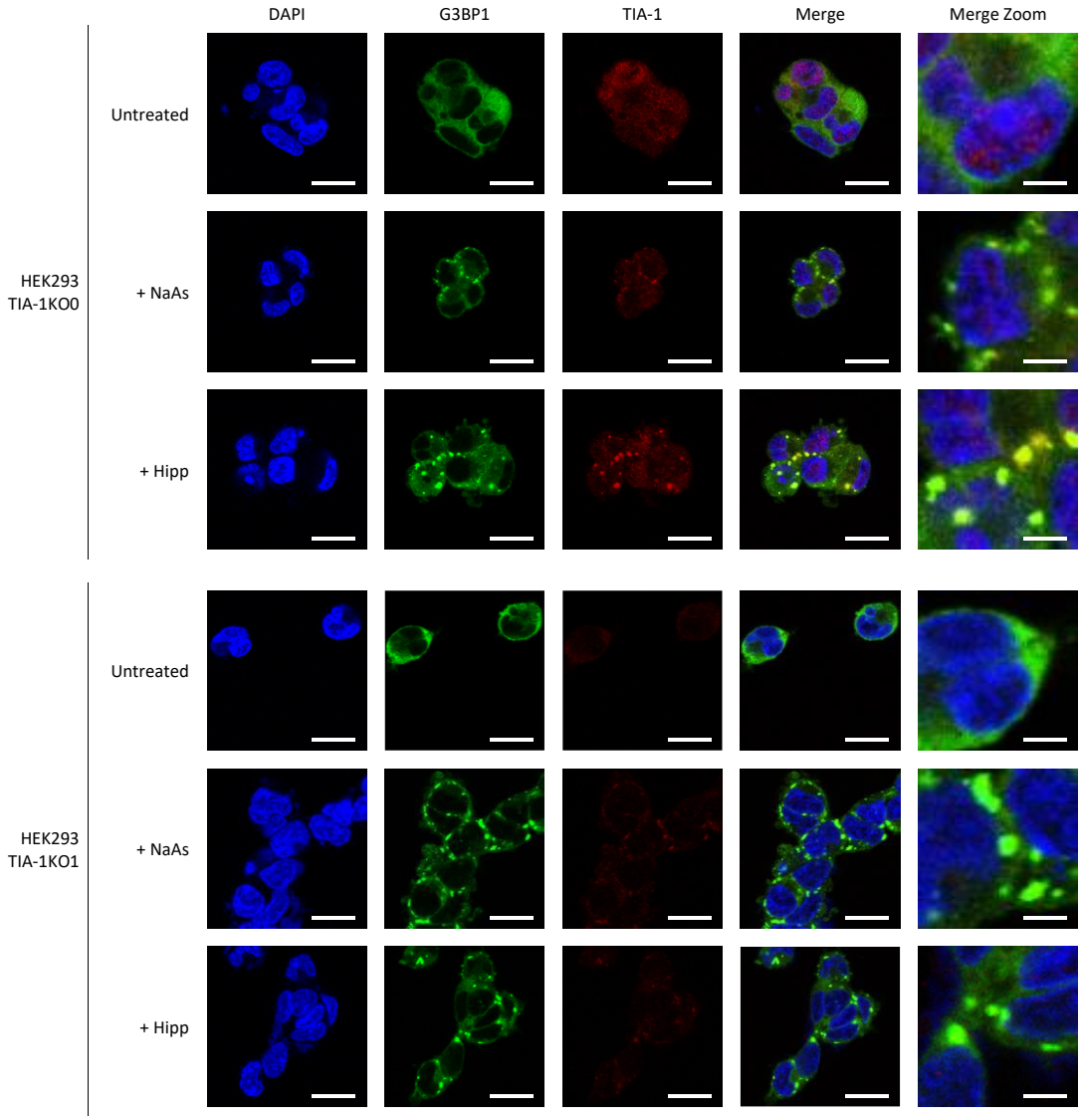

Figure 5-10 SGs still form in samples transfected with TIA-1 gRNA. SG markers TIA-1 and G3BP1 were used to show the presence of SGs following stress. HEK293 cells, either transfected with CRISPR vector lacking gRNA (KO0) or containing gRNA targeting TIA-1 (KO1) were incubated with NaAs (0.5mM), hippuristanol (1 µM) or water (untreated) for 45 minutes before fixation and permeabilization. Cells were stained for G3BP1 (green) and TIA-1 (red) using corresponding antibodies and imaged using confocal microscopy. The nuclei were stained using mounting media containing DAPI. Scale bar = 20 µm, Zoom scale bar = 5 µm.

Concurrent with these experiments, the expression of TIA-1a and TIA-1b was investigated. Using a previously published expression vector for TIA-1b (pFRT_TO_eGFP_TIA1) (Meyer et al., 2018), we suggested that TIA-1a and/or TIA-1b could be expressed back into cells lacking TIA-1, and the effects on the cell investigated.

pFRT_TO_eGFP_TIA1 was renamed pFRT_TO_eGFP_TIA1b (pTIA-1b), as the sequence lacked exon 5 and therefore expressed TIA-1b, and an additional vector using this plasmid as a backbone and including exon 5 was designed named pFRT_TO_eGFP_TIA1a (pTIA-1a), as in would express the longer TIA-1a isoform (Figure 5-11A). pTIA-1a was created through mutagenesis, using primers containing exons 5 and overlapping the original plasmid. Due to the complexity of the mutagenic primer, the manufacturer's protocol (Q5 Mutagenesis Kit; QIAGEN) was unable to provide a product, however, following lowering of the extension temperature, the vector was amplified, visualised on the DNA gel shown in Figure 5-11B. The plasmids were sequenced and the region covering exon 5 was compared to both target sequences (Figure 5-11C). The sequence of the plasmids confirms the presence (TIA-1a) and exclusion (TIA-1b) of exon 5.

A

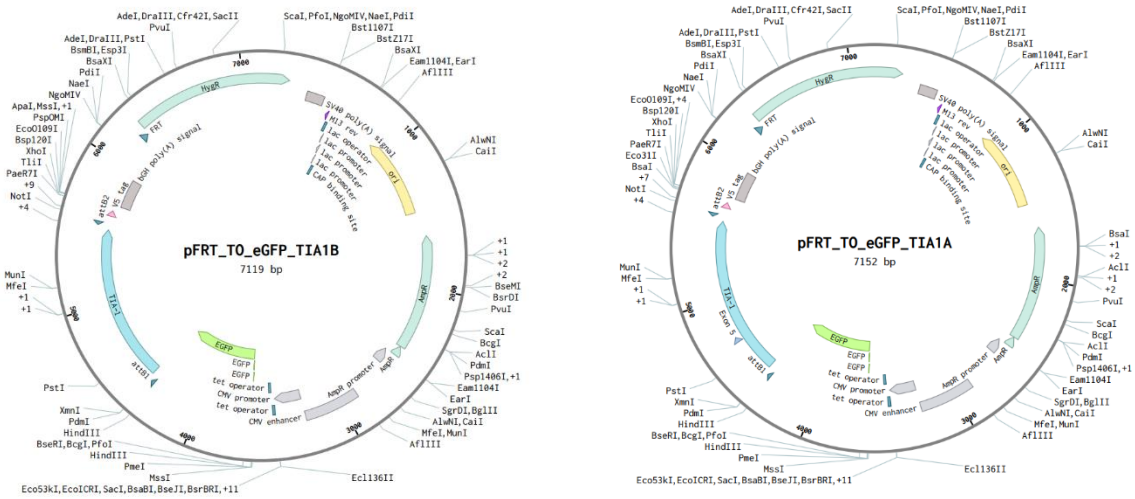

B

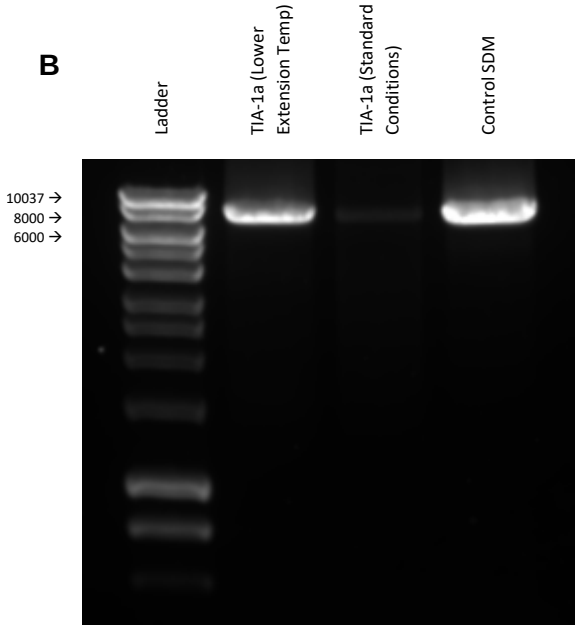

C

```
                                4628                                4677
pFRT_TO_eGFP_TIA1B              agtcaaagtgaattgggcaacaacccctagcagtcaaaagaaagatacaa
Plasmid - pFRT_TO_eGFP_TIA1B    AGTCAAAGTGAATTGGGCAACAACCCCTAGCAGTCAAAAGAAAGATACAA
pFRT_TO_eGFP_TIA1A              agtcaaagtgaattgggcaacaacccctagcagtcaaaagaaagatacaa
Plasmid - pFRT_TO_eGFP_TIA1A    AGTCAAAGTGAATTGGGCAACAACCCCTAGCAGTCAAAAGAAAGATACAA

                                4678                                4727
pFRT_TO_eGFP_TIA1B              gca---------------------------------atcatttccatgtc
Plasmid - pFRT_TO_eGFP_TIA1B    GCA---------------------------------ATCATTTCCATGTC
pFRT_TO_eGFP_TIA1A              gcAGTAGTACCGTTGTCAGCACACAGCGTTCACAAGATcatttccatgtc
Plasmid - pFRT_TO_eGFP_TIA1A    GCAGTAGTACCGTTGTCAGCACACAGCGTTCACAAGATCATTTCCATGTC

                                4728                                4777
pFRT_TO_eGFP_TIA1B              tttgttggtgatctcagcccagaaattacaactgaagatataaaagctgc
Plasmid - pFRT_TO_eGFP_TIA1B    TTTGTTGGTGATCTCAGCCCAGAAATTACAACTGAAGATATAAAAGCTGC
pFRT_TO_eGFP_TIA1A              tttgttggtgatctcagcccagaaattacaactgaagatataaaagctgc
Plasmid - pFRT_TO_eGFP_TIA1A    TTTGTTGGTGATCTCAGCCCAGAAATTACAACTGAAGATATAAAAGCTGC

                                4778          4796
pFRT_TO_eGFP_TIA1B              ttttgcaccatttggaaga
Plasmid - pFRT_TO_eGFP_TIA1B    TTTTGCACCATTTGGAAGA
pFRT_TO_eGFP_TIA1A              ttttgcaccatttggaaga
Plasmid - pFRT_TO_eGFP_TIA1A    TTTTGCACCATTTGGAAGA
```

Figure 5-11 Development of TIA-1a and TIA-1b expression vectors. (A) pFRT_TO_eGFP_TIA1B vector was obtained from Addgene and expresses eGFP-TIA-1b. Mutagenesis was performed on this plasmid, using NEB Q5 mutagenesis kit, to include the missing exon 5 creating pFRT_TO_eGFP_TIA1A, the expression vector for eGFP-TIA1b. **(B)** NEB Q5 mutagenesis kit was used to incorporate primers including exon 5 into the amplification of the plasmid, before the original backbone was digested by DpnI. Standard PCR conditions did not provide a product, and instead extension temperatures were lowered due to AT rich primers. Control SDM represents mutagenesis control. **(C)** pFRT_TO_eGFP_TIA1A and pFRT_TO_eGFP_TIA1B plasmids were sequenced and aligned against the expected products, focussing on exon 5 region.

Finally, these expression plasmids were used to induce TIA-1a and TIA-1b in the knockout sample, KO1. Whilst the polyclonal antibody had revealed the presence of TIA-1 within KO1, the original antibody was used to optimise this technique with these cell lines for future use.

TIA-1 on each expression vector was associated with eGFP, which not only allowed for cells to be sorted but provided a variation in size against endogenous TIA-1. Figure 5-12 shows the protein expression of TIA-1 following transfection of each plasmid into the KO1 cell line. TIA-1 presents as the familiar multiple isoform bands in wt HEK293 cells, whilst is absent in all conditions in KO1 cells (Figure 5-12A). Following transfection of either TIA-1a or TIA-1b, a larger TIA-1 product is observed, representing the eGFP-associated protein. Whilst the transfected negative cells, do not show a TIA-1 product at either endogenous sized TIA-1 or eGFP associated. This data was quantified (Figure 5-12B) showing that TIA-1a expression was greater than TIA-1b in the transfected samples.

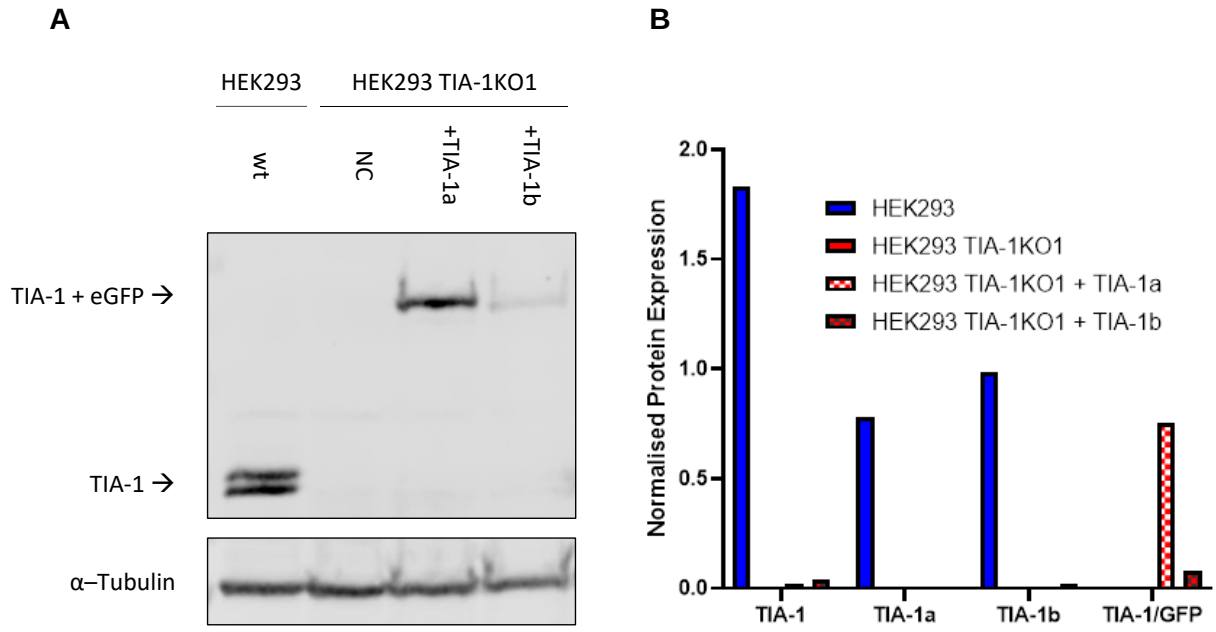

Figure 5-12 TIA-1a/b can be expressed in HEK293 cells. (A) HEK293 TIA-1KO1 cells were transfected with pFRT_TO_eGFP_TIA1A (+TIA-1a), pFRT_TO_eGFP_TIA1B (+TIA-1b) or without a vector (NC) for 48 hours. Samples containing the vectors were FACS sorted to only contain GFP+ cells. Protein was extracted from each sample, along with wt HEK293 cells and resolved on 10% SDS-PAGE gel before immunoblotting against TIA-1 and loading control, α-tubulin. **(B)** Quantification of WB (A) showing protein levels of TIA-1, TIA-1a, TIA-1B and eGFP-TIA-1(a/b) normalised against α-tubulin. n=1.

5.3 Discussion

TIA-1 has several functions within the cell. Firstly, regarding stress, TIA-1 is a key SG protein and is a constitutive component. It has been demonstrated that overexpression of TIA-1 can induce the formation of SGs, whilst depletion of TIA-1 prevents their accumulation (Gilks et al., 2004; Kedersha et al., 1999, 2000). TIA-1 has also been shown to be involved in translational silencing through association with mRNA to maintain a repressed state (Yamasaki et al., 2007). Third, and potentially most relevant in this chapter, TIA-1 can function as a regulator of alternative splicing (Förch et al., 2000; Smith & Valcárcel, 2000). Finally, it has also been shown that TIA-1 expresses both tumour suppressor and oncogenic functions (Carrascoso et al., 2018; Hamada et al., 2016; Sánchez-Jiménez et al., 2015).

The results presented in this chapter, show a significant decrease in TIA-1 protein expression following latent EBV infection, compared to uninfected cells (Figure 5-2). Whilst this decrease is shown in total TIA-1 levels (encompassing all isoforms), it is TIA-1b specifically that exhibits this decrease. This decrease was also shown in the mRNA (Figure 5-4), in which overall levels of TIA-1 mRNA were lower in latent EBV-infected cells, but the larger isoform was preferentially spliced maintaining similar levels to the uninfected cell line. Furthermore, the lack of an mRNA degradation phenotype in EBV infected cells (Figure 5-5, Figure 5-6), suggests that TIA-1 is transcriptionally controlled, to reduce mRNA in EBV infection, and TIA-1a is preferentially spliced over TIA-1b, resulting in similar levels of TIA-1a, but lower levels of TIA-1b compared to uninfected cells. A protein degradation phenotype, in which EBV promoted the increased degradation of TIA-1 was also ruled out following treatment with cycloheximide (Figure 5-7), as TIA-1 protein half-life did not change between EBV^+ and EBV^- cells.

This study originally aimed to investigate the role in which SGs played in EBV infection, however, our finding that TIA-1 mRNA was lower in latent EBV infected cells, compared

to uninfected samples, correlated to data showing TIA-1 levels differ in EBV^+ and EBV^- BL patient samples (Kaymaz et al., 2017). Further investigation concluding that it is TIA-1b levels that are lower whilst TIA-1a remained similar, caused us to speculate that this may contribute to EBV-associated oncogenesis. It is understood that latent EBV promotes the proliferation of B cells, and evades apoptosis, mechanisms that are commonly associated with cancer development (Price et al., 2017). To understand how this may link to each isoform of TIA-1, the first question that was asked, was how might TIA-1b depletion benefit the latent virus.

Whilst TIA-1a and TIA-1b differ by one exon, only 33 bp in length, their function appears to differ somewhat (Izquierdo & Valcárcel, 2007b). As a regulator of alternative splicing, TIA-1 can affect many mechanisms by promoting a variety of splicing products (Förch et al., 2000). It was shown that TIA-1a and TIA-1b display distinct splicing activity (Izquierdo & Valcárcel, 2007b). Other RBPs have also been shown to have alternate isoform functions. AUF1, a key factor associated with mRNA stability and decay, was found to have differing RNA binding potential, and specificity, depending on the inclusion/exclusion of a 19 amino acid region (Kajita et al., 1995; Loflin et al., 1999; Pullmann et al., 2007; Xu et al., 2001). It may be speculated that isoform specificity may be a feature of several other RBPs, to regulate a large number of functions relating to mRNA turnover and translation.

TIA-1 specific isoform function appears to have a dramatic difference regarding tumour suppression. TIA-1a was shown to promote proliferation and have an oncogenic function, while TIA-1b inhibited cell proliferation and induced cell death (Hamada et al., 2016). Current research is only beginning to investigate TIA-1 isoform-specific roles in cancer, with many previous studies concluding that TIA-1 is a tumour suppressor (Hamdollah Zadeh et al., 2015; Izquierdo et al., 2011; Tian et al., 1991). It was shown that depletion of TIA-1 increased cell proliferation, whilst the addition of TIA-1 promotes apoptosis (Reyes et al., 2009; Tian et al., 1991). It is thought to exert its tumour

suppressor function through regulation of oncogenes inhibiting proliferation, whilst promoting apoptosis through alterative splicing of Fas, a key death receptor within the cell (Izquierdo et al., 2005; Reyes et al., 2009). Interestingly, regulation of Fas splicing has been shown to be associated with TIA-1b (Izquierdo & Valcárcel, 2007a, 2007b). TIA-1b promotes the inclusion of Fas exon 6, which is involved a positive feedback loop inducing increased levels of proapoptotic forms of Fas. TIA-1a on the other hand promoted exclusion of this exon, decreasing apoptosis. In contrast, TIA-1 has also been shown to promote tumour activity (Hamada et al., 2016). This group found that knockdown of TIA-1 inhibited proliferation and suggested that TIA-1 increased tumour activity through the regulation of several cancer-associated transcripts. However, this study concluded that it was TIA-1a responsible for this oncogenic activity, whilst TIA-1b inhibited proliferation and promoted apoptosis.

The conflicting function of each isoform may exist as a fragile balance between a tumour suppressor and oncogenic mechanism, which latent EBV may alter to benefit its replication. The loss of TIA-1b and its inhibitory effect on cell proliferation would aid EBV replication, allowing the virus to spread as cells divide. However, this may also promote the development of EBV-associated cancer, through the loss of a tumour suppressor gene, leaving only the oncogenic TIA-1a isoform.

The next process was to determine how TIA-1 expression and splicing were regulated. Interestingly, it has been shown that several RBPs, linked to mRNA turnover and translation, including AUF1, TIAR, HuR and TIA-1, may control their expression (Pullmann et al., 2007). Furthermore, HuR isoform expression was affected by EBV infection, along with 23 other RBP (Homa et al., 2013). This study revealed that latent EBV, confirmed through the presence of latent protein LMP1, promoted the expression of a shorter HuR isoform containing a smaller 3’ UTR. However, it remains unclear as to whether this is just a response to the stress caused by proliferating cells or a direct effect of the virus. Previously, it had been revealed that cellular stress, including arsenite-

induced stress, can promote the global shortening of 3’ UTRs (Zheng et al., 2018). This process of expressing alternative 3’ UTR isoforms is controlled by either alternative polyadenylation, a process involving alternative cleavage and polyadenylation, or alternative splicing of the last exon (Mattioli et al., 2019; Wu et al., 2011). The effect that preferential expression of the shorter 3’ UTR has on HuR function remains inconclusive; however, this would likely prevent binding and therefore regulation by other RBPs, either promoting or repressing translation of the protein.

TIA-1 expression was found to be controlled by at least two other RBPs, including HuR (Pullmann et al., 2007). HuR and TIAR were shown to bind to TIA-1 transcripts and either promote expression or repress translation respectively. While data shown in this chapter reveals that TIAR protein expression of either isoform does not change in response to latent EBV infection (Figure 5-3), HuR isoform mRNA expression does (Figure 5-8). This data reinforces the study by Homa et al. (2013), showing the preferential expression of HuR consisting of a shorter 3’ UTR.

It was shown that TIA-1 can bind more efficiently to longer 3’ UTRs, and, coming back to the original aim of this project, binding efficiency correlated to an increased association with SG assembly (Zheng et al., 2018). This group found that mRNA with longer 3’UTRs facilitated binding to TIA-1, which in turn promoted efficient recruitment to SGs.

HuR and TIA-1 have been linked in multiple studies. One study found that reduction in HuR caused a decrease in TIA-1 protein levels, whilst silencing of TIA-1 increased HuR and speculated on a potential negative feedback loop (Tomoko Kawai et al., 2006). This study also confirmed that HuR and TIA-1 were able to bind the mRNA of the other. Due to the nature of RBP, binding likely occurred in the 3’UTR of the mRNA, and shortening this would potentially prevent binding. Pullmann et al. (2007) also observed that HuR directly regulates TIA-1 protein levels.

A potential mechanism of action may occur in the preferential expression of shorter 3' UTRs. The expression of shorter HuR 3' UTRs may reduce SG formation in latent EBV-infected cells. As shown in previous chapters, latent EBV infection is not sufficient to promote SG assembly. Reduced binding of TIA-1 and HuR may play a factor, along with previously discussed mechanisms, in inhibiting SG assembly.

Whether or not HuR 3' UTR shortening plays a role in TIA-1a protein expression remains unclear. If the shortening of the 3' UTR reduces the function of HuR, it could be suggested that this, as shown in previous studies, would decrease TIA-1 levels. However, this requires further research to fully understand.

Finally, in this chapter a method for determining the effect that decreased TIA-1 has on mRNA regulation and protein expression was examined. Firstly, a knockdown was performed, to investigate any changes that might occur to several target genes and proteins. The data presented in this chapter, show the effect that TIA-1 siRNA has on both BL31 and EBV-infected BL31wtBAC (Figure 10-5). TIA-1 protein levels decrease but are not entirely silenced. Furthermore, following qPCR, no change in mRNA levels was detected in any of the siRNA-treated cells. Therefore, we suggested that a KO would be more efficient for this process. The proposed mechanism was to first KO global TIA-1, before reintroducing TIA-1a, TIA-1b or both as expression vectors. Each vector contained TIA-1a/b associated with GFP, which allowed for sorting via FACs and differentiation from endogenous TIA-1 in further analysis. The KO of TIA-1 has been shown previously using a vector containing Cas9, eGFP and the gRNA targetting TIA-1 (Meyer et al., 2018). Following transfection of this plasmid into HEK293 cells, FACS allowed for only cells that had taken in the vector to be sorted and grown into single colonies. Of the four colonies chosen for initial sequencing, all displayed mutations and errors after the PAM site (Figure 5-9A). As this CRISPR plasmid contained only one gRNA, it was expected to cut at one site (3 bps upstream from the PAM site) and

following non-homologous end joining, several errors be created promoting a loss of function mutation.

The data shown in the DNA gel, reveals no large size difference in each KO sample, compared to the negative control (Figure 5-9B). The most intriguing part of this experiment was shown in Figure 5-9C, in which the monoclonal antibody, used throughout this project to detect TIA-1, did not show the presence of TIA-1 in the KO samples, whilst confirming TIA-1 in the negative control. To confirm that mutation had knocked out the gene, rather than just interfered with the antibody epitope, additional probing using a polyclonal antibody was performed, which revealed TIA-1 within all samples. As the polyclonal antibody binds to multiple epitopes within TIA-1, this was still able to bind to the protein and produce a signal. Therefore, it can be concluded that each mutation created on the KO samples, caused an interference with the epitope of the monoclonal antibody, but did not knock out the gene.

Next, the mRNA levels were investigated, to confirm whether any decrease in gene expression had occurred (Figure 5-9D). KO samples 1-3 revealed no differences in TIA-1a, TIA-1b or total TIA-1 mRNA expression compared to the negative control. KO4 however, did exhibit a 50% reduction in TIA-1a, TIA-1b and total TIA-1 mRNA expression. This would suggest that KO4 contains a heterozygous KO, in which the gene has been successfully silenced in one allele but remains in the other.

Following this, although mRNA and protein were revealed to not have been sufficiently reduced, SG function was examined. As the KO samples had shown interference with the epitope of the monoclonal antibody (targetting the C-terminal region), it was suggested that a conformational change may have occurred, affecting function. The data shown in Figure 5-10, shows that SG assembly still occurs in KO1. TIA-1 has been implicated as a vital SG assembly protein, and depletion of TIA-1 inhibits SG formation

(Gilks et al., 2004; Kedersha et al., 1999, 2000). Therefore, as in this experiment, SGs still form, and it can be concluded that TIA-1 is not being knocked out.

Whilst a successful knockout had not been obtained, the remainder of the experiment was still optimized. First, the expression plasmid containing TIA-1b was obtained (Meyer et al., 2018), and was modified to include exon 5 to express TIA-1a (Figure 5-11). Following the transfection of each vector into HEK293 KO1 cells, containing a mutation affecting epitope binding of the monoclonal antibody, it can be seen that each isoform is expressed (Figure 5-12). This method, along with further RNA-seq, and proteomics, may provide vital insight into how the loss of TIA-1b affects gene regulation, as latent EBV would.

6 Stress granule formation during lytic EBV infection

6.1 Introduction

Lytic phase is the viral phase in which the virus is actively replicating, producing infectious virions (Sixbey et al., 1983). Much like the other herpesviruses, EBV can enter the lytic cycle as well as latent. Lytic EBV infection, however, generally occurs during initial infection, actively replicating in oropharyngeal cells, before eventually reaching B cells and developing a persistent latent infection. This preferential progress into latency likely evades many antiviral responses of the host and contributes to EBV being one of the most abundant human viruses.

In contrast to the other herpesviruses, most lytic EBV infections are not considered to be associated with serious diseases (Kenney, 2007). The most common illness associated with primary infection and lytic EBV is infectious mononucleosis (IM) (Cohen, 2001; Jenson, 2000). IM is common in children and adolescents and causes fatigue, fever, pharyngitis, swelling of lymph nodes, and lymphocytosis, among other symptoms (Ebell, 2004).

Upon primary infection, the virus commonly infects epithelial cells whilst in lytic cycle before then infecting B cells and entering latency (Kenney, 2007). Whilst in B cells, the virus may be stimulated to be reactivated and enter lytic cycle (Odumade et al., 2011). Activation of lytic cycle from latent *in vivo* is not fully understood (Murata, 2014), however, it is thought to be linked to the differentiation of epithelial and B cells, potentially due to unrelated infections (Laichalk & Thorley-Lawson, 2005; Odumade et al., 2011; C. C. Sun & Thorley-Lawson, 2007; Tovey et al., 1978; L. S. Young et al., 1991).

There are three groups of lytic gene products, described by the phase in which they are expressed in lytic cycle, immediate-early (IE), early (E) and late (L) (Tsurumi et al., 2005). The IE genes, BZLF1 and BRLF1 (encoding for ZEBRA/Zta and Rta respectively) are

regularly expressed first, following lytic induction and act to facilitate the transcription of several E genes, driving entry into lytic cycle (G. Miller et al., 2007). Interestingly, when expressed alone, the transcription factor Zta is capable of inducing the complete replication cycle, including the production of infectious virions (Grogan et al., 1987), confirming the importance of this viral gene product in the activation of lytic phase. During lytic cycle, there is a wider range of viral gene products produced than latent, many of which are involved in the active replication of the virus and immune system evasion (Odumade et al., 2011; Quinn et al., 2014). The increased expression of viral products would suggest that this phase has the potential to activate the stress response, and require a mechanism to evade it.

Lytic cycle is inducible in several EBV cell culture *in vitro* systems, through the addition of several agents including phorbol 12-myristate 13-acetate (PMA) (Hausen et al., 1978), Ig cross-linking antibodies (Takada, 1984; Takada & Ono, 1989; Tovey et al., 1978), transforming growth factor β (TGF-β) (di Renzo et al., 1994), and transfection of BZLF1 or BRLF1 (Ragoczy et al., 1998). This provides several mechanisms that allow lytic cycle to be induced *in vitro* and for the effects of this viral phase to be investigated.

In other studies that have investigated the effects of SG formation and viral infection, the majority have looked at viruses that are actively replicating, rather than in a dormant phase such as latency exhibited by herpesviruses (J. P. White & Lloyd, 2012). Furthermore, studies that have investigated SG formation and herpesviruses specifically, near exclusively focus on lytic phase (Dauber et al., 2016; Finnen et al., 2016; Sharma et al., 2017; Ziehr et al., 2016). Sharma et al. (2017) briefly investigated latent KSHV effects on SG formation and found no differences between latent and uninfected cell lines but did find that lytic KSHV inhibited this process. Therefore, we raised the question as to whether this also occurred in EBV.

Studies relating to HSV-1 and HSV-2, have identified the lytic viral protein, virion host shut-off (VHS), as key to inhibiting the SG response within infected cells (Dauber et al., 2016; Finnen et al., 2016). VHS is an endoribonuclease encoded by the UL41 gene, that targets both host and viral mRNA, acting to shut off host translation and provide the mRNA access to translational machinery (Smiley et al., 2001). VHS was also revealed to target dsRNA limiting its accumulation and preventing activation of PKR and in turn SG formation (Dauber et al., 2016; Finnen et al., 2016). The ɣ-herpesviruses do not express a protein/gene homologous to VHS/UL41, however, the host shut-off function is adopted by the endonucleases SOX/BGLF5 (KSHV/EBV) (Glaunsinger & Ganem, 2004; Rowe et al., 2007). Interestingly, SOX was shown to inhibit SG formation (Sharma et al., 2017), presumably through a similar mechanism of dsRNA degradation to VHS, however, this remains to be determined. BGLF5 on the other hand had not been investigated regarding SG formation and is discussed later in this section.

Another viral lytic product implicated in SG evasion in herpesvirus was ORF57 (Sharma et al., 2017). ORF57 is a posttranscriptional regulator responsible for efficient KSHV gene expression (Majerciak & Zheng, 2015). Its roles include increasing RNA stability, promoting RNA splicing and promoting translation. Sharma et al. (2017) found that ORF57 blocked PKR activation and SG formation, through binding to both PKR and its activating protein, PACT, preventing activation of PKR and downstream signalling. The homologous protein in EBV is EB2 (SM), however, only shares 30% homology (Majerciak & Zheng, 2009). Interestingly, EB2 was shown to not inhibit SG formation (Sharma et al., 2017). In HSV-1, VHS and ORF57 homologue, ICP27, have been suggested to work together to confer specificity during host shut-off (Rowe et al., 2007; Taddeo et al., 2010). We speculated that BGLF5 and EB2 may be doing the same in SG inhibition.

6.2 Results

6.2.1 ZTA induces lytic cycle and inhibits SG formation in Zta-AK cells

This study first aimed to develop a means by which lytic cycle could be effectively induced providing a basis to investigate the role that the lytic virus has in stress granule formation.

Zta expression drives entry into lytic cycle and can be used to reactivate lytic EBV (Ramasubramanyan et al., 2015). A system had been previously described in which EBV^+ Akata cells contained a Zta expression vector under the control of a doxycycline-regulated promoter (Ramasubramanyan et al., 2015), and was kindly gifted to this study by Prof. Alison Sinclair. The expression vector contained a truncated neuronal growth factor receptor (NGFR), GFP, and either the BZLF1 gene (Zta) in the correct orientation or reversed, to act as a negative control, and was controlled by a bi-directional doxycycline-regulated promoter. NGFR allowed for the purification of cells expressing the vector, whilst GFP provided a means for visualisation. Akata cell lines expressing each vector were named Zta-AK (representing Zta in the correct orientation) and Rev-AK (representing Zta in the reverse orientation).

To assess the effectiveness of these cell lines, the initial process was to first confirm the expression of Zta in doxycycline-induced Zta-AK cells, and its absence in Rev-AK. Figure 6-1A shows Zta-AK and Rev-AK protein expression on a WB in the presence or absence of doxycycline. Following a significant overexposure, shown in the bleaching of the loading control α-tubulin, Zta expression is shown exclusively in Zta-AK following doxycycline treatment and remains absent in untreated Zta-AK and both conditions of Rev-AK. This suggests that Zta-AK is induced into lytic cycle following doxycycline treatment. To further assess this process, doxycycline-induced Zta-AK and Rev-AK were isolated using anti-NGFR antibodies coupled with magnetic beads. Cells in which the vector had been activated (positive bead) were able to be separated

from those containing the inactivated vector (negative bead). Zta expression following doxycycline induction can be seen in the isolated sample of Zta-AK, while a faint band is shown in the un-isolated (negative bead) sample, this is likely due to the beads being saturated and some induced sample failing to bind (Figure 6-1B). In both Rev-AK samples, Zta is not present, confirming that these samples do not express Zta in the presence of doxycycline, regardless of vector activation.

Following confirmation that Zta-AK cells express Zta following doxycycline-induction, and therefore are in lytic cycle, whilst Rev-Ak do not, the doxycycline-treated cell lines were subjected to stress induction (Figure 6-1C). Cells were treated with arsenite, hippuristanol or water (untreated control), and imaged using stress granule marker antibodies, G3BP1 and TIA-1. The expression vector also contains GFP, allowing for cells that have the vector activated to be visualised. Figure 6-1C shows that in all doxycycline-treated cells, a small number express GFP and show the activation of the vector, however, as shown in Figure 6-1B, Rev-AK cells cannot express Zta and are therefore considered not to have entered lytic cycle. The first observation made is that the untreated cells thought to be in lytic cycle, GFP^+ Zta-AK, do not exhibit SGs, suggesting that the lytic virus either does not promote SG formation or evades the process. Interestingly, following chemical stress in the form of arsenite and hippuristanol, cells undergoing lytic cycle either do not exhibit SGs or show a significantly reduced response when compared to the same cell line that is not in lytic cycle, GFP^- Zta-AK. In contrast, Rev-AK cells, show a similar SG response in both GFP^+ and GFP^- cells. Revealing that the lytic virus acts to prevent SG formation in both arsenite and hippuristanol treated conditions.

Figure 6-1D shows SG quantification from Figure 6-1C using Cell Profiler, and the previously described workflow (Figure 4-3), however, modified to recognise G3BP1 SGs, rather than TIA-1, as for this cell line, G3BP1 provided a clearer visualisation of SGs. Quantification reveals a compelling image, showing that the number of SGs per cell in

GFP^- cells, does not significantly differ between Rev-AK and Zta-AK for each condition. However, when considering cells that are GFP^+, this image drastically changes. Rev-AK cells show a similar response to each chemical as their GFP^- counterparts, whilst Zta-AK cells reveal a significantly tempered SG response, in which arsenite treated cells failed to show SGs, and hippuristanol treated cells exhibited a significantly reduced response compared to GFP^- cells in the same condition.

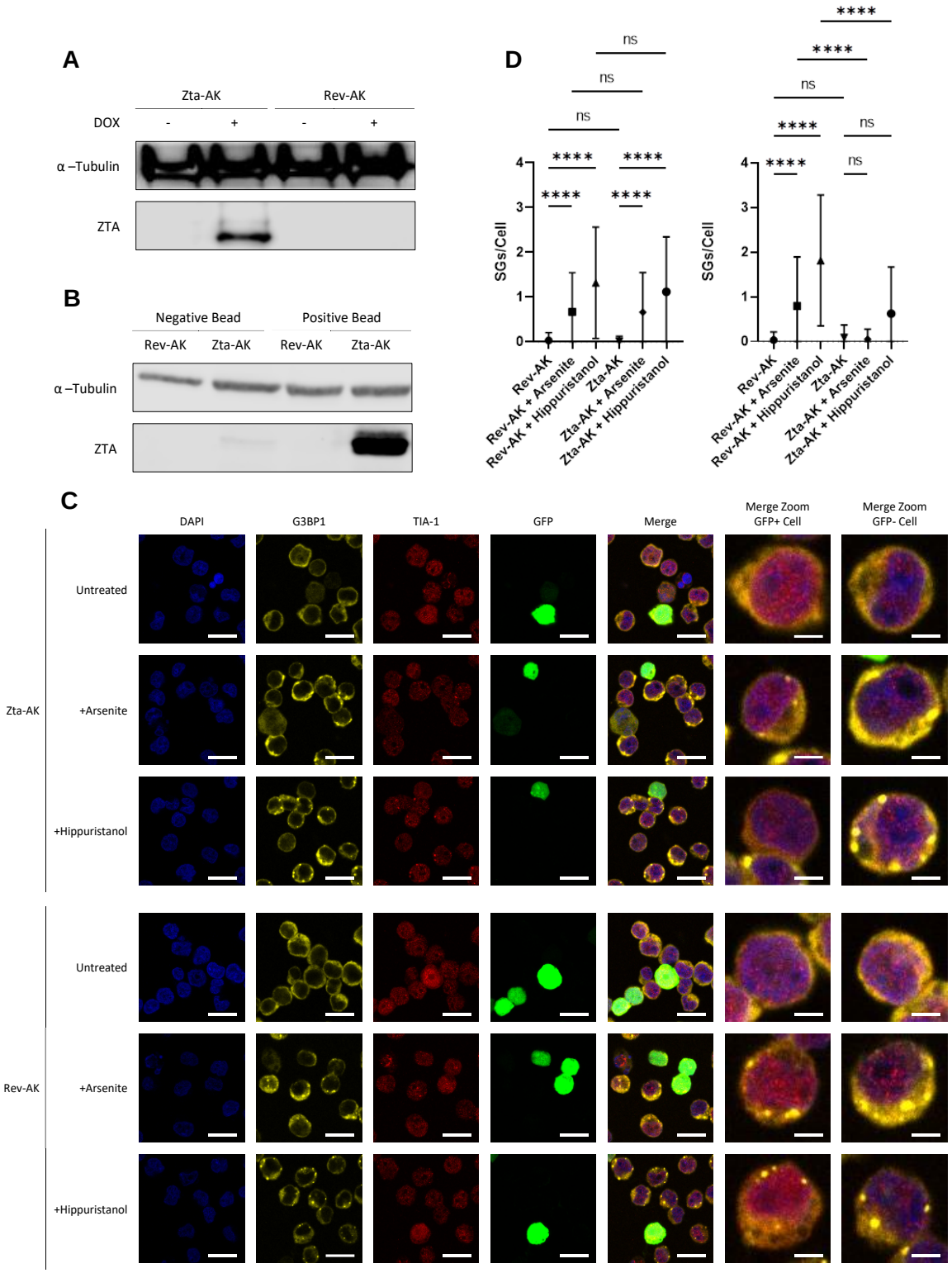

Figure 6-1 Zta-expressing cells inhibit SG formation. (A) Protein was extracted from Zta-AK and Rev-AK cells following incubation with doxycycline (500 ng/ml) or untreated. **(B)** Zta-AK and Rev-AK cell lines were incubated with doxycycline (500 ng/ml) for 24 hours before being magnetically sorted by anti-NGFR associated beads and immunoblotted. Negative bead represents cells that did not associate to the bead, whilst positive bead represents cells that did. (A & B) Protein was resolved on 10% SDS-PAGE and western blotted using antibodies against ZTA and loading control, α-tubulin. **(C)** Cells were incubated with NaAs (0.5mM), hippuristanol (1 μM) or water (untreated) for 45 minutes before fixation and permeabilization. Cells were stained for G3BP1 (green) and TIA-1 (red) using corresponding antibodies and imaged using confocal microscopy. The nuclei were stained using mounting media containing DAPI (blue), and GFP signifies cells containing the activated vector. Scale bar = 20 μm, Zoom scale bar = 5 μm. **(D)** Quantification of IF (C) was performed using cell profiler to count G3BP1+ stress granules per cell. Total number of cells per condition >48. Error bars represent s.e.m. n=3 (Two-way ANOVA, ns = $P > 0.05$, * = $P \leq 0.05$, ** = $P \leq 0.01$, *** = $P \leq 0.001$, **** = $P \leq 0.0001$).

6.2.2 eIF2αK activation in lytic Zta-AK

The cell lines used in this experiment are all EBV$^+$ Akata (Burkitt Lymphoma) cell lines, thought to be primarily in latency 1 (Fujiwara et al., 1999). This latency phase is one of the most restrictive in terms of viral gene expression, only expressing EBERs, EBNA1 and miRNAs. Following on from previous chapters, this study aimed to investigate the role of eIF2α and its kinases, in this instance, following entry into lytic cycle.

The first observation that was made, was that the phosphorylation state of eIF2α was consistent between all cell lines, regardless of whether it had the expression vector activated by doxycycline, or whether it had entered lytic cycle (Figure 6-2). Figure 6-2A shows the protein levels of total and phosphorylated eIF2α, and quantified in Figure 6-2B. It was revealed that although Zta-AK cells that have associated with the beads and therefore express Zta and are in lytic cycle, this does not induce eIF2α phosphorylation.

The activation of PERK and PKR were also investigated. Following doxycycline induction of the expression vector in both Zta-AK and Rev-AK, PKR phosphorylation was lower than compared to cells which do not contain the expression vector or are not activated. This is interesting as it would suggest that the expression vector may be interfering with PKR phosphorylation, however, as there is little difference between cells expressing Zta and entering lytic, and those expressing the non-functional reverse Zta, this response is not controlled by the virus.

PERK activation is also affected in cells expressing the vector, both expressing Zta or reverse Zta, however, as opposed to PKR, it is increased in these cells, compared to those containing the inactive vector, or none (Figure 6-2A-B). This slight increase, although not significant, may suggest that the expression of products from the vector is increasing ER stress and activation of PERK, however, this response, along with PKR, does not affect the phosphorylation of eIF2α in any cell line.

ATF4 protein expression, controlled by eIF2α phosphorylation, does not reveal a significant difference between the cell lines and conditions (Figure 6-2C). A moderate increase is shown between Rev-Ak cells that do not express the vector, compared to those that do and both conditions of Zta-AK. However, these cell lines and conditions exhibit a similar level of ATF4 expression, suggesting that first, the lytic virus does not affect ATF4 expression, as no difference is seen between bead-associated and associated Zta-AK cells. Secondly, no difference is seen between non-lytic (Rev-AK) bead-associated cells and both conditions of Zta-AK. Only two biological repeats of this experiment were possible due to the scale, complexity, and consumable limitation of this experiment.

Finally, Figure 6-2D shows TIA-1 protein expression between each cell line and condition. There is no significant difference observed between cells expressing Zta and entering lytic, and those that are not. This data suggests that lytic activation does not alter the expression of TIA-1 proteins.

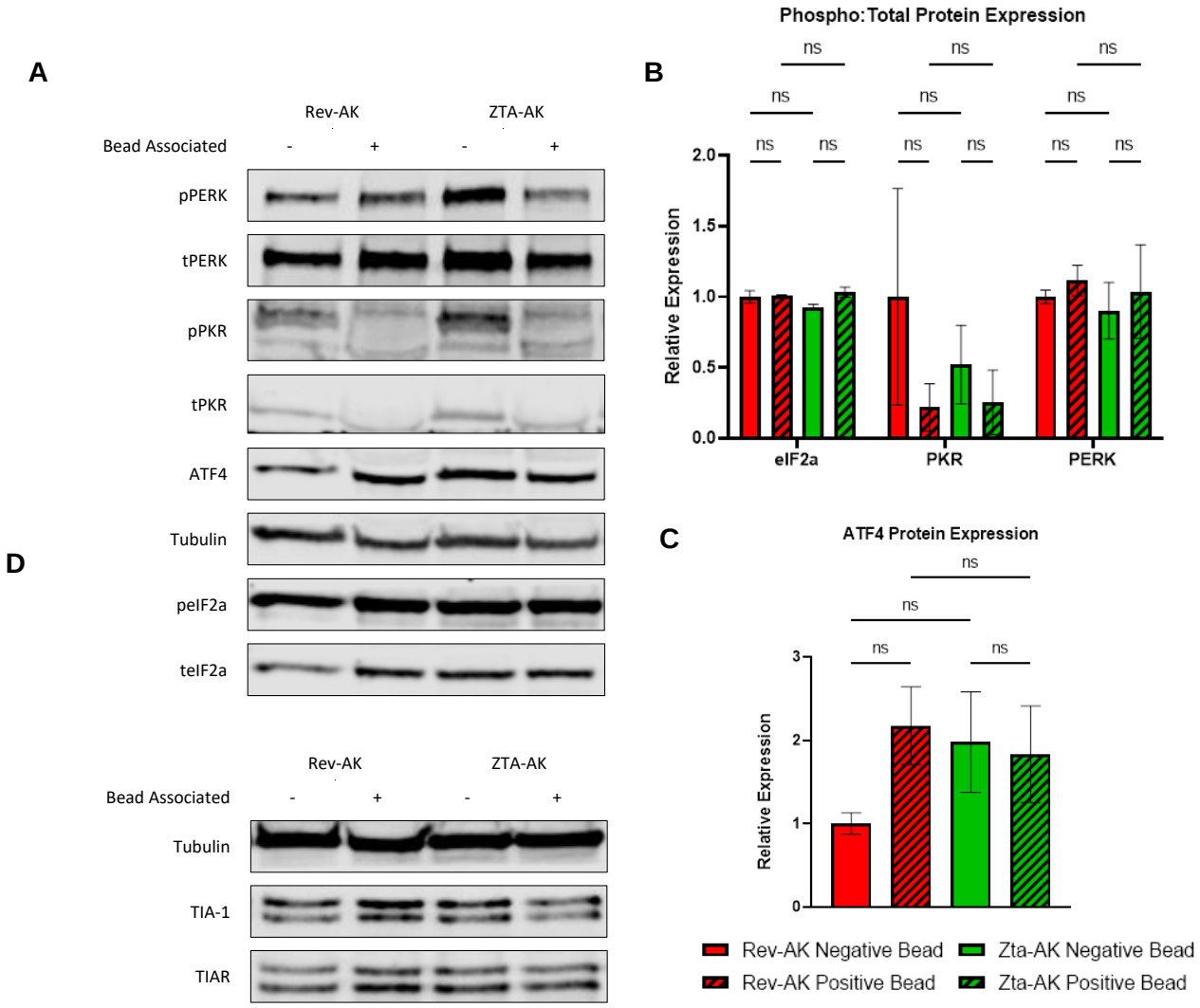

Figure 6-2 Lytic EBV does not induce eIF2α phosphorylation, or expression of TIA-1. (A) Zta-AK and Rev-AK cell lines were incubated with doxycycline (500 ng/ml) for 24 hours before being magnetically sorted by anti-NGFR associated beads and immunoblotted. Negative bead represents cells that did not associate to the bead, whilst positive bead represents cells that did. Protein was resolved on 10% SDS-PAGE and immunoblotted using antibodies against phosphor/total PERK, PKR, eIF2α along with ATF4 and loading control, α-tubulin. **(B)** Quantification of WB (A) showing protein expression levels of phosphorylated eIF2α, PKR and PERK, when normalised against the total. Expression levels are relative to the Rev-AK Negative Bead condition. **(C)** Quantification of ATF4 protein expression levels (A) relative to Rev-AK Negative Bead condition. (B & C) Error bars represent s.e.m. n=2 (Two-way ANOVA, ns = $P > 0.05$, * = $P \leq 0.05$, ** = $P \leq 0.01$, *** = $P \leq 0.001$, **** = $P \leq 0.0001$). **(D)** Samples from (A) resolved on 10% SDS-PAGE and immunoblotted using antibodies against TIA-1 and loading control, α-tubulin.

6.2.3 SG formation during lytic EBV infection of adherent cells

Although reactivation of EBV *in vivo* is considered to occur mainly in B cells, primary infection is thought to occur in oral epithelial cells whilst the virus is in lytic cycle (Kenney, 2007). Therefore, it was important to consider the effect that the lytic virus has on epithelial cells.

AGS is an epithelial gastric adenocarcinoma cell line, that has previously successfully been infected with recombinant EBV derived from the Akata cell line (H. J. Shin et al., 2011). EBV is associated with nearly 10% of all gastric carcinoma cases (reviewed in Iizasa et al., 2012), therefore AGS is a model cell line to investigate the role of EBV further. AGS EBV AK1 and AGS EBV AK2 are two cell lines that have been infected with the recombinant Akata EBV virus, which contained a neomycin resistance gene and are collectively referred to as AGS EBV AK. AGS A1 and AGS A2 are EBV^- cell lines that have undergone the infection process without the virus referred to as AGS A. Finally, AGS is the EBV^- parental cell line from which the previous cell lines were derived. These cell lines were kindly gifted by Manal Moalwi and Prof. Alison Sinclair.

As shown in previous studies, lytic cycle can be induced through the addition of phorbol 12-myristate 13-acetate (PMA) (Hausen et al., 1978). PMA activates the protein kinase C (PKC) pathway, which in turn promotes the expression of several transcription factors that induce Zta/BZLF1 expression, driving entry into lytic cycle (Baumann et al., 1998). Following incubation of each cell line with PMA (50 ng/ml) for 24 hours, Zta was expressed in a small number of cells containing the virus (Figure 6-3A). Stress induction then revealed that cells exhibiting Zta accumulated significantly fewer SGs than cells lacking Zta. The cells infected with the recombinant EBV virus but not expressing Zta showed a similar SG response to EBV^- infection control, AGSA (Figure 6-3A-B) and the parental cell line, AGS (IF not shown/Figure 6-3B). As noted previously, hippuristanol induces a stronger SG response, equating to more SGs/cell than arsenite, when

quantified by Cell Profiler. However, in cells expressing Zta, and therefore considered to contain lytic EBV, both hippuristanol and arsenite-induced SG formation is dampened to similar levels as untreated cells.

Many cells were analysed per condition, with each cell line undergoing induction and stress treatment in triplicate, however, due to the inefficiency of the EBV cells in entering lytic cycle, the number of cells counted for these conditions was significantly lower than cells not expressing the lytic virus.

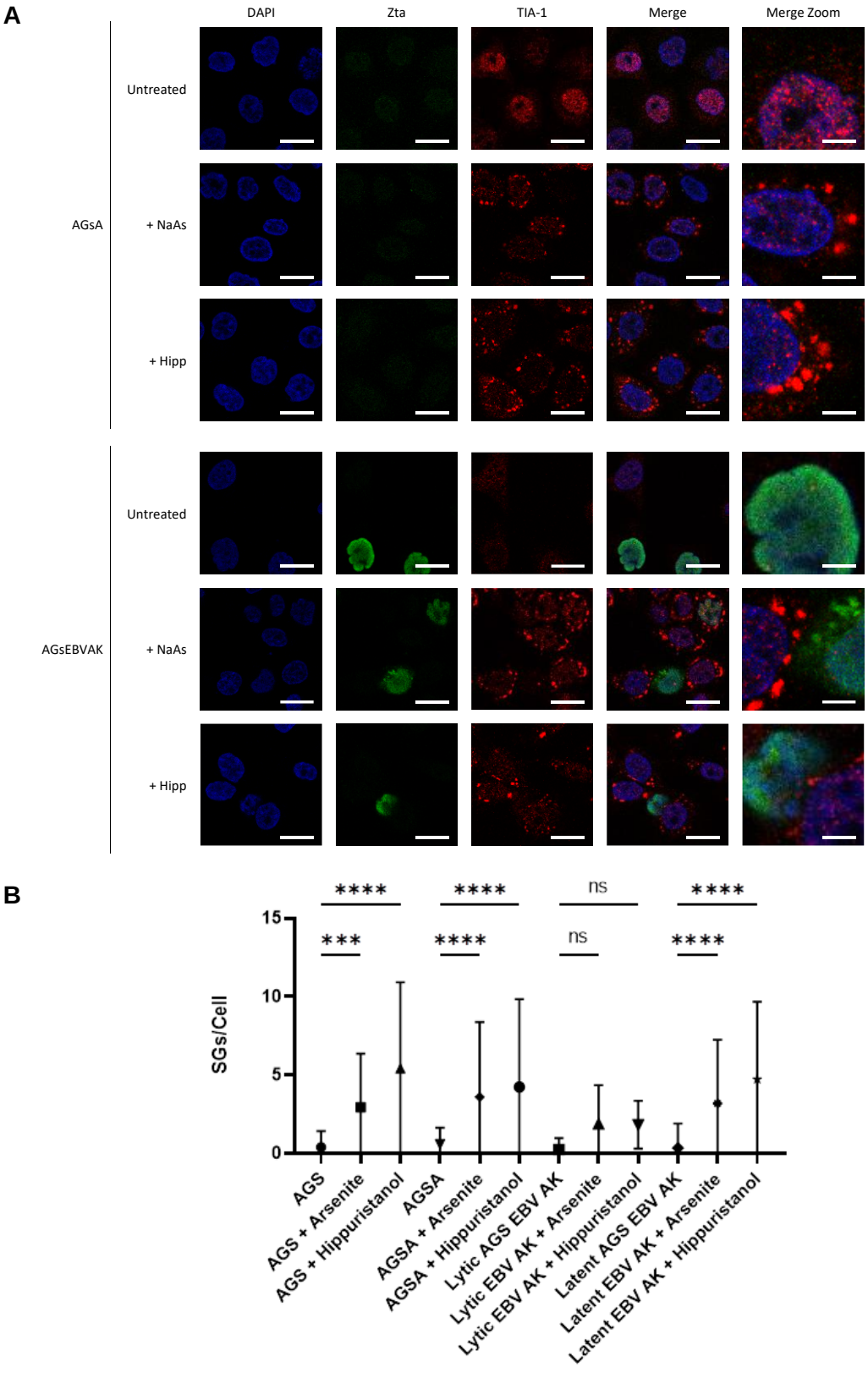

Figure 6-3 Lytic EBV-infected AGS cells inhibit induced SG formation. (A) EBV positive AGS cells (AGS EBV AK) and EBV negative AGS cells (AGS A) were seeded onto coverslips and incubated with PMA (50 ng/ml) for 24 hours, before stressing cells with NaAs (0.5 mM), Hippuristanol (1 µM) or water (untreated) for 45 minutes. Cells were fixed, permeabilized and stained for Zta (green) and TIA-1 (red) using corresponding antibodies and imaged using confocal microscopy. The nuclei were stained using mounting media containing DAPI. Scale bar = 20 µm, Zoom scale bar = 5 µm. **(B)** Quantification of TIA-1+ SGs by cell profiler in AGS cells (cell line control), AGSA (EBV-) and AGS EBV AK (EBV+). Lytic EBV AK cells represent cells expressing Zta, Latent EBV AK are cells without Zta. Total number of cells per condition >12. Error bars represent s.e.m. n=6 (Two-way ANOVA, ns = $P > 0.05$, * = $P \leq 0.05$, ** = $P \leq 0.01$, *** = $P \leq 0.001$, **** = $P \leq 0.0001$).

6.2.4 The role that BGLF5 has on SG formation during lytic EBV infection

The initial data discovered in this study, pointed to lytic EBV preventing SG formation through an eIF2α independent pathway, shown through the lytic virus's ability to inhibit both arsenite and hippuristanol-induced SG formation. As this effect is not exhibited in the latent virus, it can be speculated that one or more lytic viral products are responsible for this inhibition.

The first step in determining how lytic EBV may be preventing chemical-induced SG formation was to look at how the other human herpesviruses performed a similar function. HSV-1 and HSV-2 employ a mechanism involving lytic viral protein VHS, which inhibits SG formation through the degradation of dsRNA that would otherwise activate PKR and the ISR. Although no homolog exists in ɣ-herpesvirus to this α-herpesvirus protein, SOX (KSHV) and BGLF5 (EBV) adopt a similar host shut-off function to VHS (Glaunsinger & Ganem, 2004; Rowe et al., 2007). SOX was shown to prevent SG formation in KSHV infection (Sharma et al., 2017), however, BGLF5, remains to be investigated.

Secondly, KSHV employs an additional method to inhibit SG formation. Sharma et al. (2017) revealed that viral posttranscriptional regulator, ORF57, inhibited PKR activation through binding to PKR and its binding partner, PACT, and in turn prevented SG formation. This study went on to investigate the EBV homolog of ORF57, EB2 (SM) but found that it did not exhibit the same inhibitory function. VHS and the HSV-1 ORF57 homologue, ICP27, have been shown to work together to infer a specificity on host shut-off (Rowe et al., 2007; Taddeo et al., 2010). Therefore, we raised the question, of whether this occurs in EBV with EB2 working with BGLF5 to prevent SGs.

The B95.8 EBV strain is commonly used to transform and infect B cells and was used in the creation of BL2wtBAC2 and BL31wtBAC2.2 (Anderton et al., 2008; Callard et al., 1988; Kelly et al., 2005). It is derived from an EBV^{+} primate cell line that sheds EBV

virions capable of transforming other B cells (Glaser et al., 1989). Infection of B cells with this virus produces EBV^+ cell lines that enter latency, however, are capable of being reactivated just as the virus can *in vivo*. This process was built upon by another study, in which the entire EBV genome from B95.8 cells was cloned into a vector carrying GFP and hygromycin resistance, allowing for viral mutants to be generated and transfected into several cell lines (Delecluse et al., 1998). The same group also developed several EBV mutants including BGLF5 knockout, in which the BGLF5 gene was replaced by a kanamycin resistance gene (R Feederle et al., 2009). Prof. Delecluse kindly gifted the wild-type, and BGLF5 knock-out EBV transfected HEK293 producer cell lines to this study.

Initial characterisation of the B95.8 EBV HEK293, and BGLF5 KO EBV HEK293 cell lines showed that both these cell lines contained a high percentage of cells expressing GFP in all conditions (Figure 6-4). This suggests that the EBV genome, associated with GFP in the plasmid is present and is expressed in both EBV cell lines, while the absence of GFP in the EBV^- control cell line, HEK293, reinforces this observation.

However, following induction of lytic cycle, either through transfection of BZLF1 (Zta) (Delecluse et al., 1998; R Feederle et al., 2009; Regina Feederle et al., 2009) or as performed on previous cell lines, with incubation of PMA, neither cell line express a measurable level of Zta, suggesting that the transfection and PMA activation was not successful (Figure 6-4). PMA incubation was shown to induce a few cells into lytic cycle in the BGLF5 KO EBV HEK293 cells, whilst transfection of BZLF1 into either EBV cell line did not induce Zta expression. Optimisation of BZLF1 transfection was required to successfully induce the cells into lytic, however, time limitations towards the end of this project prevented this.

Therefore, due to the inefficiency of inducing the lytic cycle by transfection of BZLF1, PMA induction was used for the subsequent experiments. Following incubation of each

cell line with PMA, cells were treated with sodium arsenite or hippuristanol, along with untreated control (Figure 6-5). As shown in Figure 6-4, both EBV^+ cell lines express high levels of GFP, signifying the presence of the GFP-associated EBV genome, however, there is a distinct absence of Zta suggesting that these cells are not in lytic cycle. Therefore, we are unable to determine the response that lytic cycle within these cells has on arsenite and hippuristanol-induced stress. Further optimisation of lytic induction in these cells would be required before any conclusion regarding BGLF5 could be made.

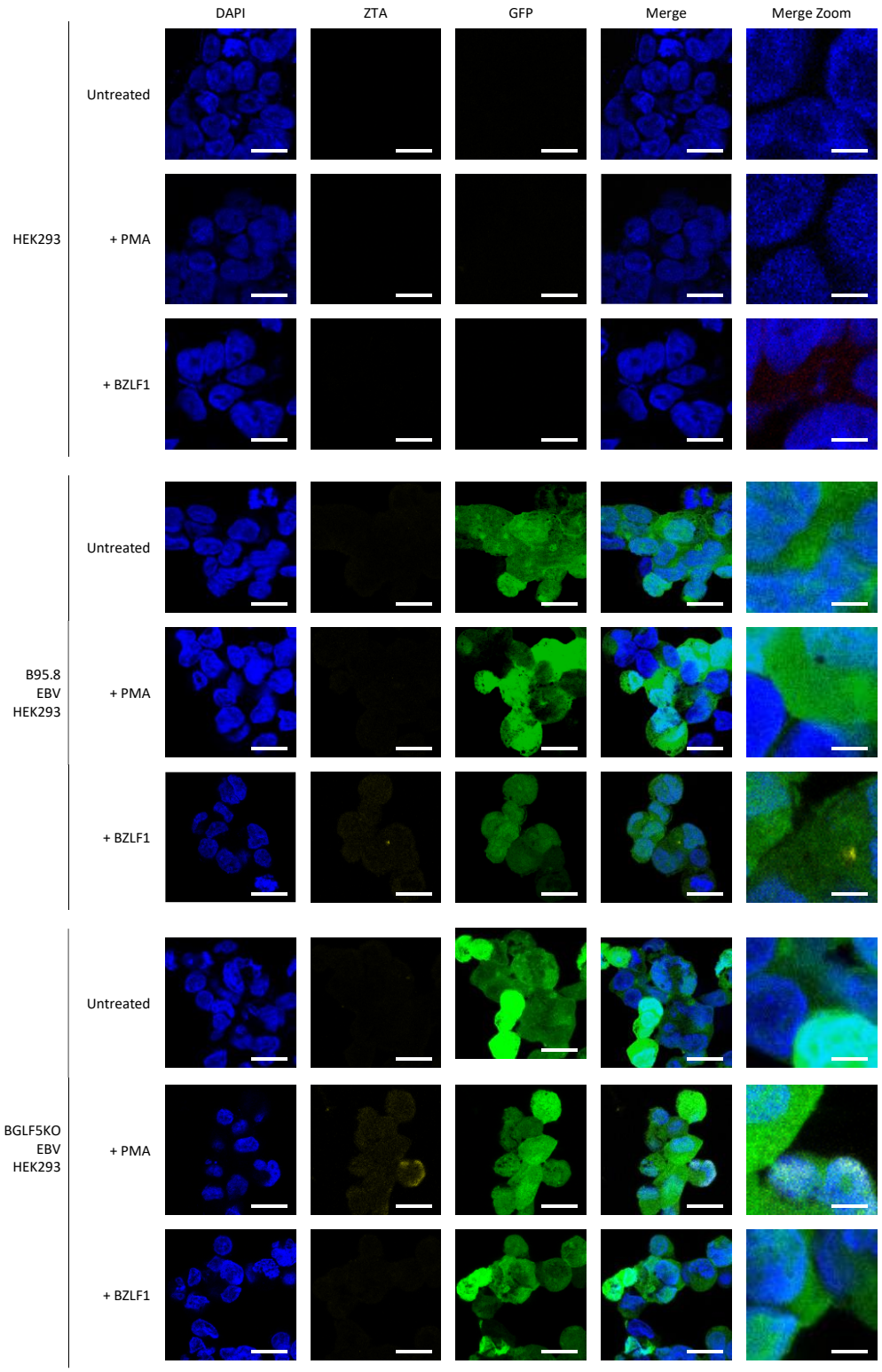

Figure 6-4 Lytic induction in EBV-infected HEK293 cells. HEK293 cells, shown in the top three panels, were transfected with EBV (B95.8 EBV HEK293) or, EBV lacking BGLF5 (BGLF5 KO EBV HEK293), both associated with GFP and hygromycin resistance. Cells seeded onto coverslips were transfected with BZLF1 (lipofectamine), incubated with PMA (50 ng/ml) or untreated for 24 hours, before fixing and permeabilizing. Cells were probed for Zta (yellow) along with corresponding secondary antibodies, and sealed onto slides with DAPI (blue) containing mounting media. Cells were imaged on confocal microscope. Scale bar = 20 µm, Zoom scale bar = 5 µm

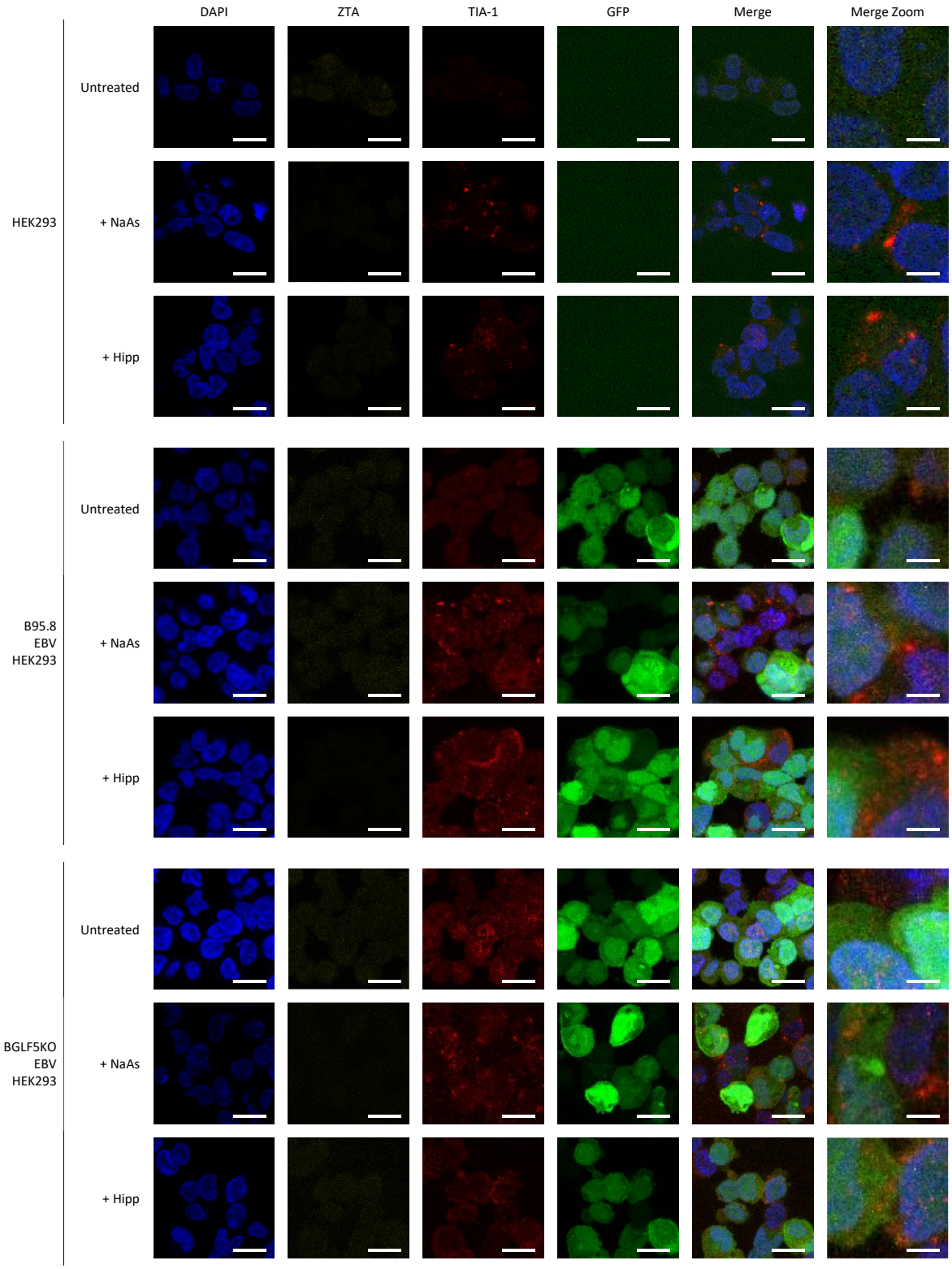

Figure 6-5 Stress treatment of PMA-treated cells. HEK293, B95.8 EBV HEK293 and BGLF5 KO EBV HEK293 were incubated with PMA (50 ng/ml) for 24 hours, before treating with NaAs (0.5 mM), Hippuristanol (1 μM) or water (untreated). Cells were fixed and permeabilized before probing for Zta (yellow) and TIA-1 (red), along with corresponding secondary antibodies, and sealed onto slides with DAPI (blue) containing mounting media. Cells were imaged on confocal microscope. Scale bar = 20 μm, Zoom scale bar = 5 μm

6.2.5 HEK293 + BGLF5

Finally, the last process that was used to investigate the role that BGLF5 has on SG accumulation, was to express the protein into a non-EBV cell line. The BGLF5 ORF was cloned into a pcDNA $3.1^{(+)}$ expression vector (kindly gifted by Prof. H-J Delecluse) which allowed it to be expressed and selected using G418.

BGLF5 was transfected into HEK293 cells which were maintained in G418 selection (500 µg/ml), to ensure only BGLF5 expressing cells were present. Stress treatment of BGLF5 expressing HEK293 (HEK293 + BGLF5), along with wt HEK293, showed that there was little difference in their abilities to accumulate SGs (Figure 6-6). Confocal microscopy images show that TIA-1^{+} (and G3BP-1^{+}) SGs accumulate in both treated conditions of both cell lines (Figure 6-6A). When these images were quantified using Cell Profiler (Figure 6-6B), there is no significant difference in SG formation between cells expressing BGLF5 and wt, and their responses to each stress induction remain similar.

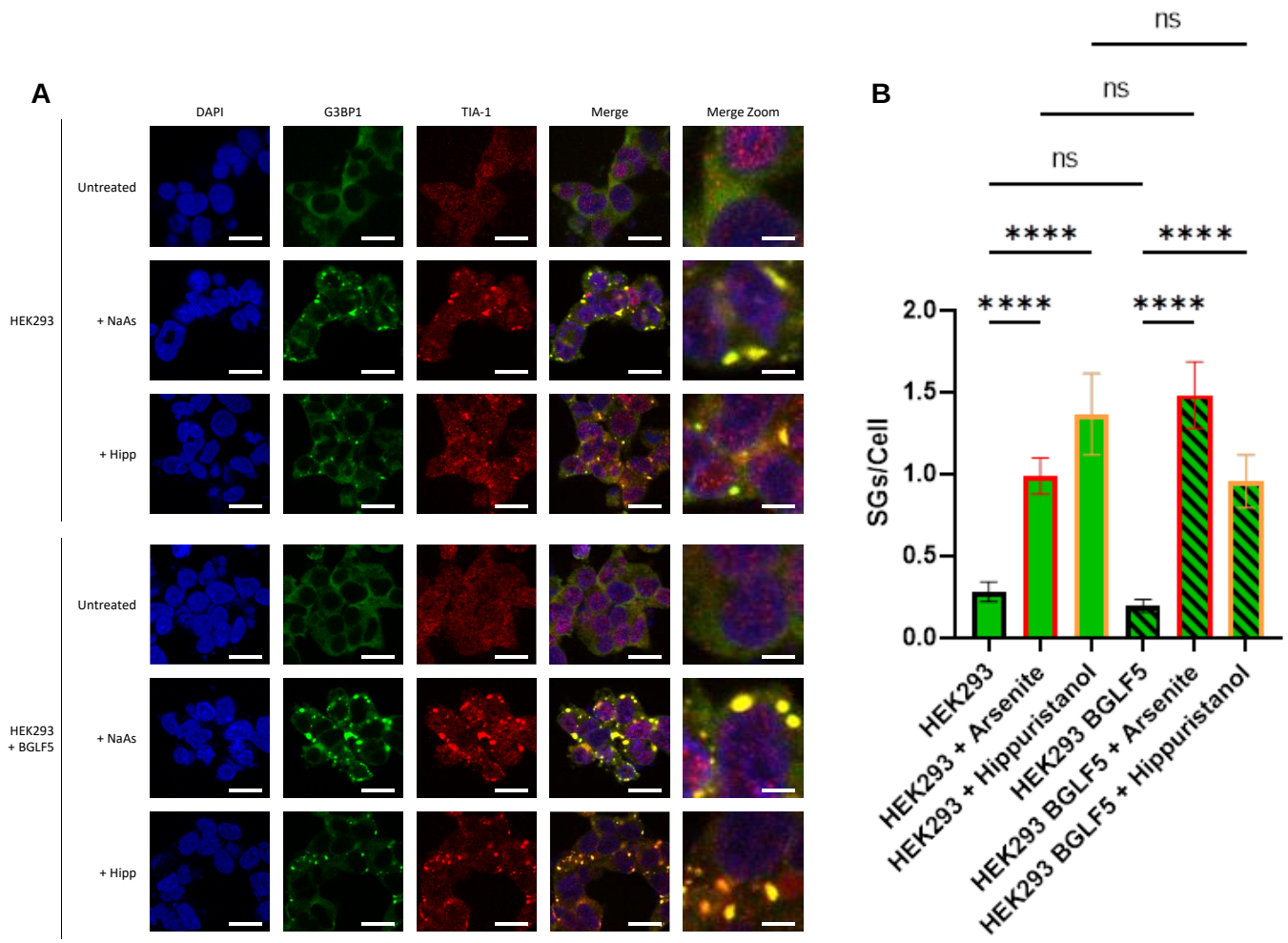

Figure 6-6 Induced SG accumulation in response to BGLF5 expression. (A) HEK293 cells were transfected with BGLF5 expression vector (Hek293 + BGLF5), or negative control (HEK293) before treatment with arsenite (0.5 mM), hippuristanol (1 µM) or water (Untreated). Cells were fixed and permeabilized before probing for G3BP1 (green) and TIA-1 (red), along with corresponding secondary antibodies, and sealed onto slides with DAPI (blue) containing mounting media. Cells were imaged on confocal microscope. Scale bar = 20 µm, Zoom scale bar = 5 µm **(B)** Quantification of IF (A) was performed using cell profiler to count TIA-1+ stress granules per cell. Total number of cells per condition >40. Error bars represent s.e.m. n=3 (Two-way ANOVA, ns = $P > 0.05$, * = $P \leq 0.05$, ** = $P \leq 0.01$, *** = $P \leq 0.001$, **** = $P \leq 0.0001$).

6.3 Discussion

Lytic EBV regularly occurs during primary infection and allows for the virus to successfully replicate and spread within host cells before it enters latency, becoming dormant and evading the host response. It was shown in previous chapters that latent EBV infection does not induce SG formation, potentially through preventing or reversing eIF2α activation, such as increasing GADD34 expression, or inhibiting PKR activation. However, only a small quantity of viral products are expressed during latency, providing an easier task for the virus in evading any host response. The lytic phase, on the other hand, produces a full complement of viral gene products (Murata, 2018), increasing the opportunity for the host to detect and combat the invading virus.

In contrast to other herpesviruses, lytic EBV is rarely linked to significant human disease instead, it is the latent growth phase that is responsible for several malignancies including cancer and multiple sclerosis (Bjornevik et al., 2022; Wong et al., 2022). This occurrence may be due to the relatively short-lived nature of lytic virus, and its preferential restriction into latency in B cells. However, lytic virus remains an important phase in the EBV lifecycle, key to producing infectious virions and spreading the virus. It is therefore important to understand whether the virus induces the host immune response, regarding eIF2α and SG formation, and whether the virus can evade this mechanism.

The initial data shown in this chapter confirms that cells can enter lytic cycle (Figure 6-1A/B). The expression of Zta alone has been shown to drive entry into lytic cycle (Zalani et al., 1996), and is expressed during early lytic phase to promote the expression of several other lytic genes (Murata, 2014). It can therefore be concluded that the presence of Zta within the cells, shown in Figure 6-1, represents that the cells are in lytic phase, and expressing viral lytic products. The most compelling data from this experiment is shown in Figure 6-1C, in which cells expressing GFP, in the cell line

containing Zta in the correct orientation within the expression vector, do not form stress granules in response to arsenite or hippuristanol-induced stress. As shown in the control cell line, and all previous experiments using these drugs, clear and obvious SGs form following exposure to arsenite or hippuristanol. This is further reinforced by internal controls within the Zta-AK cell line, where GFP^- cells, representing the absence of Zta and therefore lytic cycle, form SGs to a similar level as the control cell line, Rev-AK (Figure 6-1D). Taken together, there is striking evidence to suggest that lytic EBV infection prevents the formation of SGs in response to arsenite and hippuristanol induced stress. Hippuristanol was included in these experiments, as it provides an alternative stress to arsenite, which works through activating eIF2α phosphorylation. Hippuristanol instead inhibits eIF4A, the RNA helicase subunit of the eIF4F complex, preventing its interaction with RNA, causing stalling of translation and assembly of SGs (Cencic & Pelletier, 2016). If lytic EBV prevented SG formation relating to eIF2α phosphorylation, as with other HHVs such as HSV and KSHV (Dauber et al., 2011; Finnen et al., 2014; Sharma et al., 2017), it would be likely that hippuristanol induced stress would result in SG formation, however, this is not the case. The fact that hippuristanol-induced SG assembly is also disrupted in lytic cells, suggests that this inhibition is downstream of both eIF2α activation and eIF4A activity. This implies that EBV may inhibit SG formation through an alternative mechanism to the other known HHVs, potentially through direct interaction with specific SG components.

This data was further reinforced using a different cell line system. The AGS EBV cell system provided an alternative mechanism for lytic EBV induction. Firstly, the AGS cell line is an EBV^-, adherent, epithelial cell line derived from human gastric adenocarcinoma. These cells had been infected with recombinant Akata EBV containing neomycin resistance, allowing for selection using G418. A negative control cell line had also been created, that lacked the virus. Unlike the Zta-AK cell lines, these cells did not contain an inducible expression vector and instead were induced into lytic cycle using PMA.

Following induction of these cells, along with the same treatment using the parental cell line, AGS, and the EBV^- infection control, AGS A, cells were then subjected to stress induction (Figure 6-3). As seen with the Zta-AK cell line, cells expressing Zta exhibited an absence of SGs in the presence of arsenite or hippuristanol. Furthermore, cells in the same condition, but lacking the expression of Zta, considered to contain the latent virus, show similar levels of SGs to the uninfected controls.

Lytic virus clearly can prevent SG formation in both adherent and suspension cell lines. This is physiologically relevant as EBV is likely to first infect oral epithelial cells during primary infection, at which stage it will be in lytic phase, before spreading to B cells and entering latency. As reactivation of EBV lytic phase has been shown to occur in B cells (Laichalk & Thorley-Lawson, 2005), it is also important to understand how the lytic virus behaves in these cells. The mechanism in which lytic EBV prevents SG formation is independent of eIF2α, and eIF4A, shown through alternative stress inducers. This is interesting as several other HHVs have been shown to inhibit SG accumulation through eIF2α (Dauber et al., 2011; Finnen et al., 2014; Sharma et al., 2017), and would suggest that EBV involves a different process.

Using the Zta-AK/Rev-AK cell lines, it was possible to separate cells expressing the expression vector and those not. NGFR was also expressed along with GFP and Zta (or reverse Zta) in these cell lines, allowing for cells containing the induced vector to be extracted using magnetic beads associated with anti-NGFR antibodies. It can be assumed that all cells associated with the Zta-AK cell line were in lytic phase, as discussed previously, whilst cells that did not bind, did not contain the vector, or it was not activated. This process allowed for cells containing the lytic virus to be immunoblotted and protein levels investigated. As expected, following the SG data, eIF2α is not affected during lytic infection compared to both negative control (Rev-AK) and Zta-AK cells lacking the expression vector. Furthermore, PKR and PERK, although showing slight variation between cells containing the vector and those not, there is no difference

between cells in lytic cycle and those with the reverse Zta gene. This is also reinforced in the ATF4 protein expression. Overall, this suggests that the lytic virus does not affect PKR, PERK or eIF2α activation. PKR is regularly defined as the virus detecting kinase for eIF2α, this is because of its ability to bind to dsRNA, a product of all viral replication in ssRNA, dsRNA, and DNA viruses (Son et al., 2015; Weber et al., 2006). However, as lytic EBV does not appear to activate PKR, the question arises as to why not. Lytic EBV is the phase in which the virus is actively replicating and infecting other cells, through the production of infectious virions. Furthermore, lytic EBV would likely cause ER stress through the production of glycoproteins at increased levels in the ER eventually leading to unfolded proteins. The presence of these unfolded proteins would therefore activate PERK, however, as with PKR, this is not the case. It can be speculated, that if lytic EBV can prevent SG assembly, it may also involve mechanisms to prevent activation of pathways that may disrupt this prevention, such as eIF2α phosphorylation.

Although it remains unclear as to whether lytic EBV manipulates the eIF2α pathway, the virus is preventing chemically induced SG formation. To investigate what viral product may contribute to disrupted SG formation, EBV was compared to the other human herpesviruses. HSV-1 and HSV-2 have been shown to inhibit SG formation through the expression of viral protein VHS, which suppressed PKR and SG formation (Dauber et al., 2016; Esclatine et al., 2004b; Finnen et al., 2012, 2014). Interestingly, in HSV-2, the process of SG disruption was suggested to occur downstream of eIF2α phosphorylation, and it was also shown that hippuristanol could induce SGs in infected cells, where arsenite could not (Finnen et al., 2012). VHS acts to destabilise and reduce the accumulation of cellular and viral mRNA, including dsRNA, tempering the response by PKR (Dauber et al., 2019). Furthermore, it was also shown that during HSV-1 infection, TIA-1 accumulation occurs within the cytoplasm, however, SG formation is prevented (Esclatine et al., 2004a). These studies have focused on lytic viral products.

Although HSV-1 and HSV-2 are human herpesviruses, they fall within the α subfamily, which has several differences from EBV, a ɣ-herpesvirus. One important difference is that EBV does not have a homologue to VHS, which is responsible for preventing host protein synthesis, and aiding immune evasion in α-herpesviruses (Kwong & Frenkel, 1987; Smiley, 2004). Instead, a similar function is adopted by the exonuclease BGLF5 (Rowe et al., 2007). VHS is an endonuclease that degrades both viral and host mRNAs (Everly et al., 2002). In a similar function, BGLF5 was shown to degrade both viral and host mRNA, promoting shut-off of host protein synthesis, and potentially evading host response (Horst et al., 2012; Rowe et al., 2007). As VHS was shown to prevent SG formation in lytic HSV infection, we speculated that BGLF5 may contribute to a similar mechanism in EBV, linked to its degradation of mRNA.

Using HEK293 cells infected with EBV, and BGLF5 KO EBV infected HEK293, it was attempted to determine whether BGLF5 was responsible for SG disruption. However, as shown in Figure 6-4 and Figure 6-5, no clear expression of Zta was detected in the EBV^{+} cell lines. GFP representing the presence of the viral genome was visible suggesting that the cells were infected, however, the lack of Zta suggests that these cells were in the latent phase and had not been susceptible to induction into lytic. It is unclear why these cells displayed an inefficiency in entering lytic cycle.

Following this, the BGLF5 ORF was transfected into HEK293 cells under the selection of a hygromycin resistance gene, without the rest of the EBV genome. This allowed for BGLF5 to be expressed in HEK293 without the need for induction. The data presented in Figure 6-6, shows that expression of BGLF5 alone is not enough to prevent SG formation in response to arenite or hippuristanol stress. VHS is thought to disrupt SG formation in HSV infection through an eIF2α-dependent pathway, reducing levels of complementary transcripts, destabilising the dsRNA, and inhibiting PKR (Dauber et al., 2019). Lytic EBV, on the other hand, was shown to also prevent SG formation in response to hippuristanol-induced stress, eIF2α-independently. Therefore, it is likely that

another mechanism is in play during lytic EBV, either alone or in conjunction with a VHS-like BGLF5 function. Interestingly, another study found that ɣ-herpesvirus KSHV SOX, an exonuclease that shares high homology with EBV BGLF5, is also capable of affecting SG formation through degradation of RNA (Sharma et al., 2017).

KSHV displays an additional mechanism to disrupt SG formation during lytic infection. The virus expresses the lytic protein ORF57 which was shown to inhibit SG formation via inhibition of PKR, blocking eIF2α phosphorylation (Sharma et al., 2017). EBV expresses a homologous protein to ORF57, EB2 (BMLF1/Mta/SM), which is vital for virion production (Gruffat et al., 2002). EB2 functions as an mRNA export factor to accumulate viral mRNAs preferentially derived from intronless genes (Batisse et al., 2005; Juillard et al., 2012; Verma et al., 2009). There are conflicting views as to whether EB2 is capable of disrupting PKR activation, eIF2α phosphorylation and SG formation, like ORF57. One study found that EB2 did not function to block this pathway, and arsenite-induced SGs accumulated in cells expressing EB2, in contrast to homologs, ORF57 (KSHV) or ICP27 (HSV-1), that inhibited this process (Sharma et al., 2017). Another study, however, suggested that EB2 prevents activation of PKR through direct binding of EB2, via a repeated Arg-X-Pro (RXP) sequence, to the kinase (Poppers et al., 2003).

These conflicting studies may suggest that EBV SG disruption involves a complicated mechanism. Whilst our study was unable to investigate EB2's contribution to SG evasion, we speculate that it may work in tandem with BGLF5 to disrupt this process, as was previously been suggested for the shut-off function (Rowe et al., 2007).

.

7 Final Discussion

Biomolecular condensates have proven to be vital tools for the cellular processes involved in many mechanisms, either constantly present and functioning, such as the nucleolus or Cajal bodies, or accumulating as a response to a specific condition, such as SGs. SGs can accumulate through a variety of stresses, however, the focus of this project is to investigate the viral induction of SGs, which have been associated as an important component of the host antiviral response (Onomoto et al., 2014).

The central pathway for SG formation involves the phosphorylation of eIF2α, in which translation is stalled, accumulating mRNA, translational machinery and RNA-binding proteins into foci. Whilst four main kinases are responsible for phosphorylating eIF2α, activation of PKR and PERK have been regularly associated with viral infection. The formation of SGs prevents the translation of any foreign material, such as viral products. Therefore, in its canonical form, SG formation prevents viral replication, and many viruses have adopted processes to evade, hijack and manipulate this mechanism.

In this project, we focus on the Epstein-Barr virus, a human herpesvirus, that infects over 90% of the world population, and is responsible for several virus-associated malignancies (Thompson & Kurzrock, 2004).

Of the nine herpesviruses that affect humans, currently, only four have been shown to interfere with the SG mechanism (Table 1-5). HSV-1 and HSV-2, block the activation of PKR through the expression of viral protein VHS (Dauber et al., 2011, 2016; Finnen et al., 2014), CMV uses a similar process of blocking PKR with viral proteins pITRS1 and pIRS1 (Ziehr et al., 2016), whilst KSHV was shown to block PKR also through viral protein ORF57. Several other studies have implicated additional viral proteins in eIF2α pathway modification, however, have not directly looked at SG formation (Ambagala & Cohen, 2007; Y. Li et al., 2011; Sharon & Frenkel, 2017). EBV is one of the most prevalent viruses in the human population and has been neglected in the sense of SG

biology. Little is known about the effect that EBV infection has on this mechanism, whether it is inhibited or even activated during either life cycle of the virus. It has been shown that latent EBV protein EBNA3C can bind to GADD34 within the ISR and potentially negatively regulate its function in dephosphorylating eIF2α (Garrido et al., 2009). Whilst another latent EBV product, LMP1, has been shown to promote the activation of PERK (Dong et al., 2008). This gives rise to several questions, as these processes would encourage the cell to stall translation and form SGs, which would be detrimental to viral replication.

The first aim of this study was to determine how the ISR was affected by latent EBV infection. It can be seen by data presented in chapter 3, that PKR protein levels are increased during latent infection, suggesting that the virus is inducing the innate immune response, promoted by IFN signalling through the detection of viral PAMPs by the cell PRRs. The phosphorylation level of PKR does not correlate to this increased protein level and remains unaffected in EBV^{+} when compared to EBV^{-} cells. Whilst increased levels of PKR could be expected to detect the presence of the latent infection, our data suggests that this does not occur, and either PKR is unable to detect the presence of any activating components, such as dsRNA, or is inhibited in this process.

dsRNA has previously been detected in DNA viruses, thought to arise as intermediates during replication, through overlapping converging transcription or expression of highly structured ssRNAs (Jacobs & Langland, 1996; Majde, 2000; Weber et al., 2006). Whilst latent EBV infection produces only a few viral products, and replicates via host machinery, it can be speculated that this may not produce dsRNA that would activate PKR. miRNA produced by latent EBV may have the ability to activate PKR, however, no current studies have investigated this. EBER1 and EBER2 are ssRNA latent products produced by EBV that exhibit a considerable secondary structure (Fok et al., 2006). Both EBER1 and EBER2 have been shown to bind PKR, and exert an inhibitory effect *in vitro* (Clarke et al., 1991; Nanbo et al., 2002; Sharp et al., 1993). This mechanism remains to

be seen *in vivo* and is subject to some speculation due to EBERs localisation to the nucleus (Glickman et al., 1988; Howe & Steitz, 1986; Toczyski et al., 1994). Interestingly, the EBERs were detected in the cytoplasm during interphase, implicating them with a potential role in translation (Schwemmle et al., 1992).

It remains to be determined whether latent EBV infection can produce a component capable of activating PKR. However, data presented in this chapter shows that PKR is not activated during latent infection (Figure 3-5). PKR is either inhibited by a viral component, preventing its activation and the phosphorylation of eIF2α, or the latent virus expresses its products in such a way as to evade detection of PKR, without the need for an inhibitory process. Whilst our data cannot rule out an inhibitory mechanism, it would be reasonable to suggest that EBV does not produce products capable of activating PKR, either through the absence of dsRNA, or the reduced concentration of viral products produced during latency.

Further investigation into the direct activation of PKR in latent EBV-infected cells, using activating agents such as poly(I:C), that work to exclusively activate PKR, may provide answers to whether the virus inhibits the activation of this kinase. Whilst work to finally conclude the EBERs role and association with PKR *in vivo* would help to remove doubt over this interaction.

PERK activation was also shown not to change in latent EBV infected cells, suggesting that the cell was not detecting ER stress (Figure 3-5). This is consistent with the fact that latent EBV is not producing glycoproteins within the ER, which have previously been associated with the activation of PERK (Leung et al., 2012). Furthermore, the restricted protein expression displayed by latent EBV would potentially not overwhelm protein folding, which may occur during the lytic cycle, preventing the increased presence of unfolded proteins that would activate PERK. Whilst previous data suggested latent protein LMP1 was capable of activating PERK (Dong et al., 2008; Lam et al., 2004), it

was shown that high levels of LMP1 expression were required to induce eIF2α phosphorylation, suggesting that this may not occur within most latent EBV infected cells. Data obtained in this chapter, suggests that latent EBV does not activate PERK, and therefore LMP1 protein levels in these cell lines are not expressed to such levels as to activate PERK. Further research directly investigating LMP1 levels within latent EBV^+ cells may provide insight as to whether this latent product is capable of activating PERK during the virus's lifecycle.

eIF2α phosphorylation during latent EBV infection correlated with the lack of PKR and PERK activation, and did not differ between EBV^+ and EBV^- cells (Figure 3-5). This suggests that the ISR is not activated by any element of latent EBV infection, allowing the virus to remain hidden within the cell without inducing the stress response. Whilst ATF4 mRNA and protein levels in EBV^+ samples reinforced this observation, GADD34 provided a curious result (Figure 3-5). The increase in GADD34 mRNA following latent EBV infection, suggests that the virus employs a mechanism to prevent the phosphorylation of eIF2α. Furthermore, the lack of an increase in ATF4 expression only provides more questions as to how the virus can induce GADD34 expression without an increase in eIF2α phosphorylation or increased expression of downstream components, such as ATF4. Our data provides a potential trend, suggesting an increase in CHOP mRNA expression in EBV^+ BL2 cells compared to EBV^-, however, this is not reinforced in BL31. Investigation into GADD34 expression in several EBV KO cell lines may provide the answer as to what latent product is responsible for this novel finding, whilst the answer as to why this occurs may lie in the biphasic lifecycle of EBV, and its ability to reactivate lytic cycle. In our research, we did not investigate whether this observation was exclusive to the latent phase, as if it is also present during lytic, this may provide a useful mechanism to counteract any activation of the ISR that may occur.

Our data revealed that the latent virus did not alter the cell's response to arsenite stress regarding the ISR (Figure 3-6, Figure 3-7). Whilst we had shown the presence of a

potential mechanism to dephosphorylate eIF2α during latent infection, no significant difference was seen between EBV^+ and EBV^- cell lines. However, we must ask whether the stress induced by arsenite is so severe that the increase in GADD34 is unable to reduce the phosphorylation of eIF2α. To further understand how increased GADD34 may reduce stress-activated eIF2α phosphorylation in latently infected cells, less harsh stresses and more physiologically relevant inducers may be adopted, such as poly(I:C) that can mimic dsRNA and activate PKR. Furthermore, it would be important to understand whether GADD34 protein expression correlates to mRNA within EBV^+ cells.

While we did not observe increased eIF2α phosphorylation in latent EBV-infected cells, we next aimed to investigate SG formation in these cells. Our data revealed that the latent EBV infection did not affect SG formation within the cell (Figure 4-4). Latent infection is not sufficient to induce SG formation alone, furthermore, it did not prevent chemical induction of SGs through arsenite or hippuristanol (Figure 4-4). This is in line with studies that have investigated the other HHVs (Table 1-5). Combining this information with that obtained in the previous chapter, we suggest that latent EBV infection does affect the ISR, and therefore evades the formation of SGs.

Although SG assembly does not occur during latent EBV infection, we aimed to investigate whether levels of RBPs, commonly associated with SG formation, may have changed. G3BP1 and TIAR protein levels remained unchanged between latent EBV^+ and EBV^- cells, however, TIA-1 protein levels decreased (Figure 5-2, Figure 5-3). We found that latent EBV infection also decreased the levels of TIA-1 mRNA (Figure 5-4). Although the mechanism of downregulation was not determined, data presented in this study suggests that TIA-1 is transcriptionally controlled to downregulate the mRNA. Furthermore, TIA-1 mRNA was preferentially spliced to give basal levels of TIA-1a, but significantly lower levels of TIA-1b. Isoform specific studies of TIA-1 are only recently being investigated (Hamada et al., 2016; Izquierdo & Valcárcel, 2007b; Reyes et al., 2009; Sánchez-Jiménez et al., 2015), so much remains to be concluded regarding the

specific function of each isoform. Previous studies of TIA-1 have generalised both isoforms as one and even included TIAR at times, defining this group as TIA proteins. This has not aided the understanding of TIA-1, as through our research into this protein, it is becoming increasingly clear that not only are TIA-1 and TIAR significantly different, but TIA-1 isoforms are also. Whilst TIA-1 has previously been shown to be required for SG formation (Kedersha et al., 1999), isoform-specific SG function has not been investigated.

Importantly, several studies have implicated TIA-1a as having an oncogenic function, inducing proliferation, whilst TIA-1b was shown to have a tumour suppressor function (Hamada et al., 2016; Reyes et al., 2009; Sánchez-Jiménez et al., 2015). This is Interesting as latent EBV infection is commonly associated with several tumours and a study comparing EBV^+ and EBV^- BLs found that was approximately a 30% reduction in TIA-1 mRNA expression in EBV^+ BL, compared to EBV^- (Kaymaz et al., 2017). This reduction correlates to our data showing a similar decrease in overall TIA-1 mRNA levels during latent EBV infection (Figure 5-4). Which following isoform-specific analysis, reveals that this 30% reduction corresponds mostly to the loss of TIA-1b. Speculatively, we suggest that latent EBV aims to induce proliferation, promoting cell division and thus division of the virus. One mechanism that would allow this characteristic, is the alteration of TIA-1 isoform expression, allowing TIA-1a to continue promoting proliferation, whilst decreasing TIA-1b expression, which may prevent this. In doing so, EBV increases the proliferation of B cells, however, loses the function of the tumour suppressor TIA-1b. Whilst this is likely only one small factor in EBV tumorigenesis, it may provide additional clues as to how EBV-associated cancers develop and may offer a novel target for preventative measures. Investigating the balance of TIA-1 isoforms in healthy cells will be key to understanding their separate roles in tumour progression. Whilst further research into how TIA-1 isoform expression may be controlled by the latent virus could make use of numerous latent EBV^+ KO cell lines that currently exist.

Although no difference was observed in SG formation and latent EBV infection, we speculated that SG function may be altered during lytic EBV infection, similar to data presented for KSHV infection (Sharma et al., 2017). Sharma et al. (2017) showed that latent infection did affect chemical-induced SG accumulation, but lytic KSHV infection prevented this effect. We found that as with latent, lytic virus alone did not induce SG formation. However, following chemical-induced stress, via arsenite and hippuristanol, known to be effective SG inducers, lytic-infected cells provided some striking data. Cells expressing the lytic virus tempered SG accumulation in response to these chemicals, whilst cells in latency exhibited similar levels of SGs to uninfected cells. This has previously not been shown and provides new insight as to how EBV infection may evade this process. Interestingly, both arsenite and hippuristanol-induced stress granule formation were reduced in lytic EBV-infected cells. Arsenite promotes the activation of several eIF2αK, which phosphorylate eIF2α and induce SG formation (Gilks et al., 2004; Zhou et al., 2008). Hippuristanol, on the other hand, induces SG formation, via an eIF2α-independent pathway, inhibiting eIF4A and its helicase activity, preventing its RNA interaction by maintaining eIF4A in a closed conformation, stalling translation and promoting SG assembly (Cencic & Pelletier, 2016). The fact that lytic EBV disrupts SG formation in response to both arsenite and hippuristanol, is unlike the other HHVs that interfere with eIF2α phosphorylation to prevent SG formation. Instead, EBV employs a mechanism independent of eIF2α and downstream of both eIF2α phosphorylation and eIF4E activity.

Although our data suggested that lytic EBV may make use of an alternative mechanism to inhibit SG formation than the other HHVs. Work to identify the viral component for such a response began by comparing components responsible for the same effect in the other HHVs. Two initial targets were identified through the mechanism in which HSV-1, HSV-2 and KSHV prevent chemical-induced SG formation. The first was HSV-1/HSV-2 lytic protein VHS, responsible for host translational shut-off, which degrades dsRNA, and

prevents its accumulation and activation of PKR (Dauber et al., 2016). Whilst EBV does not have a homolog to VHS, a similar protein has adopted the host shut-off function, BGLF5 (Rowe et al., 2007). BGLF5 degrades both viral and host mRNA to shut off host protein synthesis. The second target identified was EB2, the homolog to KSHV ORF57, a protein responsible for inhibiting PKR through direct interaction, preventing eIF2α phosphorylation and blocking SG formation (Sharma et al., 2017). We remained speculative about EB2, as Sharma et al. (2017) found that EB2 did not inhibit arsenite-induced SG formation whilst homologs in KSHV and HSV-1 did. Whilst another study found that EB2 could prevent activation of PKR through direct binding, similar to ORF57 (Poppers et al., 2003).

Initial data presented by our study points towards BGLF5 not alone responsible for lytic EBV SG evasion. This conclusion was suggested through the viral effect on eIF2α-independent SG mechanisms, and BGLF5 expression into HEK293 cells not altering SG formation (Figure 6-1, Figure 6-6). Further investigation is required to completely rule out BGLF5 as a factor in lytic EBV SG evasion. Speculatively, BGLF5 may require additional viral products to exert its function. This may be assessed through monitoring cytoplasmic mRNA levels in cells expressing BGLF5, along with PKR activation.

Whilst not directly investigating EB2 in this study, there remains huge potential for this protein. Although having been ruled out by previous studies (Sharma et al., 2017), we speculate that it may still contribute to SG evasion. HSV-1 VHS is known to work in association with ORF57 HSV-1 homolog, ICP27, to provide specificity to the host shut-off function (Rowe et al., 2007; Taddeo et al., 2010). Whether this may also be the case with SG interference in EBV infection remains to be seen. Co-expression of EB2 and BGLF5 into a cell system may provide insight into the role that they play in SG inhibition.

This thesis provides the first investigation of SG assembly and associated proteins and mechanisms, during EBV infection. Latent EBV does not induce the ISR or affect SG

assembly, however, lytic EBV inhibits both eIF2α-dependent and -independent SG pathways, through currently unknown mechanisms. Furthermore, latent EBV contributes to a reduction in SG-associated RNP, TIA-1, specifically, the expression of the shorter isoform TIA-1b, which has recently been associated as a tumour suppressor. This study provides the first evidence that latent EBV decreased levels of this tumour suppressor, providing a potential mechanism that could contribute to the development of EBV-associated cancers. TIA-1b may offer an interesting novel target in future preventative measures of these cancers.

8 Published Work

Tweedie, A., & Nissan, T. (2021). Hiding in Plain Sight: Formation and Function of Stress Granules During Microbial Infection of Mammalian Cells. Frontiers in Molecular Biosciences, 8. https://doi.org/10.3389/fmolb.2021.647884

Zagorac, S., de Giorgio, A., Dabrowska, A., Kalisz, M., Casas-Vila, N., Cathcart, P., Yiu, A., Ottaviani, S., Degani, N., Lombardo, Y., Tweedie, A., Nissan, T., Vance, K. W., Ulitsky, I., Stebbing, J., & Castellano, L. (2021). SCIRT lncRNA Restrains Tumorigenesis by Opposing Transcriptional Programs of Tumour-Initiating Cells. Cancer Research, 81(3), 580–593. https://doi.org/10.1158/0008-5472.CAN-20-2612

9 References

Ablasser, A., Bauernfeind, F., Hartmann, G., Latz, E., Fitzgerald, K. A., & Hornung, V. (2009). RIG-I-dependent sensing of poly(dA:dT) through the induction of an RNA polymerase III-transcribed RNA intermediate. *Nature Immunology*, *10*(10), 1065–1072. https://doi.org/10.1038/ni.1779

Adomavicius, T., Guaita, M., Zhou, Y., Jennings, M. D., Latif, Z., Roseman, A. M., & Pavitt, G. D. (2019). The structural basis of translational control by eIF2 phosphorylation. *Nature Communications*, *10*(1). https://doi.org/10.1038/s41467-019-10167-3

Akira, S., Uematsu, S., & Takeuchi, O. (2006). Pathogen recognition and innate immunity. In *Cell* (Vol. 124, Issue 4, pp. 783–801). https://doi.org/10.1016/j.cell.2006.02.015

Akula, S. M., Naranatt, P. P., Walia, N.-S., Wang, F.-Z., Fegley, B., & Chandran, B. (2003). Kaposi's Sarcoma-Associated Herpesvirus (Human Herpesvirus 8) Infection of Human Fibroblast Cells Occurs through Endocytosis. *Journal of Virology*, *77*(14), 7978–7990. https://doi.org/10.1128/jvi.77.14.7978-7990.2003

Albornoz, A., Carletti, T., Corazza, G., & Marcello, A. (2014). The Stress Granule Component TIA-1 Binds Tick-Borne Encephalitis Virus RNA and Is Recruited to Perinuclear Sites of Viral Replication To Inhibit Viral Translation. *Journal of Virology*, *88*(12), 6611–6622. https://doi.org/10.1128/jvi.03736-13

Alexopoulou, L., Holt, A. C., Medzhitov, R., & Flavell, R. A. (2001). Recognition of double-stranded RNA and activation of NF-κB by Toll-like receptor 3. *Nature*, *413*(6857), 732–738. https://doi.org/10.1038/35099560

Algire, M. A., Maag, D., & Lorsch, J. R. (2005). Pi release from eIF2, not GTP hydrolysis, is the step controlled by start-site selection during eukaryotic translation initiation. *Molecular Cell*, *20*(2), 251–262. https://doi.org/10.1016/j.molcel.2005.09.008

Allen, M. D., Young, L. S., & Dawson, C. W. (2005). The Epstein-Barr Virus-Encoded LMP2A and LMP2B Proteins Promote Epithelial Cell Spreading and Motility. *Journal of Virology*, *79*(3), 1789–1802. https://doi.org/10.1128/jvi.79.3.1789-1802.2005

Ambagala, A. P. N., & Cohen, J. I. (2007). Varicella-Zoster Virus IE63, a Major Viral Latency Protein, Is Required To Inhibit the Alpha Interferon-Induced Antiviral Response. *Journal of Virology*, *81*(15), 7844–7851. https://doi.org/10.1128/jvi.00325-07

Ameri, K., & Harris, A. L. (2008). Activating transcription factor 4. In *International Journal of Biochemistry and Cell Biology* (Vol. 40, Issue 1, pp. 14–21). Int J Biochem Cell Biol. https://doi.org/10.1016/j.biocel.2007.01.020

Amon, W., & Farrell, P. J. (2005). Reactivation of Epstein-Barr virus from latency. In *Reviews in Medical Virology* (Vol. 15, Issue 3, pp. 149–156). John Wiley & Sons, Ltd. https://doi.org/10.1002/rmv.456

Anderson, D. M., Anderson, K. M., Chang, C. L., Makarewich, C. A., Nelson, B. R., McAnally, J. R., Kasaragod, P., Shelton, J. M., Liou, J., Bassel-Duby, R., & Olson, E. N. (2015). A micropeptide encoded by a putative long noncoding RNA regulates muscle performance. *Cell*, *160*(4), 595–606. https://doi.org/10.1016/j.cell.2015.01.009

Anderson, P. J., & Kedersha, N. (2002a). Visibly stressed: The role of eIF2, TIA-1, and stress granules in protein translation. In *Cell Stress and Chaperones* (Vol. 7, Issue 2, pp. 213–221). https://doi.org/10.1379/1466-1268(2002)007<0213:VSTROE>2.0.CO;2

Anderson, P. J., & Kedersha, N. (2002b). Stressful initiations. *Journal of Cell Science*, *115*(Pt 16), 3227–3234. http://www.ncbi.nlm.nih.gov/pubmed/12140254

Anderson, P. J., & Kedersha, N. (2008). Stress granules: the Tao of RNA triage. In *Trends in Biochemical Sciences* (Vol. 33, Issue 3, pp. 141–150). https://doi.org/10.1016/j.tibs.2007.12.003

Anderson, P. J., & Kedersha, N. (2009). Stress granules. In *Current Biology* (Vol. 19, Issue 10). Cell Press. https://doi.org/10.1016/j.cub.2009.03.013

Anderton, E., Yee, J., Smith, P., Crook, T., White, R. E., & Allday, M. J. (2008). Two Epstein-Barr virus (EBV) oncoproteins cooperate to repress expression of the proapoptotic tumour-suppressor Bim: Clues to the pathogenesis of Burkitt's lymphoma. *Oncogene*, *27*(4), 421–433. https://doi.org/10.1038/sj.onc.1210668

Annibaldi, A., Dousse, A., Martin, S., Tazi, J., & Widmann, C. (2011). Revisiting G3BP1 as a RasGAP binding protein: Sensitization of tumor cells to chemotherapy by the RasGAP 317-326 sequence does not involve G3BP1. *PLoS ONE*, *6*(12). https://doi.org/10.1371/journal.pone.0029024

Apicco, D. J., Ash, P. E. A., Maziuk, B., Leblang, C., Medalla, M., Al Abdullatif, A., Ferragud, A., Botelho, E., Ballance, H. I., Dhawan, U., Boudeau, S., Cruz, A. L., Kashy, D., Wong, A., Goldberg, L. R., Yazdani, N., Zhang, C., Ung, C. Y., Tripodis, Y., … Wolozin, B. (2018). Reducing the RNA binding protein TIA1 protects against tau-mediated neurodegeneration in vivo. *Nature Neuroscience*, *21*(1), 72–82. https://doi.org/10.1038/s41593-017-0022-z

Arimoto, K., Fukuda, H., Imajoh-Ohmi, S., Saito, H., & Takekawa, M. (2008). Formation of stress granules inhibits apoptosis by suppressing stress-responsive MAPK pathways. *Nature Cell Biology*, *10*(11), 1324–1332. https://doi.org/10.1038/ncb1791

Arvin, A., Campadelli-Fiume, G., Mocarski, E., Moore, P. S., Roizman, B., Whitley, R., & Yamanishi, K. (2007). Human herpesviruses: Biology, therapy, and immunoprophylaxis. In A. Arvin, G. Campadelli-Fiume, E. Mocarski, P. S. Moore, B. Roizman, R. Whitley, & K. Yamanishi (Eds.), *Human Herpesviruses: Biology, Therapy, and Immunoprophylaxis*. Cambridge University Press. https://doi.org/10.1017/CBO9780511545313

Asselah, T., Bièche, I., Mansouri, A., Laurendeau, I., Cazals-Hatem, D., Feldmann, G., Bedossa, P., Paradis, V., Martinot-Peignoux, M., Lebrec, D., Guichard, C., Ogier-Denis, E., Vidaud, M., Tellier, Z., Soumelis, V., Marcellin, P., & Moreau, R. (2010). In vivo hepatic endoplasmic reticulum stress in patients with chronic hepatitis C. *Journal of Pathology*, *221*(3), 264–274. https://doi.org/10.1002/path.2703

Audas, T. E., Audas, D. E., Jacob, M. D., Ho, J. J. D., Khacho, M., Wang, M., Perera, J. K., Gardiner, C., Bennett, C. A., Head, T., Kryvenko, O. N., Jorda, M., Daunert, S., Malhotra, A., Trinkle-Mulcahy, L., Gonzalgo, M. L., & Lee, S. (2016). Adaptation to Stressors by Systemic Protein Amyloidogenesis. *Developmental Cell*, *39*(2), 155–168. https://doi.org/10.1016/j.devcel.2016.09.002

Audas, T. E., Jacob, M. D., & Lee, S. (2012). Immobilization of Proteins in the Nucleolus

by Ribosomal Intergenic Spacer Noncoding RNA. *Molecular Cell*, *45*(2), 147–157. https://doi.org/10.1016/j.molcel.2011.12.012

Aulas, A., Caron, G., Gkogkas, C. G., Mohamed, N. V., Destroismaisons, L., Sonenberg, N., Leclerc, N., Alex Parker, J., & Velde, C. Vande. (2015). G3BP1 promotes stress-induced RNA granule interactions to preserve polyadenylated mRNA. *Journal of Cell Biology*, *209*(1), 73–84. https://doi.org/10.1083/jcb.201408092

Avendaño, C., & Menéndez, J. C. (2008). DNA Intercalators and Topoisomerase Inhibitors. In *Medicinal Chemistry of Anticancer Drugs* (pp. 199–228). Elsevier. https://doi.org/10.1016/b978-0-444-52824-7.00007-x

Aznaourova, M., Schmerer, N., Schmeck, B., & Schulte, L. N. (2020). Disease-Causing Mutations and Rearrangements in Long Non-coding RNA Gene Loci. In *Frontiers in Genetics* (Vol. 11). https://doi.org/10.3389/fgene.2020.527484

Babcock, G. J., Decker, L. L., Volk, M., & Thorley-Lawson, D. A. (1998). EBV persistence in memory B cells in vivo. *Immunity*, *9*(3), 395–404. https://doi.org/10.1016/S1074-7613(00)80622-6

Ballarino, M., Morlando, M., Fatica, A., & Bozzoni, I. (2016). Non-coding RNAs in muscle differentiation and musculoskeletal disease. In *Journal of Clinical Investigation* (Vol. 126, Issue 6, pp. 2021–2030). American Society for Clinical Investigation. https://doi.org/10.1172/JCI84419

Baltimore, D. (1971). Expression of animal virus genomes. *Bacteriological Reviews*, *35*(3), 235–241. https://doi.org/10.1128/br.35.3.235-241.1971

Banani, S. F., Lee, H. O., Hyman, A. A., & Rosen, M. K. (2017). Biomolecular condensates: Organizers of cellular biochemistry. In *Nature Reviews Molecular Cell Biology* (Vol. 18, Issue 5, pp. 285–298). https://doi.org/10.1038/nrm.2017.7

Banerjee, N., & Mukhopadhyay, S. (2016). Viral glycoproteins: biological role and application in diagnosis. In *VirusDisease* (Vol. 27, Issue 1, pp. 1–11). https://doi.org/10.1007/s13337-015-0293-5

Banker, G., Churchill, L., & Cotman, C. W. (1974). Proteins of the postsynaptic density. *Journal of Cell Biology*, *63*(2), 456–465. https://doi.org/10.1083/jcb.63.2.456

Baradaran-Heravi, Y., Van Broeckhoven, C., & van der Zee, J. (2020). Stress granule mediated protein aggregation and underlying gene defects in the FTD-ALS spectrum. In *Neurobiology of Disease* (Vol. 134, p. 104639). Academic Press. https://doi.org/10.1016/j.nbd.2019.104639

Batisse, J., Manet, E., Middeldorp, J. M., Sergeant, A., & Gruffat, H. (2005). Epstein-Barr Virus mRNA Export Factor EB2 Is Essential for Intranuclear Capsid Assembly and Production of gp350. *Journal of Virology*, *79*(22), 14102–14111. https://doi.org/10.1128/jvi.79.22.14102-14111.2005

Baumann, M., Mischak, H., Dammeier, S., Kolch, W., Gires, O., Pich, D., Zeidler, R., Delecluse, H.-J., & Hammerschmidt, W. (1998). Activation of the Epstein-Barr Virus Transcription Factor BZLF1 by 12- O -Tetradecanoylphorbol-13-Acetate-Induced Phosphorylation. *Journal of Virology*, *72*(10), 8105–8114. https://doi.org/10.1128/jvi.72.10.8105-8114.1998

Bazot, Q., Deschamps, T., Tafforeau, L., Siouda, M., Leblanc, P., Harth-Hertle, M. L., Rabourdin-Combe, C., Lotteau, V., Kempkes, B., Tommasino, M., Gruffat, H., &

Manet, E. (2014). Epstein-Barr virus nuclear antigen 3A protein regulates CDKN2B transcription via interaction with MIZ-1. *Nucleic Acids Research*, *42*(15), 9700–9716. https://doi.org/10.1093/nar/gku697

Bazzini, A. A., Johnstone, T. G., Christiano, R., MacKowiak, S. D., Obermayer, B., Fleming, E. S., Vejnar, C. E., Lee, M. T., Rajewsky, N., Walther, T. C., & Giraldez, A. J. (2014). Identification of small ORFs in vertebrates using ribosome footprinting and evolutionary conservation. *EMBO Journal*, *33*(9), 981–993. https://doi.org/10.1002/embj.201488411

Bechtel, J. T., Liang, Y., Hvidding, J., & Ganem, D. (2003). Host Range of Kaposi's Sarcoma-Associated Herpesvirus in Cultured Cells. *Journal of Virology*, *77*(11), 6474–6481. https://doi.org/10.1128/jvi.77.11.6474-6481.2003

Bernardi, R., & Pandolfi, P. P. (2007). Structure, dynamics and functions of promyelocytic leukaemia nuclear bodies. In *Nature Reviews Molecular Cell Biology* (Vol. 8, Issue 12, pp. 1006–1016). https://doi.org/10.1038/nrm2277

Bertolotti, A., Zhang, Y., Hendershot, L. M., Harding, H. P., & Ron, D. (2000). Dynamic interaction of BiP and ER stress transducers in the unfolded-protein response. *Nature Cell Biology*, *2*(6), 326–332. https://doi.org/10.1038/35014014

Bhende, P. M., Dickerson, S. J., Sun, X., Feng, W.-H., & Kenney, S. C. (2007). X-Box-Binding Protein 1 Activates Lytic Epstein-Barr Virus Gene Expression in Combination with Protein Kinase D. *Journal of Virology*, *81*(14), 7363–7370. https://doi.org/10.1128/jvi.00154-07

Bieging, K. T., Amick, A. C., & Longnecker, R. (2009). Epstein-Barr virus LMP2A bypasses p53 inactivation in a MYC model of lymphomagenesis. *Proceedings of the National Academy of Sciences of the United States of America*, *106*(42), 17945–17950. https://doi.org/10.1073/pnas.0907994106

Bjornevik, K., Cortese, M., Healy, B. C., Kuhle, J., Mina, M. J., Leng, Y., Elledge, S. J., Niebuhr, D. W., Scher, A. I., Munger, K. L., & Ascherio, A. (2022). Longitudinal analysis reveals high prevalence of Epstein-Barr virus associated with multiple sclerosis. *Science*, *375*(6578), 296–301. https://doi.org/10.1126/science.abj8222

Bley, N., Lederer, M., Pfalz, B., Reinke, C., Fuchs, T., Glaß, M., Möller, B., & Hüttelmaier, S. (2015). Stress granules are dispensable for mRNA stabilization during cellular stress. *Nucleic Acids Research*, *43*(4), 26. https://doi.org/10.1093/nar/gku1275

Boehmer, P. E., & Nimonkar, A. V. (2003). Herpes virus replication. In *IUBMB Life* (Vol. 55, Issue 1, pp. 13–22). John Wiley & Sons, Ltd. https://doi.org/10.1080/1521654031000070645

Boke, E., Ruer, M., Wühr, M., Coughlin, M., Lemaitre, R., Gygi, S. P., Alberti, S., Drechsel, D., Hyman, A. A., & Mitchison, T. J. (2016). Amyloid-like Self-Assembly of a Cellular Compartment. *Cell*, *166*(3), 637–650. https://doi.org/10.1016/j.cell.2016.06.051

Bol, G. M., Vesuna, F., Xie, M., Zeng, J., Aziz, K., Gandhi, N., Levine, A., Irving, A., Korz, D., Tantravedi, S., Heerma van Voss, M. R., Gabrielson, K., Bordt, E. A., Polster, B. M., Cope, L., Groep, P., Kondaskar, A., Rudek, M. A., Hosmane, R. S., … Raman, V. (2015). Targeting DDX 3 with a small molecule inhibitor for lung cancer therapy. *EMBO Molecular Medicine*, *7*(5), 648–669. https://doi.org/10.15252/emmm.201404368

Bond, C. S., & Fox, A. H. (2009). Paraspeckles: Nuclear bodies built on long noncoding RNA. In *Journal of Cell Biology* (Vol. 186, Issue 5, pp. 637–644). The Rockefeller University Press. https://doi.org/10.1083/jcb.200906113

Borza, C. M., & Hutt-Fletcher, L. M. (2002). Alternate replication in B cells and epithelial cells switches tropism of Epstein-Barr virus. *Nature Medicine*, *8*(6), 594–599. https://doi.org/10.1038/nm0602-594

Brandimarte, L., La Starza, R., Gianfelici, V., Barba, G., Pierini, V., Di Giacomo, D., Cools, J., Elia, L., Vitale, A., Luciano, L., Bardi, A., Chiaretti, S., Matteucci, C., Specchia, G., & Mecucci, C. (2014). DDX3X-MLLT10 fusion in adults with NOTCH1 positive T-cell acute lymphoblastic leukemia. In *Haematologica* (Vol. 99, Issue 5, p. 64). Ferrata Storti Foundation. https://doi.org/10.3324/haematol.2013.101725

Brangwynne, C. P., Eckmann, C. R., Courson, D. S., Rybarska, A., Hoege, C., Gharakhani, J., Jülicher, F., & Hyman, A. A. (2009). Germline P granules are liquid droplets that localize by controlled dissolution/condensation. *Science*, *324*(5935), 1729–1732. https://doi.org/10.1126/science.1172046

Brazão, T. F., Johnson, J. S., Müller, J., Heger, A., Ponting, C. P., & Tybulewicz, V. L. J. (2016). Long noncoding RNAs in B-cell development and activation. *Blood*, *128*(7), e10–e19. https://doi.org/10.1182/blood-2015-11-680843

Brostrom, C. O., & Brostrom, M. A. (1997). Regulation of Translational Initiation during Cellular Responses to Stress. In *Progress in Nucleic Acid Research and Molecular Biology* (Vol. 58, Issue C, pp. 79–125). Academic Press. https://doi.org/10.1016/S0079-6603(08)60034-3

Broz, P., & Dixit, V. M. (2016). Inflammasomes: Mechanism of assembly, regulation and signalling. In *Nature Reviews Immunology* (Vol. 16, Issue 7, pp. 407–420). https://doi.org/10.1038/nri.2016.58

Brush, M. H., Weiser, D. C., & Shenolikar, S. (2003). Growth Arrest and DNA Damage-Inducible Protein GADD34 Targets Protein Phosphatase 1α to the Endoplasmic Reticulum and Promotes Dephosphorylation of the α Subunit of Eukaryotic Translation Initiation Factor 2. *Molecular and Cellular Biology*, *23*(4), 1292–1303. https://doi.org/10.1128/mcb.23.4.1292-1303.2003

Buchan, J. R., Muhlrad, D., & Parker, R. (2008). P bodies promote stress granule assembly in Saccharomyces cerevisiae. *Journal of Cell Biology*, *183*(3), 441–455. https://doi.org/10.1083/jcb.200807043

Buchan, J. R., & Parker, R. (2009). Eukaryotic Stress Granules: The Ins and Outs of Translation. In *Molecular Cell* (Vol. 36, Issue 6, pp. 932–941). Howard Hughes Medical Institute. https://doi.org/10.1016/j.molcel.2009.11.020

Budkina, K., El Hage, K., Clement, M. J., Desforges, B., Bouhss, A., Joshi, V., Maucuer, A., Hamon, L., Ovchinnikov, L. P., Lyabin, D. N., & Pastre, D. (2021). YB-1 unwinds mRNA secondary structures in vitro and negatively regulates stress granule assembly in HeLa cells. *Nucleic Acids Research*, *49*(17), 10061–10081. https://doi.org/10.1093/nar/gkab748

Burgess, H. M., & Mohr, I. (2018). Defining the Role of Stress Granules in Innate Immune Suppression by the Herpes Simplex Virus 1 Endoribonuclease VHS. *Journal of Virology*, *92*(15), 829–847. https://doi.org/10.1128/JVI.00829-18

Burkitt, D. (2005). A sarcoma involving the jaws in african children. *British Journal of*

Surgery, *46*(197), 218–223. https://doi.org/10.1002/bjs.18004619704

Burýšek, L., & Pitha, P. M. (2001). Latently Expressed Human Herpesvirus 8-Encoded Interferon Regulatory Factor 2 Inhibits Double-Stranded RNA-Activated Protein Kinase. *Journal of Virology*, *75*(5), 2345–2352. https://doi.org/10.1128/jvi.75.5.2345-2352.2001

Cabili, M. N., Dunagin, M. C., McClanahan, P. D., Biaesch, A., Padovan-Merhar, O., Regev, A., Rinn, J. L., & Raj, A. (2015). Localization and abundance analysis of human lncRNAs at single-cell and single-molecule resolution. *Genome Biology*, *16*(1). https://doi.org/10.1186/s13059-015-0586-4

Calender, A., Billaud, M., Aubry, J. P., Banchereau, J., Vuillaume, M., & Lenoir, G. M. (1987). Epstein-Barr virus (EBV) induces expression of B-cell activation markers on in vitro infection of EBV-negative B-lymphoma cells. *Proceedings of the National Academy of Sciences of the United States of America*, *84*(22), 8060–8064. https://doi.org/10.1073/pnas.84.22.8060

Callard, R. E., Lau, Y. L., Shields, J. G., Smith, S. H., Cairns, J., Flores-Romo, L., & Gordon, J. (1988). The marmoset B-lymphoblastoid cell line (B95-8) produces and responds to B-cell growth and differentiation factors: Role of shed CD23 (sCD23). *Immunology*, *65*(3), 379–384.

Capelluto, D. G. S., Kutateladze, T. G., Habas, R., Finkielstein, C. V., He, X., & Overduin, M. (2002). The DIX domain targets dishevelled to actin stress fibres and vesicular membranes. *Nature*, *419*(6908), 726–729. https://doi.org/10.1038/nature01056

Carlevaro-Fita, J., Rahim, A., Guigó, R., Vardy, L. A., & Johnson, R. (2016). Cytoplasmic long noncoding RNAs are frequently bound to and degraded at ribosomes in human cells. *RNA*, *22*(6), 867–882. https://doi.org/10.1261/rna.053561.115

Carninci, P., Kasukawa, T., Katayama, S., Gough, J., Frith, M. C., Maeda, N., Oyama, R., Ravasi, T., Lenhard, B., Wells, C., Kodzius, R., Shimokawa, K., Bajic, V. B., Brenner, S. E., Batalov, S., Forrest, A. R. R., Zavolan, M., Davis, M. J., Wilming, L. G., … Hayashizaki, Y. (2005). Molecular biology: The transcriptional landscape of the mammalian genome. *Science*, *309*(5740), 1559–1563. https://doi.org/10.1126/science.1112014

Carpenter, A. E., Jones, T. R., Lamprecht, M. R., Clarke, C., Kang, I. H., Friman, O., Guertin, D. A., Chang, J. H., Lindquist, R. A., Moffat, J., Golland, P., & Sabatini, D. M. (2006). CellProfiler: image analysis software for identifying and quantifying cell phenotypes. *Genome Biology*. https://doi.org/10.1186/gb-2006-7-10-r100

Carrascoso, I., Alcalde, J., Tabas-Madrid, D., Oliveros, J. C., & Izquierdo, J. M. (2018). Transcriptome-wide analysis links the short-term expression of the b isoforms of TIA proteins to protective proteostasis-mediated cell quiescence response. *PLoS ONE*, *13*(12), e0208526. https://doi.org/10.1371/journal.pone.0208526

Cassady, K. A., Gross, M., & Roizman, B. (1998). The Herpes Simplex Virus US11 Protein Effectively Compensates for the γ134.5 Gene if Present before Activation of Protein Kinase R by Precluding Its Phosphorylation and That of the α Subunit of Eukaryotic Translation Initiation Factor 2. *Journal of Virology*, *72*(11), 8620–8626. https://doi.org/10.1128/jvi.72.11.8620-8626.1998

Cencic, R., & Pelletier, J. (2016). Hippuristanol - A potent steroid inhibitor of eukaryotic initiation factor 4A. *Translation*, *4*(1), e1137381. https://doi.org/10.1080/21690731.2015.1137381

Cesaro, T., & Michiels, T. (2021). Inhibition of PKR by Viruses. In *Frontiers in Microbiology* (Vol. 12). https://doi.org/10.3389/fmicb.2021.757238

Chan, C. P., Kok, K. H., Tang, H. M. V., Wong, C. M., & Jin, D. Y. (2013). Internal ribosome entry site-mediated translational regulation of ATF4 splice variant in mammalian unfolded protein response. *Biochimica et Biophysica Acta - Molecular Cell Research*, *1833*(10), 2165–2175. https://doi.org/10.1016/j.bbamcr.2013.05.002

Chatterjee, K., Das, P., Chattopadhyay, N. R., Mal, S., & Choudhuri, T. (2019). The interplay between Epstein-Bar virus (EBV) with the p53 and its homologs during EBV associated malignancies. In *Heliyon* (Vol. 5, Issue 11). Elsevier Ltd. https://doi.org/10.1016/j.heliyon.2019.e02624

Chen, Y., Li, Z., Chen, X., & Zhang, S. (2021). Long non-coding RNAs: From disease code to drug role. In *Acta Pharmaceutica Sinica B* (Vol. 11, Issue 2, pp. 340–354). Chinese Academy of Medical Sciences. https://doi.org/10.1016/j.apsb.2020.10.001

Chiang, W. C., Chan, P., Wissinger, B., Vincent, A., Skorczyk-Werner, A., Krawczyński, M. R., Kaufman, R. J., Tsang, S. H., Héon, E., Kohl, S., & Lin, J. H. (2017). Achromatopsia mutations target sequential steps of ATF6 activation. *Proceedings of the National Academy of Sciences of the United States of America*, *114*(2), 400–405. https://doi.org/10.1073/pnas.1606387114

Chiu, Y. F., & Sugden, B. (2016). Epstein-Barr Virus: The Path from Latent to Productive Infection. In *Annual Review of Virology* (Vol. 3, pp. 359–372). https://doi.org/10.1146/annurev-virology-110615-042358

Choi, H., Lee, H., Kim, S. R., Gho, Y. S., & Lee, S. K. (2013). Epstein-Barr Virus-Encoded MicroRNA BART15-3p Promotes Cell Apoptosis Partially by Targeting BRUCE. *Journal of Virology*, *87*(14), 8135–8144. https://doi.org/10.1128/jvi.03159-12

Choy, M. S., Yusoff, P., Lee, I. C., Newton, J. C., Goh, C. W., Page, R., Shenolikar, S., & Peti, W. (2015). Structural and Functional Analysis of the GADD34: PP1 eIF2α Phosphatase. *Cell Reports*, *11*(12), 1885–1891. https://doi.org/10.1016/j.celrep.2015.05.043

Chujo, T., & Hirose, T. (2017). Nuclear bodies built on architectural long noncoding RNAs: Unifying principles of their construction and function. In *Molecules and Cells* (Vol. 40, Issue 12, pp. 889–896). https://doi.org/10.14348/molcells.2017.0263

Clarke, P. A., Schwemmle, M., Schickinger, J., Hilse, K., & Clemens, M. J. (1991). Binding of epstein-barr virus small RNA EBER-1 to the double-stranded RNA-activated protein kinase DAI. *Nucleic Acids Research*, *19*(2), 243–248. https://doi.org/10.1093/nar/19.2.243

Cláudio, N., Dalet, A., Gatti, E., & Pierre, P. (2013). Mapping the crossroads of immune activation and cellular stress response pathways. In *EMBO Journal* (Vol. 32, Issue 9, pp. 1214–1224). https://doi.org/10.1038/emboj.2013.80

Cohen, J. I. (2001). Epstein-Barr Virus Infection. *N Engl J Med*, *343*(1), 481–492.

Cohen, J. I., Wang, F., Mannick, J., & Kieff, E. D. (1989). Epstein-Barr virus nuclear protein 2 is a key determinant of lymphocyte transformation. *Proceedings of the National Academy of Sciences of the United States of America*, *86*(23), 9558–9562. https://doi.org/10.1073/pnas.86.23.9558

Collier, N. C., & Schlesinger, M. J. (1986). The dynamic state of heat shock proteins in chicken embryo fibroblasts. *Journal of Cell Biology*, *103*(4), 1495–1507. https://doi.org/10.1083/jcb.103.4.1495

Compton, T., Nepomuceno, R. R., & Nowlin, D. M. (1992). Human cytomegalovirus penetrates host cells by PH-independent fusion at the cell surface. *Virology*, *191*(1), 387–395. https://doi.org/10.1016/0042-6822(92)90200-9

Couthouis, J., Hart, M. P., Shorter, J., DeJesus-Hernandez, M., Erion, R., Oristano, R., Liu, A. X., Ramos, D., Jethava, N., Hosangadi, D., Epstein, J., Chiang, A., Diaz, Z., Nakaya, T., Ibrahim, F., Kim, H. J., Solski, J. A., Williams, K. L., Mojsilovic-Petrovic, J., … Gitler, A. D. (2011). A yeast functional screen predicts new candidate ALS disease genes. *Proceedings of the National Academy of Sciences of the United States of America*, *108*(52), 20881–20890. https://doi.org/10.1073/pnas.1109434108

Cruz-Muñoz, M. E., & Fuentes-Panana, E. M. (2018). Beta and gamma human herpesviruses: Agonistic and antagonistic interactions with the host immune system. In *Frontiers in Microbiology* (Vol. 8, Issue JAN, p. 2521). Frontiers Media SA. https://doi.org/10.3389/fmicb.2017.02521

Cui, B. C., Sikirzhytski, V., Aksenova, M., Lucius, M. D., Levon, G. H., Mack, Z. T., Pollack, C., Odhiambo, D., Broude, E., Lizarraga, S. B., Wyatt, M. D., & Shtutman, M. (2020). Pharmacological inhibition of DEAD-Box RNA Helicase 3 attenuates stress granule assembly. *Biochemical Pharmacology*, *182*, 114280. https://doi.org/10.1016/j.bcp.2020.114280

Dauber, B., Pelletier, J., & Smiley, J. R. (2011). The Herpes Simplex Virus 1 vhs Protein Enhances Translation of Viral True Late mRNAs and Virus Production in a Cell Type-Dependent Manner. *Journal of Virology*, *85*(11), 5363–5373. https://doi.org/10.1128/JVI.00115-11

Dauber, B., Poon, D., dos Santos, T., Duguay, B. A., Mehta, N., Saffran, H. A., & Smiley, J. R. (2016). The Herpes Simplex Virus Virion Host Shutoff Protein Enhances Translation of Viral True Late mRNAs Independently of Suppressing Protein Kinase R and Stress Granule Formation. *Journal of Virology*, *90*(13), 6049–6057. https://doi.org/10.1128/jvi.03180-15

Dauber, B., Saffran, H. A., & Smiley, J. R. (2019). The herpes simplex virus host shutoff (vhs) RNase limits accumulation of double stranded RNA in infected cells: Evidence for accelerated decay of duplex RNA. *PLoS Pathogens*, *15*(10). https://doi.org/10.1371/journal.ppat.1008111

Dauber, B., & Wolff, T. (2009). Activation of the antiviral kinase PKR and viral countermeasures. In *Viruses* (Vol. 1, Issue 3, pp. 523–544). Multidisciplinary Digital Publishing Institute (MDPI). https://doi.org/10.3390/v1030523

Davison, A. J. (2002). Evolution of the herpesviruses. *Veterinary Microbiology*, *86*(1–2), 69–88. https://doi.org/10.1016/S0378-1135(01)00492-8

De Leo, A., Calderon, A., & Lieberman, P. M. (2020). Control of Viral Latency by Episome Maintenance Proteins. In *Trends in Microbiology* (Vol. 28, Issue 2, pp. 150–162). https://doi.org/10.1016/j.tim.2019.09.002

Del Gatto-Konczak, F., Bourgeois, C. F., Le Guiner, C., Kister, L., Gesnel, M., Stévenin, J., & Breathnach, R. (2000). The RNA-Binding Protein TIA-1 Is a Novel Mammalian Splicing Regulator Acting through Intron Sequences Adjacent to a 5′ Splice Site.

Molecular and Cellular Biology, *20*(17), 6287–6299. https://doi.org/10.1128/mcb.20.17.6287-6299.2000

Delecluse, H.-J., Hilsendegen, T., Pich, D., Zeidler, R., & Hammerschmidt, W. (1998). Propagation and recovery of intact, infectious Epstein-Barr virus from prokaryotic to human cells. *Proceedings of the National Academy of Sciences of the United States of America*, *95*(14), 8245–8250. https://doi.org/10.1073/pnas.95.14.8245

Dember, L. M., Kim, N. D., Liu, K. Q., & Anderson, P. J. (1996). Individual RNA recognition motifs of TIA-1 and TIAR have different RNA binding specificities. *Journal of Biological Chemistry*, *271*(5), 2783–2788. https://doi.org/10.1074/jbc.271.5.2783

Derrien, T., Johnson, R., Bussotti, G., Tanzer, A., Djebali, S., Tilgner, H., Guernec, G., Martin, D., Merkel, A., Knowles, D. G., Lagarde, J., Veeravalli, L., Ruan, X., Ruan, Y., Lassmann, T., Carninci, P., Brown, J. B., Lipovich, L., Gonzalez, J. M., … Guigó, R. (2012). The GENCODE v7 catalog of human long noncoding RNAs: Analysis of their gene structure, evolution, and expression. *Genome Research*, *22*(9), 1775–1789. https://doi.org/10.1101/gr.132159.111

di Renzo, L., Alttok, A., Klein, G., & Klein, E. (1994). Endogenous TGF-β contributes to the induction of the EBV lytic cycle in two burkitt lymphoma cell lines. *International Journal of Cancer*, *57*(6), 914–919. https://doi.org/10.1002/ijc.2910570623

Ding, X., Sun, F., Chen, J., Chen, L., Tobin-Miyaji, Y., Xue, S., Qiang, W., & Luo, S. Z. (2020). Amyloid-Forming Segment Induces Aggregation of FUS-LC Domain from Phase Separation Modulated by Site-Specific Phosphorylation. *Journal of Molecular Biology*, *432*(2), 467–483. https://doi.org/10.1016/j.jmb.2019.11.017

Dixon, D. A., Balch, G. C., Kedersha, N., Anderson, P. J., Zimmerman, G. A., Beauchamp, R. D., & Prescott, S. M. (2003). Regulation of cyclooxygenase-2 expression by the translational silencer TIA-1. *Journal of Experimental Medicine*, *198*(3), 475–481. https://doi.org/10.1084/jem.20030616

Doench, J. G., Fusi, N., Sullender, M., Hegde, M., Vaimberg, E. W., Donovan, K. F., Smith, I., Tothova, Z., Wilen, C., Orchard, R., Virgin, H. W., Listgarten, J., & Root, D. E. (2016). Optimized sgRNA design to maximize activity and minimize off-target effects of CRISPR-Cas9. *Nature Biotechnology*, *34*(2), 184–191. https://doi.org/10.1038/nbt.3437

Döhner, K., Cornelius, A., Serrero, M. C., & Sodeik, B. (2021). The journey of herpesvirus capsids and genomes to the host cell nucleus. In *Current Opinion in Virology* (Vol. 50, pp. 147–158). Elsevier B.V. https://doi.org/10.1016/j.coviro.2021.08.005

Donehower, L. A., Soussi, T., Korkut, A., Liu, Y., Schultz, A., Cardenas, M. E., Li, X., Babur, O., Hsu, T. K., Lichtarge, O., Weinstein, J. N., Akbani, R., & Wheeler, D. A. (2019). Integrated Analysis of TP53 Gene and Pathway Alterations in The Cancer Genome Atlas. *Cell Reports*, *28*(5), 1370-1384.e5. https://doi.org/10.1016/j.celrep.2019.07.001

Dong, Y. L., Sugden, B., Lee, D. Y., & Sugden, B. (2008). The LMP1 oncogene of EBV activates PERK and the unfolded protein response to drive its own synthesis. *Blood*, *111*(4), 2280–2289. https://doi.org/10.1182/blood-2007-07-100032

Dörner, T., & Radbruch, A. (2007). Antibodies and B Cell Memory in Viral Immunity. In *Immunity* (Vol. 27, Issue 3, pp. 384–392). https://doi.org/10.1016/j.immuni.2007.09.002

Dreyfuss, G., Kim, V. N., & Kataoka, N. (2002). Messenger-RNA-binding proteins and the messages they carry. In *Nature Reviews Molecular Cell Biology* (Vol. 3, Issue 3, pp. 195–205). https://doi.org/10.1038/nrm760

Drummer, H. E., Reubel, G. H., & Stnddert, M. J. (1996). Equine gammaherpesvirus 2 (EHV2) is latent in B lymphocytes. *Archives of Virology*, *141*(3–4), 495–504. https://doi.org/10.1007/BF01718313

Du, M., & Chen, Z. J. (2018). DNA-induced liquid phase condensation of cGAS activates innate immune signaling. *Science*, *361*(6403), 704–709. https://doi.org/10.1126/science.aat1022

Duan, Y., Du, A., Gu, J., Duan, G., Wang, C., Gui, X., Ma, Z., Qian, B., Deng, X., Zhang, K., Sun, L., Tian, K., Zhang, Y., Jiang, H., Liu, C., & Fang, Y. (2019). PARylation regulates stress granule dynamics, phase separation, and neurotoxicity of disease-related RNA-binding proteins. *Cell Research*, *29*(3), 233–247. https://doi.org/10.1038/s41422-019-0141-z

Dubois, M. L., & Boisvert, F. M. (2016). The nucleolus: Structure and function. In *The Functional Nucleus* (pp. 29–49). https://doi.org/10.1007/978-3-319-38882-3_2

Duggan, M., Torkzaban, B., Ahooyi, T. M., Khalili, K., & Gordon, J. (2020). Age-related neurodegenerative diseases. In *Journal of Cellular Physiology* (Vol. 235, Issue 4, pp. 3131–3141). https://doi.org/10.1002/jcp.29248

Dumetz, A. C., Chockla, A. M., Kaler, E. W., & Lenhoff, A. M. (2008). Protein phase behavior in aqueous solutions: Crystallization, liquid-liquid phase separation, gels, and aggregates. *Biophysical Journal*, *94*(2), 570–583. https://doi.org/10.1529/biophysj.107.116152

Ebell, M. H. (2004). Epstein-Barr Virus Infectious Mononucleosis - American Family Physician. In *American Family Physician* (Vol. 70, Issue 7). www.aafp.org/afp.

Egan, P. A., Sobkowiak, M., & Chan, S.-W. (2013). Hepatitis C Virus Envelope Protein E1 Binds PERK and Represses the Unfolded Protein Response. *The Open Virology Journal*, *7*(1), 37–40. https://doi.org/10.2174/1874357901307010037

Eiermann, N., Haneke, K., Sun, Z., Stoecklin, G., & Ruggieri, A. (2020). Dance with the Devil: Stress Granules and Signaling in Antiviral Responses. In *Viruses* (Vol. 12, Issue 9). Viruses. https://doi.org/10.3390/v12090984

El-Sharkawy, A., Al Zaidan, L., & Malki, A. (2018). Epstein-Barr virus-associated malignancies: Roles of viral oncoproteins in carcinogenesis. In *Frontiers in Oncology* (Vol. 8, Issue AUG, p. 265). https://doi.org/10.3389/fonc.2018.00265

Eliopoulos, A. G., Gallagher, N. J., Blake, S. M. S., Dawson, C. W., & Young, L. S. (1999). Activation of the p38 mitogen-activated protein kinase pathway by Epstein-Barr virus-encoded latent membrane protein 1 coregulates interleukin- 6 and interleukin-8 production. *Journal of Biological Chemistry*, *274*(23), 16085–16096. https://doi.org/10.1074/jbc.274.23.16085

Eliopoulos, A. G., & Young, L. S. (1998). Activation of the cJun N-terminal kinase (JNK) pathway by the Epstein-Barr virus-encoded latent membrane protein 1 (LMP1). *Oncogene*, *16*(13), 1731–1742. https://doi.org/10.1038/sj.onc.1201694

Emara, M. M., & Brinton, M. A. (2007). Interaction of TIA-1/TIAR with West Nile and dengue virus products in infected cells interferes with stress granule formation and

processing body assembly. *Proceedings of the National Academy of Sciences*, *104*(21), 9041–9046. https://doi.org/10.1073/pnas.0703348104

Epstein, M. A., Achong, B. G., & Barr, Y. M. (1964). Virus Particles In Cultured Lymphoblasts From Burkitt's Lymphoma. *The Lancet*, *283*(7335), 702–703. https://doi.org/10.1016/S0140-6736(64)91524-7

Erickson, F. L., Harding, L. D., Dorris, D. R., & Hannig, E. M. (1997). Functional analysis of homologs of translation initiation factor 2γ in yeast. *Molecular and General Genetics*, *253*(6), 711–719. https://doi.org/10.1007/s004380050375

Ernst, H., Duncan, R. F., & Hershey, J. W. B. (1987). Cloning and sequencing of complementary DNAs encoding the α-subunit of translational initiation factor eIF-2. Characterization of the protein and its messenger RNA. *Journal of Biological Chemistry*, *262*(3), 1206–1212. https://doi.org/10.1016/s0021-9258(19)75772-x

Esclatine, A., Taddeo, B., & Roizman, B. (2004a). The UL41 protein of herpes simplex virus mediates selective stabilization or degradation of cellular mRNAs. *Proceedings of the National Academy of Sciences of the United States of America*, *101*(52), 18165–18170. https://doi.org/10.1073/pnas.0408272102

Esclatine, A., Taddeo, B., & Roizman, B. (2004b). Herpes Simplex Virus 1 Induces Cytoplasmic Accumulation of TIA-1/TIAR and both Synthesis and Cytoplasmic Accumulation of Tristetraprolin, Two Cellular Proteins That Bind and Destabilize AU-Rich RNAs. *Journal of Viology*, *78*(16), 8582–8592. https://doi.org/10.1128/JVI.78.16.8582-8592.2004

Esteban, M., García, M. A., Domingo-Gil, E., Arroyo, J., Nombela, C., & Rivas, C. (2003). The latency protein LANA2 from Kaposi's sarcoma-associated herpesvirus inhibits apoptosis induced by dsRNA-activated protein kinase but not RNase L activation. *Journal of General Virology*, *84*(6), 1463–1470. https://doi.org/10.1099/vir.0.19014-0

Esteller, M. (2011). Non-coding RNAs in human disease. In *Nature Reviews Genetics* (Vol. 12, Issue 12, pp. 861–874). https://doi.org/10.1038/nrg3074

Everly, D. N., Feng, P., Mian, I. S., & Read, G. S. (2002). mRNA Degradation by the Virion Host Shutoff (Vhs) Protein of Herpes Simplex Virus: Genetic and Biochemical Evidence that Vhs Is a Nuclease. *Journal of Virology*, *76*(17), 8560–8571. https://doi.org/10.1128/jvi.76.17.8560-8571.2002

Fan, X. C., & Steitz, J. A. (1998). Overexpression of HuR, a nuclear-cytoplasmic shuttling protein, increases the in vivo stability of ARE-containing mRNAs. *EMBO Journal*, *17*(12), 3448–3460. https://doi.org/10.1093/emboj/17.12.3448

Fay, M. M., Aulas, A., Kedersha, N., Ivanov, P., Anderson, P. J., & Szaflarski, W. (2017). Methods to Classify Cytoplasmic Foci as Mammalian Stress Granules. *Journal of Visualized Experiments*, *123*, 55656. https://doi.org/10.3791/55656

Feederle, R, Bannert, H., Lips, H., Müller-Lantzsch, N., & Delecluse, H.-J. (2009). The Epstein-Barr Virus Alkaline Exonuclease BGLF5 Serves Pleiotropic Functions in Virus Replication. *Journal of Virology*, *83*(10), 4952–4962. https://doi.org/10.1128/jvi.00170-09

Feederle, Regina, Haar, J., Bernhardt, K., Linnstaedt, S. D., Bannert, H., Lips, H., Cullen, B. R., & Delecluse, H.-J. (2011). The Members of an Epstein-Barr Virus MicroRNA Cluster Cooperate To Transform B Lymphocytes. *Journal of Virology*, *85*(19), 9801–

9810. https://doi.org/10.1128/jvi.05100-11

Feederle, Regina, Mehl-Lautscham, A. M., Bannert, H., & Delecluse, H.-J. (2009). The Epstein-Barr Virus Protein Kinase BGLF4 and the Exonuclease BGLF5 Have Opposite Effects on the Regulation of Viral Protein Production. *Journal of Virology*, *83*(21), 10877–10891. https://doi.org/10.1128/jvi.00525-09

Fijen, C., & Rothenberg, E. (2021). The evolving complexity of DNA damage foci: RNA, condensates and chromatin in DNA double-strand break repair. *DNA Repair*, *105*. https://doi.org/10.1016/j.dnarep.2021.103170

Finnen, R. L., Hay, T. J. M., Dauber, B., Smiley, J. R., & Banfield, B. W. (2014). The Herpes Simplex Virus 2 Virion-Associated Ribonuclease vhs Interferes with Stress Granule Formation. *Journal of Virology*, *88*(21), 12727–12739. https://doi.org/10.1128/JVI.01554-14

Finnen, R. L., Pangka, K. R., & Banfield, B. W. (2012). Herpes Simplex Virus 2 Infection Impacts Stress Granule Accumulation. *Journal of Virology*, *86*(15), 8119–8130. https://doi.org/10.1128/JVI.00313-12

Finnen, R. L., Zhu, M., Li, J., Romo, D., & Banfield, B. W. (2016). Herpes Simplex Virus 2 Virion Host Shutoff Endoribonuclease Activity Is Required To Disrupt Stress Granule Formation. *Journal of Virology*, *90*(17), 7943–7955. https://doi.org/10.1128/JVI.00947-16

Fiola, S., Gosselin, D., Takada, K., & Gosselin, J. (2010). TLR9 Contributes to the Recognition of EBV by Primary Monocytes and Plasmacytoid Dendritic Cells. *The Journal of Immunology*, *185*(6), 3620–3631. https://doi.org/10.4049/jimmunol.0903736

Fish, K., Chen, J., & Longnecker, R. (2014). Epstein-Barr virus latent membrane protein 2A enhances MYC-driven cell cycle progression in a mouse model of B lymphoma. *Blood*, *123*(4), 530–540. https://doi.org/10.1182/blood-2013-07-517649

Fok, V., Mitton-Fry, R. M., Grech, A., & Steitz, J. A. (2006). Multiple domains of EBER 1, an Epstein-Barr virus noncoding RNA, recruit human ribosomal protein L22. *RNA*, *12*(5), 872–882. https://doi.org/10.1261/rna.2339606

Förch, P., Puig, O., Kedersha, N., Martínez, C., Granneman, S., Séraphin, B., Anderson, P. J., & Valcárcel, J. (2000). The apoptosis-promoting factor TIA-1 is a regulator of alternative pre-mRNA splicing. *Molecular Cell*, *6*(5), 1089–1098. https://doi.org/10.1016/S1097-2765(00)00107-6

Förch, P., Puig, O., Martínez, C., Séraphin, B., & Valcárcel, J. (2002). The splicing regulator TIA-1 interacts with U1-C to promote U1 snRNP recruitment to 5′ splice sites. *EMBO Journal*, *21*(24), 6882–6892. https://doi.org/10.1093/emboj/cdf668

Fox, A. H., Bond, C. S., & Lamond, A. I. (2005). P54nrb forms a heterodimer with PSP1 that localizes to paraspeckles in an RNA-dependent manner. *Molecular Biology of the Cell*, *16*(11), 5304–5315. https://doi.org/10.1091/mbc.E05-06-0587

Fox, A. H., Lam, Y. W., Leung, A. K. L., Lyon, C. E., Andersen, J., Mann, M., & Lamond, A. I. (2002). Paraspeckles: A novel nuclear domain. *Current Biology*, *12*(1), 13–25. https://doi.org/10.1016/S0960-9822(01)00632-7

Franchi, L., Warner, N., Viani, K., & Nuñez, G. (2009). Function of Nod-like receptors in microbial recognition and host defense. In *Immunological Reviews* (Vol. 227, Issue

1, pp. 106–128). NIH Public Access. https://doi.org/10.1111/j.1600-065X.2008.00734.x

Fugl, A., & Andersen, C. L. (2019). Epstein-Barr virus and its association with disease - A review of relevance to general practice. In *BMC Family Practice* (Vol. 20, Issue 1). https://doi.org/10.1186/s12875-019-0954-3

Fujimura, K., Sasaki, A. T., & Anderson, P. J. (2012). Selenite targets eIF4E-binding protein-1 to inhibit translation initiation and induce the assembly of non-canonical stress granules. *Nucleic Acids Research*, *40*(16), 8099–8110. https://doi.org/10.1093/nar/gks566

Fujiwara, S., Nitadori, Y., Nakamura, H., Nagaishi, T., & Ono, Y. (1999). Epstein-Barr Virus (EBV) Nuclear Protein 2-Induced Disruption of EBV Latency in the Burkitt's Lymphoma Cell Line Akata: Analysis by Tetracycline-Regulated Expression. *Journal of Virology*, *73*(6), 5214–5219. https://doi.org/10.1128/jvi.73.6.5214-5219.1999

Fukuda, M., & Kawaguchi, Y. (2014). Role of the Immunoreceptor Tyrosine-Based Activation Motif of Latent Membrane Protein 2A (LMP2A) in Epstein-Barr Virus LMP2A-Induced Cell Transformation. *Journal of Virology*, *88*(9), 5189–5194. https://doi.org/10.1128/jvi.03714-13

Furnari, F. B., Adams, M. D., & Pagano, J. S. (1992). Regulation of the Epstein-Barr virus DNA polymerase gene. *Journal of Virology*, *66*(5), 2837–2845. https://doi.org/10.1128/jvi.66.5.2837-2845.1992

Gall, J. G., Bellini, M., Wu, Z., & Murphy, C. (1999). Assembly of the nuclear transcription and processing machinery: Cajal bodies (coiled bodies) and transcriptosomes. *Molecular Biology of the Cell*, *10*(12), 4385–4402. https://doi.org/10.1091/mbc.10.12.4385

Garrido, J. L., Maruo, S., Takada, K., & Rosendorff, A. (2009). EBNA3C interacts with Gadd34 and counteracts the unfolded protein response. *Virology Journal*, *6*(1), 231. https://doi.org/10.1186/1743-422X-6-231

Gaspar, N. J., Kinzy, T. G., Scherer, B. J., Humbelin, M., Hershey, J. W. B., & Merrick, W. C. (1994). Translation initiation factor eIF-2. Cloning and expression of the human cDNA encoding the γ-subunit. *Journal of Biological Chemistry*, *269*(5), 3415–3422. https://doi.org/10.1016/s0021-9258(17)41878-3

Gass, J. N., Gifford, N. M., & Brewer, J. W. (2002). Activation of an unfolded protein response during differentiation of antibody-secreting B cells. *Journal of Biological Chemistry*, *277*(50), 49047–49054. https://doi.org/10.1074/jbc.M205011200

Gaudreault, E., Fiola, S., Olivier, M., & Gosselin, J. (2007). Epstein-Barr Virus Induces MCP-1 Secretion by Human Monocytes via TLR2. *Journal of Virology*, *81*(15), 8016–8024. https://doi.org/10.1128/jvi.00403-07

Gershon, A. A., Chen, J., Davis, L., Krinsky, C., Cowles, R., Reichard, R., & Gershon, M. (2012). Latency of varicella zoster virus in dorsal root, cranial, and enteric ganglia in vaccinated children. *Transactions of the American Clinical and Climatological Association*, *123*.

Gibson, B. A., Doolittle, L. K., Schneider, M. W. G., Jensen, L. E., Gamarra, N., Henry, L., Gerlich, D. W., Redding, S., & Rosen, M. K. (2019). Organization of Chromatin by Intrinsic and Regulated Phase Separation. *Cell*, *179*(2), 470-484.e21.

https://doi.org/10.1016/j.cell.2019.08.037

Gilks, N., Kedersha, N., Ayodele, M., Shen, L., Stoecklin, G., Dember, L. M., & Anderson, P. J. (2004). Stress granule assembly is mediated by prion-like aggregation of TIA-1. *Molecular Biology of the Cell*, *15*(12), 5383–5398. https://doi.org/10.1091/mbc.E04-08-0715

Gill, A. L., Premasiri, A. S., & Vieira, F. G. (2021). Hypothesis and Theory: Roles of Arginine Methylation in C9orf72-Mediated ALS and FTD. *Frontiers in Cellular Neuroscience*, *15*, 23. https://doi.org/10.3389/fncel.2021.633668

Girardin, S. E., Cuziol, C., Philpott, D. J., & Arnoult, D. (2020). The eIF2α kinase HRI in innate immunity, proteostasis, and mitochondrial stress. In *FEBS Journal* (Vol. 288, Issue 10, pp. 3094–3107). FEBS J. https://doi.org/10.1111/febs.15553

Glaser, R., Tarr, K. L., & Dangel, A. W. (1989). The transforming prototype of epstein-barr virus (B95-8) is also a lytic virus. *International Journal of Cancer*, *44*(1), 95–100. https://doi.org/10.1002/ijc.2910440118

Glauninger, H., Wong Hickernell, C. J., Bard, J. A. M., & Drummond, D. A. (2022). Stressful steps: Progress and challenges in understanding stress-induced mRNA condensation and accumulation in stress granules. *Molecular Cell*. https://doi.org/10.1016/j.molcel.2022.05.014

Glaunsinger, B., & Ganem, D. (2004). Lytic KSHV infection inhibits host gene expression by accelerating global mRNA turnover. *Molecular Cell*, *13*(5), 713–723. https://doi.org/10.1016/S1097-2765(04)00091-7

Glickman, J. N., Howe, J. G., & Steitz, J. A. (1988). Structural analyses of EBER1 and EBER2 ribonucleoprotein particles present in Epstein-Barr virus-infected cells. *Journal of Virology*, *62*(3), 902–911. https://doi.org/10.1128/jvi.62.3.902-911.1988

Glisovic, T., Bachorik, J. L., Yong, J., & Dreyfuss, G. (2008). RNA-binding proteins and post-transcriptional gene regulation. In *FEBS Letters* (Vol. 582, Issue 14, pp. 1977–1986). https://doi.org/10.1016/j.febslet.2008.03.004

Glynn, F. J., Mackle, T., & Kinsella, J. (2007). Upper airway obstruction in infectious mononucleosis. *European Journal of Emergency Medicine*, *14*(1), 41–42. https://doi.org/10.1097/01.mej.0000224431.36376.71

Gordiyenko, Y., Llácer, J. L., & Ramakrishnan, V. (2019). Structural basis for the inhibition of translation through eIF2α phosphorylation. *Nature Communications*, *10*(1), 1–11. https://doi.org/10.1038/s41467-019-10606-1

Gregorovic, G., Boulden, E. A., Bosshard, R., Elgueta Karstegl, C., Skalsky, R., Cullen, B. R., Gujer, C., Rämer, P. C., Münz, C., & Farrell, P. J. (2015). Epstein-Barr Viruses (EBVs) Deficient in EBV-Encoded RNAs Have Higher Levels of Latent Membrane Protein 2 RNA Expression in Lymphoblastoid Cell Lines and Efficiently Establish Persistent Infections in Humanized Mice. *Journal of Virology*, *89*(22), 11711–11714. https://doi.org/10.1128/jvi.01873-15

Gregory, C. D., Rowe, M., & Rickinson, A. B. (1990). Different Epstein-Barr virus-B cell interactions in phenotypically distinct clones of a Burkitt's lymphoma cell line. *Journal of General Virology*, *71*(7), 1481–1495. https://doi.org/10.1099/0022-1317-71-7-1481

Gribskov, M. (1992). Translational initiation factors IF-1 and eIF-2α share an RNA-

binding motif with prokaryotic ribosomal protein S1 and polynucleotide phosphorylase. *Gene*, *119*(1), 107–111. https://doi.org/10.1016/0378-1119(92)90073-X

Grogan, E., Jenson, H. B., Countryman, J., Heston, L., Gradoville, L., & Miller, G. (1987). Transfection of a rearranged viral DNA fragment, WZhet, stably converts latent Epstein-Barr viral infection to productive infection in lymphoid cells. *Proceedings of the National Academy of Sciences of the United States of America*, *84*(5), 1332–1336. https://doi.org/10.1073/pnas.84.5.1332

Gruffat, H., Batisse, J., Pich, D., Neuhierl, B., Manet, E., Hammerschmidt, W., & Sergeant, A. (2002). Epstein-Barr Virus mRNA Export Factor EB2 Is Essential for Production of Infectious Virus. *Journal of Virology*, *76*(19), 9635–9644. https://doi.org/10.1128/jvi.76.19.9635-9644.2002

Guillén-Boixet, J., Kopach, A., Holehouse, A. S., Wittmann, S., Jahnel, M., Schlüßler, R., Kim, K., Trussina, I. R. E. A., Wang, J., Mateju, D., Poser, I., Maharana, S., Ruer-Gruß, M., Rickinson, A. B., Zhang, X., Chang, Y. T., Guck, J., Honigmann, A., Mahamid, J., … Franzmann, T. M. (2020). RNA-Induced Conformational Switching and Clustering of G3BP Drive Stress Granule Assembly by Condensation. *Cell*, *181*(2), 346-361.e17. https://doi.org/10.1016/j.cell.2020.03.049

Haeussler, M., Schönig, K., Eckert, H., Eschstruth, A., Mianné, J., Renaud, J. B., Schneider-Maunoury, S., Shkumatava, A., Teboul, L., Kent, J., Joly, J. S., & Concordet, J. P. (2016). Evaluation of off-target and on-target scoring algorithms and integration into the guide RNA selection tool CRISPOR. *Genome Biology*, *17*(1). https://doi.org/10.1186/s13059-016-1012-2

Hamada, J., Shoda, K., Masuda, K., Fujita, Y., Naruto, T., Kohmoto, T., Miyakami, Y., Watanabe, M., Kudo, Y., Fujiwara, H., Ichikawa, D., Otsuji, E., & Imoto, I. (2016). Tumor-promoting function and prognostic significance of the RNA-binding protein T-cell intracellular antigen-1 in esophageal squamous cell carcinoma. *Oncotarget*, *7*(13), 17111–17128. https://doi.org/10.18632/oncotarget.7937

Hamdollah Zadeh, M. A., Amin, E. M., Hoareau-Aveilla, C., Domingo, E., Symonds, K. E., Ye, X., Heesom, K. J., Salmon, A. H. J., D'Silva, O., Betteridge, K. B., Williams, A. C., Kerr, D. J., Oltean, S., Midgley, R. S., Ladomery, M. R., Harper, S. J., Varey, A. H. R., & Bates, D. O. (2015). Alternative splicing of TIA-1 in human colon cancer regulates VEGF isoform expression, angiogenesis, tumour growth and bevacizumab resistance. *Molecular Oncology*, *9*(1), 167–178. https://doi.org/10.1016/j.molonc.2014.07.017

Hamilton-Dutoit, S. J., Rea, D., Raphael, M., Sandvej, K., Delecluse, H.-J., Gisselbrecht, C., Marelle, L., Van Krieken, J. H. J. M., & Pallesen, G. (1993). Epstein-Barr virus-latent gene expression and tumor cell phenotype in acquired immunodeficiency syndrome-related non-Hodgkin's lymphoma: Correlation of lymphoma phenotype with three distinct patterns of viral latency. *American Journal of Pathology*, *143*(4), 1072–1085. /pmc/articles/PMC1887058/?report=abstract

Han, J., Back, S. H., Hur, J., Lin, Y. H., Gildersleeve, R., Shan, J., Yuan, C. L., Krokowski, D., Wang, S., Hatzoglou, M., Kilberg, M. S., Sartor, M. A., & Kaufman, R. J. (2013). ER-stress-induced transcriptional regulation increases protein synthesis leading to cell death. *Nature Cell Biology*, *15*(5), 481–490. https://doi.org/10.1038/ncb2738

Haneklaus, M., Gerlic, M., Kurowska-Stolarska, M., Rainey, A.-A., Pich, D., McInnes, I. B., Hammerschmidt, W., O'Neill, L. A. J., & Masters, S. L. (2012). Cutting Edge: miR-223 and EBV miR-BART15 Regulate the NLRP3 Inflammasome and IL-1β

Production. *The Journal of Immunology*, *189*(8), 3795–3799. https://doi.org/10.4049/jimmunol.1200312

Harada, S., & Kieff, E. D. (1997). Epstein-Barr virus nuclear protein LP stimulates EBNA-2 acidic domain-mediated transcriptional activation. *Journal of Virology*, *71*(9), 6611–6618. https://doi.org/10.1128/jvi.71.9.6611-6618.1997

Harding, H. P., Novoa, I., Zhang, Y., Zeng, H., Wek, R. C., Schapira, M., & Ron, D. (2000). Regulated translation initiation controls stress-induced gene expression in mammalian cells. *Molecular Cell*, *6*(5), 1099–1108. https://doi.org/10.1016/S1097-2765(00)00108-8

Hardy, W. B. (1905). Colloidal solution. The globulins. *The Journal of Physiology*, *33*(4–5), 251–337. https://doi.org/10.1113/jphysiol.1905.sp001126

Hardy, W. B. (1912). The tension of composite fluid surfaces and the mechanical stability of films of fluid. *Proceedings of the Royal Society of London. Series A, Containing Papers of a Mathematical and Physical Character*, *86*(591), 610–635. https://doi.org/10.1098/rspa.1912.0053

Harth-Hertle, M. L., Scholz, B. A., Erhard, F., Glaser, L. V., Dölken, L., Zimmer, R., & Kempkes, B. (2013). Inactivation of Intergenic Enhancers by EBNA3A Initiates and Maintains Polycomb Signatures across a Chromatin Domain Encoding CXCL10 and CXCL9. *PLoS Pathogens*, *9*(9). https://doi.org/10.1371/journal.ppat.1003638

Hausen, H. Zur, O'Neill, F. J., Freese, U. K., & Hecker, E. (1978). Persisting oncogenic herpesvirus induced by the tumour promoter TPA. *Nature*, *272*(5651), 373–375. https://doi.org/10.1038/272373a0

Hayden, M. S., West, A. P., & Ghosh, S. (2006). NF-κB and the immune response. In *Oncogene* (Vol. 25, Issue 51, pp. 6758–6780). https://doi.org/10.1038/sj.onc.1209943

He, J., Liu, L., Tang, F., Zhou, Y., Liu, H., Lu, C., Feng, D., Zhu, H., Mao, Y., Li, Z., Zhang, L., Duan, Y., Xiao, Z., Zeng, M., Weng, L., & Sun, L. Q. (2021). Paradoxical effects of DNA tumor virus oncogenes on epithelium-derived tumor cell fate during tumor progression and chemotherapy response. *Signal Transduction and Targeted Therapy*, *6*(1). https://doi.org/10.1038/s41392-021-00787-x

Hemmi, H., Takeuchi, O., Kawai, T., Kaisho, T., Sato, S., Sanjo, H., Matsumoto, M., Hoshino, K., Wagner, H., Takeda, K., & Akira, S. (2000). A Toll-like receptor recognizes bacterial DNA. *Nature*, *408*(6813), 740–745. https://doi.org/10.1038/35047123

Herbst, H., Dallenbach, F., Hummel, M., Niedobitek, G., Pileri, S., Muller-Lantzsch, N., & Stein, H. (1991). Epstein-Barr virus latent membrane protein expression in Hodgkin and Reed-Sternberg cells. *Proceedings of the National Academy of Sciences of the United States of America*, *88*(11), 4766–4770. https://doi.org/10.1073/pnas.88.11.4766

Hershey, J. W. B. (1989). Protein phosphorylation controls translation rates. In *Journal of Biological Chemistry* (Vol. 264, Issue 35, pp. 20823–20826). http://www.jbc.org/content/264/35/20823.full.pdf

Hinman, M. N., & Lou, H. (2008). Diverse molecular functions of Hu proteins. In *Cellular and Molecular Life Sciences* (Vol. 65, Issue 20, pp. 3168–3181). https://doi.org/10.1007/s00018-008-8252-6

Hinnebusch, A. G., & Lorsch, J. R. (2012). The mechanism of eukaryotic translation initiation: New insights and challenges. *Cold Spring Harbor Perspectives in Biology*, *4*(10). https://doi.org/10.1101/cshperspect.a011544

Hofmann, S., Kedersha, N., Anderson, P. J., & Ivanov, P. (2021). Molecular mechanisms of stress granule assembly and disassembly. In *Biochimica et Biophysica Acta - Molecular Cell Research* (Vol. 1868, Issue 1). Biochim Biophys Acta Mol Cell Res. https://doi.org/10.1016/j.bbamcr.2020.118876

Hofweber, M., & Dormann, D. (2019). Friend or foe-Post-translational modifications as regulators of phase separation and RNP granule dynamics. In *Journal of Biological Chemistry* (Vol. 294, Issue 18, pp. 7137–7150). American Society for Biochemistry and Molecular Biology. https://doi.org/10.1074/jbc.TM118.001189

Hollyoake, M., Stühler, A., Farrell, P. J., Sinclair, A. J., & Gordon, J. (1995). The Normal Cell Cycle Activation Program Is Exploited during the Infection of Quiescent B Lymphocytes by Epstein-Barr Virus. *Cancer Research*, *55*(21), 4784–4787. https://pubmed.ncbi.nlm.nih.gov/7585505/

Homa, N. J., Salinas, R., Forte, E., Robinson, T. J., Garcia-Blanco, M. A., & Luftig, M. A. (2013). Epstein-Barr Virus Induces Global Changes in Cellular mRNA Isoform Usage That Are Important for the Maintenance of Latency. *Journal of Virology*, *87*(22), 12291–12301. https://doi.org/10.1128/jvi.02464-13

Horst, D., Burmeister, W. P., Boer, I. G. J., van Leeuwen, D., Buisson, M., Gorbalenya, A. E., Wiertz, E. J., & Ressing, M. E. (2012). The “Bridge” in the Epstein-Barr Virus Alkaline Exonuclease Protein BGLF5 Contributes to Shutoff Activity during Productive Infection. *Journal of Virology*, *86*(17), 9175–9187. https://doi.org/10.1128/jvi.00309-12

Houmani, J. L., Davis, C. I., & Ruf, I. K. (2009). Growth-Promoting Properties of Epstein-Barr Virus EBER-1 RNA Correlate with Ribosomal Protein L22 Binding. *Journal of Virology*, *83*(19), 9844–9853. https://doi.org/10.1128/jvi.01014-09

Hoving, J. C., Wilson, G. J., & Brown, G. D. (2014). Signalling C-type lectin receptors, microbial recognition and immunity. In *Cellular Microbiology* (Vol. 16, Issue 2, pp. 185–194). Wiley-Blackwell. https://doi.org/10.1111/cmi.12249

Howe, J. G., & Steitz, J. A. (1986). Localization of Epstein-Barr virus-encoded small RNAs by in situ hybridization. *Proceedings of the National Academy of Sciences of the United States of America*, *83*(23), 9006–9010. https://doi.org/10.1073/pnas.83.23.9006

Hu, F. L., Chen, F. Y., Zheng, X., Ernberg, I., Cao, S. L., Christensson, B., Klein, G., & Winberg, G. (1993). Clonability and tumorigenicity of human epithelial cells expressing the EBV encoded membrane protein LMP1. *Oncogene*, *8*(6), 1575–1583. https://europepmc.org/article/med/8389032

Hu, S., Sun, H., Yin, L., Li, J., Mei, S., Xu, F., Wu, C., Liu, X., Zhao, F., Zhang, D., Huang, Y., Ren, L., Cen, S., Wang, J., Liang, C., & Guo, F. (2019). PKR-dependent cytosolic cGAS foci are necessary for intracellular DNA sensing. *Science Signaling*, *12*(609). https://doi.org/10.1126/scisignal.aav7934

Huang, C., Chen, Y., Dai, H., Zhang, H., Xie, M., Zhang, H., Chen, F., Kang, X., Bai, X., & Chen, Z. (2020). UBAP2L arginine methylation by PRMT1 modulates stress granule assembly. *Cell Death and Differentiation*, *27*(1), 227–241. https://doi.org/10.1038/s41418-019-0350-5

Huang, S., Deerinck, T. J., Ellisman, M. H., & Spector, D. L. (1998). The perinucleolar compartment and transcription. *Journal of Cell Biology*, *143*(1), 35–47. https://doi.org/10.1083/jcb.143.1.35

Hutchinson, J. N., Ensminger, A. W., Clemson, C. M., Lynch, C. R., Lawrence, J. B., & Chess, A. (2007). A screen for nuclear transcripts identifies two linked noncoding RNAs associated with SC35 splicing domains. *BMC Genomics*, *8*(1), 1–16. https://doi.org/10.1186/1471-2164-8-39

Hyman, A. A., Weber, C. A., & Jülicher, F. (2014). Liquid-liquid phase separation in biology. In *Annual review of cell and developmental biology* (Vol. 30, pp. 39–58). Annual Reviews. https://doi.org/10.1146/annurev-cellbio-100913-013325

ICTV. (2021). *Virus Taxonomy: 2021 Release*. International Committee on Taxonomy of Viruses. https://talk.ictvonline.org/taxonomy/

Iizasa, H., Kim, H., Kartika, A. V., Kanehiro, Y., & Yoshiyama, H. (2020). Role of Viral and Host microRNAs in Immune Regulation of Epstein-Barr Virus-Associated Diseases. In *Frontiers in Immunology* (Vol. 11, p. 367). https://doi.org/10.3389/fimmu.2020.00367

Iizasa, H., Nanbo, A., Nishikawa, J., Jinushi, M., & Yoshiyama, H. (2012). Epstein-barr virus (EBV)-associated gastric carcinoma. In *Viruses* (Vol. 4, Issue 12, pp. 3420–3439). https://doi.org/10.3390/v4123420

Ivashkiv, L. B., & Donlin, L. T. (2014). Regulation of type i interferon responses. In *Nature Reviews Immunology* (Vol. 14, Issue 1, pp. 36–49). https://doi.org/10.1038/nri3581

Iwakiri, D., Zhou, L., Samanta, M., Matsumoto, M., Ebihara, T., Seya, T., Imai, S., Fujieda, M., Kawa, K., & Takada, K. (2009). Epstein-Barr virus (EBV)-encoded small RNA is released from EBV-infected cells and activates signaling from toll-like receptor 3. *Journal of Experimental Medicine*, *206*(10), 2091–2099. https://doi.org/10.1084/jem.20081761

Izquierdo, J. M. (2008). Hu antigen R (HuR) functions as an alternative pre-mRNA splicing regulator of Fas apoptosis-promoting receptor on exon definition. *Journal of Biological Chemistry*, *283*(27), 19077–19084. https://doi.org/10.1074/jbc.M800017200

Izquierdo, J. M., Alcalde, J., Carrascoso, I., Reyes, R., & Ludeña, M. D. (2011). Knockdown of T-cell intracellular antigens triggers cell proliferation, invasion and tumour growth. *Biochemical Journal*, *435*(2), 337–344. https://doi.org/10.1042/BJ20101030

Izquierdo, J. M., Majós, N., Bonnal, S., Martínez, C., Castelo, R., Guigó, R., Bilbao, D., & Valcárcel, J. (2005). Regulation of fas alternative splicing by antagonistic effects of TIA-1 and PTB on exon definition. *Molecular Cell*, *19*(4), 475–484. https://doi.org/10.1016/j.molcel.2005.06.015

Izquierdo, J. M., & Valcárcel, J. (2007a). Fas-activated Serine/Threonine Kinase (FAST K) synergizes with TIA-1/TIAR proteins to regulate Fas alternative splicing. *Journal of Biological Chemistry*, *282*(3), 1539–1543. https://doi.org/10.1074/jbc.C600198200

Izquierdo, J. M., & Valcárcel, J. (2007b). Two isoforms of the T-cell Intracellular Antigen 1 (TIA-1) splicing factor display distinct splicing regulation activities: Control of TIA-1 isoform ratio by TIA-1-related protein. *Journal of Biological Chemistry*, *282*(27),

19410–19417. https://doi.org/10.1074/jbc.M700688200

Izumi, K. M., Kaye, K. M., & Kieff, E. D. (1997). The Epstein-Barr virus LMP1 amino acid sequence that engages tumor necrosis factor receptor associated factors is critical for primary B lymphocyte growth transformation. *Proceedings of the National Academy of Sciences of the United States of America*, *94*(4), 1447–1452. https://doi.org/10.1073/pnas.94.4.1447

Jacobs, B. L., & Langland, J. O. (1996). When Two Strands Are Better Than One: The Mediators and Modulators of the Cellular Responses to Double-Stranded RNA. In *Virology* (Vol. 219, Issue 2, pp. 339–349). https://doi.org/10.1006/viro.1996.0259

Jacquemont, B., & Roizman, B. (1975). RNA synthesis in cells infected with herpes simplex virus. X. Properties of viral symmetric transcripts and of double-stranded RNA prepared from them. *Journal of Virology*, *15*(4), 707–713. https://doi.org/10.1128/jvi.15.4.707-713.1975

Jain, S., Wheeler, J. R., Walters, R. W., Agrawal, A., Barsic, A., & Parker, R. (2016). ATPase-Modulated Stress Granules Contain a Diverse Proteome and Substructure. *Cell*, *164*(3), 487–498. https://doi.org/10.1016/j.cell.2015.12.038

Jaramillo, M. L., Abraham, N., & Bell, J. C. (1995). Molecular biology: The interferon system: A review with emphasis on the role of PKR in growth control. In *Cancer Investigation* (Vol. 13, Issue 3, pp. 327–338). Taylor & Francis. https://doi.org/10.3109/07357909509094468

Jeffery-Smith, A., & Riddell, A. (2021). Herpesviruses. In *Medicine (United Kingdom)* (Vol. 49, Issue 12, pp. 780–784). University of Texas Medical Branch at Galveston. https://doi.org/10.1016/j.mpmed.2021.09.011

Jenson, H. B. (2000). Acute complications of Epstein-Barr virus infectious mononucleosis. *Current Opinion in Pediatrics*, *12*(3), 263–268. https://doi.org/10.1097/00008480-200006000-00016

Ji, P., Diederichs, S., Wang, W., Böing, S., Metzger, R., Schneider, P. M., Tidow, N., Brandt, B., Buerger, H., Bulk, E., Thomas, M., Berdel, W. E., Serve, H., & Müller-Tidow, C. (2003). MALAT-1, a novel noncoding RNA, and thymosin β4 predict metastasis and survival in early-stage non-small cell lung cancer. *Oncogene*, *22*(39), 8031–8041. https://doi.org/10.1038/sj.onc.1206928

Jiang, L., Gu, Z. H., Yan, Z. X., Zhao, X., Xie, Y. Y., Zhang, Z. G., Pan, C. M., Hu, Y., Cai, C. P., Dong, Y., Huang, J. Y., Wang, L., Shen, Y., Meng, G., Zhou, J. F., Hu, J. Da, Wang, J. F., Liu, Y. H., Yang, L. H., … Chen, S. J. (2015). Exome sequencing identifies somatic mutations of DDX3X in natural killer/T-cell lymphoma. *Nature Genetics*, *47*(9), 1061–1066. https://doi.org/10.1038/ng.3358

Jiang, S., Fagman, J. B., Chen, C., Alberti, S., & Liu, B. (2020). Protein phase separation and its role in tumorigenesis. *ELife*, *9*, 1–27. https://doi.org/10.7554/eLife.60264

Jin, M., Han, T., Yao, Y., Alessi, A. F., Freeberg, M. A., Inoki, K., Klionsky, D. J., Kim, J. K., Karnovsky, A., Moresco, J. J., Yates, J. R., Baba, M., Gitler, A. D., Fuller, G. G., Alessi, A. F., & Roach, N. P. (2017). Glycolytic Enzymes Coalesce in G Bodies under Hypoxic Stress. *Cell Reports*, *20*(4), 895–908. https://doi.org/10.1016/j.celrep.2017.06.082

Joaquina Delás, M., Sabin, L. R., Dolzhenko, E., Knott, S. R., Maravilla, E. M., Jackson, B. T., Wild, S. A., Kovacevic, T., Stork, E. M., Zhou, M., Erard, N., Lee, E., Kelley,

D. R., Roth, M., Barbosa, I. A., Zuber, J., Rinn, J. L., Smith, A. D., & Hannon, G. J. (2017). lncRNA requirements for mouse acute myeloid leukemia and normal differentiation. *ELife*, *6*. https://doi.org/10.7554/eLife.25607

Jordan, R., Wang, L., Graczyk, T. M., Block, T. M., & Romano, P. R. (2002). Replication of a Cytopathic Strain of Bovine Viral Diarrhea Virus Activates PERK and Induces Endoplasmic Reticulum Stress-Mediated Apoptosis of MDBK Cells. *Journal of Virology*, *76*(19), 9588–9599. https://doi.org/10.1128/jvi.76.19.9588-9599.2002

Jousse, C., Oyadomari, S., Novoa, I., Lu, P. D., Zhang, Y., Harding, H. P., & Ron, D. (2003). Inhibition of a constitutive translation initiation factor 2α phosphatase, CReP, promotes survival of stressed cells. *Journal of Cell Biology*, *163*(4), 767–775. https://doi.org/10.1083/jcb.200308075

Juillard, F., Bazot, Q., Mure, F., Tafforeau, L., MacRi, C., Rabourdin-Combe, C., Lotteau, V., Manet, E., & Gruffat, H. (2012). Epstein-Barr virus protein EB2 stimulates cytoplasmic mRNA accumulation by counteracting the deleterious effects of SRp20 on viral mRNAs. *Nucleic Acids Research*, *40*(14), 6834–6849. https://doi.org/10.1093/nar/gks319

Kaiser, C., Laux, G., Eick, D., Jochner, N., Bornkamm, G. W., & Kempkes, B. (1999). The Proto-Oncogene c- myc Is a Direct Target Gene of Epstein-Barr Virus Nuclear Antigen 2. *Journal of Virology*, *73*(5), 4481–4484. https://doi.org/10.1128/jvi.73.5.4481-4484.1999

Kajita, Y., Nakayama, J. I., Aizawa, M., & Ishikawa, F. (1995). The UUAG-specific RNA binding protein, heterogeneous nuclear ribonucleoprotein D0: Common modular structure and binding properties of the 2xRBD-Gly family. *Journal of Biological Chemistry*, *270*(38), 22167–22175. https://doi.org/10.1074/jbc.270.38.22167

Kamagata, K., Kanbayashi, S., Honda, M., Itoh, Y., Takahashi, H., Kameda, T., Nagatsugi, F., & Takahashi, S. (2020). Liquid-like droplet formation by tumor suppressor p53 induced by multivalent electrostatic interactions between two disordered domains. *Scientific Reports*, *10*(1). https://doi.org/10.1038/s41598-020-57521-w

Kanai, Y., Dohmae, N., & Hirokawa, N. (2004). Kinesin transports RNA: Isolation and characterization of an RNA-transporting granule. *Neuron*, *43*(4), 513–525. https://doi.org/10.1016/j.neuron.2004.07.022

Kandasamy, K., Joseph, K., Subramaniam, K., Raymond, J. R., & Tholanikunnel, B. G. (2005). Translational control of β2-adrenergic receptor mRNA by T-cell-restricted intracellular antigen-related protein. *Journal of Biological Chemistry*, *280*(3), 1931–1943. https://doi.org/10.1074/jbc.M405937200

Kang, W., Wang, Y., Yang, W., Zhang, J., Zheng, H., & Li, D. (2021). Research Progress on the Structure and Function of G3BP. In *Frontiers in Immunology* (Vol. 12). https://doi.org/10.3389/fimmu.2021.718548

Kapranov, P., Cheng, J., Dike, S., Nix, D. A., Duttagupta, R., Willingham, A. T., Stadler, P. F., Hertel, J., Hackermüller, J., Hofacker, I. L., Bell, I., Cheung, E., Drenkow, J., Dumais, E., Patel, S., Helt, G., Ganesh, M., Ghosh, S., Piccolboni, A., … Gingeras, T. R. (2007). RNA maps reveal new RNA classes and a possible function for pervasive transcription. *Science*, *316*(5830), 1484–1488. https://doi.org/10.1126/science.1138341

Kawai, Taro, & Akira, S. (2009). The roles of TLRs, RLRs and NLRs in pathogen

recognition. In *International Immunology* (Vol. 21, Issue 4, pp. 317–337). https://doi.org/10.1093/intimm/dxp017

Kawai, Tomoko, Lal, A., Yang, X., Galban, S., Mazan-Mamczarz, K., & Gorospe, M. (2006). Translational Control of Cytochrome c by RNA-Binding Proteins TIA-1 and HuR. *Molecular and Cellular Biology*, *26*(8), 3295–3307. https://doi.org/10.1128/mcb.26.8.3295-3307.2006

Kaye, K. M., Izumi, K. M., & Kieff, E. D. (1993). Epstein-Barr virus latent membrane protein 1 is essential for B-lymphocyte growth transformation. *Proceedings of the National Academy of Sciences of the United States of America*, *90*(19), 9150–9154. https://doi.org/10.1073/pnas.90.19.9150

Kaymaz, Y., Oduor, C. I., Yu, H., Otieno, J. A., Ong'echa, J. M., Moormann, A. M., & Bailey, J. A. (2017). Comprehensive Transcriptome and Mutational Profiling of Endemic Burkitt Lymphoma Reveals EBV Type–Specific Differences. *Molecular Cancer Research*, *15*(5), 563–576. https://doi.org/10.1158/1541-7786.mcr-16-0305-t

Kedersha, N., & Anderson, P. J. (2002). Stress granules: Sites of mRNA triage that regulate mRNA stability and translatability. *Biochemical Society Transactions*, *30*(6), 963–969. https://doi.org/10.1042/BST0300963

Kedersha, N., Cho, M. R., Li, W., Yacono, P. W., Chen, S., Gilks, N., Golan, D. E., & Anderson, P. J. (2000). Dynamic shuttling of TIA-1 accompanies the recruitment of mRNA to mammalian stress granules. *Journal of Cell Biology*, *151*(6), 1257–1268. https://doi.org/10.1083/jcb.151.6.1257

Kedersha, N., Gupta, M., Li, W., Miller, I., & Anderson, P. J. (1999). RNA-binding proteins TIA-1 and TIAR link the phosphorylation of eIF-2α to the assembly of mammalian stress granules. *Journal of Cell Biology*, *147*(7), 1431–1441. https://doi.org/10.1083/jcb.147.7.1431

Kedersha, N., Panas, M. D., Achorn, C. A., Lyons, S. M., Tisdale, S., Hickman, T., Thomas, M., Lieberman, J., McInerney, G. M., Ivanov, P., & Anderson, P. J. (2016). G3BP-Caprin1-USP10 complexes mediate stress granule condensation and associate with 40S subunits. *Journal of Cell Biology*, *212*(7), 845–860. https://doi.org/10.1083/jcb.201508028

Kedersha, N., Stoecklin, G., Ayodele, M., Yacono, P., Lykke-Andersen, J., Fitzler, M. J., Scheuner, D., Kaufman, R. J., Golan, D. E., & Anderson, P. J. (2005). Stress granules and processing bodies are dynamically linked sites of mRNP remodeling. *Journal of Cell Biology*, *169*(6), 871–884. https://doi.org/10.1083/jcb.200502088

Kelly, G. L., Milner, A. E., Tierney, R. J., Croom-Carter, D. S. G., Altmann, M., Hammerschmidt, W., Bell, A. I., & Rickinson, A. B. (2005). Epstein-Barr Virus Nuclear Antigen 2 (EBNA2) Gene Deletion Is Consistently Linked with EBNA3A, -3B, and -3C Expression in Burkitt's Lymphoma Cells and with Increased Resistance to Apoptosis. *Journal of Virology*, *79*(16), 10709–10717. https://doi.org/10.1128/jvi.79.16.10709-10717.2005

Kenney, S. C. (2007). Reactivation and lytic replication of EBV. In *Human Herpesviruses: Biology, Therapy, and Immunoprophylaxis* (pp. 403–433). Cambridge University Press. https://doi.org/10.1017/CBO9780511545313.026

Kenney, S. C., & Mertz, J. E. (2014). Regulation of the latent-lytic switch in Epstein-Barr virus. In *Seminars in Cancer Biology* (Vol. 26, pp. 60–68).

https://doi.org/10.1016/j.semcancer.2014.01.002

Khalfallah, Y., Kuta, R., Grasmuck, C., Prat, A., Durham, H. D., & Vande Velde, C. (2018). TDP-43 regulation of stress granule dynamics in neurodegenerative disease-relevant cell types. *Scientific Reports*, *8*(1). https://doi.org/10.1038/s41598-018-25767-0

Khan, G., & Hashim, M. J. (2014). Global burden of deaths from epstein-barr virus attributable malignancies 1990-2010. *Infectious Agents and Cancer*, *9*(1), 1–11. https://doi.org/10.1186/1750-9378-9-38

Khan, G., Miyashita, E. M., Yang, B., Babcock, G. J., & Thorley-Lawson, D. A. (1996). Is EBV persistence in vivo a model for B cell homeostasis? *Immunity*, *5*(2), 173–179. https://doi.org/10.1016/S1074-7613(00)80493-8

Khaperskyy, D. A., Hatchette, T. F., & McCormick, C. (2012). Influenza A virus inhibits cytoplasmic stress granule formation. *The FASEB Journal*, *26*(4), 1629–1639. https://doi.org/10.1096/fj.11-196915

Khoo, D., Perez, C., & Mohr, I. (2002). Characterization of RNA Determinants Recognized by the Arginine- and Proline-Rich Region of Us11, a Herpes Simplex Virus Type 1-Encoded Double-Stranded RNA Binding Protein That Prevents PKR Activation. *Journal of Virology*, *76*(23), 11971–11981. https://doi.org/10.1128/jvi.76.23.11971-11981.2002

Khyatti, M., Patel, P. C., Stefanescu, I., & Menezes, J. (1991). Epstein-Barr virus (EBV) glycoprotein gp350 expressed on transfected cells resistant to natural killer cell activity serves as a target antigen for EBV-specific antibody-dependent cellular cytotoxicity. *Journal of Virology*, *65*(2), 996–1001. https://doi.org/10.1128/jvi.65.2.996-1001.1991

Kim, T. H., Song, J., Kim, S. H., Parikh, A. K., Mo, X., Palanichamy, K., Kaur, B., Yu, J., Yoon, S. O., Nakano, I., & Kwon, C. H. (2014). Piperlongumine treatment inactivates peroxiredoxin 4, exacerbates endoplasmic reticulum stress, and preferentially kills high-grade glioma cells. *Neuro-Oncology*, *16*(10), 1354–1364. https://doi.org/10.1093/neuonc/nou088

Kim, W. J., Kim, J. H., & Jang, S. K. (2007). Anti-inflammatory lipid mediator 15d-PGJ2 inhibits translation through inactivation of eIF4A. *EMBO Journal*, *26*(24), 5020–5032. https://doi.org/10.1038/sj.emboj.7601920

Kim, Y. K., Shin, J. S., & Nahm, M. H. (2016). NOD-like receptors in infection, immunity, and diseases. In *Yonsei Medical Journal* (Vol. 57, Issue 1, pp. 5–14). https://doi.org/10.3349/ymj.2016.57.1.5

Kimball, S. R., Heinzinger, N. K., Horetsky, R. L., & Jefferson, L. S. (1998). Identification of interprotein interactions between the subunits of eukaryotic initiation factors eIF2 and eIF2B. *Journal of Biological Chemistry*, *273*(5), 3039–3044. https://doi.org/10.1074/jbc.273.5.3039

Kitagawa, M., Kitagawa, K., Kotake, Y., Niida, H., & Ohhata, T. (2013). Cell cycle regulation by long non-coding RNAs. In *Cellular and Molecular Life Sciences* (Vol. 70, Issue 24, pp. 4785–4794). https://doi.org/10.1007/s00018-013-1423-0

Ko, Y. H. (2015). EBV and human cancer. In *Experimental and Molecular Medicine* (Vol. 47, Issue 1). https://doi.org/10.1038/emm.2014.109

Kojima, E., Takeuchi, A., Haneda, M., Yagi, A., Hasegawa, T., Yamaki, K. ichi, Takeda, K., Akira, S., Shimokata, K., & Isobe, K. ichi. (2003). The function of GADD34 is a recovery from a shutoff of protein synthesis induced by ER stress: elucidation by GADD34-deficient mice. *The FASEB Journal : Official Publication of the Federation of American Societies for Experimental Biology*, *17*(11), 1573–1575. https://doi.org/10.1096/fj.02-1184fje

Komano, J., Maruo, S., Kurozumi, K., Oda, T., & Takada, K. (1999). Oncogenic Role of Epstein-Barr Virus-Encoded RNAs in Burkitt's Lymphoma Cell Line Akata. *Journal of Virology*, *73*(12), 9827–9831. https://doi.org/10.1128/jvi.73.12.9827-9831.1999

Kondo, K., & Yamanishi, K. (2007). HHV-6A, 6B, and 7: Molecular basis of latency and reactivation. In *Human Herpesviruses: Biology, Therapy, and Immunoprophylaxis* (pp. 843–849). Cambridge University Press. https://doi.org/10.1017/CBO9780511545313.048

Kopp, M. C., Larburu, N., Durairaj, V., Adams, C. J., & Ali, M. M. U. (2019). UPR proteins IRE1 and PERK switch BiP from chaperone to ER stress sensor. *Nature Structural and Molecular Biology*, *26*(11), 1053–1062. https://doi.org/10.1038/s41594-019-0324-9

Koyama, S., Ishii, K. J., Coban, C., & Akira, S. (2008). Innate immune response to viral infection. In *Cytokine* (Vol. 43, Issue 3, pp. 336–341). Academic Press. https://doi.org/10.1016/j.cyto.2008.07.009

Kozak, M., & Roizman, B. (1975). RNA synthesis in cells infected with herpes simplex virus. IX. Evidence for accumulation of abundant symmetric transcripts in nuclei. *Journal of Virology*, *15*(1), 36–40. https://doi.org/10.1128/jvi.15.1.36-40.1975

Kozireva, S., Rudevica, Z., Baryshev, M., Leonciks, A., Kashuba, E., & Kholodnyuk, I. (2018). Upregulation of the chemokine receptor CCR2B in Epstein-Barr Virus-positive Burkitt lymphoma cell lines with the latency III program. *Viruses*, *10*(5). https://doi.org/10.3390/v10050239

Kroschwald, S., Maharana, S., Mateju, D., Malinovska, L., Nüske, E., Poser, I., Rickinson, A. B., & Alberti, S. (2015). Promiscuous interactions and protein disaggregases determine the material state of stress-inducible RNP granules. *ELife*, *4*(AUGUST2015). https://doi.org/10.7554/eLife.06807

Krummenacher, C., Carfí, A., Eisenberg, R. J., & Cohen, G. H. (2013). Entry of herpesviruses into cells: The enigma variations. *Advances in Experimental Medicine and Biology*, *790*, 178–195. https://doi.org/10.1007/978-1-4614-7651-1_10

Kuhen, K. L., & Samuel, C. E. (1997). Isolation of the interferon-inducible RNA-dependent protein kinase Pkr promoter and identification of a novel DNA element within the 5'-flanking region of human and mouse Pkr genes. *Virology*, *227*(1), 119–130. https://doi.org/10.1006/viro.1996.8306

Kuhen, K. L., & Samuel, C. E. (1999). Mechanism of interferon action: Functional characterization of positive and negative regulatory domains that modulate transcriptional activation of the human RNA-dependent protein kinase Pkr promoter. *Virology*, *254*(1), 182–195. https://doi.org/10.1006/viro.1998.9536

Kumar, V. (2021). The Trinity of cGAS, TLR9, and ALRs Guardians of the Cellular Galaxy Against Host-Derived Self-DNA. In *Frontiers in Immunology* (Vol. 11, p. 1). https://doi.org/10.3389/fimmu.2020.624597

Kwong, A. D., & Frenkel, N. (1987). Herpes simplex virus-infected cells contain a function(s) that destabilizes both host and viral mRNAs. *Proceedings of the National Academy of Sciences of the United States of America*, *84*(7), 1926–1930. https://doi.org/10.1073/pnas.84.7.1926

Lafontaine, D. L. J., Riback, J. A., Bascetin, R., & Brangwynne, C. P. (2021). The nucleolus as a multiphase liquid condensate. In *Nature Reviews Molecular Cell Biology* (Vol. 22, Issue 3, pp. 165–182). https://doi.org/10.1038/s41580-020-0272-6

Laichalk, L. L., & Thorley-Lawson, D. A. (2005). Terminal Differentiation into Plasma Cells Initiates the Replicative Cycle of Epstein-Barr Virus In Vivo. *Journal of Virology*, *79*(2), 1296–1307. https://doi.org/10.1128/jvi.79.2.1296-1307.2005

Lallemand-Breitenbach, V., & de Thé, H. (2010). PML nuclear bodies. In *Cold Spring Harbor perspectives in biology* (Vol. 2, Issue 5). https://doi.org/10.1101/cshperspect.a000661

Lam, N., Sandberg, M. L., & Sugden, B. (2004). High Physiological Levels of LMP1 Result in Phosphorylation of eIF2α in Epstein-Barr Virus-Infected Cells. *Journal of Virology*, *78*(4), 1657–1664. https://doi.org/10.1128/jvi.78.4.1657-1664.2004

Lamond, A. I. (1993). The Spliceosome. In *BioEssays* (Vol. 15, Issue 9, pp. 595–603). Bioessays. https://doi.org/10.1002/bies.950150905

Laporte, D., Salin, B., Daignan-Fornier, B., & Sagot, I. (2008). Reversible cytoplasmic localization of the proteasome in quiescent yeast cells. *Journal of Cell Biology*, *181*(5), 737–745. https://doi.org/10.1083/jcb.200711154

Le Guiner, C., Lejeune, F., Galiana, D., Kister, L., Breathnach, R., Stévenin, J., & Del Gatto-Konczak, F. (2001). TIA-1 and TIAR Activate Splicing of Alternative Exons with Weak 5′ Splice Sites followed by a U-rich Stretch on Their Own Pre-mRNAs. *Journal of Biological Chemistry*, *276*(44), 40638–40646. https://doi.org/10.1074/jbc.M105642200

Lee, C. H., Yu, C. C., Wang, B. Y., & Chang, W. W. (2016). Tumorsphere as an effective in vitro platform for screening anticancer stem cell drugs. *Oncotarget*, *7*(2), 1215–1226. https://doi.org/10.18632/oncotarget.6261

Lee, Y. Y., Cevallos, R. C., & Jan, E. (2009). An upstream open reading frame regulates translation of GADD34 during cellular stresses that induce eIF2phosphorylation. *Journal of Biological Chemistry*, *284*(11), 6661–6673. https://doi.org/10.1074/jbc.M806735200

Lefkowitz, E. J., Dempsey, D. M., Hendrickson, R. C., Orton, R. J., Siddell, S. G., & Smith, D. B. (2018). Virus taxonomy: The database of the International Committee on Taxonomy of Viruses (ICTV). *Nucleic Acids Research*, *46*(D1), D708–D717. https://doi.org/10.1093/nar/gkx932

Lemaire, P. A., Anderson, E., Lary, J., & Cole, J. L. (2008). Mechanism of PKR Activation by dsRNA. *Journal of Molecular Biology*, *381*(2), 351–360. https://doi.org/10.1016/j.jmb.2008.05.056

Leung, H. J., Duran, E. M., Kurtoglu, M., Andreansky, S., Lampidis, T. J., & Mesri, E. A. (2012). Activation of the Unfolded Protein Response by 2-Deoxy-d-Glucose Inhibits Kaposi's Sarcoma-Associated Herpesvirus Replication and Gene Expression. *Antimicrobial Agents and Chemotherapy*, *56*(11), 5794–5803.

https://doi.org/10.1128/aac.01126-12

Levy, C. B., Stumbo, A. C., Ano Bom, A. P. D., Portari, E. A., Carneiro, Y., Silva, J. L., & De Moura-Gallo, C. V. (2011). Co-localization of mutant p53 and amyloid-like protein aggregates in breast tumors. *International Journal of Biochemistry and Cell Biology*, *43*(1), 60–64. https://doi.org/10.1016/j.biocel.2010.10.017

Levy, D. E., & Darnell, J. E. (2002). STATs: Transcriptional control and biological impact. In *Nature Reviews Molecular Cell Biology* (Vol. 3, Issue 9, pp. 651–662). https://doi.org/10.1038/nrm909

Lewy, T. G., Grabowski, J. M., & Bloom, M. E. (2017). BiP: Master regulator of the unfolded protein response and crucial factor in flavivirus biology. In *Yale Journal of Biology and Medicine* (Vol. 90, Issue 2, pp. 291–300). Yale Journal of Biology and Medicine. /pmc/articles/PMC5482305/

Lewy, T. G., Offerdahl, D. K., Grabowski, J. M., Kellman, E., Mlera, L., Chiramel, A., & Bloom, M. E. (2020). PERK-mediated unfolded protein response signaling restricts replication of the tick-borne flavivirus langat virus. *Viruses*, *12*(3). https://doi.org/10.3390/v12030328

Li, D., & Wu, M. (2021). Pattern recognition receptors in health and diseases. In *Signal Transduction and Targeted Therapy* (Vol. 6, Issue 1, pp. 1–24). Nature Publishing Group. https://doi.org/10.1038/s41392-021-00687-0

Li, L., Roy, K., Katyal, S., Sun, X., Bléoo, S., & Godbout, R. (2006). Dynamic nature of cleavage bodies and their spatial relationship to DDX1 bodies, cajal bodies, and gems. *Molecular Biology of the Cell*, *17*(3), 1126–1140. https://doi.org/10.1091/mbc.E05-08-0768

Li, Y., Zhang, C., Chen, X., Yu, J., Wang, Y., Yang, Y., Du, M., Jin, H., Ma, Y., He, B., & Cao, Y. (2011). ICP34.5 protein of herpes simplex virus facilitates the initiation of protein translation by bridging eukaryotic initiation factor 2α (eIF2α) and protein phosphatase 1. *Journal of Biological Chemistry*, *286*(28), 24785–24792. https://doi.org/10.1074/jbc.M111.232439

Lin, J., Johannsen, E. C., Robertson, E. S., & Kieff, E. D. (2002). Epstein-Barr Virus Nuclear Antigen 3C Putative Repression Domain Mediates Coactivation of the LMP1 Promoter with EBNA-2. *Journal of Virology*, *76*(1), 232–242. https://doi.org/10.1128/jvi.76.1.232-242.2002

Linero, F. N., Thomas, M. G., Boccaccio, G. L., & Scolaro, L. A. (2011). Junín virus infection impairs stress-granule formation in Vero cells treated with arsenite via inhibition of eiF2α phosphorylation. *Journal of General Virology*, *92*(12), 2889–2899. https://doi.org/10.1099/vir.0.033407-0

Liu, J. L., & Gall, J. G. (2007). U bodies are cytoplasmic structures that contain uridine-rich small nuclear ribonucleoproteins and associate with P bodies. *Proceedings of the National Academy of Sciences of the United States of America*, *104*(28), 11655–11659. https://doi.org/10.1073/pnas.0704977104

Liu, Q., & Dreyfuss, G. (1996). A novel nuclear structure containing the survival of motor neurons protein. *EMBO Journal*, *15*(14), 3555–3565. https://doi.org/10.1002/j.1460-2075.1996.tb00725.x

Liu, Y., Wang, M., Cheng, A., Yang, Q., Wu, Y., Jia, R., Liu, M., Zhu, D., Chen, S., Zhang, S., Zhao, X. X., Huang, J., Mao, S., Ou, X., Gao, Q., Wang, Y., Xu, Z., Chen, Z.,

Zhu, L., … Chen, X. (2020). The role of host eIF2α in viral infection. In *Virology Journal* (Vol. 17, Issue 1). https://doi.org/10.1186/s12985-020-01362-6

Liu, Z., Lv, Y., Zhao, N., Guan, G., & Wang, J. (2015). Protein kinase R-like ER kinase and its role in endoplasmic reticulum stress-decided cell fate. In *Cell Death and Disease* (Vol. 6, Issue 7). https://doi.org/10.1038/cddis.2015.183

Liu, Z. S., Cai, H., Xue, W., Wang, M., Xia, T., Li, W. J., Xing, J. Q., Zhao, M., Huang, Y. J., Chen, S., Wu, S. M., Wang, X., Liu, X., Pang, X., Zhang, Z. Y., Li, T., Dai, J., Dong, F., Xia, Q., … Li, T. (2019). G3BP1 promotes DNA binding and activation of cGAS. *Nature Immunology*, *20*(1), 18–28. https://doi.org/10.1038/s41590-018-0262-4

Lloyd, R. E. (2012). How do viruses interact with stress-associated RNA granules? *PLoS Pathogens*, *8*(6). https://doi.org/10.1371/journal.ppat.1002741

Loflin, P., Chen, C.-Y. A., & Shyu, A.-B. (1999). Unraveling a cytoplasmic role for hnRNP d in the in vivo mRNA destabilization directed by the AU-rich element. *Genes and Development*, *13*(14), 1884–1897. https://doi.org/10.1101/gad.13.14.1884

Lozon, T. I., Eastman, A. J., Matute-Bello, G., Chen, P., Hallstrand, T. S., & Altemeier, W. A. (2011). PKR-dependent CHOP induction limits hyperoxia-induced lung injury. *American Journal of Physiology - Lung Cellular and Molecular Physiology*, *300*(3), 422–429. https://doi.org/10.1152/ajplung.00166.2010

Lu, P. D., Harding, H. P., & Ron, D. (2004). Translation reinitiation at alternative open reading frames regulates gene expression in an integrated stress response. *Journal of Cell Biology*, *167*(1), 27–33. https://doi.org/10.1083/jcb.200408003

Lunde, B. M., Moore, C., & Varani, G. (2007). RNA-binding proteins: Modular design for efficient function. In *Nature Reviews Molecular Cell Biology* (Vol. 8, Issue 6, pp. 479–490). https://doi.org/10.1038/nrm2178

Lussignol, M., Queval, C., Bernet-Camard, M.-F., Cotte-Laffitte, J., Beau, I., Codogno, P., & Esclatine, A. (2013). The Herpes Simplex Virus 1 Us11 Protein Inhibits Autophagy through Its Interaction with the Protein Kinase PKR. *Journal of Virology*, *87*(2), 859–871. https://doi.org/10.1128/jvi.01158-12

Lyabin, D. N., Eliseeva, I. A., & Ovchinnikov, L. P. (2014). YB-1 protein: Functions and regulation. In *Wiley Interdisciplinary Reviews: RNA* (Vol. 5, Issue 1, pp. 95–110). John Wiley & Sons, Ltd. https://doi.org/10.1002/wrna.1200

Lyon, A. S., Peeples, W. B., & Rosen, M. K. (2021). A framework for understanding the functions of biomolecular condensates across scales. In *Nature Reviews Molecular Cell Biology* (Vol. 22, Issue 3, pp. 215–235). Nature Publishing Group. https://doi.org/10.1038/s41580-020-00303-z

Lypowy, J., Chen, I. Y., & Abdellatif, M. (2005). An alliance between Ras GTPase-activating protein, filamin C, and Ras GTPase-activating protein SH3 domain-binding protein regulates myocyte growth. *Journal of Biological Chemistry*, *280*(27), 25717–25728. https://doi.org/10.1074/jbc.M414266200

Ma, W., & Mayr, C. (2018). A Membraneless Organelle Associated with the Endoplasmic Reticulum Enables 3′UTR-Mediated Protein-Protein Interactions. *Cell*, *175*(6), 1492-1506.e19. https://doi.org/10.1016/j.cell.2018.10.007

Ma, Y., Brewer, J. W., Alan Diehl, J., & Hendershot, L. M. (2002). Two distinct stress

signaling pathways converge upon the CHOP promoter during the mammalian unfolded protein response. *Journal of Molecular Biology*, *318*(5), 1351–1365. https://doi.org/10.1016/S0022-2836(02)00234-6

Ma, Y., & Hendershot, L. M. (2003). Delineation of a negative feedback regulatory loop that controls protein translation during endoplasmic reticulum stress. *Journal of Biological Chemistry*, *278*(37), 34864–34873. https://doi.org/10.1074/jbc.M301107200

Mackenzie, I. R., Nicholson, A. M., Sarkar, M., Messing, J., Purice, M. D., Pottier, C., Annu, K., Baker, M., Perkerson, R. B., Kurti, A., Matchett, B. J., Mittag, T., Temirov, J., Hsiung, G. Y. R., Krieger, C., Murray, M. E., Kato, M., Fryer, J. D., Petrucelli, L., … Rademakers, R. (2017). TIA1 Mutations in Amyotrophic Lateral Sclerosis and Frontotemporal Dementia Promote Phase Separation and Alter Stress Granule Dynamics. *Neuron*, *95*(4), 808-816.e9. https://doi.org/10.1016/j.neuron.2017.07.025

Macville, M., Schröck, E., Padilla-Nash, H., Keck, C., Ghadimi, B. M., Zimonjic, D., Popescu, N., & Ried, T. (1999). Comprehensive and definitive molecular cytogenetic characterization of HeLa cells by spectral karyotyping. *Cancer Research*, *59*(1), 141–150. https://aacrjournals.org/cancerres/article/59/1/141/505037/Comprehensive-and-Definitive-Molecular-Cytogenetic

Mahboubi, H., Kodiha, M., & Stochaj, U. (2013). Automated detection and quantification of granular cell compartments. *Microscopy and Microanalysis*, *19*(3), 617–628. https://doi.org/10.1017/S1431927613000159

Mahboubi, H., Seganathy, E., Kong, D., & Stochaj, U. (2013). Identification of Novel Stress Granule Components That Are Involved in Nuclear Transport. *PLoS ONE*, *8*(6). https://doi.org/10.1371/journal.pone.0068356

Majde, J. A. (2000). Viral Double-Stranded RNA, Cytokines, and the Flu. *Journal of Interferon & Cytokine Research*, *20*(3), 259–272. https://doi.org/10.1089/107999000312397

Majerciak, V., & Zheng, Z. M. (2009). Kaposi's sarcoma-associated herpesvirus ORF57 in viral RNA processing. *Frontiers in Bioscience*, *14*(4), 1516–1528. https://doi.org/10.2741/3322

Majerciak, V., & Zheng, Z. M. (2015). KSHV ORF57, a protein of many faces. In *Viruses* (Vol. 7, Issue 2, pp. 604–633). https://doi.org/10.3390/v7020604

Mancao, C., Altmann, M., Jungnickel, B., & Hammerschmidt, W. (2005). Rescue of "crippled" germinal center B cells from apoptosis by Epstein-Barr virus. *Blood*, *106*(13), 4339–4344. https://doi.org/10.1182/blood-2005-06-2341

Mancao, C., & Hammerschmidt, W. (2007). Epstein-Barr virus latent membrane protein 2A is a B-cell receptor mimic and essential for B-cell survival. *Blood*, *110*(10), 3715–3721. https://doi.org/10.1182/blood-2007-05-090142

Manche, L., Green, S. R., Schmedt, C., & Mathews, M. B. (1992). Interactions between double-stranded RNA regulators and the protein kinase DAI. *Molecular and Cellular Biology*, *12*(11), 5238–5248. https://doi.org/10.1128/mcb.12.11.5238

Mannick, J. B., Cohen, J. I., Birkenbach, M., Marchini, A., & Kieff, E. D. (1991). The Epstein-Barr virus nuclear protein encoded by the leader of the EBNA RNAs is

important in B-lymphocyte transformation. *Journal of Virology*, *65*(12), 6826–6837. https://doi.org/10.1128/jvi.65.12.6826-6837.1991

Mao, Y. S., Zhang, B., & Spector, D. L. (2011). Biogenesis and function of nuclear bodies. In *Trends in Genetics* (Vol. 27, Issue 8, pp. 295–306). https://doi.org/10.1016/j.tig.2011.05.006

Marciniak, S. J., Yun, C. Y., Oyadomari, S., Novoa, I., Zhang, Y., Jungreis, R., Nagata, K., Harding, H. P., & Ron, D. (2004). CHOP induces death by promoting protein synthesis and oxidation in the stressed endoplasmic reticulum. *Genes and Development*, *18*(24), 3066–3077. https://doi.org/10.1101/gad.1250704

Margolis, T. P., Imai, Y., Yang, L., Vallas, V., & Krause, P. R. (2007). Herpes Simplex Virus Type 2 (HSV-2) Establishes Latent Infection in a Different Population of Ganglionic Neurons than HSV-1: Role of Latency-Associated Transcripts. *Journal of Virology*, *81*(4), 1872–1878. https://doi.org/10.1128/jvi.02110-06

Marmor-Kollet, H., Siany, A., Kedersha, N., Knafo, N., Rivkin, N., Danino, Y. M., Moens, T. G., Olender, T., Sheban, D., Cohen, N., Dadosh, T., Addadi, Y., Ravid, R., Eitan, C., Toth Cohen, B., Hofmann, S., Riggs, C. L., Advani, V. M., Higginbottom, A., … Hornstein, E. (2020). Spatiotemporal Proteomic Analysis of Stress Granule Disassembly Using APEX Reveals Regulation by SUMOylation and Links to ALS Pathogenesis. *Molecular Cell*, *80*(5), 876-891.e6. https://doi.org/10.1016/j.molcel.2020.10.032

Maruo, S., Zhao, B., Johannsen, E. C., Kieff, E. D., Zou, J., & Takada, K. (2011). Epstein-Barr virus nuclear antigens 3C and 3A maintain lymphoblastoid cell growth by repressing p16INK4A and p14ARF expression. *Proceedings of the National Academy of Sciences of the United States of America*, *108*(5), 1919–1924. https://doi.org/10.1073/pnas.1019599108

Matar, C. G., Rangaswamy, U. S., Wakeman, B. S., Iwakoshi, N., & Speck, S. H. (2014). Murine Gammaherpesvirus 68 Reactivation from B Cells Requires IRF4 but Not XBP-1. *Journal of Virology*, *88*(19), 11600–11610. https://doi.org/10.1128/jvi.01876-14

Matouk, I. J., Mezan, S., Mizrahi, A., Ohana, P., Abu-lail, R., Fellig, Y., DeGroot, N., Galun, E., & Hochberg, A. (2010). The oncofetal H19 RNA connection: Hypoxia, p53 and cancer. *Biochimica et Biophysica Acta - Molecular Cell Research*, *1803*(4), 443–451. https://doi.org/10.1016/j.bbamcr.2010.01.010

Mattioli, C. C., Rom, A., Franke, V., Imami, K., Arrey, G., Terne, M., Woehler, A., Akalin, A., Ulitsky, I., & Chekulaeva, M. (2019). Alternative 3 UTRs direct localization of functionally diverse protein isoforms in neuronal compartments. *Nucleic Acids Research*, *47*(5), 2560–2573. https://doi.org/10.1093/nar/gky1270

Maurya, P. K., Mishra, A., Yadav, B. S., Singh, S., Kumar, P., Chaudhary, A., Srivastava, S., Murugesan, S. N., & Mani, A. (2017). Role of Y box protein-1 in cancer: As potential biomarker and novel therapeutic target. In *Journal of Cancer* (Vol. 8, Issue 10, pp. 1900–1907). Ivyspring International Publisher. https://doi.org/10.7150/jca.17689

Mazroui, R., Sukarieh, R., Bordeleau, M. E., Kaufman, R. J., Northcote, P., Tanaka, J., Gallouzi, I., & Pelletier, J. (2006). Inhibition of ribosome recruitment induces stress granule formation independently of eukaryotic initiation factor 2α phosphorylation. *Molecular Biology of the Cell*, *17*(10), 4212–4219. https://doi.org/10.1091/mbc.E06-04-0318

McCormick, C., & Khaperskyy, D. A. (2017). Translation inhibition and stress granules in the antiviral immune response. In *Nature Reviews Immunology* (Vol. 17, Issue 10, pp. 647–660). Nature Publishing Group. https://doi.org/10.1038/nri.2017.63

McInerney, G. M., Kedersha, N., Kaufman, R. J., Anderson, P. J., & Liljestrom, P. (2005). Importance of eIF2alpha phosphorylation and stress granule assembly in alphavirus translation regulation. *Mol Biol Cell*, *16*(8), 3753–3763. https://doi.org/10.1091/mbc.E05-02-0124

McKenna, S. A., Lindhout, D. A., Shimoike, T., Aitken, C. E., & Puglisi, J. D. (2007). Viral dsRNA Inhibitors Prevent Self-association and Autophosphorylation of PKR. *Journal of Molecular Biology*, *372*(1), 103–113. https://doi.org/10.1016/j.jmb.2007.06.028

McNab, F., Mayer-Barber, K., Sher, A., Wack, A., & O'Garra, A. (2015). Type I interferons in infectious disease. In *Nature Reviews Immunology* (Vol. 15, Issue 2, pp. 87–103). https://doi.org/10.1038/nri3787

Mercer, T. R., Dinger, M. E., & Mattick, J. S. (2009). Long non-coding RNAs: Insights into functions. In *Nature Reviews Genetics* (Vol. 10, Issue 3, pp. 155–159). Nature Publishing Group. https://doi.org/10.1038/nrg2521

Merrick, W. C., & Pavitt, G. D. (2018). Protein synthesis initiation in eukaryotic cells. *Cold Spring Harbor Perspectives in Biology*, *10*(12). https://doi.org/10.1101/cshperspect.a033092

Meyer, C., Garzia, A., Mazzola, M., Gerstberger, S., Molina, H., & Tuschl, T. (2018). The TIA1 RNA-Binding Protein Family Regulates EIF2AK2-Mediated Stress Response and Cell Cycle Progression. *Molecular Cell*, *69*(4), 622-635.e6. https://doi.org/10.1016/j.molcel.2018.01.011

Miller, G., El-Guindy, A., Countryman, J., Ye, J., & Gradoville, L. (2007). Lytic Cycle Switches of Oncogenic Human Gammaherpesviruses. In *Advances in Cancer Research* (Vol. 97, pp. 81–109). https://doi.org/10.1016/S0065-230X(06)97004-3

Miller, N., & Hutt-Fletcher, L. M. (1992). Epstein-Barr virus enters B cells and epithelial cells by different routes. *Journal of Virology*, *66*(6), 3409–3414. https://doi.org/10.1128/jvi.66.6.3409-3414.1992

Minks, M. A., West, D. K., Benvin, S., & Baglioni, C. (1979). Structural requirements of double-stranded RNA for the activation of 2',5'-oligo(A) polymerase and protein kinase of interferon-treated HeLa cells. *Journal of Biological Chemistry*, *254*(20), 10180–10183. https://doi.org/10.1016/s0021-9258(19)86690-5

Mittelman, D., & Wilson, J. H. (2013). The fractured genome of HeLa cells. *Genome Biology*, *14*(4), 1–4. https://doi.org/10.1186/gb-2013-14-4-111

Miyake, F., Yoshikawa, T., Sun, H., Kakimi, A., Ohashi, M., Akimoto, S., Nishiyama, Y., & Asano, Y. (2006). Latent infection of human herpesvirus 7 in CD4+ T lymphocytes. *Journal of Medical Virology*, *78*(1), 112–116. https://doi.org/10.1002/jmv.20511

Modrow, S., Falke, D., Truyen, U., & Schätzl, H. (2013). Viruses: Definition, Structure, Classification. In *Molecular Virology* (pp. 17–30). Nature Publishing Group. https://doi.org/10.1007/978-3-642-20718-1_2

Molliex, A., Temirov, J., Lee, J., Coughlin, M., Kanagaraj, A. P., Kim, H. J., Mittag, T., &

Taylor, J. P. (2015). Phase Separation by Low Complexity Domains Promotes Stress Granule Assembly and Drives Pathological Fibrillization. *Cell*, *163*(1), 123–133. https://doi.org/10.1016/j.cell.2015.09.015

Montgomery, T. S. H. (1898). Comparative cytological studies, with special regard to the morphology of the nucleolus. *Journal of Morphology*, *15*(2), 265–582. https://doi.org/10.1002/jmor.1050150204

Morales-Sánchez, A., & Fuentes-Panana, E. M. (2018). The immunomodulatory capacity of an epstein-barr virus abortive lytic cycle: Potential contribution to viral tumorigenesis. In *Cancers* (Vol. 10, Issue 4). https://doi.org/10.3390/cancers10040098

Morrison, J. A., & Raab-Traub, N. (2005). Roles of the ITAM and PY Motifs of Epstein-Barr Virus Latent Membrane Protein 2A in the Inhibition of Epithelial Cell Differentiation and Activation of β-Catenin Signaling. *Journal of Virology*, *79*(4), 2375–2382. https://doi.org/10.1128/jvi.79.4.2375-2382.2005

Mosialos, G., Birkenbacht, M., Yalamanchill, R., Van Arsdale, T., Ware, C., & Kleff, E. (1995). The Epstein-Barr virus transforming protein LMP1 engages signaling proteins for the tumor necrosis factor receptor family. *Cell*, *80*(3), 389–399. https://doi.org/10.1016/0092-8674(95)90489-1

Mrozek-Gorska, P., Buschle, A., Pich, D., Schwarzmayr, T., Fechtner, R., Scialdone, A., & Hammerschmidt, W. (2019). Epstein–Barr virus reprograms human B lymphocytes immediately in the prelatent phase of infection. *Proceedings of the National Academy of Sciences of the United States of America*, *116*(32), 16046–16055. https://doi.org/10.1073/pnas.1901314116

Muralidharan, S., & Mandrekar, P. (2013). Cellular stress response and innate immune signaling: integrating pathways in host defense and inflammation. *Journal of Leukocyte Biology*, *94*(6), 1167–1184. https://doi.org/10.1189/jlb.0313153

Murata, T. (2014). Regulation of Epstein-Barr virus reactivation from latency. In *Microbiology and Immunology* (Vol. 58, Issue 6, pp. 307–317). John Wiley & Sons, Ltd. https://doi.org/10.1111/1348-0421.12155

Murata, T. (2018). Encyclopedia of EBV-encoded lytic genes: An update. In *Advances in Experimental Medicine and Biology* (Vol. 1045, pp. 395–412). Springer, Singapore. https://doi.org/10.1007/978-981-10-7230-7_18

Murata, T., Sugimoto, A., Inagaki, T., Yanagi, Y., Watanabe, T., Sato, Y., & Kimura, H. (2021). Molecular basis of epstein–barr virus latency establishment and lytic reactivation. In *Viruses* (Vol. 13, Issue 12). https://doi.org/10.3390/v13122344

Nanbo, A., Inoue, K., Adachi-Takasawa, K., & Takada, K. (2002). Epstein-Barr virus RNA confers resistance to interferon-α-induced apoptosis in Burkitt's lymphoma. *EMBO Journal*, *21*(5), 954–965. https://doi.org/10.1093/emboj/21.5.954

Naranda, T., Sirangelo, I., Fabbri, B. J., & Hershey, J. W. B. (1995). Mutations in the NKXD consensus element indicate that GTP binds to the γ-subunit of translation initiation factor eIF2. *FEBS Letters*, *372*(2–3), 249–252. https://doi.org/10.1016/0014-5793(95)00993-J

Nathaniel Roybal, C., Hunsaker, L. A., Barbash, O., Vander Jagt, D. L., & Abcouwer, S. F. (2005). The oxidative stressor arsenite activates vascular endothelial growth factor mRNA transcription by an ATF4-dependent mechanism. *Journal of Biological*

Chemistry, *280*(21), 20331–20339. https://doi.org/10.1074/jbc.M411275200

Nemerow, G. R., Mold, C., Schwend, V. K., Tollefson, V., & Cooper, N. R. (1987). Identification of gp350 as the viral glycoprotein mediating attachment of Epstein-Barr virus (EBV) to the EBV/C3d receptor of B cells: sequence homology of gp350 and C3 complement fragment C3d. *Journal of Virology*, *61*(5), 1416–1420. https://doi.org/10.1128/jvi.61.5.1416-1420.1987

Neumann, M., Sampathu, D. M., Kwong, L. K., Truax, A. C., Micsenyi, M. C., Chou, T. T., Bruce, J., Schuck, T., Grossman, M., Clark, C. M., McCluskey, L. F., Miller, B. L., Masliah, E., Mackenzie, I. R., Feldman, H., Feiden, W., Kretzschmar, H. A., Trojanowski, J. Q., & Lee, V. M. Y. (2006). Ubiquitinated TDP-43 in frontotemporal lobar degeneration and amyotrophic lateral sclerosis. *Science*, *314*(5796), 130–133. https://doi.org/10.1126/science.1134108

Newton, K., Petfalski, E., Tollervey, D., & Cáceres, J. F. (2003). Fibrillarin Is Essential for Early Development and Required for Accumulation of an Intron-Encoded Small Nucleolar RNA in the Mouse. *Molecular and Cellular Biology*, *23*(23), 8519–8527. https://doi.org/10.1128/mcb.23.23.8519-8527.2003

Nicoll, M. P., Proença, J. T., & Efstathiou, S. (2012). The molecular basis of herpes simplex virus latency. In *FEMS Microbiology Reviews* (Vol. 36, Issue 3, pp. 684–705). Wiley-Blackwell. https://doi.org/10.1111/j.1574-6976.2011.00320.x

Niedobitek, G., Agathanggelou, A., Rowe, M., Jones, E. L., Jones, D. B., Turyaguma, P., Oryema, J., Wright, D. H., & Young, L. S. (1995). Heterogeneous expression of Epstein-Barr virus latent proteins in endemic Burkitt's lymphoma. *Blood*, *86*(2), 659–665. https://doi.org/10.1182/blood.v86.2.659.bloodjournal862659

Nizami, Z., Deryusheva, S., & Gall, J. G. (2010). The Cajal body and histone locus body. In *Cold Spring Harbor perspectives in biology* (Vol. 2, Issue 7). Cold Spring Harbor Laboratory Press. https://doi.org/10.1101/cshperspect.a000653

Novoa, I., Zeng, H., Harding, H. P., & Ron, D. (2001). Feedback inhibition of the unfolded protein response by GADD34-mediated dephosphorylation of eIF2α. *Journal of Cell Biology*, *153*(5), 1011–1021. https://doi.org/10.1083/jcb.153.5.1011

Novoa, I., Zhang, Y., Zeng, H., Jungreis, R., Harding, H. P., & Ron, D. (2003). Stress-induced gene expression requires programmed recovery from translational repression. *EMBO Journal*, *22*(5), 1180–1187. https://doi.org/10.1093/emboj/cdg112

Obrig, T. G., Culp, W. J., McKeehan, W. L., & Hardesty, B. (1971). The mechanism by which cycloheximide and related glutarimide antibiotics inhibit peptide synthesis on reticulocyte ribosomes. *Journal of Biological Chemistry*, *246*(1), 174–181. https://doi.org/10.1016/s0021-9258(18)62546-3

Odumade, O. A., Hogquist, K. A., & Balfour, H. H. (2011). Progress and problems in understanding and managing primary epstein-barr virus infections. *Clinical Microbiology Reviews*, *24*(1), 193–209. https://doi.org/10.1128/CMR.00044-10

Ohn, T., & Anderson, P. J. (2010). The role of posttranslational modifications in the assembly of stress granules. In *Wiley Interdisciplinary Reviews: RNA* (Vol. 1, Issue 3, pp. 486–493). Wiley-Blackwell. https://doi.org/10.1002/wrna.23

Ojha, J., Secreto, C. R., Rabe, K. G., Van Dyke, D. L., Kortum, K. M., Slager, S. L., Shanafelt, T. D., Fonseca, R., Kay, N. E., & Braggio, E. (2015). Identification of

recurrent truncated DDX3X mutations in chronic lymphocytic leukaemia. In *British Journal of Haematology* (Vol. 169, Issue 3, pp. 445–448). Br J Haematol. https://doi.org/10.1111/bjh.13211

Okazaki, Y., Furuno, M., Kasukawa, T., Adachi, J., Bono, H., Kondo, S., Nikaido, I., Osato, N., Saito, R., Suzuki, H., Yamanaka, I., Kiyosawa, H., Yagi, K., Tomaru, Y., Hasegawa, Y., Nogami, A., Schönbach, C., Gojobori, T., Baldarelli, R., … Hayashizaki, Y. (2002). Analysis of the mouse transcriptome based on functional annotation of 60,770 full-length cDNAs. *Nature*, *420*, 563. http://www.informatics.jax.org/mgihome/

Onomoto, K., Jogi, M., Yoo, J. S., Narita, R., Morimoto, S., Takemura, A., Sambhara, S., Kawaguchi, A., Osari, S., Nagata, K., Matsumiya, T., Namiki, H., Yoneyama, M., & Fujita, T. (2012). Critical role of an antiviral stress granule containing RIG-I and PKR in viral detection and innate immunity. *PLoS ONE*, *7*(8), 43031. https://doi.org/10.1371/journal.pone.0043031

Onomoto, K., Yoneyama, M., Fung, G., Kato, H., & Fujita, T. (2014). Antiviral innate immunity and stress granule responses. In *Trends in Immunology* (Vol. 35, Issue 9, pp. 420–428). Elsevier Ltd. https://doi.org/10.1016/j.it.2014.07.006

Osato, T., & Imai, S. (1996). Epstein-Barr virus and gastric carcinoma. *Seminars in Cancer Biology*, *7*(4), 175–182. https://doi.org/10.1006/scbi.1996.0024

Pakos-Zebrucka, K., Koryga, I., Mnich, K., Ljujic, M., Samali, A., & Gorman, A. M. (2016). The integrated stress response. *EMBO Reports*, *17*(10), 1374–1395. https://doi.org/10.15252/embr.201642195

Palam, L. R., Baird, T. D., & Wek, R. C. (2011). Phosphorylation of eIF2 facilitates ribosomal bypass of an inhibitory upstream ORF to enhance CHOP translation. *Journal of Biological Chemistry*, *286*(13), 10939–10949. https://doi.org/10.1074/jbc.M110.216093

Palazzo, A. F., & Lee, E. S. (2015). Non-coding RNA: What is functional and what is junk? *Frontiers in Genetics*, *5*(JAN). https://doi.org/10.3389/fgene.2015.00002

Panas, M. D., Ivanov, P., & Anderson, P. J. (2016). Mechanistic insights into mammalian stress granule dynamics. In *Journal of Cell Biology* (Vol. 215, Issue 3, pp. 313–323). The Rockefeller University Press. https://doi.org/10.1083/jcb.201609081

Papesch, M., & Watkins, R. (2001). Epstein-Barr virus infectious mononucleosis. In *Clinical Otolaryngology and Allied Sciences* (Vol. 26, Issue 1, pp. 3–8). https://doi.org/10.1046/j.1365-2273.2001.00431.x

Parker, F., Maurier, F., Delumeau, I., Duchesne, M., Faucher, D., Debussche, L., Dugue, A., & Tocque, B. (1996). A Ras-GTPase-Activating Protein SH3-Domain-Binding Protein. *Molecular and Cellular Biology*, *16*(6), 2561–2569. https://www.ncbi.nlm.nih.gov/pmc/articles/PMC231246/pdf/162561.pdf

Paschos, K., Smith, P., Anderton, E., Middeldorp, J. M., White, R. E., & Allday, M. J. (2009). Epstein-Barr virus latency in B cells leads to epigenetic repression and CpG methylation of the tumour suppressor gene Bim. *PLoS Pathogens*, *5*(6). https://doi.org/10.1371/journal.ppat.1000492

Patel, A., Lee, H. O., Jawerth, L., Maharana, S., Jahnel, M., Hein, M. Y., Stoynov, S., Mahamid, J., Saha, S., Franzmann, T. M., Pozniakovski, A., Poser, I., Maghelli, N., Royer, L. A., Weigert, M., Myers, E. W., Grill, S., Drechsel, D., Hyman, A. A., &

Alberti, S. (2015). A Liquid-to-Solid Phase Transition of the ALS Protein FUS Accelerated by Disease Mutation. *Cell*, *162*(5), 1066–1077. https://doi.org/10.1016/j.cell.2015.07.047

Pavio, N., Romano, P. R., Graczyk, T. M., Feinstone, S. M., & Taylor, D. R. (2003). Protein Synthesis and Endoplasmic Reticulum Stress Can Be Modulated by the Hepatitis C Virus Envelope Protein E2 through the Eukaryotic Initiation Factor 2α Kinase PERK. *Journal of Virology*, *77*(6), 3578–3585. https://doi.org/10.1128/jvi.77.6.3578-3585.2003

Peeples, W. B., & Rosen, M. K. (2020). Phase Separation Can Increase Enzyme Activity by Concentration and Molecular Organization. *BioRxiv*, 2020.09.15.299115. https://doi.org/10.1101/2020.09.15.299115

Peltonen, K., Colis, L., Liu, H., Jäämaa, S., Moore, H. M., Enbäck, J., Laakkonen, P., Vaahtokari, A., Jones, R. J., af Hällström, T. M., & Laiho, M. (2010). Identification of novel p53 Pathway activating Small-molecule compounds reveals unexpected similarities with known therapeutic agents. *PLoS ONE*, *5*(9), e12996. https://doi.org/10.1371/journal.pone.0012996

Peltonen, K., Colis, L., Liu, H., Trivedi, R., Moubarek, M. S., Moore, H. M., Bai, B., Rudek, M. A., Bieberich, C. J., & Laiho, M. (2014). A targeting modality for destruction of RNA polymerase I that possesses anticancer activity. *Cancer Cell*, *25*(1), 77–90. https://doi.org/10.1016/j.ccr.2013.12.009

Piecyk, M., Wax, S., Beck, A. R. P., Kedersha, N., Gupta, M., Maritim, B., Chen, S., Gueydan, C., Kruys, V., Streuli, M., & Anderson, P. J. (2000). TIA-1 is a translational silencer that selectively regulates the expression of TNF-α. *EMBO Journal*, *19*(15), 4154–4163. https://doi.org/10.1093/emboj/19.15.4154

Piovan, E., Tosello, V., Indraccolo, S., Cabrelle, A., Baesso, I., Trentin, L., Zamarchi, R., Tamamura, H., Fujii, N., Semenzato, G., Chieco-Bianchi, L., & Amadori, A. (2005). Chemokine receptor expression in EBV-associated lymphoproliferation in hu/SCID mice: Implications for CXCL12/CXCR4 axis in lymphoma generation. *Blood*, *105*(3), 931–939. https://doi.org/10.1182/blood-2004-03-0799

Pirrotta, V., & Li, H. B. (2012). A view of nuclear Polycomb bodies. In *Current Opinion in Genetics and Development* (Vol. 22, Issue 2, pp. 101–109). https://doi.org/10.1016/j.gde.2011.11.004

Poppers, J., Mulvey, M., Perez, C., Khoo, D., & Mohr, I. (2003). Identification of a Lytic-Cycle Epstein-Barr Virus Gene Product That Can Regulate PKR Activation. *Journal of Virology*, *77*(1), 228–236. https://doi.org/10.1128/jvi.77.1.228-236.2003

Portal, D., Zhou, H., Zhao, B., Kharchenko, P. V., Lowry, E., Wong, L., Quackenbush, J., Holloway, D., Jiang, S., Lu, Y., & Kieff, E. D. (2013). Epstein-Barr virus nuclear antigen leader protein localizes to promoters and enhancers with cell transcription factors and EBNA2. *Proceedings of the National Academy of Sciences of the United States of America*, *110*(46), 18537–18542. https://doi.org/10.1073/pnas.1317608110

Price, A. M., Dai, J., Bazot, Q., Patel, L., Nikitin, P. A., Djavadian, R., Winter, P. S., Salinas, C. A., Barry, A. P., Wood, K. C., Johannsen, E. C., Letai, A., Allday, M. J., & Luftig, M. A. (2017). Epstein-barr virus ensures B cell survival by uniquely modulating apoptosis at early and late times after infection. *ELife*, *6*. https://doi.org/10.7554/eLife.22509

Pullmann, R., Kim, H. H., Abdelmohsen, K., Lal, A., Martindale, J. L., Yang, X., & Gorospe, M. (2007). Analysis of Turnover and Translation Regulatory RNA-Binding Protein Expression through Binding to Cognate mRNAs. *Molecular and Cellular Biology*, *27*(18), 6265–6278. https://doi.org/10.1128/mcb.00500-07

Puthenveetil, S., Whitby, L., Ren, J., Kelnar, K., Krebs, J. F., & Beal, P. A. (2006). Controlling activation of the RNA-dependent protein kinase by siRNAs using site-specific chemical modification. *Nucleic Acids Research*, *34*(17), 4900–4911. https://doi.org/10.1093/nar/gkl464

Quinn, L. L., Zuo, J., Abbott, R. J. M., Shannon-Lowe, C., Tierney, R. J., Hislop, A. D., & Rowe, M. (2014). Cooperation between Epstein-Barr Virus Immune Evasion Proteins Spreads Protection from CD8+ T Cell Recognition across All Three Phases of the Lytic Cycle. *PLoS Pathogens*, *10*(8). https://doi.org/10.1371/journal.ppat.1004322

Quiroz, F. G., Fiore, V. F., Levorse, J., Polak, L., Wong, E., Pasolli, H. A., & Fuchs, E. (2020). Liquid-liquid phase separation drives skin barrier formation. *Science (New York, N.Y.)*, *367*(6483). https://doi.org/10.1126/science.aax9554

Ragoczy, T., Heston, L., & Miller, G. (1998). The Epstein-Barr Virus Rta Protein Activates Lytic Cycle Genes and Can Disrupt Latency in B Lymphocytes. *Journal of Virology*, *72*(10), 7978–7984. https://doi.org/10.1128/jvi.72.10.7978-7984.1998

Ramasubramanyan, S., Osborn, K., Al-Mohammad, R., Naranjo Perez-Fernandez, I. B., Zuo, J., Balan, N., Godfrey, A., Patel, H., Peters, G., Rowe, M., Jenner, R. G., & Sinclair, A. J. (2015). Epstein-Barr virus transcription factor Zta acts through distal regulatory elements to directly control cellular gene expression. *Nucleic Acids Research*, *43*(7), 3563–3577. https://doi.org/10.1093/nar/gkv212

Rampersad, S., & Tennant, P. (2018). Replication and Expression Strategies of Viruses. In *Viruses: Molecular Biology, Host Interactions, and Applications to Biotechnology* (pp. 55–82). Academic Press. https://doi.org/10.1016/B978-0-12-811257-1.00003-6

Ran, F. A., Hsu, P. D., Wright, J., Agarwala, V., Scott, D. A., & Zhang, F. (2013). Genome engineering using the CRISPR-Cas9 system. *Nature Protocols*, *8*(11), 2281–2308. https://doi.org/10.1038/nprot.2013.143

Ratnadiwakara, M., & Änkö, M.-L. (2018). mRNA Stability Assay Using Transcription Inhibition by Actinomycin D in Mouse Pluripotent Stem Cells. *Bio-Protocol*, *8*(21). https://doi.org/10.21769/bioprotoc.3072

Ray, S., Singh, N., Kumar, R., Patel, K., Pandey, S., Datta, D., Mahato, J., Panigrahi, R., Navalkar, A., Mehra, S., Gadhe, L., Chatterjee, D., Sawner, A. S., Maiti, S., Bhatia, S., Gerez, J. A., Chowdhury, A., Kumar, A., Padinhateeri, R., … Maji, S. K. (2020). α-Synuclein aggregation nucleates through liquid–liquid phase separation. *Nature Chemistry*, *12*(8), 705–716. https://doi.org/10.1038/s41557-020-0465-9

Rayman, J. B., & Kandel, E. R. (2017). TIA-1 is a functional prion-like protein. In *Cold Spring Harbor Perspectives in Biology* (Vol. 9, Issue 5). https://doi.org/10.1101/cshperspect.a030718

Rechsteiner, M. P., Berger, C., Zauner, L., Sigrist, J. A., Weber, M., Longnecker, R., Bernasconi, M., & Nadal, D. (2008). Latent Membrane Protein 2B Regulates Susceptibility to Induction of Lytic Epstein-Barr Virus Infection. *Journal of Virology*, *82*(4), 1739–1747. https://doi.org/10.1128/jvi.01723-07

Reineke, L. C., Dougherty, J. D., Pierre, P., & Lloyd, R. E. (2012). Large G3BP-induced granules trigger eIF2α phosphorylation. *Molecular Biology of the Cell*, *23*(18), 3499–3510. https://doi.org/10.1091/mbc.E12-05-0385

Reineke, L. C., Kedersha, N., Langereis, M. A., van Kuppeveld, F. J. M., & Lloyd, R. E. (2015). Stress granules regulate double-stranded RNA-dependent protein kinase activation through a complex containing G3BP1 and Caprin1. *MBio*, *6*(2), e02486-14. https://doi.org/10.1128/mBio.02486-14

Reineke, L. C., & Lloyd, R. E. (2015). The Stress Granule Protein G3BP1 Recruits Protein Kinase R To Promote Multiple Innate Immune Antiviral Responses. *Journal of Virology*, *89*(5), 2575–2589. https://doi.org/10.1128/jvi.02791-14

Reisman, D., Yates, J. R., & Sugden, B. (1985). A putative origin of replication of plasmids derived from Epstein-Barr virus is composed of two cis-acting components. *Molecular and Cellular Biology*, *5*(8), 1822–1832. https://doi.org/10.1128/mcb.5.8.1822

Reyes, R., Alcalde, J., & Izquierdo, J. M. (2009). Depletion of T-cell intracellular antigen proteins promotes cell proliferation. *Genome Biology*, *10*(8), 87. https://doi.org/10.1186/gb-2009-10-8-r87

Roll-Mecak, A., Alone, P., Cao, C., Dever, T. E., & Burley, S. K. (2004). X-ray Structure of Translation Initiation Factor eIF2γ: Implications for tRNA and eIF2α binding. *Journal of Biological Chemistry*, *279*(11), 10634–10642. https://doi.org/10.1074/jbc.M310418200

Ron, D., & Habener, J. F. (1992). CHOP, a novel developmentally regulated nuclear protein that dimerizes with transcription factors C/EBP and LAP and functions as a dominant-negative inhibitor of gene transcription. *Genes and Development*, *6*(3), 439–453. https://doi.org/10.1101/gad.6.3.439

Rovedo, M., & Longnecker, R. (2007). Epstein-Barr Virus Latent Membrane Protein 2B (LMP2B) Modulates LMP2A Activity. *Journal of Virology*, *81*(1), 84–94. https://doi.org/10.1128/jvi.01302-06

Rowe, M., Glaunsinger, B., Van Leeuwen, D., Zuo, J., Sweetman, D., Ganem, D., Middeldorp, J. M., Wiertz, E. J., & Ressing, M. E. (2007). Host shutoff during productive Epstein-Barr virus infection is mediated by BGLF5 and may contribute to immune evasion. *Pnas*, *104*(9), 3366–3371. https://doi.org/10.1073/pnas.0611128104

Rowe, M., Rowe, D. T., Gregory, C. D., Young, L. S., Farrell, P. J., Rupani, H., & Rickinson, A. B. (1987). Differences in B cell growth phenotype reflect novel patterns of Epstein-Barr virus latent gene expression in Burkitt's lymphoma cells. *The EMBO Journal*, *6*(9), 2743–2751. https://doi.org/10.1002/j.1460-2075.1987.tb02568.x

Ruf, I. K., Lackey, K. A., Warudkar, S., & Sample, J. T. (2005). Protection from Interferon-Induced Apoptosis by Epstein-Barr Virus Small RNAs Is Not Mediated by Inhibition of PKR. *Journal of Virology*, *79*(23), 14562–14569. https://doi.org/10.1128/JVI.79.23.14562-14569.2005

Ruggieri, A., Dazert, E., Metz, P., Hofmann, S., Bergeest, J. P., Mazur, J., Bankhead, P., Hiet, M. S., Kallis, S., Alvisi, G., Samuel, C. E., Lohmann, V., Kaderali, L., Rohr, K., Frese, M., Stoecklin, G., & Bartenschlager, R. (2012). Dynamic Oscillation of Translation and Stress Granule Formation Mark the Cellular Response to Virus

Infection. *Cell Host and Microbe*, *12*(1), 71–85. https://doi.org/10.1016/j.chom.2012.05.013

Ryu, J. K., Rafalski, V. A., Meyer-Franke, A., Adams, R. A., Poda, S. B., Rios Coronado, P. E., Pedersen, L. Ø., Menon, V., Baeten, K. M., Sikorski, S. L., Bedard, C., Hanspers, K., Bardehle, S., Mendiola, A. S., Davalos, D., Machado, M. R., Chan, J. P., Plastira, I., Petersen, M. A., … Akassoglou, K. (2018). Fibrin-targeting immunotherapy protects against neuroinflammation and neurodegeneration. *Nature Immunology*, *19*(11), 1212–1223. https://doi.org/10.1038/s41590-018-0232-x

Rzymski, T., Milani, M., Pike, L., Buffa, F., Mellor, H. R., Winchester, L., Pires, I., Hammond, E., Ragoussis, I., & Harris, A. L. (2010). Regulation of autophagy by ATF4 in response to severe hypoxia. *Oncogene*, *29*(31), 4424–4435. https://doi.org/10.1038/onc.2010.191

Saha, A., Bamidele, A., Murakami, M., & Robertson, E. S. (2011). EBNA3C Attenuates the Function of p53 through Interaction with Inhibitor of Growth Family Proteins 4 and 5. *Journal of Virology*, *85*(5), 2079–2088. https://doi.org/10.1128/jvi.02279-10

Saha, A., Halder, S., Upadhyay, S. K., Lu, J., Kumar, P., Murakami, M., Cai, Q., & Robertson, E. S. (2011). Epstein-Barr virus nuclear antigen 3c facilitates G1-S transition by stabilizing and enhancing the function of Cyclin D1. *PLoS Pathogens*, *7*(2). https://doi.org/10.1371/journal.ppat.1001275

Saha, A., & Robertson, E. S. (2011). Functional modulation of the metastatic suppressor Nm23-H1 by oncogenic viruses. In *FEBS Letters* (Vol. 585, Issue 20, pp. 3174–3184). NIH Public Access. https://doi.org/10.1016/j.febslet.2011.08.007

Saha, A., & Robertson, E. S. (2019). Mechanisms of B-Cell Oncogenesis Induced by Epstein-Barr Virus. *Journal of Virology*, *93*(13). https://doi.org/10.1128/jvi.00238-19

Salghetti, S. E., Kim, S. Y., & Tansey, W. P. (1999). Destruction of Myc by ubiquitin-mediated proteolysis: Cancer-associated and transforming mutations stabilize Myc. *EMBO Journal*, *18*(3), 717–726. https://doi.org/10.1093/emboj/18.3.717

Samanta, M., Iwakiri, D., Kanda, T., Imaizumi, T., & Takada, K. (2006). EB virus-encoded RNAs are recognized by RIG-I and activate signaling to induce type I IFN. *EMBO Journal*, *25*(18), 4207–4214. https://doi.org/10.1038/sj.emboj.7601314

Samir, P., Kesavardhana, S., Patmore, D. M., Gingras, S., Malireddi, R. K. S., Karki, R., Guy, C. S., Briard, B., Place, D. E., Bhattacharya, A., Sharma, B. R., Nourse, A., King, S. V., Pitre, A., Burton, A. R., Pelletier, S., Gilbertson, R. J., & Kanneganti, T. D. (2019). DDX3X acts as a live-or-die checkpoint in stressed cells by regulating NLRP3 inflammasome. *Nature*, *573*(7775), 590–594. https://doi.org/10.1038/s41586-019-1551-2

Sánchez-Jiménez, C., Ludeña, M. D., & Izquierdo, J. M. (2015). T-cell intracellular antigens function as tumor suppressor genes. *Cell Death and Disease*, *6*(3). https://doi.org/10.1038/cddis.2015.43

Sanders, D. W., Kedersha, N., Lee, D. S. W., Strom, A. R., Drake, V., Riback, J. A., Bracha, D., Eeftens, J. M., Iwanicki, A., Wang, A., Wei, M. T., Whitney, G., Lyons, S. M., Anderson, P. J., Jacobs, W. M., Ivanov, P., & Brangwynne, C. P. (2020). Competing Protein-RNA Interaction Networks Control Multiphase Intracellular Organization. *Cell*, *181*(2), 306-324.e28. https://doi.org/10.1016/j.cell.2020.03.050

Sandqvist, A., & Sistonen, L. (2004). Nuclear stress granules: The awakening of a sleeping beauty? In *Journal of Cell Biology* (Vol. 164, Issue 1, pp. 15–17). The Rockefeller University Press. https://doi.org/10.1083/jcb.200311102

Sarwari, N. M., Khoury, J. D., & Hernandez, C. M. R. (2016). Chronic Epstein Barr virus infection leading to classical Hodgkin lymphoma. *BMC Hematology*, *16*(1), 1–6. https://doi.org/10.1186/s12878-016-0059-3

Saunus, J. M., Edwards, S. L., French, J. D., Smart, C. E., & Brown, M. A. (2007). Regulation of BRCA1 messenger RNA stability in human epithelial cell lines and during cell cycle progression. *FEBS Letters*, *581*(18), 3435–3442. https://doi.org/10.1016/j.febslet.2007.06.046

Sbih-Lammali, F., Djennaoui, D., Belaoui, H., Bouguermouh, A., Decaussin, G., & Ooka, T. (1996). Transcriptional expression of Epstein-Barr virus genes and proto-oncogenes in North African nasopharyngeal carcinoma. *Journal of Medical Virology*, *49*(1), 7–14. https://doi.org/10.1002/(SICI)1096-9071(199605)49:1<7::AID-JMV2>3.0.CO;2-A

Schlick, S. N., Wood, C. D., Gunnell, A., Webb, H. M., Khasnis, S., Schepers, A., & West, M. J. (2011). Upregulation of the cell-cycle regulator RGC-32 in epstein-barr virus-immortalized cells. *PLoS ONE*, *6*(12). https://doi.org/10.1371/journal.pone.0028638

Schneider-Poetsch, T., Ju, J., Eyler, D. E., Dang, Y., Bhat, S., Merrick, W. C., Green, R., Shen, B., & Liu, J. O. (2010). Inhibition of eukaryotic translation elongation by cycloheximide and lactimidomycin. *Nature Chemical Biology*, *6*(3), 209–217. https://doi.org/10.1038/nchembio.304

Schwemmle, M., Clemens, M. J., Hilse, K., Pfeifer, K., Tröster, H., Müller, W. E. G., & Bachmann, M. (1992). Localization of Epstein-Barr virus-encoded RNAs EBER-1 and EBER-2 in interphase and mitotic Burkitt lymphoma cells. *Proceedings of the National Academy of Sciences of the United States of America*, *89*(21), 10292–10296. https://doi.org/10.1073/pnas.89.21.10292

Sciortino, M. T., Parisi, T., Siracusano, G., Mastino, A., Taddeo, B., & Roizman, B. (2013). The Virion Host Shutoff RNase Plays a Key Role in Blocking the Activation of Protein Kinase R in Cells Infected with Herpes Simplex Virus 1. *Journal of Virology*, *87*(6), 3271–3276. https://doi.org/10.1128/JVI.03049-12

Seto, E., Moosmann, A., Grömminger, S., Walz, N., Grundhoff, A., & Hammerschmidt, W. (2010). Micro RNAS of epstein-barr virus promote cell cycle progression and prevent apoptosis of primary human B cells. *PLoS Pathogens*, *6*(8), 69–70. https://doi.org/10.1371/journal.ppat.1001063

Sharma, N. R., Majerciak, V., Kruhlak, M. J., & Zheng, Z. M. (2017). KSHV inhibits stress granule formation by viral ORF57 blocking PKR activation. *PLoS Pathogens*, *13*(10). https://doi.org/10.1371/journal.ppat.1006677

Sharma, N. R., & Zheng, Z.-M. (2022). RNA Granules in Antiviral Innate Immunity: A Kaposi's Sarcoma-Associated Herpesvirus Journey. *Frontiers in Microbiology*, *12*, 4038. https://doi.org/10.3389/fmicb.2021.794431

Sharon, E., & Frenkel, N. (2017). Human Herpesvirus 6A Exhibits Restrictive Propagation with Limited Activation of the Protein Kinase R-eIF2α Stress Pathway. *Journal of Virology*, *91*(9). https://doi.org/10.1128/jvi.02120-16

Sharp, T. V, Schwemmle, M., Jeffrey, I., Laing, K., Mellor, H., Proud, C. G., Hilse, K., &

Clemens, M. J. (1993). Comparative analysis of the regulation of the interferon-inducible protein kinase PKR by Epstein-Barr virus RNAs EBER-1 and EBER-2 and adenovirus VA1 RNA. *Nucleic Acids Research*, *21*(19), 4483–4490. https://www.ncbi.nlm.nih.gov/pmc/articles/PMC311179/pdf/nar00068-0061.pdf

Sheth, U., & Parker, R. (2003). Decapping and decay of messenger RNA occur in cytoplasmic processing bodies. *Science*, *300*(5620), 805–808. https://doi.org/10.1126/science.1082320

Shih, J. W., Wang, W. T., Tsai, T. Y., Kuo, C. Y., Li, H. K., & Wu Lee, Y. H. (2012). Critical roles of RNA helicase DDX3 and its interactions with eIF4E/PABP1 in stress granule assembly and stress response. *Biochemical Journal*, *441*(1), 119–129. https://doi.org/10.1042/BJ20110739

Shin, H. J., Kim, D. N., & Lee, S. K. (2011). Association between epstein-barr virus infection and chemoresistance to docetaxel in gastric carcinoma. *Molecules and Cells*, *32*(2), 173–179. https://doi.org/10.1007/s10059-011-0066-y

Shin, V. Y., Chen, J., Cheuk, I. W. Y., Siu, M. T., Ho, C. W., Wang, X., Jin, H., & Kwong, A. (2019). Long non-coding RNA NEAT1 confers oncogenic role in triple-negative breast cancer through modulating chemoresistance and cancer stemness. *Cell Death and Disease*, *10*(4). https://doi.org/10.1038/s41419-019-1513-5

Shin, Y., & Brangwynne, C. P. (2017). Liquid phase condensation in cell physiology and disease. In *Science* (Vol. 357, Issue 6357). American Association for the Advancement of Science. https://doi.org/10.1126/science.aaf4382

Sinclair, A. J., Yarranton, S., & Schelcher, C. (2006). DNA-damage response pathways triggered by viral replication. In *Expert Reviews in Molecular Medicine* (Vol. 8, Issue 5, pp. 1–11). https://doi.org/10.1017/S1462399406010544

Sirey, T. M., Roberts, K., Haerty, W., Bedoya-Reina, O., Rogatti-Granados, S., Tan, J. Y., Li, N., Heather, L. C., Carter, R. N., Cooper, S., Finch, A. J., Wills, J., Morton, N. M., Marques, A. C., & Ponting, C. P. (2019). Erratum: Correction: The long non-coding RNA Cerox1 is a post transcriptional regulator of mitochondrial complex I catalytic activity (eLife (2019) 8 PII: e50980). In *eLife* (Vol. 8). https://doi.org/10.7554/eLife.50980

Sivachandran, N., Wang, X., & Frappier, L. (2012). Functions of the Epstein-Barr Virus EBNA1 Protein in Viral Reactivation and Lytic Infection. *Journal of Virology*, *86*(11), 6146–6158. https://doi.org/10.1128/jvi.00013-12

Sixbey, J. W., Vesterinen, E. H., Nedrud, J. G., Raab-traub, N., Walton, L. A., & Pagano, J. S. (1983). Replication of Epstein-Barr virus in human epithelial cells infected in vitro. *Nature*, *306*(5942), 480–483. https://doi.org/10.1038/306480a0

Sizova, D. V., Kolupaeva, V. G., Pestova, T. V., Shatsky, I. N., & Hellen, C. U. T. (1998). Specific Interaction of Eukaryotic Translation Initiation Factor 3 with the 5′ Nontranslated Regions of Hepatitis C Virus and Classical Swine Fever Virus RNAs. *Journal of Virology*, *72*(6), 4775–4782. https://doi.org/10.1128/jvi.72.6.4775-4782.1998

Sledz, C. A., Holko, M., De Veer, M. J., Silverman, R. H., & Williams, B. R. G. (2003). Activation of the interferon system by short-interfering RNAs. *Nature Cell Biology*, *5*(9), 834–839. https://doi.org/10.1038/ncb1038

Smalley, M. J., Signoret, N., Robertson, D., Tilley, A., Hann, A., Ewan, K., Ding, Y.,

Paterson, H., & Dale, T. C. (2005). Dishevelled (Dvl-2) activates canonical Wnt signalling in the absence of cytoplasmic puncta. *Journal of Cell Science*, *118*(22), 5279–5289. https://doi.org/10.1242/jcs.02647

Smiley, J. R. (2004). Herpes Simplex Virus Virion Host Shutoff Protein: Immune Evasion Mediated by a Viral RNase? *Journal of Virology*, *78*(3), 1063–1068. https://doi.org/10.1128/jvi.78.3.1063-1068.2004

Smiley, J. R., Elgadi, M. M., & Saffran, H. A. (2001). Herpes simplex virus vhs protein. In *Methods in Enzymology* (Vol. 342, pp. 440–451). Academic Press. https://doi.org/10.1016/S0076-6879(01)42565-1

Smith, C. W. J., & Valcárcel, J. (2000). Alternative pre-mRNA splicing: the logic of combinatorial control. In *Trends in Biochemical Sciences* (Vol. 25, Issue 8, pp. 381–388). https://doi.org/10.1016/S0968-0004(00)01604-2

Sohn, J., & Hur, S. (2016). Filament assemblies in foreign nucleic acid sensors. In *Current Opinion in Structural Biology* (Vol. 37, pp. 134–144). NIH Public Access. https://doi.org/10.1016/j.sbi.2016.01.011

Somasekharan, S. P., El-Naggar, A., Leprivier, G., Cheng, H., Hajee, S., Grunewald, T. G. P., Zhang, F., Ng, T., Delattre, O., Evdokimova, V., Wang, Y., Gleave, M., & Sorensen, P. H. (2015). YB-1 regulates stress granule formation and tumor progression by translationally activating G3BP1. *Journal of Cell Biology*, *208*(7), 913–929. https://doi.org/10.1083/jcb.201411047

Son, K.-N., Liang, Z., & Lipton, H. L. (2015). Double-Stranded RNA Is Detected by Immunofluorescence Analysis in RNA and DNA Virus Infections, Including Those by Negative-Stranded RNA Viruses. *Journal of Virology*, *89*(18), 9383–9392. https://doi.org/10.1128/JVI.01299-15

Sonenberg, N., & Hinnebusch, A. G. (2009). Regulation of Translation Initiation in Eukaryotes: Mechanisms and Biological Targets. In *Cell* (Vol. 136, Issue 4, pp. 731–745). NIH Public Access. https://doi.org/10.1016/j.cell.2009.01.042

Spannl, S., Tereshchenko, M., Mastromarco, G. J., Ihn, S. J., & Lee, H. O. (2019). Biomolecular condensates in neurodegeneration and cancer. In *Traffic* (Vol. 20, Issue 12, pp. 890–911). https://doi.org/10.1111/tra.12704

Spector, D. L., & Lamond, A. I. (2011). Nuclear speckles. *Cold Spring Harbor Perspectives in Biology*, *3*(2), 1–12. https://doi.org/10.1101/cshperspect.a000646

Sreedharan, J., Blair, I. P., Tripathi, V. B., Hu, X., Vance, C., Rogelj, B., Ackerley, S., Durnall, J. C., Williams, K. L., Buratti, E., Baralle, F., De Belleroche, J., Mitchell, J. D., Leigh, P. N., Al-Chalabi, A., Miller, C. C., Nicholson, G. A., & Shaw, C. E. (2008). TDP-43 mutations in familial and sporadic amyotrophic lateral sclerosis. *Science*, *319*(5870), 1668–1672. https://doi.org/10.1126/science.1154584

Stetson, D. B., & Medzhitov, R. (2006). Type I Interferons in Host Defense. In *Immunity* (Vol. 25, Issue 3, pp. 373–381). https://doi.org/10.1016/j.immuni.2006.08.007

Strambio-De-Castillia, C., Niepel, M., & Rout, M. P. (2010). The nuclear pore complex: Bridging nuclear transport and gene regulation. In *Nature Reviews Molecular Cell Biology* (Vol. 11, Issue 7, pp. 490–501). https://doi.org/10.1038/nrm2928

Strom, A. R., Emelyanov, A. V, Mir, M., Fyodorov, D. V, Darzacq, X., & Karpen, G. H. (2017). Phase separation drives heterochromatin domain formation. *Nature*,

547(7662), 241–245. https://doi.org/10.1038/nature22989

Su, H.-L., Liao, C.-L., & Lin, Y.-L. (2002). Japanese Encephalitis Virus Infection Initiates Endoplasmic Reticulum Stress and an Unfolded Protein Response. *Journal of Virology*, *76*(9), 4162–4171. https://doi.org/10.1128/jvi.76.9.4162-4171.2002

Sugden, B., Marsh, K., & Yates, J. R. (1985). A vector that replicates as a plasmid and can be efficiently selected in B-lymphoblasts transformed by Epstein-Barr virus. *Molecular and Cellular Biology*, *5*(2), 410–413. https://doi.org/10.1128/mcb.5.2.410

Sun, C. C., & Thorley-Lawson, D. A. (2007). Plasma Cell-Specific Transcription Factor XBP-1s Binds to and Transactivates the Epstein-Barr Virus BZLF1 Promoter. *Journal of Virology*, *81*(24), 13566–13577. https://doi.org/10.1128/jvi.01055-07

Sun, X., & Wong, D. (2016). Long non-coding RNA-mediated regulation of glucose homeostasis and diabetes. In *American Journal of Cardiovascular Disease* (Vol. 6, Issue 2, pp. 17–25). www.AJCD.us

Suragani, R. N. V. S., Zachariah, R. S., Velazquez, J. G., Liu, S., Sun, C. W., Townes, T. M., & Chen, J. J. (2012). Heme-regulated eIF2α kinase activated Atf4 signaling pathway in oxidative stress and erythropoiesis. *Blood*, *119*(22), 5276–5284. https://doi.org/10.1182/blood-2011-10-388132

Swanson-Mungerson, M., Bultema, R., & Longnecker, R. (2010). Epstein-Barr virus LMP2A imposes sensitivity to apoptosis. *Journal of General Virology*, *91*(9), 2197–2202. https://doi.org/10.1099/vir.0.021444-0

Taddeo, B., Zhang, W., & Roizman, B. (2010). Role of Herpes Simplex Virus ICP27 in the Degradation of mRNA by Virion Host Shutoff RNase. *Journal of Virology*, *84*(19), 10182–10190. https://doi.org/10.1128/jvi.00975-10

Takada, K. (1984). Cross-linking of cell surface immunoglobulins induces epstein-barr virus in burkitt lymphoma lines. *International Journal of Cancer*, *33*(1), 27–32. https://doi.org/10.1002/ijc.2910330106

Takada, K., & Ono, Y. (1989). Synchronous and sequential activation of latently infected Epstein-Barr virus genomes. *Journal of Virology*, *63*(1), 445–449. https://doi.org/10.1128/jvi.63.1.445-449.1989

Tardif, K. D., Mori, K., Kaufman, R. J., & Siddiqui, A. (2004). Hepatitis C Virus Suppresses the IRE1-XBP1 Pathway of the Unfolded Protein Response. *Journal of Biological Chemistry*, *279*(17), 17158–17164. https://doi.org/10.1074/jbc.M312144200

Taylor, G. M., Raghuwanshi, S. K., Rowe, D. T., Wadowsky, R. M., & Rosendorff, A. (2011). Endoplasmic reticulum stress causes EBV lytic replication. *Blood*, *118*(20), 5528–5539. https://doi.org/10.1182/blood-2011-04-347112

Thompson, M. P., & Kurzrock, R. (2004). Epstein-Barr Virus and Cancer. In *Clinical Cancer Research* (Vol. 10, Issue 3, pp. 803–821). American Association for Cancer Research. https://doi.org/10.1158/1078-0432.CCR-0670-3

Thorley-Lawson, D. A., & Babcock, G. J. (1999). A model for persistent infection with Epstein-Barr virus: The stealth virus of human B cells. In *Life Sciences* (Vol. 65, Issue 14, pp. 1433–1453). Pergamon. https://doi.org/10.1016/S0024-3205(99)00214-3

Thorley-Lawson, D. A., Hawkins, J. B., Tracy, S. I., & Shapiro, M. (2013). The

pathogenesis of Epstein-Barr virus persistent infection. In *Current Opinion in Virology* (Vol. 3, Issue 3, pp. 227–232). Elsevier. https://doi.org/10.1016/j.coviro.2013.04.005

Tian, Q., Streuli, M., Saito, H., Schlossman, S. F., & Anderson, P. J. (1991). A polyadenylate binding protein localized to the granules of cytolytic lymphocytes induces DNA fragmentation in target cells. *Cell*, *67*(3), 629–639. https://doi.org/10.1016/0092-8674(91)90536-8

Toczyski, D. P., Matera, A. G., Ward, D. C., & Steitz, J. A. (1994). The Epstein-Barr virus (EBV) small RNA EBER1 binds and relocalizes ribosomal protein L22 in EBV-infected human B lymphocytes. *Proceedings of the National Academy of Sciences of the United States of America*, *91*(8), 3463–3467. https://doi.org/10.1073/pnas.91.8.3463

Tolay, N., & Buchberger, A. (2021). Comparative profiling of stress granule clearance reveals differential contributions of the ubiquitin system. *Life Science Alliance*, *4*(5). https://doi.org/10.26508/LSA.202000927

Tourrière, H., Chebli, K., Zekri, L., Courselaud, B., Blanchard, J. M., Bertrand, E., & Tazi, J. (2003). The RasGAP-associated endoribonuclease G3BP assembles stress granules. *Journal of Cell Biology*, *160*(6), 823–831. https://doi.org/10.1083/jcb.200212128

Tourrière, H., Gallouzi, I., Chebli, K., Capony, J. P., Mouaikel, J., van der Geer, P., & Tazi, J. (2001). RasGAP-Associated Endoribonuclease G3BP: Selective RNA Degradation and Phosphorylation-Dependent Localization. *Molecular and Cellular Biology*, *21*(22), 7747–7760. https://doi.org/10.1128/mcb.21.22.7747-7760.2001

Tovey, M. G., Begon-Lours, J., & Lenoir, G. (1978). Activation of latent Epstein-Barr virus by antibody to human IgM. In *Nature* (Vol. 276, Issue 5685, pp. 270–272). Springer. https://doi.org/10.1038/276270a0

Tran, H., Maurer, F., & Nagamine, Y. (2003). Stabilization of Urokinase and Urokinase Receptor mRNAs by HuR Is Linked to Its Cytoplasmic Accumulation Induced by Activated Mitogen-Activated Protein Kinase-Activated Protein Kinase 2. *Molecular and Cellular Biology*, *23*(20), 7177–7188. https://doi.org/10.1128/mcb.23.20.7177-7188.2003

Tsai, N. P., Ho, P. C., & Wei, L. N. (2008). Regulation of stress granule dynamics by Grb7 and FAK signalling pathway. *EMBO Journal*, *27*(5), 715–726. https://doi.org/10.1038/emboj.2008.19

Tsai, W. C., Gayatri, S., Reineke, L. C., Sbardella, G., Bedford, M. T., & Lloyd, R. E. (2016). Arginine demethylation of G3BP1 promotes stress granule assembly. *Journal of Biological Chemistry*, *291*(43), 22671–22685. https://doi.org/10.1074/jbc.M116.739573

Tsang, C. M., Deng, W., Yip, Y. L., Zeng, M. S., Lo, K. W., & Tsao, S. W. (2014). Epstein-Barr virus infection and persistence in nasopharyngeal epithelial cells. In *Chinese Journal of Cancer* (Vol. 33, Issue 11, pp. 549–555). BioMed Central. https://doi.org/10.5732/cjc.014.10169

Tsurumi, T., Fujita, M., & Kudoh, A. (2005). Latent and lytic Epstein-Barr virus replication strategies. In *Reviews in Medical Virology* (Vol. 15, Issue 1, pp. 3–15). https://doi.org/10.1002/rmv.441

Tu, Y.-C., Yu, C.-Y., Liang, J.-J., Lin, E., Liao, C.-L., & Lin, Y.-L. (2012). Blocking Double-Stranded RNA-Activated Protein Kinase PKR by Japanese Encephalitis Virus Nonstructural Protein 2A. *Journal of Virology*, *86*(19), 10347–10358. https://doi.org/10.1128/jvi.00525-12

Valentin-Vega, Y. A., Wang, Y. D., Parker, M., Patmore, D. M., Kanagaraj, A. P., Moore, J., Rusch, M., Finkelstein, D., Ellison, D. W., Gilbertson, R. J., Zhang, J., Kim, H. J., & Taylor, J. P. (2016). Cancer-associated DDX3X mutations drive stress granule assembly and impair global translation. *Scientific Reports*, *6*. https://doi.org/10.1038/srep25996

Van de Velde, L. A., Guo, X. Z. J., Barbaric, L., Smith, A. M., Oguin, T. H., Thomas, P. G., & Murray, P. J. (2016). Stress Kinase GCN2 Controls the Proliferative Fitness and Trafficking of Cytotoxic T Cells Independent of Environmental Amino Acid Sensing. *Cell Reports*, *17*(9), 2247–2258. https://doi.org/10.1016/j.celrep.2016.10.079

Van Heesch, S., Van Iterson, M., Jacobi, J., Boymans, S., Essers, P. B., De Bruijn, E., Hao, W., MacInnes, A. W., Cuppen, E., & Simonis, M. (2014). Extensive localization of long noncoding RNAs to the cytosol and mono- and polyribosomal complexes. *Genome Biology*, *15*(1), R6. https://doi.org/10.1186/gb-2014-15-1-r6

Vanderweyde, T. E., Apicco, D. J., Youmans-Kidder, K., Ash, P. E. A., Cook, C., Lummertz da Rocha, E., Jansen-West, K., Frame, A. A., Citro, A., Leszyk, J. D., Ivanov, P., Abisambra, J. F., Steffen, M., Li, H., Petrucelli, L., & Wolozin, B. (2016). Interaction of tau with the RNA-Binding Protein TIA1 Regulates tau Pathophysiology and Toxicity. *Cell Reports*, *15*(7), 1455–1466. https://doi.org/10.1016/j.celrep.2016.04.045

Vanderweyde, T. E., Yu, H., Varnum, M., Liu-Yesucevitz, L., Citro, A., Ikezu, T., Duff, K., & Wolozin, B. (2012). Contrasting Pathology of the Stress Granule Proteins TIA-1 and G3BP in Tauopathies. *Journal of Neuroscience*, *32*(24), 8270–8283. https://doi.org/10.1523/jneurosci.1592-12.2012

Vassilev, L. T., Tovar, C., Chen, S., Knezevic, D., Zhao, X., Sun, H., Heimbrook, D. C., & Chen, L. (2006). Selective small-molecule inhibitor reveals critical mitotic functions of human CDK1. *Proceedings of the National Academy of Sciences of the United States of America*, *103*(28), 10660–10665. https://doi.org/10.1073/pnas.0600447103

Vattem, K. M., & Wek, R. C. (2004). Reinitiation involving upstream ORFs regulates ATF4 mRNA translation in mammalian cells. *Proceedings of the National Academy of Sciences of the United States of America*, *101*(31), 11269–11274. https://doi.org/10.1073/pnas.0400541101

Verma, D., Ling, C., Johannsen, E. C., Nagaraja, T., & Swaminathan, S. (2009). Negative Autoregulation of Epstein-Barr Virus (EBV) Replicative Gene Expression by EBV SM Protein. *Journal of Virology*, *83*(16), 8041–8050. https://doi.org/10.1128/jvi.00382-09

Visser, L. J., Medina, G. N., Rabouw, H. H., de Groot, R. J., Langereis, M. A., de los Santos, T., & van Kuppeveld, F. J. M. (2018). Foot-and-Mouth Disease Virus Leader Protease Cleaves G3BP1 and G3BP2 and Inhibits Stress Granule Formation. *Journal of Virology*, *93*(2). https://doi.org/10.1128/jvi.00922-18

Voronina, E., Seydoux, G., Sassone-Corsi, P., & Nagamori, I. (2011). RNA granules in germ cells. In *Cold Spring Harbor Perspectives in Biology* (Vol. 3, Issue 12).

https://doi.org/10.1101/cshperspect.a002774

Vuyisich, M., Spanggord, R. J., & Beal, P. A. (2002). The binding site of the RNA-dependent protein kinase (PKR) on EBER1 RNA from Epstein-Barr virus. *EMBO Reports*, *3*(7), 622–627. https://doi.org/10.1093/embo-reports/kvf137

Wagner, B. J., DeMaria, C. T., Sun, Y., Wilson, G. M., & Brewer, G. (1998). Structure and genomic organization of the human AUF1 gene: Alternative pre-mRNA splicing generates four protein isoforms. *Genomics*, *48*(2), 195–202. https://doi.org/10.1006/geno.1997.5142

Walsh, D., McCarthy, J., O'Driscoll, C., & Melgar, S. (2013). Pattern recognition receptors-Molecular orchestrators of inflammation in inflammatory bowel disease. In *Cytokine and Growth Factor Reviews* (Vol. 24, Issue 2, pp. 91–104). https://doi.org/10.1016/j.cytogfr.2012.09.003

Walter, H. (1999). Consequences of Phase Separation in Cytoplasm. *International Review of Cytology*, *192*, 331–343. https://doi.org/10.1016/s0074-7696(08)60533-1

Walter, H., & Brooks, D. E. (1995). Phase separation in cytoplasm, due to macromolecular crowding, is the basis for microcompartmentation. *FEBS Letters*, *361*(2–3), 135–139. https://doi.org/10.1016/0014-5793(95)00159-7

Walter, P., & Ron, D. (2011). The unfolded protein response: From stress pathway to homeostatic regulation. In *Science* (Vol. 334, Issue 6059, pp. 1081–1086). American Association for the Advancement of Science. https://doi.org/10.1126/science.1209038

Walters, R. W., & Parker, R. (2015). Coupling of Ribostasis and Proteostasis: Hsp70 Proteins in mRNA Metabolism. In *Trends in Biochemical Sciences* (Vol. 40, Issue 10, pp. 552–559). Elsevier Current Trends. https://doi.org/10.1016/j.tibs.2015.08.004

Wang, D., Liebowitz, D., & Kieff, E. D. (1985). An EBV membrane protein expressed in immortalized lymphocytes transforms established rodent cells. *Cell*, *43*(3 PART 2), 831–840. https://doi.org/10.1016/0092-8674(85)90256-9

Wang, L. W., Jiang, S., & Gewurz, B. E. (2017). Epstein-Barr Virus LMP1-Mediated Oncogenicity. *Journal of Virology*, *91*(21). https://doi.org/10.1128/JVI.01718-16/ASSET/5A4577F8-F12B-4020-BA25-482C68157F70/ASSETS/GRAPHIC/ZJV9991830360002.JPEG

Wang, X., Hu, X., Song, W., Xu, H., Xiao, Z., Huang, R., Bai, Q., Zhang, F., Chen, Y., Liu, Y., Fang, J., Li, X., Shen, Q., Zhao, H., & Yang, X. (2021). Mutual dependency between lncRNA LETN and protein NPM1 in controlling the nucleolar structure and functions sustaining cell proliferation. *Cell Research*, *31*(6), 664–683. https://doi.org/10.1038/s41422-020-00458-6

Wang, Y., Chen, L., Chen, B., Li, X., Kang, J., Fan, K., Hu, Y., Xu, J., Yi, L., Yang, J., Huang, Y., Cheng, L., Li, Y., Wang, C., Li, K., Li, X., Xu, J., & Wang, D. (2013). Mammalian ncRNA-disease repository: A global view of ncRNA-mediated disease network. In *Cell Death and Disease* (Vol. 4, Issue 8). https://doi.org/10.1038/cddis.2013.292

Wang, Yiliang, Huang, L., Wang, Y., Luo, W., Li, F., Xiao, J., Qin, S., Wang, Z., Song, X., Wang, Y., Jin, F., & Wang, Y. (2020). Single-cell RNA-sequencing analysis

identifies host long noncoding RNA MAMDC2-as1 as a co-factor for HSV-1 nuclear transport. *International Journal of Biological Sciences*, *16*(9), 1586–1603. https://doi.org/10.7150/ijbs.42556

Weber, F., Wagner, V., Rasmussen, S. B., Hartmann, R., & Paludan, S. R. (2006). Double-Stranded RNA Is Produced by Positive-Strand RNA Viruses and DNA Viruses but Not in Detectable Amounts by Negative-Strand RNA Viruses. *Journal of Virology*, *80*(10), 5059–5064. https://doi.org/10.1128/JVI.80.10.5059-5064.2006

Weiss, L. M., Movahed, L. A., Warnke, R. A., & Sklar, J. (1989). Detection of Epstein–Barr Viral Genomes in Reed–Sternberg Cells of Hodgkin's Disease. *New England Journal of Medicine*, *320*(8), 502–506. https://doi.org/10.1056/nejm198902233200806

Wek, R. C. (2018). Role of eIF2α kinases in translational control and adaptation to cellular stress. *Cold Spring Harbor Perspectives in Biology*, *10*(7). https://doi.org/10.1101/cshperspect.a032870

Welsh, G. I., Price, N. T., Bladergroen, B. A., Bloomberg, G., & Proud, C. G. (1994). Identification of novel phosphorylation sites in the β-subunit of translation initiation factor eIF-2. *Biochemical and Biophysical Research Communications*, *201*(3), 1279–1288. https://doi.org/10.1006/bbrc.1994.1843

Wheeler, J. R., Matheny, T., Jain, S., Abrisch, R., & Parker, R. (2016). Distinct stages in stress granule assembly and disassembly. *ELife*, *5*(Se). https://doi.org/10.7554/eLife.18413

White, J. P., Cardenas, A. M., Marissen, W. E., & Lloyd, R. E. (2007). Inhibition of Cytoplasmic mRNA Stress Granule Formation by a Viral Proteinase. *Cell Host and Microbe*, *2*(5), 295–305. https://doi.org/10.1016/j.chom.2007.08.006

White, J. P., & Lloyd, R. E. (2011). Poliovirus Unlinks TIA1 Aggregation and mRNA Stress Granule Formation. *Journal of Virology*, *85*(23), 12442–12454. https://doi.org/10.1128/jvi.05888-11

White, J. P., & Lloyd, R. E. (2012). Regulation of stress granules in virus systems. In *Trends in Microbiology* (Vol. 20, Issue 4, pp. 175–183). https://doi.org/10.1016/j.tim.2012.02.001

White, R. E., Groves, I. J., Turro, E., Yee, J., Kremmer, E., & Allday, M. J. (2010). Extensive co-operation between the Epstein-Barr virus EBNA3 proteins in the manipulation of host gene expression and epigenetic chromatin modification. *PLoS ONE*, *5*(11), e13979. https://doi.org/10.1371/journal.pone.0013979

White, R. E., Rämer, P. C., Naresh, K. N., Meixlsperger, S., Pinaud, L., Rooney, C., Savoldo, B., Coutinho, R., Bödör, C., Gribben, J., Ibrahim, H. A., Bower, M., Nourse, J. P., Gandhi, M. K., Middeldorp, J. M., Cader, F. Z., Murray, P., Münz, C., & Allday, M. J. (2012). EBNA3B-deficient EBV promotes B cell lymphomagenesis in humanized mice and is found in human tumors. *Journal of Clinical Investigation*, *122*(4), 1487–1502. https://doi.org/10.1172/JCI58092

Wills, M. R., Poole, E., Lau, B., Krishna, B., & Sinclair, J. H. (2015). The immunology of human cytomegalovirus latency: Could latent infection be cleared by novel immunotherapeutic strategies? In *Cellular and Molecular Immunology* (Vol. 12, Issue 2, pp. 128–138). https://doi.org/10.1038/cmi.2014.75

Wilson, S. J., Tsao, E. H., Webb, B. L. J., Ye, H., Dalton-Griffin, L., Tsantoulas, C., Gale,

C. V., Du, M.-Q., Whitehouse, A., & Kellam, P. (2007). X Box Binding Protein XBP-1s Transactivates the Kaposi's Sarcoma-Associated Herpesvirus (KSHV) ORF50 Promoter, Linking Plasma Cell Differentiation to KSHV Reactivation from Latency. *Journal of Virology*, *81*(24), 13578–13586. https://doi.org/10.1128/jvi.01663-07

Wippich, F., Bodenmiller, B., Trajkovska, M. G., Wanka, S., Aebersold, R., & Pelkmans, L. (2013). Dual specificity kinase DYRK3 couples stress granule condensation/ dissolution to mTORC1 signaling. *Cell*, *152*(4), 791–805. https://doi.org/10.1016/j.cell.2013.01.033

Witten, J. T., & Ule, J. (2011). Understanding splicing regulation through RNA splicing maps. In *Trends in Genetics* (Vol. 27, Issue 3, pp. 89–97). https://doi.org/10.1016/j.tig.2010.12.001

Wolf, H., Zur Hausen, H., & Becker, V. (1973). EB viral genomes in epithelial nasopharyngeal carcinoma cells. *Nature New Biology*, *244*(138), 245–247. https://doi.org/10.1038/newbio244245a0

Wolozin, B., & Ivanov, P. (2019). Stress granules and neurodegeneration. In *Nature Reviews Neuroscience* (Vol. 20, Issue 11, pp. 649–666). NIH Public Access. https://doi.org/10.1038/s41583-019-0222-5

Wong, Y., Meehan, M. T., Burrows, S. R., Doolan, D. L., & Miles, J. J. (2022). Estimating the global burden of Epstein–Barr virus-related cancers. In *Journal of Cancer Research and Clinical Oncology* (Vol. 148, Issue 1, pp. 31–46). https://doi.org/10.1007/s00432-021-03824-y

Wu, X., Liu, M., Downie, B., Liang, C., Ji, G., Li, Q. Q., & Hunt, A. G. (2011). Genome-wide landscape of polyadenylation in Arabidopsis provides evidence for extensive alternative polyadenylation. *Proceedings of the National Academy of Sciences of the United States of America*, *108*(30), 12533–12538. https://doi.org/10.1073/pnas.1019732108

Xia, T., O'Hara, A., Araujo, I., Barreto, J., Carvalho, E., Sapucaia, J. B., Ramos, J. C., Luz, E., Pedroso, C., Manrique, M., Toomey, N. L., Brites, C., Dittmer, D. P., & Harrington, W. J. (2008). EBV microRNAs in primary lymphomas and targeting of CXCL-11 by ebv-mir-BHRF1-3. *Cancer Research*, *68*(5), 1436–1442. https://doi.org/10.1158/0008-5472.CAN-07-5126

Xie, S. Q., Martin, S., Guillot, P. V., Bentley, D. L., & Pombo, A. (2006). Splicing speckles are not reservoirs of RNA polymerase II, but contain an inactive form, phosphorylated on serine2 residues of the C-terminal domain. *Molecular Biology of the Cell*, *17*(4), 1723–1733. https://doi.org/10.1091/mbc.E05-08-0726

Xing, Y. H., Yao, R. W., Zhang, Y., Guo, C. J., Jiang, S., Xu, G., Dong, R., Yang, L., & Chen, L. L. (2017). SLERT Regulates DDX21 Rings Associated with Pol I Transcription. *Cell*, *169*(4), 664-678.e16. https://doi.org/10.1016/j.cell.2017.04.011

Xu, N., Chen, C.-Y. A., & Shyu, A.-B. (2001). Versatile Role for hnRNP D Isoforms in the Differential Regulation of Cytoplasmic mRNA Turnover. *Molecular and Cellular Biology*, *21*(20), 6960–6971. https://doi.org/10.1128/mcb.21.20.6960-6971.2001

Yamasaki, S., Stoecklin, G., Kedersha, N., Simarro, M., & Anderson, P. J. (2007). T-cell intracellular antigen-1 (TIA-1)-induced translational silencing promotes the decay of selected mRNAs. *Journal of Biological Chemistry*, *282*(41), 30070–30077. https://doi.org/10.1074/jbc.M706273200

Yang, P., Mathieu, C., Kolaitis, R. M., Zhang, P., Messing, J., Yurtsever, U., Yang, Z., Wu, J., Li, Y., Pan, Q., Yu, J., Martin, E. W., Mittag, T., Kim, H. J., & Taylor, J. P. (2020). G3BP1 Is a Tunable Switch that Triggers Phase Separation to Assemble Stress Granules. *Cell*, *181*(2), 325-345.e28. https://doi.org/10.1016/J.CELL.2020.03.046

Yasukawa, M., Ohminami, H., Sada, E., Yakushijin, Y., Kaneko, M., Yanagisawa, K., Kohno, H., Bando, S., & Fujita, S. (1999). Latent infection and reactivation of human herpesvirus 6 in two novel myeloid cell lines. *Blood*, *93*(3), 991–999. https://doi.org/10.1182/blood.v93.3.991.403a13_991_999

Yates, J. R., Warren, N., Reisman, D., & Sugden, B. (1984). A cis-acting element from the Epstein-Barr viral genome that permits stable replication of recombinant plasmids in latently infected cells. *Proceedings of the National Academy of Sciences of the United States of America*, *81*(12 I), 3806–3810. https://doi.org/10.1073/pnas.81.12.3806

Yates, J. R., Warren, N., & Sugden, B. (1985). Stable replication of plasmids derived from Epstein-Barr virus in various mammalian cells. *Nature*, *313*(6005), 812–815. https://doi.org/10.1038/313812a0

Ye, J., Rawson, R. B., Komuro, R., Chen, X., Davé, U. P., Prywes, R., Brown, M. S., & Goldstein, J. L. (2000). ER stress induces cleavage of membrane-bound ATF6 by the same proteases that process SREBPs. *Molecular Cell*, *6*(6), 1355–1364. https://doi.org/10.1016/S1097-2765(00)00133-7

Yoneyama, M., Kikuchi, M., Natsukawa, T., Shinobu, N., Imaizumi, T., Miyagishi, M., Taira, K., Akira, S., & Fujita, T. (2004). The RNA helicase RIG-I has an essential function in double-stranded RNA-induced innate antiviral responses. *Nature Immunology*, *5*(7), 730–737. https://doi.org/10.1038/ni1087

Young, L. S., Dawson, C. W., & Eliopoulos, A. G. (2000). The expression and function of Epstein-Barr virus encoded latent genes. In *Journal of Clinical Pathology - Molecular Pathology* (Vol. 53, Issue 5, pp. 238–247). https://doi.org/10.1136/mp.53.5.238

Young, L. S., Lau, R., Rowe, M., Niedobitek, G., Packham, G., Shanahan, F., Rowe, D. T., Greenspan, D., Greenspan, J. S., & Rickinson, A. B. (1991). Differentiation-associated expression of the Epstein-Barr virus BZLF1 transactivator protein in oral hairy leukoplakia. *Journal of Virology*, *65*(6), 2868–2874. https://doi.org/10.1128/jvi.65.6.2868-2874.1991

Young, S. K., & Wek, R. C. (2016). Upstream open reading frames differentially regulate gene-specific translation in the integrated stress response. In *Journal of Biological Chemistry* (Vol. 291, Issue 33, pp. 16927–16935). American Society for Biochemistry and Molecular Biology. https://doi.org/10.1074/jbc.R116.733899

Young, S. K., Willy, J. A., Wu, C., Sachs, M. S., & Wek, R. C. (2015). Ribosome reinitiation directs gene-specific translation and regulates the integrated stress response. *Journal of Biological Chemistry*, *290*(47), 28257–28271. https://doi.org/10.1074/jbc.M115.693184

Yu, F., Feng, J., Harada, J. N., Chanda, S. K., Kenney, S. C., & Sun, R. (2007). B cell terminal differentiation factor XBP-1 induces reactivation of Kaposi's sarcoma-associated herpesvirus. *FEBS Letters*, *581*(18), 3485–3488. https://doi.org/10.1016/j.febslet.2007.06.056

Yuan, J. hang, Yang, F., Wang, F., Ma, J. zhao, Guo, Y. jun, Tao, Q. fei, Liu, F., Pan, W., Wang, T. tian, Zhou, C. chuan, Wang, S. bing, Wang, Y. zhao, Yang, Y., Yang, N., Zhou, W. ping, Yang, G. shun, & Sun, S. han. (2014). A Long Noncoding RNA Activated by TGF-β promotes the invasion-metastasis cascade in hepatocellular carcinoma. *Cancer Cell*, *25*(5), 666–681. https://doi.org/10.1016/j.ccr.2014.03.010

Zacharogianni, M., Gomez, A. A., Veenendaal, T., Smout, J., & Rabouille, C. (2014). A stress assembly that confers cell viability by preserving ERES components during amino-acid starvation. *ELife*, *3*(November), 1–25. https://doi.org/10.7554/eLife.04132

Zagorac, S., de Giorgio, A., Dabrowska, A., Kalisz, M., Casas-Vila, N., Cathcart, P., Yiu, A., Ottaviani, S., Degani, N., Lombardo, Y., Tweedie, A., Nissan, T., Vance, K. W., Ulitsky, I., Stebbing, J., & Castellano, L. (2021). SCIRT lncRNA Restrains Tumorigenesis by Opposing Transcriptional Programs of Tumor-Initiating Cells. *Cancer Research*, *81*(3), 580–593. https://doi.org/10.1158/0008-5472.CAN-20-2612

Zähringer, U., Lindner, B., Inamura, S., Heine, H., & Alexander, C. (2008). TLR2 - promiscuous or specific? A critical re-evaluation of a receptor expressing apparent broad specificity. *Immunobiology*, *213*(3–4), 205–224. https://doi.org/10.1016/j.imbio.2008.02.005

Zalani, S., Holley-Guthrie, E., & Kenney, S. (1996). Epstein-Barr viral latency is disrupted by the immediate-early BRLF1 protein through a cell-specific mechanism. *Proceedings of the National Academy of Sciences of the United States of America*, *93*(17), 9194–9199. https://doi.org/10.1073/pnas.93.17.9194

Zenz, R., Eferl, R., Scheinecker, C., Redlich, K., Smolen, J., Schonthaler, H. B., Kenner, L., Tschachler, E., & Wagner, E. F. (2008). Activator protein 1 (Fos/Jun) functions in inflammatory bone and skin disease. In *Arthritis Research and Therapy* (Vol. 10, Issue 1). https://doi.org/10.1186/ar2338

Zhang, B., Kracker, S., Yasuda, T., Casola, S., Vanneman, M., Hömig-Hölzel, C., Wang, Z., Derudder, E., Li, S., Chakraborty, T., Cotter, S. E., Koyama, S., Currie, T., Freeman, G. J., Kutok, J. L., Rodig, S. J., Dranoff, G., & Rajewsky, K. (2012). Immune surveillance and therapy of lymphomas driven by Epstein-Barr virus protein LMP1 in a mouse model. *Cell*, *148*(4), 739–751. https://doi.org/10.1016/j.cell.2011.12.031

Zhang, P., Fan, B., Yang, P., Temirov, J., Messing, J., Kim, H. J., & Taylor, J. P. (2019). Chronic optogenetic induction of stress granules is cytotoxic and reveals the evolution of ALS-FTD pathology. *ELife*, *8*. https://doi.org/10.7554/eLife.39578

Zhang, T., Delestienne, N., Huez, G., Kruys, V., & Gueydan, C. (2005). Identification of the sequence determinants mediating the nucleo-cytoplasmic shuttling of TIAR and TIA-1 RNA-binding proteins. *Journal of Cell Science*, *118*(23), 5453–5463. https://doi.org/10.1242/jcs.02669

Zhang, W., Han, D., Wan, P., Pan, P., Cao, Y., Liu, Y., Wu, K., & Wu, J. (2016). ERK/c-Jun Recruits Tet1 to Induce Zta Expression and Epstein-Barr Virus Reactivation through DNA Demethylation. *Scientific Reports*, *6*(1), 1–11. https://doi.org/10.1038/srep34543

Zhang, Y., Xu, L., Chang, Y., Li, Y. J., Butler, W., Jin, E., Wang, A., Tao, Y., Chen, X., Liang, C., & Huang, J. (2020). Therapeutic potential of ReACp53 targeting mutant p53 protein in CRPC. *Prostate Cancer and Prostatic Diseases*, *23*(1), 160–171.

https://doi.org/10.1038/s41391-019-0172-z

Zhao, B., Zou, J., Wang, H., Johannsen, E. C., Peng, C. W., Quackenbush, J., Mar, J. C., Morton, C. C., Freedman, M. L., Blacklow, S. C., Aster, J. C., Bernstein, B. E., & Kieff, E. D. (2011). Epstein-Barr virus exploits intrinsic B-lymphocyte transcription programs to achieve immortal cell growth. *Proceedings of the National Academy of Sciences of the United States of America*, *108*(36), 14902–14907. https://doi.org/10.1073/pnas.1108892108

Zhao, C., & Zhao, W. (2020). NLRP3 Inflammasome—A Key Player in Antiviral Responses. In *Frontiers in Immunology* (Vol. 11, p. 211). Frontiers Media S.A. https://doi.org/10.3389/fimmu.2020.00211

Zhao, W., Zhao, J., Hou, M., Wang, Y., Zhang, Y., Zhao, X., Zhang, C., & Guo, D. (2014). HuR and TIA1/TIAL1 are involved in regulation of alternative splicing of SIRT1 pre-mRNA. *International Journal of Molecular Sciences*, *15*(2), 2946–2958. https://doi.org/10.3390/ijms15022946

Zheng, D., Wang, R., Ding, Q., Wang, T., Xie, B., Wei, L., Zhong, Z., & Tian, B. (2018). Cellular stress alters 3′UTR landscape through alternative polyadenylation and isoform-specific degradation. *Nature Communications*, *9*(1). https://doi.org/10.1038/s41467-018-04730-7

Zhou, D., Palam, L. R., Jiang, L., Narasimhan, J., Staschke, K. A., & Wek, R. C. (2008). Phosphorylation of eIF2 directs ATF5 translational control in response to diverse stress conditions. *Journal of Biological Chemistry*, *283*(11), 7064–7073. https://doi.org/10.1074/jbc.M708530200

Ziehr, B., Vincent, H. A., & Moorman, N. J. (2016). Human Cytomegalovirus pTRS1 and pIRS1 Antagonize Protein Kinase R To Facilitate Virus Replication. *Journal of Virology*, *90*(8), 3839–3848. https://doi.org/10.1128/JVI.02714-15

Zwicker, D., Decker, M., Jaensch, S., Hyman, A. A., & Jülicher, F. (2014). Centrosomes are autocatalytic droplets of pericentriolar material organized by centrioles. *Proceedings of the National Academy of Sciences of the United States of America*, *111*(26). https://doi.org/10.1073/pnas.1404855111

10 Appendix

10.1 Integrated stress response during latent EBV infection

10.1.1 Phosphorylated eIF2α fluctuation during latent EBV infection

Fluctuation in eIF2α phosphorylation levels have previously been associated with the oscillation of SGs in virus-infected cells (Ruggieri et al., 2012). To investigate whether phosphorylation of eIF2α was fluctuating in our cells the protein was extracted at varying time points with total and phosphorylated levels of eIF2α measured. Each cell line (BL2, BL2wtBAC, BL31, BL31wtBAC) was passaged 1:1 into a large volume and grown for 24 hours, prior to protein extractions taking place every 30 minutes. The protein was extracted from each sample, and western blotted with antibodies specific to total eIF2α, phosphorylated eIF2α, and ATF4, allowing for not only the phosphorylation level of eIF2α but also the induction of downstream protein, ATF4.

It was shown in Figure 10-2B that the phosphorylation of eIF2α (phosphorylated eIF2α normalised against total eIF2α) fluctuated in both uninfected and EBV-infected BL31 cells. At several time points, phosphorylation of viral infected cells was greater than uninfected, whilst at others, the uninfected cell showed increased phosphorylation of eIF2α. This was not observed in BL2 cells, which showed an increased level of phosphorylated eIF2α in uninfected than infected BL2, throughout the experiment, albeit gradually fluctuating in both cell lines. Interestingly, when shown without normalisation to the uninfected cell lines (Figure 10-1), BL31, BL31wtBAC and BL2wtBAC are comparable, expressing a similar phosphorylation ratio, whilst BL2 shows a much greater level of eIF2α phosphorylation. This started at nearly twice the level of the other cell lines.

ATF4 protein levels revealed a similar result, showing similar levels of expression between BL31 and BL31wtBAC, with increased expression fluctuating between the uninfected and infected cell lines. This suggests that a natural oscillation of eIF2α

phosphorylation occurs in the parent cell and is unrelated to the virus. BL2 on the other hand shows the same pattern in ATF4 expression as seen in the phosphorylation levels of eIF2α. ATF4 protein levels are much greater in the uninfected cells throughout the experiment, rising to roughly double at several time points. Once again, however, a fluctuation is occurring in ATF4 expression in both cell lines, noticeable most in BL2, comparing 24 hours to 29.5 hours, where ATF4 expression decreases by about half. Due to the complexity of the extractions and volume required for this experiment, it was only possible to obtain one repeat per condition at the initial stage. Unfortunately, any repeats taken at another time, would not be comparable, as should the fluctuation of eIF2α phosphorylation be occurring, these levels would be different.

We speculated that the differences seen in eIF2α phosphorylation may be a result of the cells being at a different stage of the cell cycle, and consequently, a normal oscillation within these cells. To assess this, the cell lines were synchronised at the same stage of the cell cycle before being released and the phosphorylation levels of eIF2α were monitored. The CDK1 inhibitor, RO-3306 has been previously shown to block cells at the G2/M checkpoint within the cell cycle, providing an effective mechanism to synchronise the cells in mitosis (Vassilev et al., 2006). RO-3306 was incubated with each cell line for 20 hours promoting cell stalling at G2/M, before being washed out, allowing for the cells to continue through the cell cycle, in synchronisation. It was shown that BL2 has a dramatically different eIF2α phosphorylation profile (Figure 10-3B), compared to the previously unsynchronised samples (Figure 10-2B). Figure 10-3 reveals that both the uninfected and EBV-infected BL2 cell lines have similar levels of eIF2α phosphorylation at each stage of the experiment after ~3 hours of the CDK1 inhibitor being washed out. Interestingly, the phosphorylation levels at 1 and 2 hours following removal of the inhibitor show a similar phosphorylation level to the unsynchronised samples, with the infected sample exhibiting a ~50% decrease in the phosphorylation of eIF2α, however,

this difference is sharply corrected by 3 hours post removal, where the phosphorylation of eIF2α in uninfected BL2 falls below that of EBV infected samples.

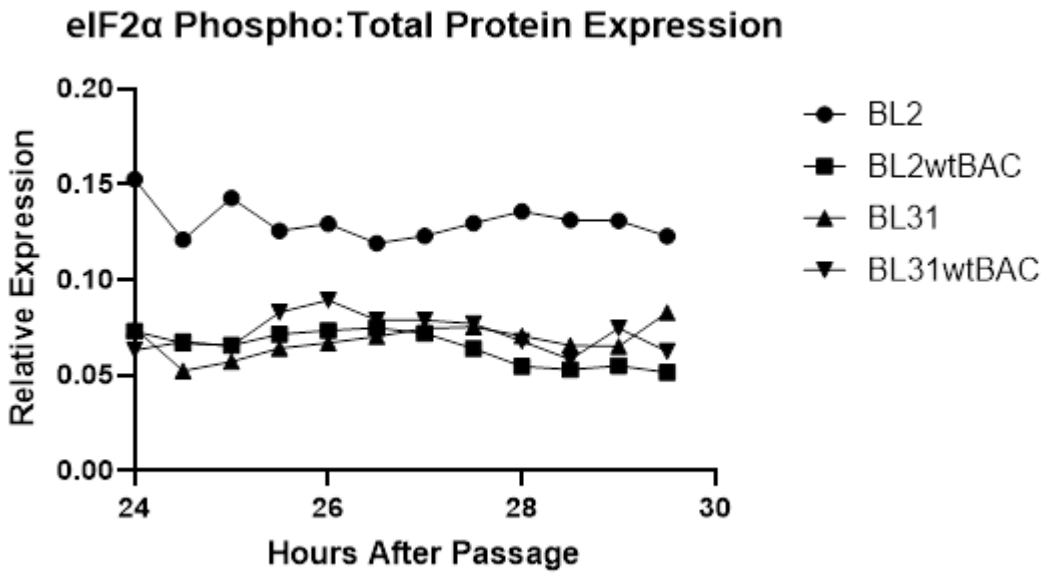

Figure 10-1 Fluctuating eIF2α phosphorylation levels in BL2 and BL31 (EBV$^{+/-}$). Expression levels of phosphorylated eIF2α, normalised against total eIF2α protein expression for BL2, BL31 and EBV^{+} counterparts, during a time course taken from Figure 10-2.

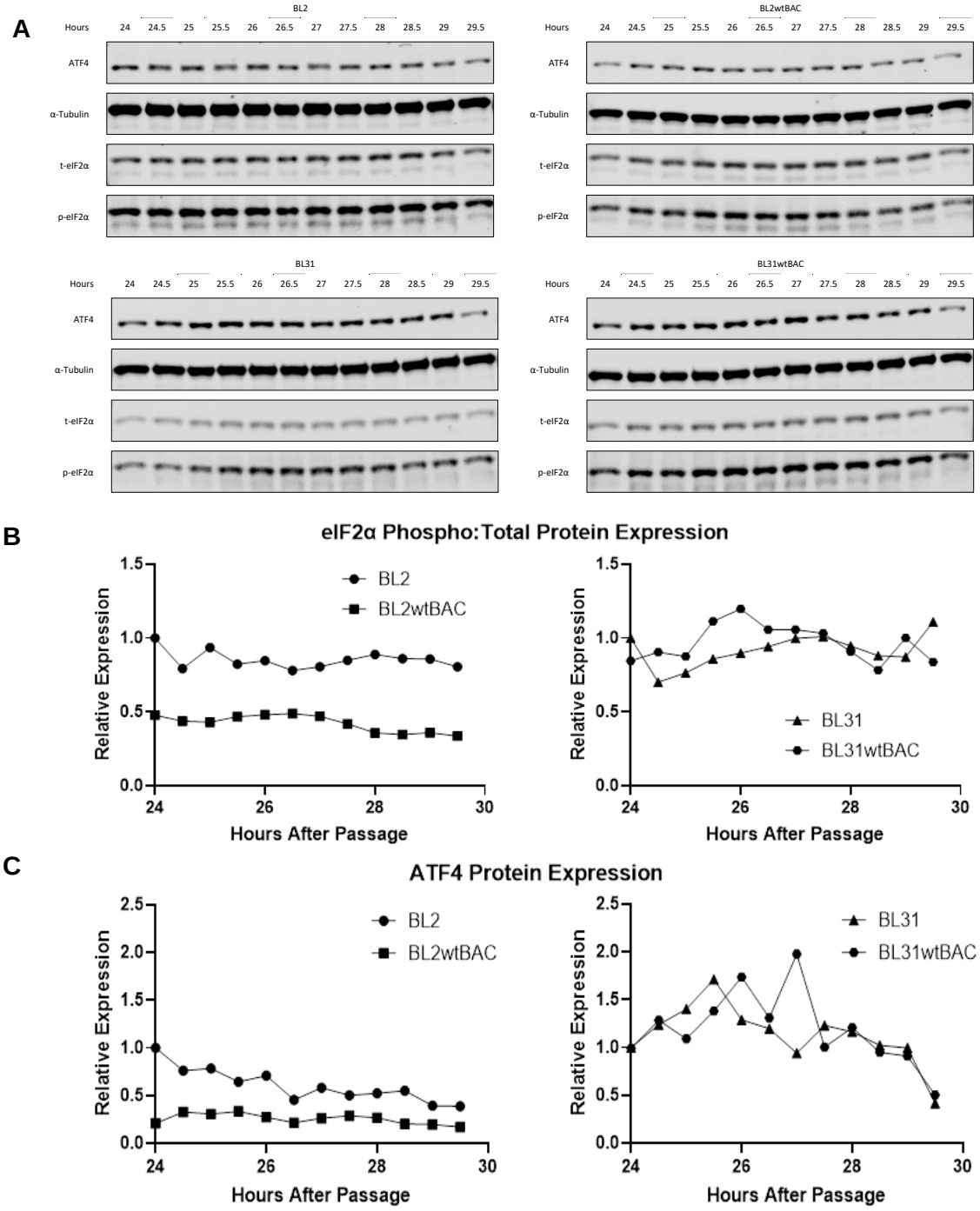

Figure 10-2 eIF2α fluctuation during latent EBV infection. (A) WB analysis of BL2, BL31 and their latent EBV+ counterparts. Protein extractions were taken 30 minutes apart 24 hours after 1:1 passage, for 6.5 hours. Protein was resolved on 10% SDS-PAGE and immunoblotted with antibodies probing for phosphorylated and total eIF2α, ATF4 and α-tubulin. **(B)** Quantification of WB (A), showing phosphorylated eIF2α normalised against total eIF2α, relative to uninfected sample at 24 hours. **(C)** Quantification of ATF4 protein levels from WB (A), normalised against α-tubulin and relative to uninfected samples at 24 hours.

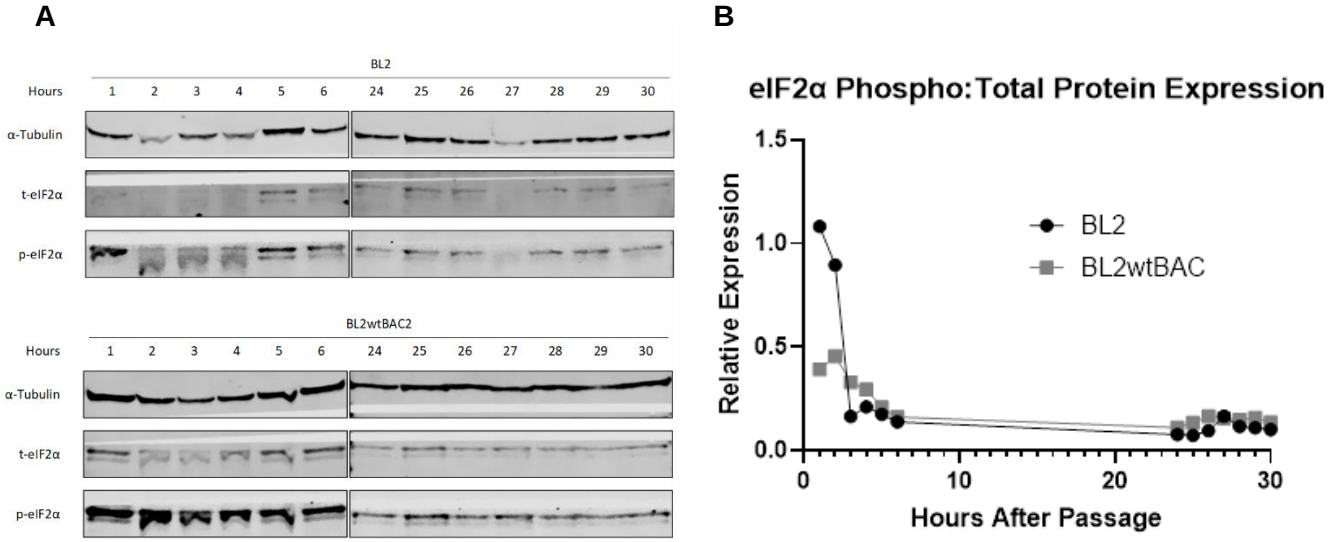

Figure 10-3 eIF2α phosphorylation during latent EBV infection following cell synchronisation. (A) WB analysis of BL2 and BL2wtBAC samples, following cell cycle arrest by CDK1 inhibitor, RO-3306. Protein extractions were taken at 1-hour intervals over 2 days. Protein was resolved on 10% SDS-PAGE and immunoblotted with antibodies probing for phosphorylated and total eIF2α and loading control α-tubulin. **(B)** Quantification of WB (A), showing phosphorylated eIF2α normalised against total eIF2α.

In both time-course experiments (Figure 10-2, Figure 10-3), for cells synchronised in the cell cycle and not, a fluctuation of eIF2α phosphorylation levels (and ATF4 protein expression) is observed in all cell lines, $EBV^{+/-}$, at similar levels. This suggests that any difference seen in eIF2α phosphorylation may be due to natural oscillation in the cell line and not caused by the virus. It can be speculated that latent EBV infection evades further eIF2α phosphorylation. The high levels of GADD34 mRNA in both EBV^{+} cell lines reinforce this hypothesis, as this provides the virus with the means to dephosphorylate eIF2α upon its activation. Increased GADD34 expression was consistent with previously published microarray data (R. E. White et al., 2010), revealing BL31 expressed lower levels of this transcript when compared to cell lines carrying the latent virus. GADD34 interacts with EBNA3C (Garrido et al., 2009), however, this microarray data suggests little difference between GADD34 expression in the wild-type EBV infected cells and EBNA3C knockout EBV infected cells. Further knockout samples from this data suggest that EBNA3 is not linked to increased GADD34 expression (R. E. White et al., 2010). Interestingly, GADD34 expression is controlled by eIF2α/ATF4. As ATF4 expression does not change between infected and latent EBV infected cells, GADD34 expression is potentially being induced by something other than ATF4/eIF2α. Could this be a latent viral product tasked to counteract any activation of the ISR? Further knockout latent product studies may provide answers to this.

10.1.2 ISR protein expression in response to arsenite exposure in latent EBV-infected cells

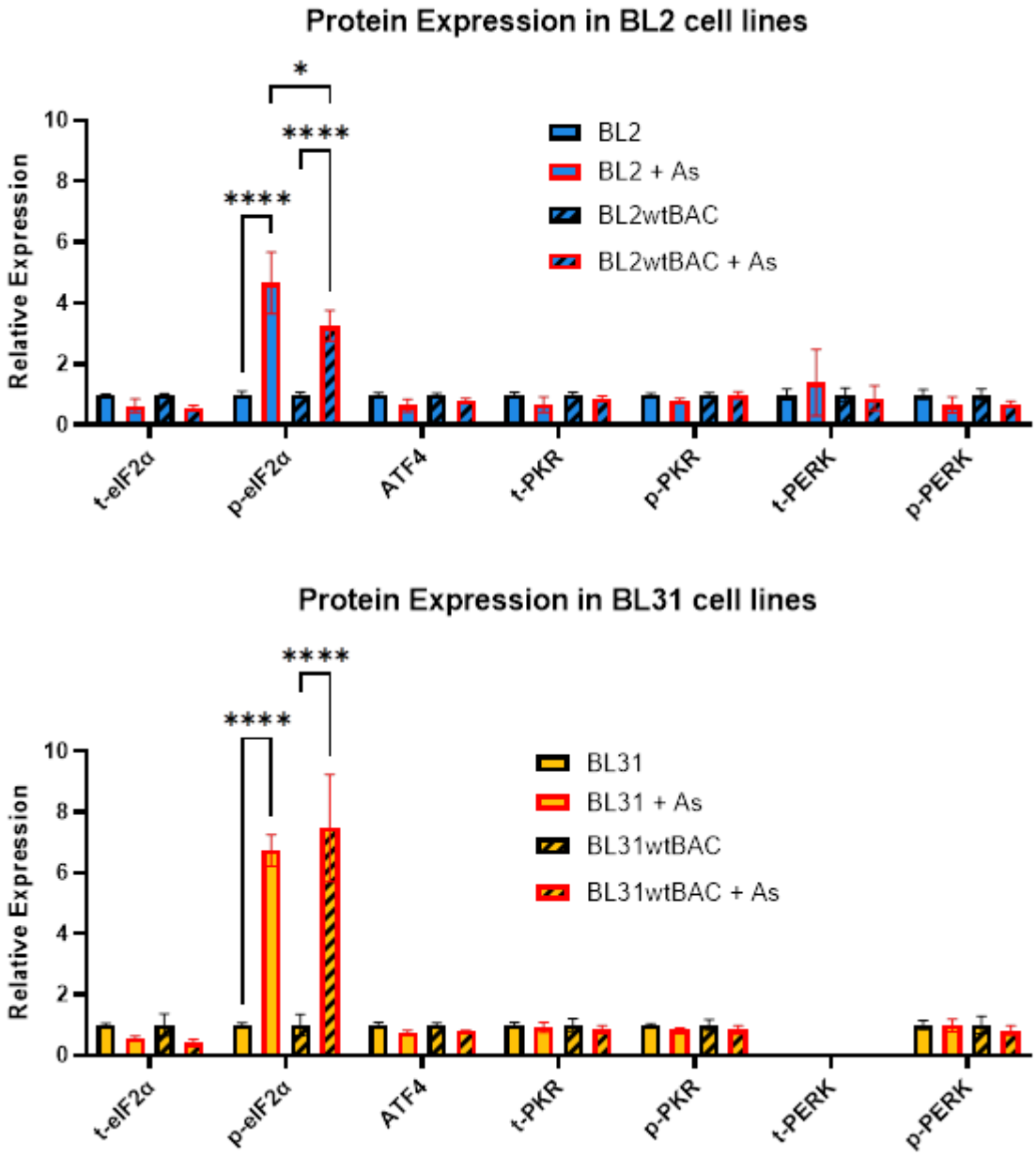

Figure 10-4 Expression of ISR-associated proteins following arsenite stress. Phosphorylated and total expression levels of ISR-associated proteins were quantified from Figure 3-6 and normalised against α-tubulin. t-PERK was undetectable in BL31 cell lines; therefore, PERK was not included in further analysis for this experiment. Error bars represent s.e.m. n=3 (Two-way ANOVA, ns = $P > 0.05$, * = $P \leq 0.05$, ** = $P \leq 0.01$, *** = $P \leq 0.001$, **** = $P \leq 0.0001$).

10.2 RNA-binding proteins and latent EBV infection

10.2.1 TIA-1 knockdown

The next stages of this project were to investigate the effect that decreased TIA-1 levels have on the cell. To achieve this, it was first attempted to knockdown TIA-1 in both infected and uninfected cells, using siRNA. A siRNA pool targeting several locations along the TIA-1 gene allowed for all isoforms to be targeted.

Figure 10-5 shows the results following the knockdown of TIA-1 in BL31 and EBV^+ BL31wtBAC. TIA-1 protein levels decrease in both siRNA-treated cell lines; however, a faint band remains suggesting that there was not a complete knockdown, only partial. Furthermore, the resolution of the TIA-1 protein does not separate TIA-1a and TIA-1b, which, in this experiment is not important, however going forward, it would be prudent to observe any differences in knockdown efficiency between isoforms. These cells were also investigated for mRNA levels; however, this did not show any observable decrease in TIA-1 levels following siRNA treatment (data not shown).

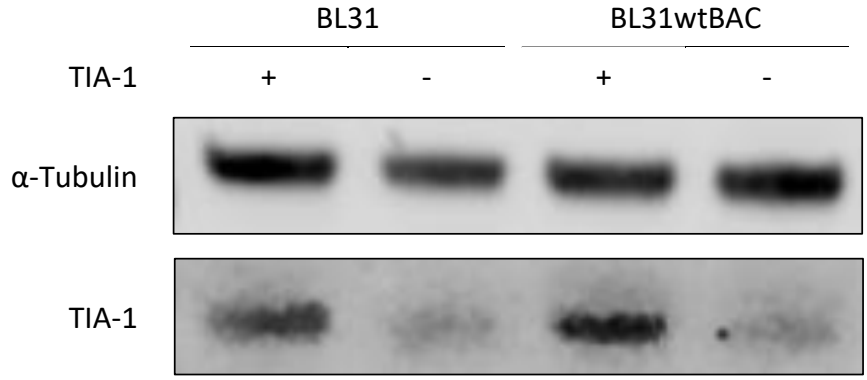

Figure 10-5 TIA-1 knockdown in EBV – and + BL31. BL31 and latent EBV BL31wtBAC cells were transfected with TIA-1 siRNA pool (TIA-1 -) or non-targeting NC siRNA (TIA-1 +) for 24 hours. Protein was extracted and resolved on 10% SDS-PAGE before immunoblotting with antibodies probing by TIA-1 and loading control α-tubulin.

10.3 SCIRT lncRNA and nuclear bodies in cancer

10.3.1 Introduction

The mammalian genome encodes for a vast amount of transcripts, the majority of which, do not code for protein (Carninci et al., 2005; Kapranov et al., 2007). These non-protein-associated transcripts are known as non-coding RNA (ncRNA). Whilst considered non-coding, they remain associated with various biological functions (Palazzo & Lee, 2015). rRNA, the most abundant RNA within the cell, is a ncRNA that along with ribosomal proteins, forms the ribosomal subunits. tRNA, used during translation to transport amino acids to the ribosome, is also an example of a ncRNA. Other examples include siRNA and microRNA, two similar RNA molecules that function to silence gene expression. This chapter focuses on another type of ncRNA, long non-coding RNA (lncRNA), a broad group of ncRNAs that are over 200 nucleotides in size and are involved in numerous biological functions, whilst also implicated in several human diseases (Derrien et al., 2012).

First described in a complex sequencing study performed on mouse cells (Okazaki et al., 2002), lncRNA encompasses many non-functional and functional ncRNAs. The functions of lncRNA include chromatin modification, transcriptional control and post-transcriptional processing and may act through molecular interactions as a guide, decoy and scaffold (reviewed Aznaourova et al., 2020; Mercer et al., 2009) (Figure 10-6). Whilst classified as ncRNA, there have been several studies that have shown that some lncRNA are translated into protein (D. M. Anderson et al., 2015; Bazzini et al., 2014).

A growing number of studies have associated lncRNA with several human diseases, including cancer, cardiovascular diseases and many others (reviewed in Chen et al., 2021). One example of this is the lncRNA H19, which was shown to be expressed at increased levels in several human cancers, and played an inhibitory role with p53 (Matouk et al., 2010). Another lncRNA, lncRNA nuclear paraspeckle assembly transcript

1 (NEAT1), was shown to be highly expressed in many tumour tissues, correlating with poor prognosis and contributing to chemoresistance (V. Y. Shin et al., 2019). The mechanisms in which these lncRNAs affect cancer development are still being elucidated, however, their broad range of functions affecting gene expression is likely to play a role in their association with disease.

The lncRNA, Stem Cell Inhibitory RNA Transcript (SCIRT), is upregulated in tumorspheres, a three-dimensional culturing technique, in which tumour initiating cells (TIC) form a spherical structure comparable to the formation of *in vivo* tumours (Zagorac et al., 2021). However, unlike, the previous two examples, appears to act as a tumour suppressor rather than an inducer. It was shown that while SCIRT was upregulated in tumorspheres derived from breast cancer cell lines, MCF7 and MB-MDA-231, it counteracted the aggressive growth properties induced by several cancer-associated transcription factors (Zagorac et al., 2021). We discovered that SCIRT formed nuclear foci in both breast cancer cell lines, which forms part of the data presented in this chapter.

lncRNA has been associated with nuclear bodies (Chujo & Hirose, 2017). In paraspeckles, for example, lncRNA has been shown to act as a scaffold in which several RNA and protein interactions are built around this core (Bond & Fox, 2009). This then provides a basis for the function of paraspeckles in influencing gene regulation. We aimed to confirm that SCIRT is forming nuclear foci, along with the nature of these foci, before dissecting its function.

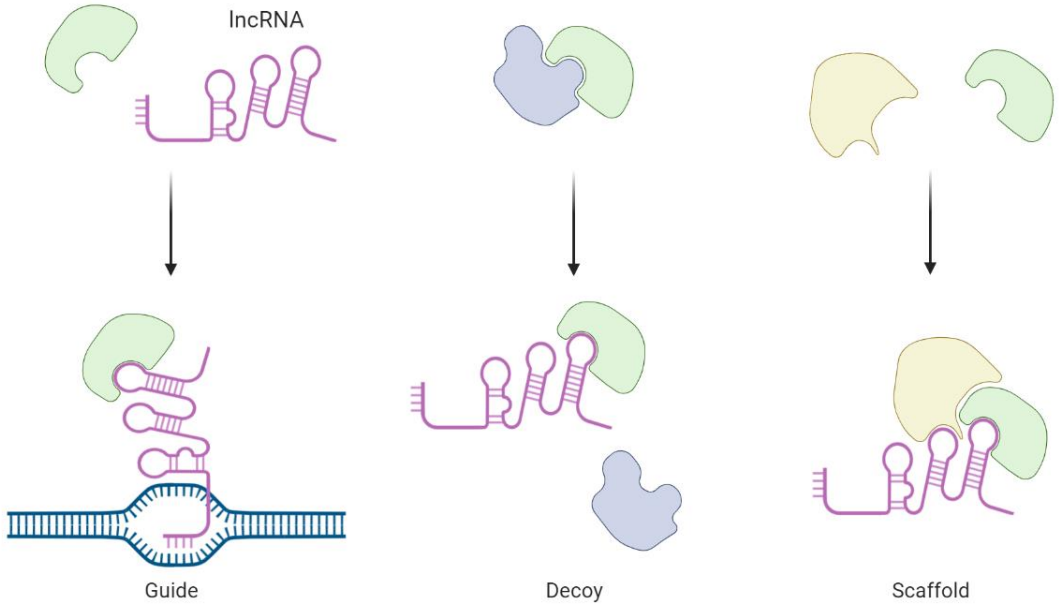

Figure 10-6 lncRNA has multiple functions through different molecular interactions. lncRNA can affect chromatin modification, transcriptional regulation, and post transcriptional modification. These functions are elicited through binding of lncRNA to DNA and protein. lncRNA may act to guide protein such as transcription factors to DNA, block protein interacts or aid the assembly of protein complexes through acting as a a scaffold. Figure adapted from Aznaourova et al. (2020).

10.3.2 Results

10.3.2.1 lncRNA SCIRT accumulates into nuclear bodies in breast cancer cell lines

lncRNA has been shown to form nuclear bodies, and act as a scaffold for their accumulation (reviewed in Chujo & Hirose, 2017). The lncRNA SCIRT, which was significantly upregulated in TIC-enriched spheres derived from primary breast cancer samples (Zagorac et al., 2021), was thought to localise within the nucleus. This study set out to confirm the localisation of SCIRT within the nucleus and determine whether this lncRNA accumulated into nuclear bodies within these tumour cell lines. In contrast to previous chapters, localisation experiments were performed using RNA rather than protein. Therefore, alternative techniques were used, and previous methods were modified.

To visualise the localisation of SCIRT within the cell, Fluorescence In Situ Hybridization (FISH) was performed. FISH enables RNA to be labelled and imaged, providing a means for SCIRT to be visualised. The breast cancer cell line, MCF7, was used throughout this chapter, whilst further data was obtained with an additional breast cancer cell line, MDA-MB-231 (MM231).

SCIRT was knocked down using two siRNAs targeting different regions of the SCIRT locus (siRNA 1B, siRNA c1B, kindly gifted by Prof. Leandro Castellano), and FISH was performed to determine the localisation of the SCIRT. As shown in Figure 10-7A, mRNA expression of SCIRT is reduced by over 75% using either siRNA, compared to cells treated with off-target negative control siRNA (siNC).

FISH reveals that SCIRT is exclusively located within the nucleus, and forms localised foci within it (Figure 10-7B). Furthermore, KD samples, treated with either siRNA 1B or siRNA c1B have a reduced SCIRT signal compared to negative control-treated cells. The nuclear accumulation of SCIRT decreases following the silencing of the lncRNA. Metastasis-associated lung adenocarcinoma transcript 1 (MALAT1), a lncRNA that has

been associated with several cancers (Hutchinson et al., 2007; Ji et al., 2003), was used to investigate whether any colocalization with SCIRT occurred in these cells, and as a positive control for FISH. It can be seen in Figure 10-7B, that MALAT1 also forms nuclear foci within MCF7 cells, however, fewer than seen in SCIRT. Furthermore, these foci do not appear to colocalise with SCIRT, suggesting that these nuclear bodies are not connected.

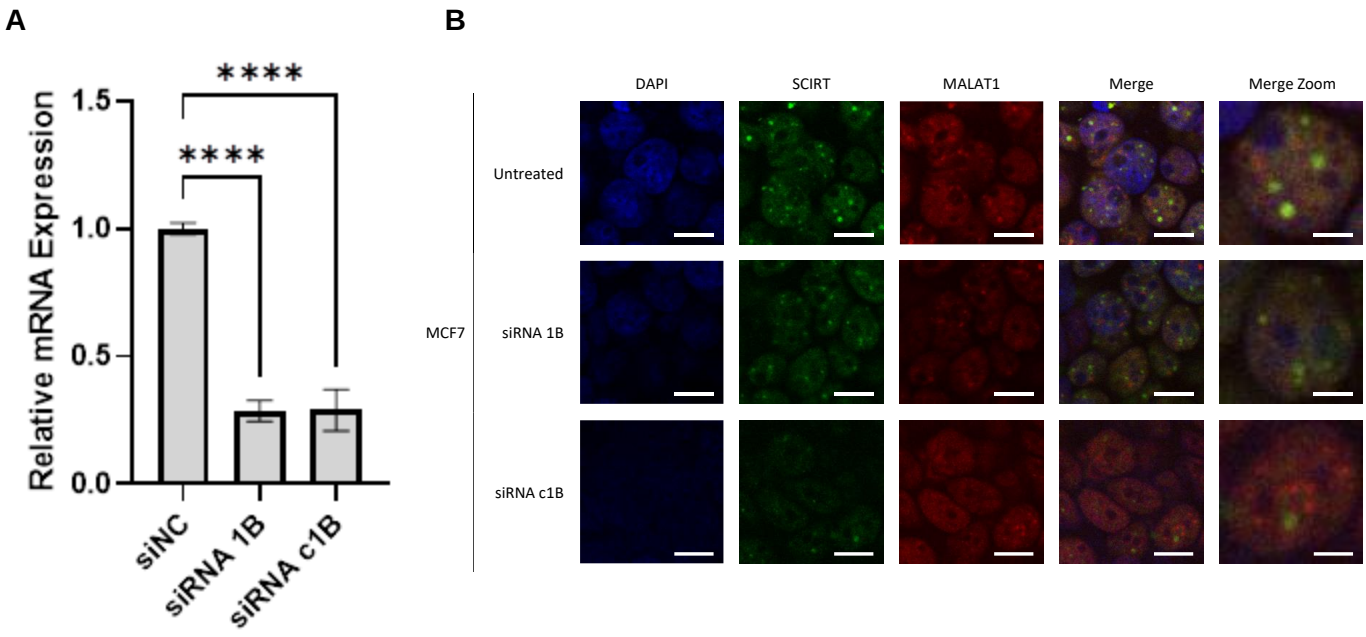

Figure 10-7 Knockdown of SCIRT decreases nuclear SCIRT foci. (A) mRNA levels of SCIRT in MCF7 cells following treatment with siRNA targeting SCIRT (siRNA 1B, siRNA c1B) or NC off-target siRNA (siNC). mRNA levels SCIRT were normalised against GAPDH and set relative to siNC. Error bars represent s.e.m. n=1 (Two-way ANOVA, ns = P > 0.05, * = P ≤ 0.05, ** = P ≤ 0.01, *** = P ≤ 0.001, **** = P ≤ 0.0001). **(B)** Immunofluorescent images of RNA FISH experiment probing for SCIRT and MALAT1 in MCF7 cells from (A). Scale bar = 20 µm, Zoom scale bar = 5 µm.

10.3.2.2 SCIRT nuclear bodies are found within the nucleolus

The nucleolus is an example of a biomolecular condensate (Mao et al., 2011). Formed through LLPS, the nucleolus is the site of ribosome biogenesis but has also been shown to capture and immobilise protein through the manipulation of several lncRNA (Audas et al., 2012). It is thought that this process is linked to the posttranslational regulation of these proteins.

The data presented in the previous section suggests that SCIRT forms nuclear bodies within breast cancer cells. We aimed to determine whether these nuclear bodies were associated with the nucleolus.

Fibrillarin, a protein associated with the C/D box small nucleolar ribonucleoproteins (snoRNPs) is localised within the nucleolus (Newton et al., 2003). Therefore, using fibrillarin as a marker, we can visualise the nucleolus with the cell. When used alongside SCIRT probing, we can determine whether SCIRT may localise to the same regions as fibrillarin, and therefore be associated with the nucleolus. A method was developed to combine both FISH and IF, allowing for the visualisation of both the RNA, SCIRT, and protein, fibrillarin.

It was shown that following the silencing of SCIRT, the signal and SCIRT nuclear bodies, decrease in MCF7 and MM231 cells, suggesting that the signal observed is that of SCIRT (Figure 10-8). The signal showing fibrillarin provides a clear visualisation of the nucleolus, in both cell lines, and in each KD condition. SCIRT is shown to localise with fibrillarin in both cell lines, suggesting that it is accumulating within the nucleolus of these cells.

It was next investigated whether the SCIRT nucleolar foci could be dispersed with the disruption of the nucleolus. BMH-21 is a small molecule, possessing antitumorigenic activity, that binds to and represses RNA-polymerase I promoting the disintegration of the nucleolus (Peltonen et al., 2010, 2014). Following treatment of MCF7 and MM231

cells with BMH-21 the fibrillarin signal begins to disperse into smaller foci and spread throughout the nucleus, suggesting that the nucleolus had been disintegrated. SCIRT foci disappeared following BMH-21 treatment whilst seen in the negative control samples, treated with DMSO (Figure 10-9). This suggests that SCIRT may be associated with nucleolar bodies within the nucleolus and upon disruption of the nucleolus, these bodies disperse. However, inhibition of rRNA transcription by BMH-21 may have additional effects on SCIRT expression levels and localisation, and further investigation is required to confirm that it is the disruption of the nucleolus itself that disperses SCIRT foci.

Interestingly, SCIRT within a relatively healthy control tissue, MRC-5, a non-cancerous lung cell line, showed the same nucleolar localisation as both breast cancer cell lines, and the dispersal following disruption of the nucleolus (Figure 10-9). This would suggest that either, SCIRT localisation into nucleolar bodies is a general characteristic of the lncRNA, rather than just in cancer cells, or the SCIRT probes are un-specifically binding to rRNA within the nucleolus.

Whilst localisation of SCIRT with the fibrillarin signal may suggest that the lncRNA is associated within the nucleus, other foci have been shown to closely associate with the nucleolus whilst remaining structurally distinct, such as the perinucleolar compartment (S. Huang et al., 1998). To further reinforce whether SCIRT is localised within the nucleolus or just closely associated, we isolated the nucleolus fraction from each cell line. Figure 10-10 reveals that both fibrillarin and SCIRT are present in this fraction, suggesting that SCIRT does localise within the nucleolus.

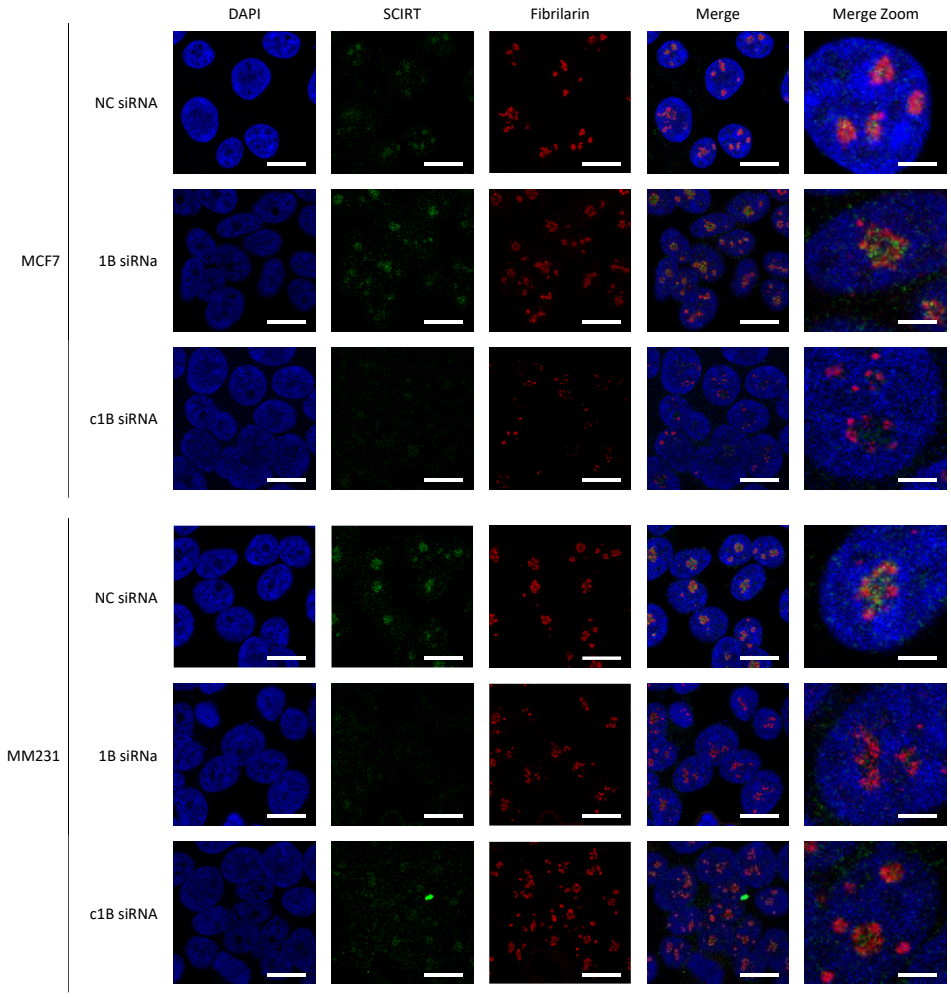

Figure 10-8 SCIRT is localised to the nucleolus. Confocal images of RNA FISH experiments probing for SCIRT and Fibrillarin, and the nuclear marker DAPI. Cells were treated with siRNA targeting SCIRT (1B siRNA, c1B siRNA) or off-target NC siRNA before fixation and probing. Scale bars represent 20 µm, and 5 µm in zoomed images.

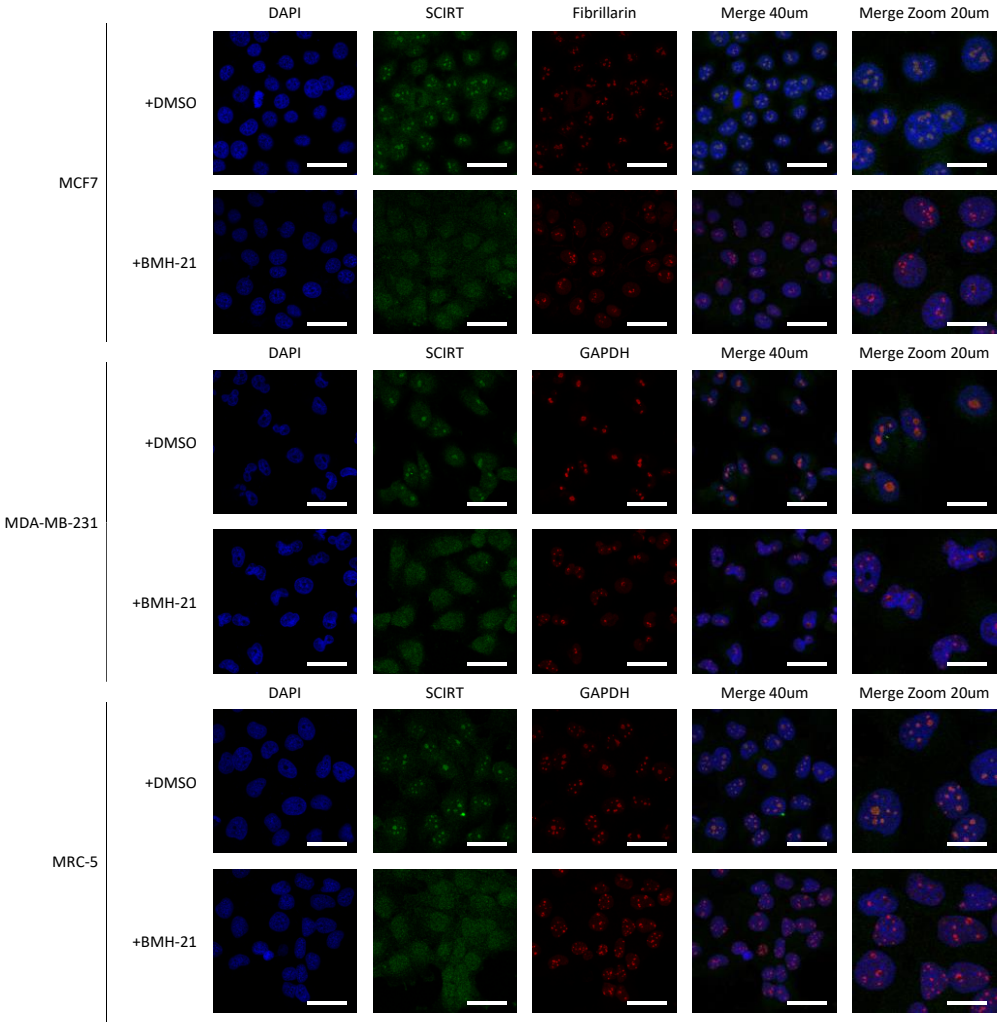

Figure 10-9 RNA FISH following PolI inhibition shows the disruption of the nucleolus and dispersal of SCIRT. Images showing IF/RNA FISH probing for lncRNA SCIRT and Fibrillarin, along with nuclear marker DAPI, in MCF7, MM231 and MRC-5. Cells were either treated with BMH-21 (1 µM) or DMSO (control) for 3 hours before fixation, permeabilsation and probing. Scale bars represent 40 µm, and 20 µm in zoomed images.

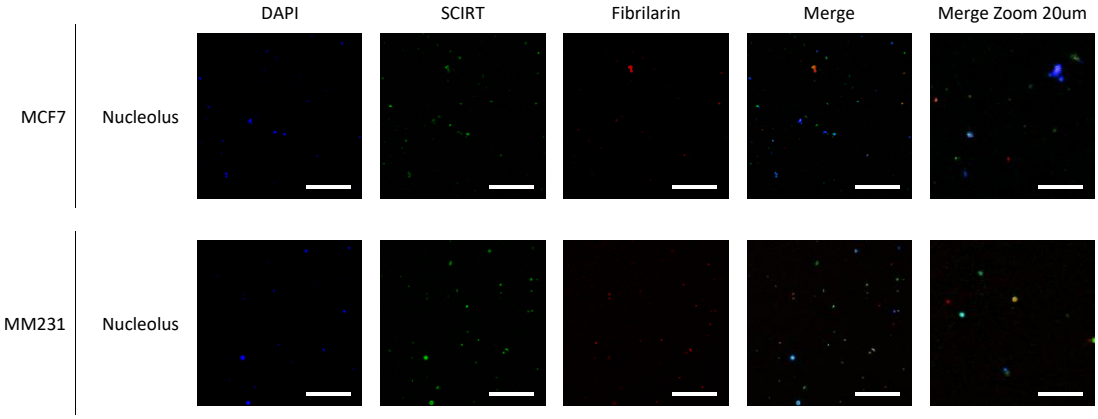

Figure 10-10 RNA FISH used in combination with IF on purified nucleolus samples show colocalization of SCIRT and Fibrillarin. Nucleoli were purified from MCF and MM231 and IF probed for Fibrillarin before fixation and RNA FISH probing for SCIRT. DAPI was used as a nuclear marker. Scale bars represent 40 µm, and 20 µm in zoomed images.

10.3.2.3 Cell growth and confluency affect SCIRT localisation

SCIRT is upregulated in tumorspheres, concentrated groups of tumour-initiating cells derived from a single cell that forms a sphere, compared to cells growing as a monolayer (Zagorac et al., 2021). Therefore, we speculated that SCIRT expression and localisation may be altered by cell-to-cell contact. We observed a change in the localisation of SCIRT foci during the optimisation of these experiments (data not shown) and aimed to determine whether the confluency of the cells or growth duration affected these foci.

Two experiments were set up to investigate how SCIRT foci changed over 3 days following seeding, and whether seed density may affect this.

First, cells were seeded at $0.2x10^6$ cells onto coverslips and grown for up to 3 days. Figure 10-11 shows that in MCF7, SCIRT foci were present in all samples ranging from 0 to 3 days following seeding, however, the quantity and intensity of SCIRT granules appear to be increased at 3 days, compared to earlier samples. Whilst results for MM231 and MRC-5 show a similar response, this difference is not as apparent.

When seed density was examined, there was no clear difference in SCIRT foci between samples seeded at different densities in either MCF7 or MM231 (Figure 10-12).

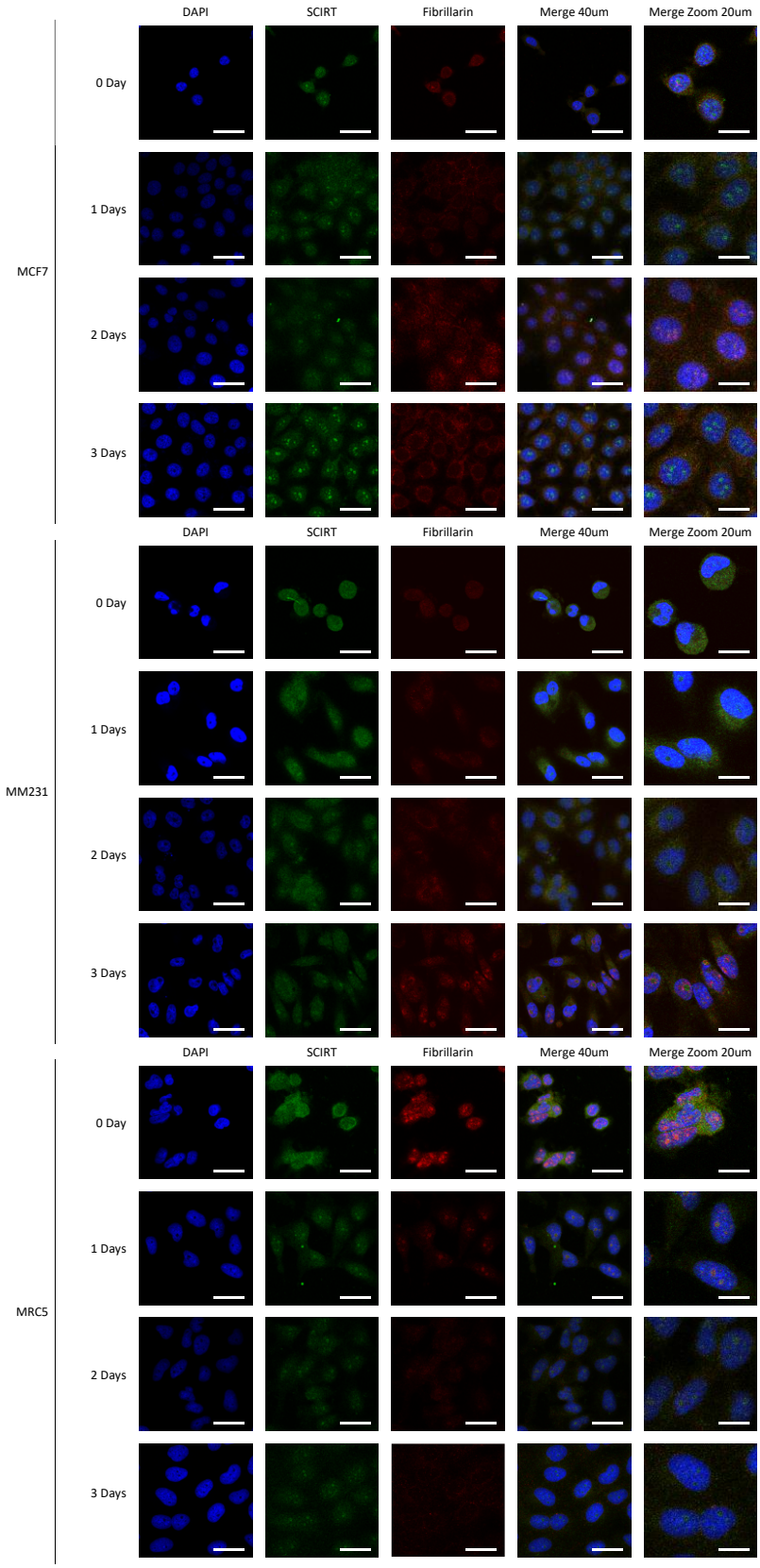

Figure 10-11 SCIRT localisation over time. Images showing RNA FISH experiments probing for SCIRT and Fibrillarin, and the nuclear marker DAPI. Cells were seeded at $0.2x10^6$ cells and allowed to grow for periods of time before fixation and probing. Scale bars represent 40 µm, and 20 µm in zoomed images

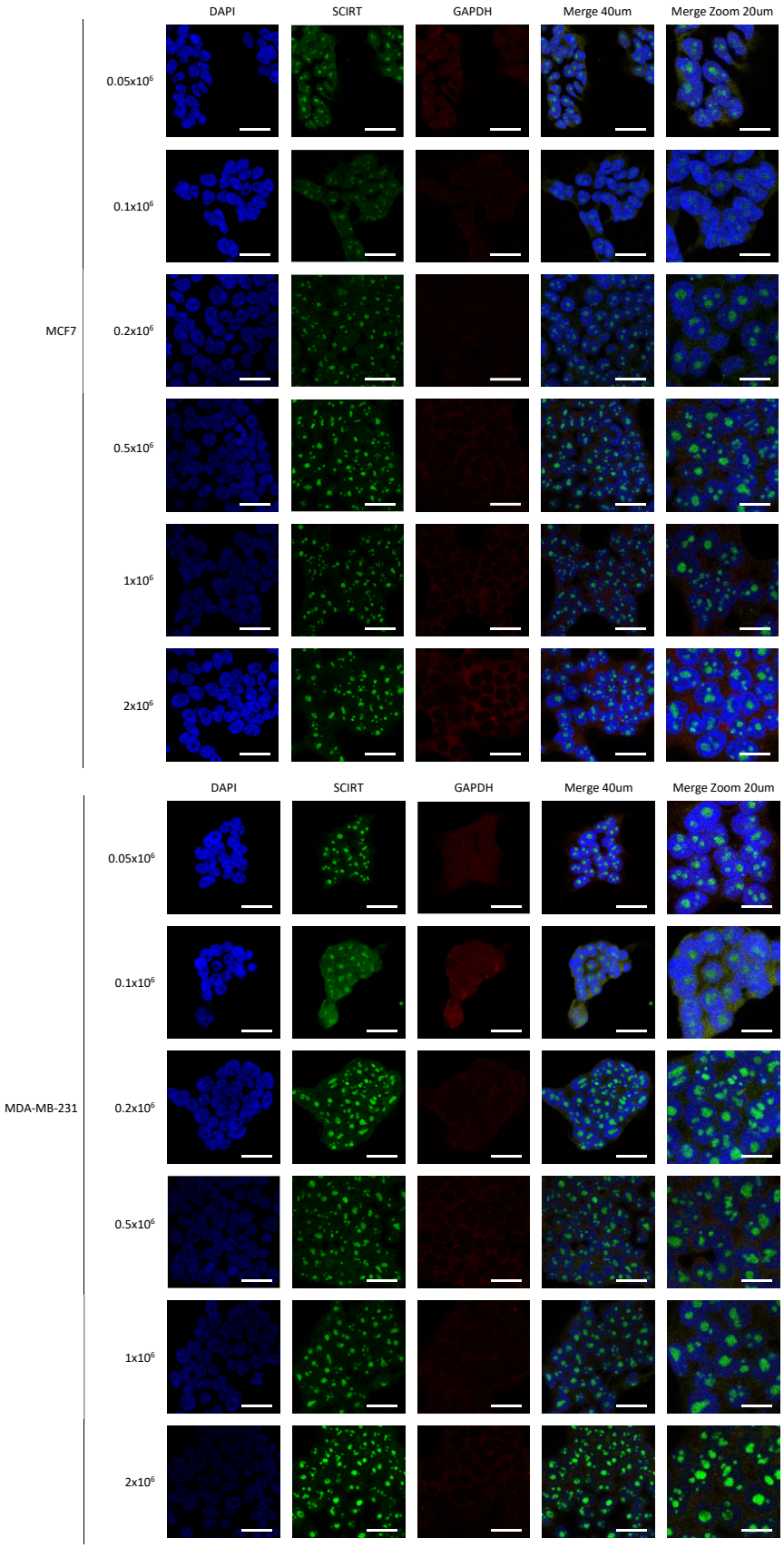

Figure 10-12 SCIRT localisation in response to cell density. Confocal images of RNA FISH experiments probing for SCIRT and Fibrillarin, and the nuclear marker DAPI. Cells were seeded at varying cell densities and and grown for 24 hours before fixation and probing. Scale bars represent 40 µm, and 20 µm in zoomed images.

10.3.2.4 Generation of a SCIRT knockout cell line

As a relatively recently discovered lncRNA, the mechanistic function of SCIRT remains unknown. However, it is thought to act as a tumour suppressor in breast cancer as it is highly expressed in tumorigenic cells, whilst suppressing their aggressive properties (Zagorac et al., 2021).

The next stages of this study were to develop a SCIRT KO cell line, which would allow for further investigation into how SCIRT may elicit its function. Not only as a tumour suppressor but how this lncRNA may also affect healthy cells, as suggested by its presence in MRC-5. A KO cell line will provide complete elimination of SCIRT, as opposed to the KD previously shown, that only provided a transient reduction in its expression.

Whilst the creation of a $SCIRT^-$ cell line would allow for functional investigation, RNA and proteomic analysis, it would also provide a useful negative control for future FISH and other probing experiments.

SCIRT is around 80 kb in length and several ORFs fall within its locus, therefore, to decrease the chances of a fatal KO or detrimentally affecting the cell, we adopted three strategies targeting alternative regions within the gene (Table 10-1, Figure 10-13). The first strategy was to remove the entire locus, this would potentially cause the most adverse effects, through the removal of a large amount of DNA from the genome. The second strategy was to remove exons 2 to 5. Exon 1 is followed by a large intron of around 70 kb, therefore by targeting only the last four exons, a much smaller region could be removed. Finally, the third strategy was the removal of the promotor region alone, chr6:44,037,857-44,044,916. Each strategy involved the incorporation of two gRNAs, one upstream and one downstream of each target region, into separate CRISPR-Cas9 plasmids. These plasmids were then transfected into MCF7 cells, allowing for the KO to

occur, followed by selection and single colony growth, this workflow is summarised in Figure 10-14.

CRISPR Strategy	Location
Deletion of Promoter Region	hg38 chr6:44,037,857-44,044,916
Deletion of Exons 2 - 5	hg38 chr6:43,995,723-44,001,116
Deletion of Entire Locus	hg38 chr6:43,995,723-44,074,652

Table 10-1 CRISPR targeting location for each SCIRT KO strategy.

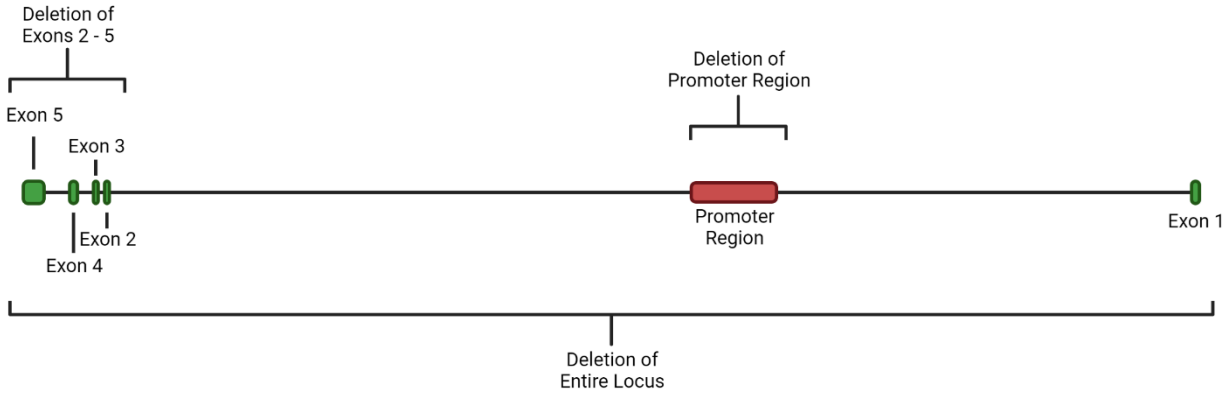

Figure 10-13 Location of each SCIRT KO strategy. Schematic diagram representing the ~80 kb gene of SCIRT with exons 1 to 5, and the promoter region. The strategy targeting the entire locus aims to induce a cut at either end of the gene for its complete removal. Deletion of the promoter region targets an area understood to consist of the SCIRT promoter. Whilst deletion of exons 2 – 5 aims to removed the majority of exons without removal of excess genetic material.

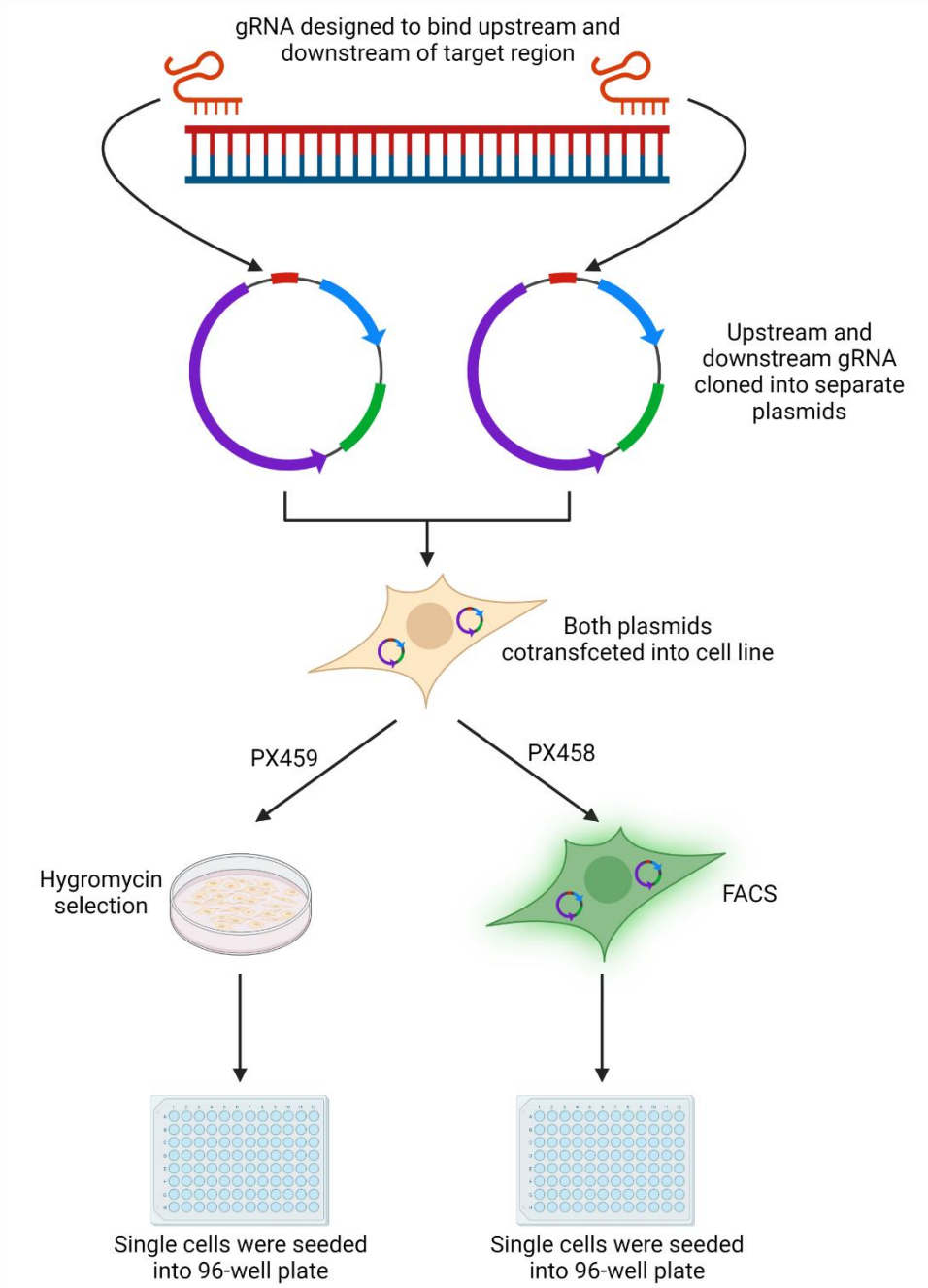

Figure 10-14 SCIRT knockout was performed using CRISPR. Upstream and downstream gRNA was designed to target partiocular regions within the SCIRT gene. These gRNAs were cloned into separate plasmids containing a Cas9 gene, along with a form of selection, GFP (PX458) or hygromycin resistance (PX459). Plasmids containing upstream and downstream gRNA were co-transfected into MCF7 cells, before selection was performed. PX459 transfected cells were exposure to hygromycin, whilst PX458 transfected cells were sorted using FACs. Cells containing the plasmid were seeded as single cells into 96-well plates, either through serial dilution (PX459) or using FACS (PX458).

Each gRNA locates and binds to the region identical to CRISPR RNA (crRNA) region on the DNA known as a protospacer and recruits the Cas9 nuclease via the trans-activating RNA (tracrRNA) region. The region on the target DNA directly downstream of the protospacer with the sequence of 5′-NGG-3′ is known as the protospacer adjacent motif (PAM) site and is the site of Cas9 binding. The Cas9 nuclease cuts the DNA three nucleotides upstream from the PAM site, inducing a double-strand break. The use of two gRNAs produces a break on either side of the target region, with the aim for NHEJ to then repair the DNA with this region absent.

gRNA was designed using Genome Browser (genome.ucsc.edu/) which identified 20-nucleotides sequences within the range of a PAM site. Genome browser provided efficiency and off-target scores (Doench et al., 2016; Haeussler et al., 2016) for each gRNA and two pairs for each region with the highest scores were chosen. Each gRNA was incorporated into both PX458 and PX459 plasmids. These two plasmids are similar, however, PX458 contains the GFP gene, whilst PX459 contains a hygromycin resistance gene. Each of these plasmids allows for a different selection method to be adopted. The correct construction of each plasmid was confirmed through sequencing, and each gRNA-plasmid pair was transfected into MCF7 cells using Lipofectamine 3000, before selection.

Initially, each gRNA was cloned into the PX459 plasmid, however, following exposure to hygromycin selection, and subsequently, single-cell dilution, colonies did not grow as expected. At this point, the PX458 plasmid system was adopted. As the function of SCIRT is unknown, the consequence of its KO is also unclear. Whether it may have proven fatal to cells, or altered the cells' susceptibility to apoptosis is unknown, therefore, to reduce any additional stress which may be brought on by exposure to hygromycin, GFP was used to sort the cells instead. As cells expressing the plasmid produced GFP along with the gRNA and Cas9 nuclease, it was possible to sort cells using FACS. This allowed for single cells to be seeded and grown without any additional stress.

Cells isolated via FACs also failed to grow from single cells, suggesting that KO of SCIRT may be fatal to the cell. This may be assessed in the future by further CRISPR processes. Using additional cell lines would allow for any cell variability to be determined, whilst additional strategies targeting other regions, and using only one gRNA may provide a viable clone. Furthermore, the development of a heterozygous knockout, allowing for SCIRT to be knocked out on one allele but remain on the other, may also provide insight as to whether SCIRT KO is fatal to cells.

10.3.3 Discussion

Over the past decade, lncRNAs are becoming an increasingly studied field, however, much remains to be understood regarding their function, localisation, and even their coding ability. As lncRNA is broadly defined as any ncRNA over 200-nt in length, their function varies significantly. They are central to many processes, including metabolism, cell cycle and differentiation (Ballarino et al., 2016; Brazão et al., 2016; Joaquina Delás et al., 2017; Kitagawa et al., 2013; Sirey et al., 2019; X. Sun & Wong, 2016), whilst also being associated in several diseases (Esteller, 2011; Y. Wang et al., 2013; Yuan et al., 2014). In more recent years, studies have also linked lncRNA to viral infection (Yiliang Wang et al., 2020). This study found that the lncRNA MAMDC2-AS1 aided the nuclear transport of viral proteins responsible for the initiation of viral gene expression.

The lncRNA SCIRT has only recently been defined, through its association and upregulation with several breast cancers (Zagorac et al., 2021). However, its function remains unknown. The data presented in this chapter investigates the localisation of this lncRNA and how this may be linked to its function.

First, SCIRT is located exclusively in the nucleus (Figure 10-7). It has been shown that the majority of lncRNA are found within the nucleus, however, may also be located in the cytoplasm (Cabili et al., 2015; Carlevaro-Fita et al., 2016; Van Heesch et al., 2014). The localisation of SCIRT exclusively to the nucleus would suggest that this lncRNA is not involved with cytoplasmic function, or shuttling. Furthermore, in both breast cancer cell lines, SCIRT is shown to form foci within the nucleolus (Figure 10-8). Nucleolar localisation of lncRNA has previously been associated with a function relating to ribosome biogenesis, such as the lncRNA SLERT (snoRNA-ended lncRNA enhances pre-ribosomal RNA transcription) (Xing et al., 2017). SLERT was shown to promote pre-ribosomal RNA transcription through interaction with proteins acting on Pol I. Another lncRNA associated with the nucleolus is LETN (lncRNA essential for tumour cell

proliferation via NPM1) (X. Wang et al., 2021). This study found that LETN was key to the structure of the nucleolus and linked to proliferation in tumour cells. This information would suggest that lncRNA associated with the nucleolus is tightly linked to nucleolar structure and function. Further nucleolar localisation analysis, including nucleolar disintegration (Figure 10-9) and purification (Figure 10-10) reinforces the finding that SCIRT is found within the nucleolus. Interestingly, SCIRT signal was also detected to similar levels and localisation in MRC-5 cells, a non-cancerous lung-derived cell line, and dispersed following nucleolar disintegration (Figure 10-9). Whilst initial findings suggested that SCIRT was upregulated in the formation of tumorspheres, a spherical formation formed through the proliferation of one cancer cell (Zagorac et al., 2021). Data presented in this chapter suggests that SCIRT localisation and expression in cancer cells *in vitro,* not in tumorspheres*,* is similar that that of non-cancerous cells. This implies that SCIRT localisation observed in this study is a general property displayed in all cells, and may potentially change upon the formation of tumorspheres. It has been suggested that tumorspheres provide a more translatable insight into anti-cancer drug effectiveness than a monolayer culture (C. H. Lee et al., 2016). Taken together, it may be speculated that SCIRT localisation and expression differ within tumours from that observed in this chapter.

To assess whether the growing conditions of the cells affected SCIRT localisation, cell growth and confluency experiments were undertaken. As SCIRT expression appeared to differ in results obtained in this study, from those previously reported (Zagorac et al., 2021), it was considered whether cell-to-cell contact may play a role in SCIRT localisation. The data presented in this chapter suggests that whilst no observable difference was seen following cell growth at increasing cell density (Figure 10-12), it could be argued that SCIRT foci within the nucleolus increase over time (Figure 10-11). However, further investigation into this effect is required, as several factors may be responsible for the observed change. One such factor may be linked to cellular stress,

caused by prolonged growth without passaging. Whilst the cells were regularly provided with fresh media, the confluency at the later time points may have contributed to nutrient competition and deprivation, along with inhibition of growth through limited space. Whilst this may also have occurred in cells seeded at a high density (Figure 10-12), the time in which the cells were grown and were able to present this stress may not have been long enough.

Taken together, there is still much to understand as to how SCIRT elicits its function, whether in the nucleolus or not. However, it remains clear that this function may differ in tumours. It would be prudent to further analyse SCIRT foci observed in both non-cancerous and cancer cell lines, whilst also probing this response in tumorspheres, which may provide greater insight as to how SCIRT is behaving at the site of tumours within the body.

One technique that would provide useful information, is the development of a SCIRT^{-} cell lines. The initial development of a KO cell line in this study has not provided a viable product, therefore, further research and investigation are required to understand whether it is possible to remove SCIRT without a fatal response. This would allow initial insight into the role which SCIRT may play in cell function.